TRANSPORTATION RESEARCH RECORD 1041

Cathodic Protection, Concrete and Bituminous Maintenance, and Bridge Repainting

TRB
TRANSPORTATION RESEARCH BOARD
NATIONAL RESEARCH COUNCIL
WASHINGTON, D.C. 1985

Transportation Research Record 1041
Price $12.20
Editor: Naomi C. Kassabian
Compositor: Lucinda Reeder
Layout: Betty L. Hawkins

mode
1 highway transportation

subject areas
25 structures design and performance
32 cement and concrete
34 general materials
40 maintenance

Transportation Research Board publications are available by ordering directly from TRB. They may also be obtained on a regular basis through organizational or individual affiliation with TRB; affiliates or library subscribers are eligible for substantial discounts. For further information, write to the Transportation Research Board, National Research Council, 2101 Constitution Avenue, N.W., Washington, D.C. 20418.

Printed in the United States of America

Library of Congress Cataloging-in-Publication Data
National Research Council. Transportation Research Board.

Cathodic protection, concrete and bituminous maintenance, and bridge repainting.

(Transportation research record ; 1041)
1. Bridges–Maintenance and repair–Congresses.
2. Pavements–Maintenance and repair–Congresses.
I. National Research Council (U.S.). Transportation Research Board. II. Series.
TE7.H5 no. 1041 380.5 s 86-5455
[TG315] [625.8]
ISBN 0-309-03957-6 ISSN 0361-1981

Contents

Addresses of Authors

Appleman, Bernard R., Steel Structures Painting Council, 4400 Fifth Avenue, Pittsburgh, Pa. 15213

Biswas, Mrinmay, Transportation and Infrastructure Research Center, School of Engineering, Duke University, Durham, N.C. 27706

Burns, William E., Division of Highways, Illinois Department of Transportation, 126 East Ash Street, Springfield, Ill. 62704-4766

Crovetti, J. A., ERES International, Inc., P.O. Box 1003, Champaign, Ill. 61820

Darter, M. I., Department of Civil Engineering, University of Illinois, 111 Talbot Lab, 104 S. Wright Street, Urbana, Ill. 61801

Fontana, Jack J., Brookhaven National Laboratory, Associated Universities, Inc., Upton, N.Y. 11973

Foshee, Forrest W., Soil and Materials Engineers, 3018 Gilliouville Road, Albany, Ga. 31707

Ghattas, Omar N., Transportation and Infrastructure Research Center, School of Engineering, Duke University, Durham, N.C. 27706

Halverson, Andrew D., Minnesota Department of Transportation, Transportation Building, St. Paul, Minn. 55155

Jordan, John W., Jr., Figg and Muller Engineers, Inc., 424 North Calhoun Street, Tallahassee, Fla. 32301

Klosowski, Jerry M., Construction Group, Technical Service and Development, Dow Corning Corporation, Midland, Mich. 48640-0994

Knight, Norman E., Pennsylvania Department of Transportation, 1009 Transportation and Safety Building, Harrisburg, Pa. 17120

Korfhage, Glenn R., Minnesota Department of Transportation, Transportation Building, St. Paul, Minn. 55155

Manning, David G., Ontario Ministry of Transportation and Communications, 1201 Wilson Avenue, Downsview, Ontario M3M 1J8, Canada

Moore, Raymond K., Civil Engineering Department, University of Kansas, Lawrence, Kans. 66045

Parker, Jr., Frazier, Civil Engineering Department, Auburn University, Auburn, Ala. 36849

Peter, Mary M., Division of Highways, Illinois Department of Transportation, 126 East Ash Street, Springfield, Ill. 62704-4766

Ramey, G. Edward, Civil Engineering Department, Auburn University, Auburn, Ala. 36849

Schell, Hannah C., Ontario Ministry of Transportation and Communications, 1201 Wilson Avenue, Downsview, Ontario M3M 1J8, Canada

Slifer, James C., Division of Highways, Illinois Department of Transportation, 126 East Ash Street, Springfield, Ill. 62704-4766

Spells, Sherwood, Construction Group, Technical Service and Development, Dow Corning Corporation, Midland, Mich. 48640-0994

Strickland, A. Mark, Alabama Highway Department, Montgomery, Ala. 36130

Vladimirou, Ilercules, Transportation and Infrastructure Research Center, School of Engineering, Duke University, Durham, N.C. 27706

Webster, Ronald P., Brookhaven National Laboratory, Associated Universities, Inc., Upton, N.Y. 11973

Electrically Conductive Polymer-Concrete Overlays

JACK J. FONTANA and RONALD P. WEBSTER

ABSTRACT

The use of cathodic protection to prevent the corrosion of reinforcing steel in concrete structures has been well established. Application of a durable, skid-resistant electrically conductive polymer-concrete overlay would advance the use of cathodic protection in highway engineering. Laboratory studies indicate that electically conductive polymer-concrete overlays with conductive fillers, such as calcined coke breeze, in conjunction with polyester or vinyl ester resins have resistivities of 1 to 10 ohm-cm. Both multiple-layer and premixed mortar-type overlays have been made. Shear bond strengths of the conductive overlays to concrete substrates vary from 600 to 1,300 psi; the bond strengths of the premixed overlays are 50 to 100 percent higher than those of the multiple-layer overlays.

Of major concern to highway structural and maintenance engineers is the rapid deterioration of concrete bridge decks and structural members such as beams, girders, columns, and piers. Although several factors contribute to the deterioration of concrete, the primary cause is corrosion of the reinforcing steel. The heavy winter use of deicing salts releases critical quantities of chloride ions that penetrate to the reinforcing-steel level and, in the presence of moisture and oxygen, initiate the corrosion process. The corrosion products increase the volume of the reinforcing steel, thereby creating tensile stresses in the surrounding concrete. When these stresses exceed the tensile strength of the concrete, it cracks and eventually spalls or delaminates.

The repair of spalls and delaminations in concrete is a common practice in highway engineering. At times all the delaminated or deteriorated concrete to the level of the reinforcing steel is removed and replaced in an effort to extend the service life of a bridge deck. In addition, the repaired decks are covered by low-slump concrete, latex-modified concrete, or polymer-concrete (PC) overlays to prevent further intrusion of chloride or moisture into the concrete. However, neither extensive patching nor overlaying of chloride-contaminated concrete has been successful in stopping the corrosion process. The only methods available to date are the removal and replacement of all chloride-contaminated concrete or the use of cathodic protection (CP). Although the removal of chloride-contaminated concrete is technically feasible, it is often prohibitively expensive. Cathodic protection, however, is not only reliable but is considered to be economically feasible.

The use of cathodic protection to prevent the corrosion of reinforcing steel in chloride-contaminated concrete bridge decks has been well documented in the literature (1-4). In the early CP systems developed for bridge deck applications, an electrically conductive asphaltic-concrete overlay was used that performed well but required significant changes in elevations and increases in dead load (5). The Office of Research of FHWA has conducted its own research program and sponsored others to improve the highway engineer's understanding of CP systems (6-8). In addition, FHWA has applied for a patent for an electrically conductive PC mortar and overlay system (9). On the basis of this work, CP systems have been installed on 11 bridges throughout the United States by utilizing electrically conductive PC mortar in slots cut into the bridge deck surface. Approximately 1 linear foot of slot is required for every square foot of the bridge deck surface. This type of installation is tedious and costly; thus FHWA sponsored research at Brookhaven National Laboratory (BNL) to further develop an electrically conductive PC overlay that would simplify the installation of CP systems on concrete bridge decks (10).

Considerable research has been done at BNL to develop a thin sand-filled resin overlay system for use on concrete bridge decks (11-13). The overlay, consisting of three to four layers of resin and aggregate, is impermeable to water and chlorides and is considered to provide a good skid-resistant surface. This type of overlay can be made electrically conductive by replacing the silica sand in the first two or three layers with an electrically conductive filler.

LABORATORY EVALUATIONS

Test Procedures to Measure Properties of Electrically Conductive Composites

The test methods used to evaluate the electrical, physical, and mechanical properties of the overlay systems are described in the following sections.

Electrical Resistivity Test

Electrical resistivity values were determined by means of one of two methods: resistivity constant and the test circuit. In the preferred, test-circuit method, a known resistance is connected in series with the conductive composite to be measured and a current is passed through the circuit. The voltage drop across the unknown composite is compared with the voltage drop across the known resistance:

$$R_C = V_C R_k / V_k \quad (1)$$

Thus, the resistivity of the composite is

$$\rho_C = V_C R_k A_C / V_k L \quad (2)$$

where

ρ_c = resistivity of the composite,
V_c = voltage drop across the composite,
R_k = resistance of known resistor,
A_c = cross-sectional area of the composite,
v_k = voltage drop across the known resistor, and
L = length of the conductor across which the V_c is measured.

A diagram of the test specimens and test circuitry is shown in Figure 1.

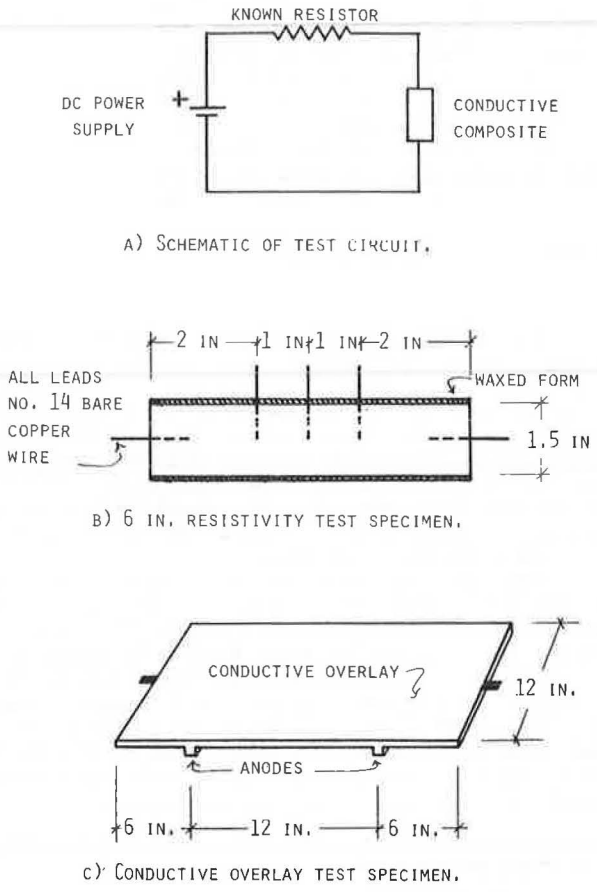

FIGURE 1 Resistivity test specimens and test circuit.

Shear Bond Strength Tests

Shear bond strengths were measured on 3-in.-diameter cores taken from overlaid portland cement concrete slabs. The bond strength is measured in direct shear by using a fixture as shown in Figure 2.

Freeze-Thaw Durability Tests

The freeze-thaw durability characteristics of electrically conductive PC overlays were evaluated according to ASTM C666 (Resistance of Concrete to Rapid Freezing and Thawing), Procedure A, and ASTM C672 (Scaling Resistance of Concrete Surfaces Exposed to Deicing Chemicals). The samples used for ASTM C666 were 3-in.-diameter cores taken from overlaid slabs, whereas the samples used for ASTM C672 were 9.5 x 8.5 x 3.625-in.-thick overlaid concrete slabs. Evaluations of the overlays in both cases were based on visual examinations and shear bond strengths.

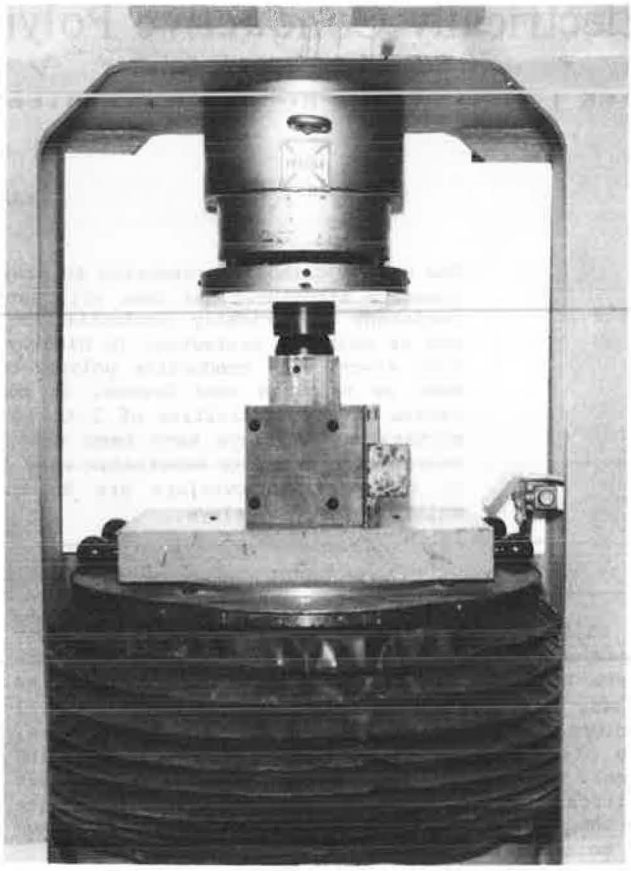

FIGURE 2 BNL shear bond strength test.

Thermal Coefficient of Expansion

The thermal coefficient of expansion was measured with a Dupont 990 Thermal Analyzer and a 943 Thermalmechanical Analyzer.

Evaluation of Electrically Conductive Composites

Conductive Fillers

The electrical conductivity of PC composites was evaluated by using all the commercially available conductive fillers and resins listed in Tables 1 and 2.

One resin, LB183-13, an orthophthalic polyester, was used to make premixed mortars with all 16 fillers. The mix proportions of filler to resin were varied for each system to obtain a smooth, workable mix in each case. The electrical resistivity of all the samples was measured and the data are summarized in Table 3.

The Shamokin coke breeze, the Asbury calcined coke breeze, and the Loresco calcined coke breeze all produced composites with electrical resistivity values of <5 ohm-cm. The calcined coke breeze composites had electrical resistivity values of 0.59 to 1.01 ohm-cm. Although the Magnamite graphite fibers also produce a conductive composite, the fibers would be considered as an additive to the coke breeze systems rather than as a filler.

Because the Loresco SWK coke breeze has a particle-size distribution of +1/4 to +No. 200, it was considered impractical for built-up or thin premixed

TABLE 1 Summary of Resins Evaluated

Resin	Manufacturer	Description	Viscosity cP (centipoise at 24° C)	Initiator/Promoter (% at 24° C)
Orthophthalic polyesters				
LB183-13	U.S.S. Chemical Company	Low-viscosity, highly resilient general-purpose resin	100-150	1.2 MEKP/0.5 CoN
MR11044	U.S.S. Chemical Company	Semiflexible casting resin	140-200	1.2 MEKP/0.5 CoN
LB802-6	U.S.S. Chemical Company	Flexible resin formulated for use as a protective coating on roads	110-135	2.0 BPO/prepromoted by supplier
MR15031-I	U.S.S. Chemical Company	Low-viscosity general-purpose resin	255	1.2 MEKP/0.5 CoN
Polylite 90-570	Reichhold Chemical Company	Low-viscosity general-purpose resin	160	1.2 MEKP/0.5 CoN
Hetron 197A	Ashland Chemical Company	Low-vicosity thixotropic resin with good resistance to acids and chlorine gas	500	1.2 MEKP/prepromoted by supplier
Isophthalic polyesters				
Polylite 98-507	Reichhold Chemical Company	Low-viscosity flexible resin	140	1.2 MEKP/prepromoted by supplier
Aropol 7532	Ashland Chemical Company	Resilient low-viscosity chemical resistant resin	450-600	1.2 MEKP/0.5 CoN
Dural 370	Dural International Corporation	Flexible low-viscosity resin	120	1.2 MEKP/0.5 CoN
Quick Deck	ODI, Inc.	Specially modified resin for bridge deck wearing surfaces	700-1,000	1.2 MEKP/prepromoted by supplier
Vinyl esters				
Epocryl DPV-701	Shell Chemical Company	Highly resilient low-viscosity resin with good chemical resistance	80-140	2.4 MEKP/0.4 CoN, 0.1 DMA
Derakane 411-C50	Dow Chemical Company	Low-viscosity casting resin with good corrosion resistance	80-160	1.8 MEKP/0.4 CoN, 0.1 DMA
Derakane XD-8084-05	Dow Chemical Company	Experimental resin with good corrosion and impact resistance	460	1.0 MEKP/0.2 CoN, 0.05 DMA
Epoxies				
Duralith	Dural International Corporation	Low-temperature high-modulus high-strength epoxy	500-1,000	2 parts base/1 part hardener
Flexolith	Dural International Corporation	Low-temperature low-modulus high-early-strength epoxy	700-1,000	2 parts base/1 part hardener
Duralcast Conductive	Dural International Corporation	Conductive epoxy binder of thin-set terrazzo floors	>1,000	4 parts base/1 part hardener
Others				
60% MMA, -35% PMMA, -5% TMPTMA	Blended at BNL	Low-viscosity methyl methacrylate-based system	225	4.7 BPO/1.0 DMA, 0.05 DMT
55.5% Sty, -4.5% PSty, -40% TMPTMA	Blended at BNL	Low-viscosity styrene-based system	10-15	2.5 BPO, 0.5 AIBN/ 1.0 DMA (oven cured at 90° C)

Note: MEKP = methyl ethyl ketone peroxide, CoN = cobalt naphthenate, BPO = benzoyl peroxide, DMA = dimethyl aniline, DMT = dimethyl-p-toluidine, AIBN = azobis (isobutyronitrile), MMA = methyl methacrylate, PMMA = poly(methyl methacrylate), TMPTMA = trimethylolpropane trimethacrylate, Sty = styrene, Psty = polystyrene.

TABLE 2 Summary of Conductive Fillers Evaluated

Filler	Manufacturer
Carbon blacks	
Statex 160	Cities Service Company
Statex M 568	Cities Service Company
Statex MT	Cities Service Company
Conductex SC	Cities Service Company
Ketjenblack EC	Armack Company
Coke breeze	
Shamokin coke breeze	Shamokin Filler Company
Calcined coke breeze	
Asbury 4335	Asbury Graphite Mills
Loresco DW1	Cathodic Engineering Equipment
Loresco DW2	Cathodic Engineering Equipment
Loresco SWK	Cathodic Engineering Equipment
Acetylene black	
Shawinigan acetylene black	Shawinigan Products
Gulf acetylene black-50	Gulf Oil Chemicals Company
Fibers	
Magnamite graphite fibers, Type AS, 1/4 in. and 0.44 in. long	Hercules, Inc.
Others	
Austin Black 325 bituminous fine black	Slab Fork Coal Company
Silicon carbide grit, 150RA	Union Carbide
Graphite powder (grade 38)	Fischer Scientific

TABLE 3 Resistivity Test Results for Various Filler Systems

Filler	Mix Proportions (wt%) Resin[a]	Filler	Resistivity (ohm-cm)
Carbon blacks			
Statex 160	76	24	18,500
Statex M 568	72	28	3,360
Statex MT	55	45	>20,000,000
Conductex SC	85	15	1,480
Ketjenblack EC	95	5	2,970
Coke breeze			
Shamokin	33	67	3.02
Calcined coke breeze			
Asbury 4335	26	74	0.85
Loresco DW1	30	70	0.99
Loresco DW2	30	70	1.01
Loresco SWK	30	70	0.59
Acetylene black			
Shawinigan	88	12	310
Gulf-50 compression	95	5	2,500
Fibers			
Magnamite graphite fibers, type AS, 1/4 in.	94	6	2.48
Others			
Austin Black 325, bituminous fine black	55	45	>20,000,000
Silicon carbide grit, 150RA	31	69	>20,000,000
Graphite powder (grade 38)	63	37	1,510

[a] LB183-13 polyester with 1.2 wt% MEKP initiator and 0.5 wt% CoN promoter.

TABLE 4 Resistivity Test Results for Various Resin Systems

Resin	Mix Proportions (wt%) Resin	Filler[a]	Resistivity[b] (ohm-cm)
Orthophthalic polyesters			
LB183-13	30	70	0.87
MR11044	30	70	0.97
LB802-6	30	70	9.26
MR15031-I	30	70	0.87
Polylite 90-570	30	70	0.70
Hetron 197A	30	70	2.14
Isophthalic polyesters			
Polylite 98-507	30	70	1.37
Aropol 7532	30	70	2.02
Dural 370	30	70	0.79
Quick Deck	37	63	2.00
Vinyl esters			
Epocryl DPV-701	30	70	1.20
Derakane 411-C50	30	70	1.12
Derakane XD-8084-05	30	70	1.14
Epoxies			
Duralith	30	70	30.62[c]
Flexolith	30	70	50.78[c]
Duralcast Conductive	27	73	14.34[c]
Others			
MMA-based system[d]	30	70	65.71[c]
Styrene-based system[d]	30	70	–[e]

[a] Asbury 4335 calcined coke breeze.
[b] Resistivity measured by using test circuit method unless otherwise noted.
[c] Resistivity = resistance (ohms) x 2.1 cm (resistivity constant).
[d] Refer to Table 1 for monomer formulation.
[e] Too high to be measured with available test equipment.

overlays and was eliminated from further consideration in this program. The Loresco DW2 was basically the same as the DW1 except that it was designed for pumping applications, so it also was eliminated. Therefore, it was decided to evaluate the Asbury 4335 and the Loresco DW1 calcined coke breezes as the primary electrically conductive fillers.

Resin Systems

A total of 18 resins, described in Table 1, were used in conjunction with Asbury 4335 calcined coke breeze to make electrically conductive composites. A mix proportion of 30 percent by weight of resin and 70 percent by weight of filler was used wherever possible to make the conductive composites. The test results are summarized in Table 4.

The electrical resistivity values varied from 0.70 to 65.71 ohm-cm, with 12 of the 18 systems exhibiting resistivity values of <5 ohm-cm. The Polylite 90-570 orthophthalic polyester resin had the lowest resistivity at 0.70 ohm-cm. In general, all the polyesters and vinyl esters that were tested, with the exception of LB802-6, can be used to make electrically conductive polymer concrete with a resistivity of <5 ohm-cm.

Evaluation of Multiple-Layer Conductive Overlay Systems

Determination of Layers Required for Conductive Overlays

Resistivity tests were performed to determine the optimum number of layers of conductive filler required to make an electrically conductive overlay. Two resins were used in this study: LB183-13 polyester and the DPV-701 vinyl ester. Each overlay consisted of five applications of Asbury 4335 calcined coke breeze and resin; the resistivity was measured after the placement of each successive layer. The overlays were allowed to cure for a minimum of 4 hr before the resistivity was measured. The results are graphically presented in Figure 3. The test results indicate that the resistivity values of the overlay made with LB183-13 are fairly constant beyond two layers of conductive filler. The vinyl ester DPV-701, on the other hand, is slightly more variable and it appears that at least three layers are necessary for adequate performance as a conductive overlay.

Evaluation of Multiple-Layer Conductive Overlays by Using Asbury 4335 or Loresco DW1 Calcined Coke Breeze

In the initial studies, conductive PC mortars made with Asbury 4335 or Loresco DW1 calcined coke breeze had essentially the same resistivity values. Studies were made with both fillers in multiple-layer overlays. The overlays were made by using the LB183-13 polyester and the DPV-701 vinyl ester. The results, as shown in Figure 4, indicate that the resistivities of overlays made with the Asbury 4335 calcined coke breeze are slightly lower than those made with the Loresco DW1 calcined coke breeze. Therefore, the rest of the work in this program was done with the Asbury 4335 calcined coke breeze.

Electrical Resistivity Values of Several Multiple-Layer Overlay Systems

The original resistivity tests were made on premixed mortars by using various resins. Evaluations of similar systems were made on multiple-layer overlays. In general, each overlay consisted of three layers of Asbury 4335 calcined coke breeze and two layers of No. 2 silica sand to provide a skid-resistant surface for the overlay. Resistivity values were obtained after each layer had cured for a minimum of 4 hr. The test results are summarized in Table 5. The resistivities of five of these systems varied from 0.86 to 2.81 ohm-cm: LB183-13, MR11044, Polylite

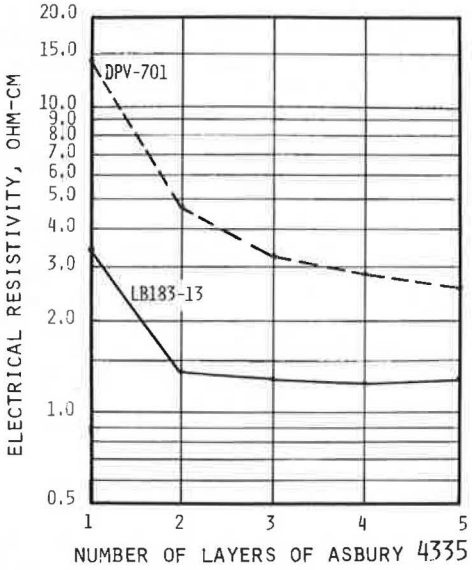

FIGURE 3 Variation of electrical resistivity with number of layers of Asbury 4335 calcined coke breeze.

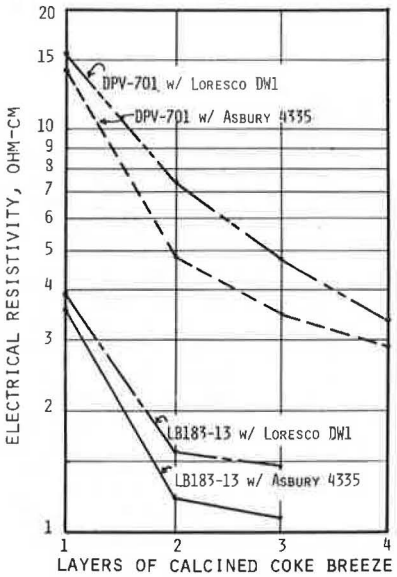

FIGURE 4 Electrical resistivity values of overlays made with Asbury 4335 and Loresco DW1 calcined coke breeze.

TABLE 5 Resistivity Test Results for Various Built-Up Systems

Resin	Electrical Resistivity (ohm-cm) by Layer[a]				
	1	2	3	4	5
Orthophthalic polyesters					
LB183-13	3.62	1.22	1.01	1.32	1.26
MR11044	1.33	1.16	0.94	1.02	1.01
Polylite 90-570	2.17	1.32	1.23	1.49	1.46
Isophthalic polyesters					
Polylite 98-507	11.13	6.86	6.46	21.03	27.27
Aropol 7532	1.53	0.88	0.89	0.88	0.86
Dural 370	21.08	3.97	6.98	25.54	66.69
Vinyl esters					
Epocryl DPV-701	14.15	4.69	3.25	2.93	2.81
Derakane XD-8084-05	18.86	22.64	5.53	8.21	7.58

[a] First three layers were placed by using Asbury 4335 calcined coke breeze. The fourth and fifth layers were placed by using No. 2 silica sand.

90-570, and Aropol 7532 polyesters and the DPV-701 vinyl ester. The resistivity of the Derakane XD-8084-05 vinyl ester was 7.58 ohm-cm, and those of the Polylite 98-507 and Dural 370 vinyl esters were 27.27 and 66.99 ohm-cm, respectively. Both the Polylite 98-507 and the Dural 370 polyesters are difficult to fully cure in thin layers, which is probably why their resistivities were so high.

Evaluation of Premixed Electrically Conductive Mortars

Resistivity Versus Resin Content

Electrically conductive PC mortars were made with Asbury 4335 calcined coke breeze and LB183-13 polyester resin. The resin content was varied from 75 to 25 percent by weight for the total mix. The results presented in Table 6 indicate that resin contents of 25 to 40 percent by weight all produce conductive composites with resistivities of <5 ohm-cm. The recommended mix is 30 percent by weight of resin and 70 percent by weight of filler; these proportions produce a workable mixture that does not show any excess resin upon curing.

TABLE 6 Variation of Electrical Resistivity with Resin Content

Mix Proportions (wt%)		
Resin[a]	Filler[b]	Resistivity (ohm-cm)
100	0	>19,000,000
75	25	>19,000,000
60	40	>19,000,000
55	45	47.31
50	50	8.17
40	60	1.34
35	65	1.17
32	68	0.83
30	70	0.80
28	72	0.54
25	75	0.89

[a] LB183-13 polyester.
[b] Asbury 4335 calcined coke breeze.

Resistivity of Mixed Filler Systems

Although calcined coke breeze filler composites have excellent electrical resistivity properties, their physical properties are poor. To improve their physical properties without destroying their electrical properties, studies were made on mixed filler systems. Silica sand was used to replace a portion of the calcined coke breeze and these composites were tested for both compressive strength and electrical resistivity. The test results of the blended filler systems are summarized in Table 7 and in Figure 5.

Test results indicate that the higher the coke breeze content, the lower the electrical resistivity. Coke breeze contents of >40 percent by weight are required to obtain resistivity values of <5 ohm-cm. Compressive strengths of ~4,300 psi were measured for coke breeze contents up to 60 percent, whereas compressive strengths for composites containing more than 60 percent coke breeze average only 3,500 psi.

On the basis of these results, a filler system containing 50 percent by weight of Asbury 4335 calcined coke breeze and 50 percent by weight of blended silica sand was selected for further evaluation as a conductive overlay.

TABLE 7 Electrical Resistivity Test Results for Composites Made with Blended Filler Systems

Filler Content (wt%)		
Sand	Coke Breeze[a]	Resistivity (ohm-cm)
100	0	>19,000,000
90	10	>19,000,000
80	20	>19,000,000
75	25	186.54
70	30	23.78
60	40	6.81
52	48	3.32
50	50	2.39
40	60	1.90
30	70	1.40
20	80	1.05
0	100	0.80

Note: Composite consists of 30 wt% LB183-13 polyester and 70 wt% blended filler.

[a]Asbury 4335 calcined coke breeze.

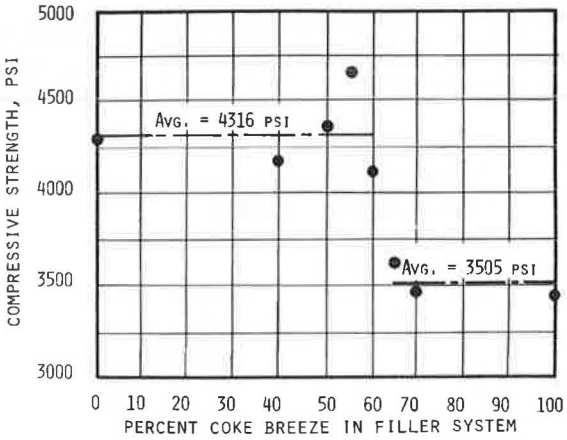

FIGURE 5 Compressive strengths of premixed mortars.

Evaluation of Electrical Resistivity of Premixed Mortars with Various Resins

Tests were done to evaluate the electrical resistivity of premixed mortar systems made with various resins. The mortar generally contained 20 percent by weight of resin and 80 percent by weight of blended filler. The blended filler used consisted of 50 percent by weight of Asbury 4335 calcined coke breeze and 50 percent by weight of blended silica sand. The test results are summarized in Table 8.

TABLE 8 Electrical Resistivity Values of Premixed Conductive Mortars

Resin	Resin Content (wt%)	Electrical Resistivity (ohm-cm)
Orthophthalic polyesters		
LB183-13	20	4.7
MR11044	20	4.0
Polylite 90-570	20	4.4
Isophthalic polyesters		
Polylite 98-507	20	3.4
Aropol 7532	30	2.0
Dural 370	20	3.7
Vinyl esters		
DPV-701	20	10.5
XD-8084-05	22	4.2

Note: Filler consisted of 50 wt% Asbury 4335 calcined coke breeze, 50 wt% blended silica sand, 2.0 wt% TiO_2 colorant.

The resistivities of the mortars varied between 2.0 and 10.5 ohm-cm, with the Aropol 7532 polyester composite exhibiting the lowest resistivity and the DPV-701 vinyl ester composite exhibiting the highest.

Evaluation of Electrical and Mechanical Properties of Multiple-Layer and Premixed Overlays

A series of tests was made to evaluate multiple-layer and premixed electrically conductive PC overlays with six different resin systems. Properties that were measured include electrical resistivity, shear bond strength, freeze-thaw durability, flexural modulus of elasticity, thermal coefficient of expansion, and the compressive strength of the premixed mortars. The test results are presented in Tables 9-11.

Electrical Resistivity

The electrical resistivities of the multiple-layer overlays varied from 2.3 to 66.7 ohm-cm; the LB183-13 resin was the lowest and the Dural 370 resin was the highest.

The electrical resistivities of the premixed overlays varied between 3.4 and 10.5 ohm-cm. The DPV-701 vinyl ester had the highest resistivity, and the Polylite 98-507 isophthalic polyester had the lowest.

Shear Bond Strength

The shear bond strength of overlays measured at the interface of the concrete substrate and the overlay should be higher than the shear strength of the base concrete (400 to 500 psi) if the overlay is to perform satisfactorily.

The shear bond strengths for the multiple-layer overlays varied between 392 and 691 psi, whereas the bond strengths of the premixed overlays varied from 928 to 1,370 psi. The bond strengths exhibited by the premixed overlays were all 50 to 100 percent higher than those of the multiple-layer overlays. This is because the coke breeze filler in the multiple-layer overlays is physically much weaker than the blended filler system used in the premixed overlay. Also, the filler in the premixed system "wets out" better and is more uniformly distributed; thus it attains better bonding characteristics.

Freeze-Thaw Durability

Freeze-thaw durability was evaluated according to ASTM C666 and ASTM C672. Generally, the rapid freeze-thaw cycling of ASTM C666 will show greater bond strength reductions than the slow cycling of ASTM C672.

The multiple-layer overlays made with Polylite 98-507 and the Dural 370 polyesters and the XD-8084-05 vinyl ester exhibited the best durability characteristics. Of the premixed overlays, the XD-8084-05 vinyl ester also exhibited the best durability characteristics.

Flexural Modulus of Elasticity

With one exception, the flexural modulus of elasticity of the multiple-layer overlays was lower than that of the premixed overlays. The modulus varied from 112,000 psi for the Dural 370 polyester to 1,442 psi for the XD-8084-05 vinyl ester in the multiple-layer overlays. In the premixed overlays,

the Polylite 98-507 polyester had the lowest modulus, 243,000 psi, which compares with a high of 734,000 psi for the DPV-701 vinyl ester.

In general, lower-modulus overlays have had a better history of not disbonding from concrete bridge decks owing to their ability to flex with the deck itself under moving traffic loads.

Thermal Coefficient of Expansion

The coefficient of expansion of portland cement concrete varies from 5.0 to 6.0 x 10^{-6} in./(in.)($°F^{-1}$). The coefficient of expansion of the electrically conductive PC overlays studied varies from 11.3 to 22.4 x 10^{-6} in./(in.)($°F^{-1}$). The multi-

TABLE 9 Properties of Built-Up and Premixed Electrically Conductive Overlays: Orthophthalic Resins

	LB183-13		Polylite 90-570	
Property	Built Up	Premixed	Built Up	Premixed
Electrical resistivity (ohm-cm)	2.3	4.7	3.3	4.4
Shear bond strength (psi)	598	1,724	691	1,370
Freeze-thaw durability bond strength (psi)				
After 100 rapid cycles	411	–	–	–
After 200 rapid cycles	464	–	–	–
After 25 slow cycles	–	–	–	–
After 50 slow cycles	433	–	495	–
Flexural modulus of elasticity (psi)	437,700	702,800	447,200	628,800
Thermal coefficient of expansion [in./(in.)($°F^{-1}$)]	19.4 x 10^{-6}	13.3 x 10^{-6}	17.0 x 10^{-6}	14.8 x 10^{-6}
Compressive strength (psi)				
Initial	–	7,917	–	6,783
After 100 rapid cycles freeze-thaw		8,132		7,013

Note: Built-up overlays consist of two to three layers of Asbury 4335 calcined coke breeze and two to three layers of sand. The premixed overlays, with two exceptions, consisted of 20 wt% resin and 80 wt% blended filler. Aropol 7532 overlays consisted of 30 wt% resin and 70 wt% blended filler and the XD-8084 overlays consisted of 22 wt% resin and 78 wt% blended filler. All values presented in this table are averages for all the data collected for each overlay system throughout the program and, as a result, may vary with data reported for specific tests.

TABLE 10 Properties of Built-Up and Premixed Electrically Conductive Overlays: Vinyl Ester Resins

	Epocryl DPV-701		Derakane XD-8084-05	
Property	Built Up	Premixed	Built Up	Premixed
Electrical resistivity (ohm-cm)	7.8	10.5	7.6	4.2
Shear bond strength (psi)	677	945	680	1,016
Freeze-thaw durability bond strength (psi)				
After 100 rapid cycles	553	–	–	–
After 200 rapid cycles	607	–	–	–
After 25 slow cycles	–	–	581	1,066
After 50 slow cycles	577	–	667	1,247
Flexural modulus of elasticity (psi)	267,000	734,200	1,442,000	632,000
Thermal coefficient of expansion [in./(in.)($°F^{-1}$)]	14.8 x 10^{-6}	12.2 x 10^{-6}	11.3 x 10^{-6}	15.6 x 10^{-6}
Compressive strength (psi)				
Initial	–	6,313	–	6,713
After 100 rapid cycles freeze-thaw		6,544		7,719

Note: Built-up overlays consist of two to three layers of Asbury 4335 calcined coke breeze and two to three layers of sand. The premixed overlays, with two exceptions, consisted of 20 wt% resin and 80 wt% blended filler. Aropol 7532 overlays consisted of 30 wt% resin and 70 wt% blended filler and the XD-8084 overlays consisted of 22 wt% resin and 78 wt% blended filler. All values presented in this table are averages for all the data collected for each overlay system throughout the program and, as a result, may vary with data reported for specific tests.

TABLE 11 Properties of Built-Up and Premixed Electrically Conductive Overlays: isophthalic Resins

	Polylite 98-507		Dural 370	
Property	Built Up	Premixed	Built Up	Premixed
Electrical resistivity (ohm-cm)	27.3	3.4	66.7	3.7
Shear bond strength (psi)	495	980	392	928
Freeze-thaw durability bond strength (psi)				
After 100 rapid cycles	–	–	–	–
After 200 rapid cycles	–	–	–	–
After 25 slow cycles	497	898	407	747
After 50 slow cycles	492	831	432	785
Flexural modulus of elasticity (psi)	199,000	243,000	112,000	393,000
Thermal coefficient of expansion [in./(in.)($°F^{-1}$)]	17.5 x 10^{-6}	15.0 x 10^{-6}	22.4 x 10^{-6}	16.3 x 10^{-6}
Compressive strength (psi)				
Initial	–	4,117	–	4,175
After 100 rapid cycles freeze-thaw		4,438		4,494

Note: Built-up overlays consist of two to three layers of Asbury 4335 calcined coke breeze and two to three layers of sand. The premixed overlays, with two exceptions, consisted of 20 wt% resin and 80 wt% blended filler. Aropol 7532 overlays consisted of 30 wt% resin and 70 wt% blended filler and the XD-8084 overlays consisted of 22 wt% resin and 78 wt% blended filler. All values presented in this table are averages for all the data collected for each overlay system throughout the program and, as a result, may vary with data reported for specific tests.

ple-layer overlays generally had a higher coefficient of expansion than the premixed overlays. This is generally because the resin content of multiple-layer overlays is higher than that in premixed overlays.

Compressive Strength of Premixed Overlays

The compressive strength of the premixed mortars used to make the electrically conductive overlays varied from 6,300 to 7,900 psi. None of the mortars tested showed any reductions of strength after being subjected to 100 freeze-thaw cycles.

Multiple-Layer Conductive Overlays in Active CP Systems

Two multiple-layer overlays were placed on reinforced-concrete slabs 4 ft x 4 ft x 8 in. thick. The slab and overlay configurations are shown in Figure 6. Each slab contained two anode slots and two mats of reinforcing steel, each of which was welded to ensure positive electrical connections.

Multiple-layer overlays with LB183-13 polyester resin and DPV-701 vinyl ester resin with Asbury 4335 calcined coke breeze were placed on the slabs. The mortar mix for the anodes consisted of 24 percent by weight of resin, 38 percent by weight of Asbury 4335 calcined coke breeze, and 38 percent by weight of blended silica sand. The primary anode wire was 0.031-in.-diameter copper-core wire clad with niobium platinum. Copper plate electrodes were incorporated into each overlay to facilitate the measurement of the electrical resistivity of the overlays. Power was supplied to each system by using a constant-current variable-voltage power supply.

The CP systems were operated for 1 year, during which time current density, operating voltage, "instant off" electrical potentials, electrical resistivity, and shear bond strengths were measured periodically to evaluate the performance characteristics of each overlay. The data are summarized in Tables 12 and 13.

The CP systems were initially activated at a current density of 2.9 mA/ft² of concrete surface area or 5.2 mA/ft² of reinforcing-steel surface area. Over the first 6 weeks, the current density was reduced to 2.12 mA/ft² of concrete surface area to keep the shift in rebar potential essentially constant.

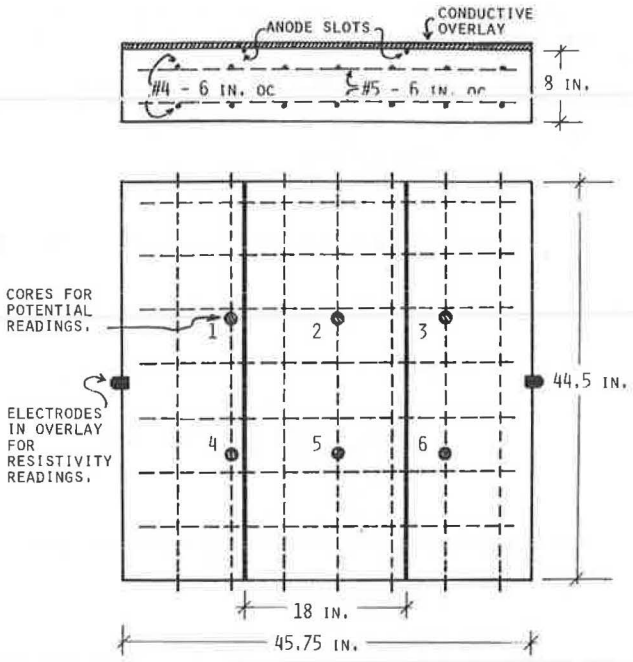

FIGURE 6 Large-scale test slabs.

Cores were taken periodically to measure any change in overlay bond strength. After 1 year of active operation, the bond strengths of both overlays were reduced by 32 percent. Visual examination of the LB183-13 overlay at the end of the year did not reveal any disbondment or deterioration. The overlay made with the DPV-701, however, had delaminations over ~2 percent of its surface area. These delaminations were characterized by a black discoloration at the overlay surface. In addition, coke breeze layers with the delaminated regions appeared to be partially disintegrated.

TABLE 12 Large-Scale Overlay Test: Slab EC356

Total Operating Time	Operating Current (mA)	Operating Voltage (V)	Avg "Instant Off" (V)[a]	Electrical Resistivity (ohm-cm)	Bond Strength (psi)	Ambient Temperature (°F)
0	–	–	-0.142	2.4	523	43
48 hr	40[b]	26.6	-0.545	–	–	53
2 wk	40	17.7	-0.618	–	–	48
3 wk	35[c]	13.9	-0.619	–	–	48
4 wk	35	8.0	-0.609	2.5	–	58
5 wk	30[d]	11.1	-0.605	–	–	49
6 wk	30	9.1	-0.607	2.5	436	53
		CP system shut down for 30 days, then restarted				
7 wk	30	5.6	-0.586	2.1	–	63
8 wk	30	2.8	-0.573	–	–	70
12 wk	30	4.0	-0.594	2.6	–	78
14 wk	30	4.3	-0.593	–	–	75
18 wk	30	3.3	-0.589	3.7	–	85
22 wk	30	3.6	-0.604	–	–	76
6 mo	30	7.5	-0.625	2.8	400	63
9 mo	30	11.2	-0.672	3.2	210	34
1 yr	30	6.5	-0.700	3.8	357	39

Note: Overlay made by using LB183-13 polyester and consisting of two noncompacted layers of Asbury 4335 calcined coke breeze and two noncompacted layers of No. 2 silica sand.

[a] Potentials measured in reference to CSE half-cell.

[b] 40 mA = 2.90 mA/ft² of concrete surface area.

[c] 35 mA = 2.48 mA/ft² of concrete surface area.

[d] 30 mA = 2.12 mA/ft² of concrete surface area.

TABLE 13 Large-Scale Overlay Test: Slab EC357

Total Operating Time	Operating Current (mA)	Operating Voltage (V)	Avg "Instant Off" (V)[a]	Electrical Resistivity (ohm-cm)	Bond Strength (psi)	Ambient Temperature (°F)
0	–	–	-0.124	8.0	583	43
48 hr	40[b]	24.0	-0.541	–	–	53
2 wk	40	16.4	-0.610	–	–	48
3 wk	35[c]	12.2	-0.609	–	–	48
4 wk	35	6.6	-0.628	7.9	–	58
5 wk	30[d]	8.7	-0.616	–	–	49
6 wk	30	7.3	-0.610	7.3	474	53
		CP system shut down for 30 days, then restarted				
7 wk	30	5.0	-0.580	7.4	–	63
8 wk	30	2.6	-0.550	–	–	70
12 wk	30	3.8	-0.596	7.6	–	78
14 wk	30	4.3	-0.593	–	–	75
18 wk	30	3.3	-0.581	6.9	–	85
22 wk	30	3.7	-0.595	–	–	76
6 mo	30	8.2	-0.622	8.2	509	63
9 mo	30	12.0	-0.662	9.3	514	34
1 yr	30	7.0	-0.667	8.9	392	39

Note: Overlay made by using DPV-701 vinyl ester and consisting of three noncompacted layers of Asbury 4335 calcined coke breeze and two noncompacted layers of No. 2 silica sand.

[a]Potentials measured in reference to CSE half-cell.

[b]40 mA = 2.90 mA/ft^2 (31.3 mA/m^2) of concrete surface area.

[c]35 mA = 2.48 mA/ft^2 (26.9 mA/m^2) of concrete surface area.

[d]30 mA = 2.12 mA/ft^2 (22.9 mA/m^2) of concrete surface area.

CONCLUSIONS AND RECOMMENDATIONS

Multiple-layer electrically conductive PC overlays have been made by using conductive fillers. Resistivity of such overlays varies from 1 to 8 ohm-cm depending on the type of resin used and the number of conductive layers applied. Studies of such overlays with an operating CP system indicate that the bond strength of the overlay to the concrete substrate is reduced by 32 percent within 1 year of operation.

On the basis of physical and mechanical properties, three resin systems show the greatest promise for use in multiple-layer overlays. These resins are LB183-13 and Polylite 90-570 polyesters and DPV-701 vinyl ester. The electrical resistivities of these overlays average 2.3 to 7.8 ohm-cm with initial bond strengths of 600 to 700 psi.

The major disadvantage of multiple-layer conductive overlays appears to be the inherent weakness of the calcined coke breeze. In addition, the calcined coke breeze appears to be subject to deterioration due to oxidation from the gases emitted during operation of the CP system.

The premixed electrically conductive PC overlays appear to be more promising at this time. They exhibit bond strengths that are 50 to 100 percent higher than those of multiple-layer overlays. In addition, they appear to have better freeze-thaw durability and more reliable curing characteristics. The filler particles are coated better in premixed systems and therefore should be less subject to deterioration due to off-gassing of the concrete when it is under an operating CP system. Although the electrical resistivities (3 to 10 ohm-cm) of premixed conductive overlays are slightly higher than those of multiple-layer overlays, they are still low enough to operate in CP systems.

The major emphasis of this study was on multiple-layer overlays, and it is believed that additional research work is necessary to obtain such information on premixed overlays as curing shrinkage, placement techniques, skid resistance, and performance under actual traffic conditions.

The two resin systems that would be recommended for premixed overlays are Polylite 90-570 polyester and XD-8084-05 vinyl ester. In addition, both the Polylite 98-507 and Dural 370 isophthalic polyesters should also be considered for premixed conductive overlay systems.

ACKNOWLEDGMENT

This work was performed under the auspices of the U.S. Department of Energy.

REFERENCES

1. R.C. Robinson. Cathodic Protection of Steel in Concrete. ACI Special Publ. 49-7. American Concrete Institute, Detroit, Mich., 1973, pp. 83-93.
2. D.A. Hausmann. Cathodic Protection of Steel in Concrete. In Proc., 24th Conference of the National Association of Corrosion Engineers, March 18-22, 1968, NACE, Houston, Tex., 1969, pp. 310-313.
3. J.B. Lankes. Cathodic Protection of Reinforcing Bars. American Concrete Institute Journal, April 1976, pp. 191-192.
4. J.B. Vrable. Cathodic Protection for Reinforcing Steel in Concrete. In Chloride Corrosion of Steel in Concrete. ASTM Special Technical Publ. 629, ASTM, Philadelphia, Pa., 1977, pp. 124-149.
5. H.J. Fromm. Electrically Conductive Asphalt Mixes for the Cathodic Protection of Concrete Bridge Decks. Proc., Association of Asphalt Paving Technologists, Vol. 45, 1976, pp. 382-399.
6. K.C. Clear. FCP Annual Progress Report--Year Ending September 30, 1981, Project No. 4K: Cost-Effective Rigid Concrete Construction and Rehabilitation in Adverse Environments. FHWA, U.S. Department of Transportation, 1981.
7. Y.P. Virmani. FCP Annual Progress Report--Year Ending September 30, 1982, Project No. 4K: Cost-Effective Rigid Concrete Construction and Rehabilitation in Adverse Environments. FHWA, U.S. Department of Transportation, 1982.
8. Y.P. Virmani. FCP Annual Progress Report--Year Ending September 30, 1983, Project No. 5Q: Corrosion Protection and Bridge Maintenance.

FHWA, U.S. Department of Transportation, 1983.
9. K.C. Clear, Y.P. Virmani, and J. Bartholomew. Cathodic Protection Using Conductive Polymer Concrete. Patent Applications DOT H-10013. Feb. 1982.
10. R.P. Webster, J.J. Fontana, and W. Reams. Electrically Conductive Polymer Concrete Overlays. Final Report BNL 35036. Brookhaven National Laboratory, Upton, N.Y., May 1984.
11. J.J. Fontana and R.P. Webster. Thin Sand-Filled Resin Overlays. BNL 24079-R. Brookhaven National Laboratory, Upton, N.Y., 1978.
12. R. Webster, J.J. Fontana, and L.E. Kukacka. Thin Polymer Concrete Overlays Interim User's Manual Method B. Report FHWA-TS-78-225. FHWA, U.S. Department of Transportation, Feb. 1978.
13. J.J. Fontana and J. Bartholomew. Use of Concrete Polymer Materials in the Transportation Industry. ACI Publication SP-69. American Concrete Institute, Detroit, Mich., 1981.

Publication of this paper sponsored by Committee on Corrosion.

Bridge Deck Rehabilitation by Using Cathodic Protection with a Low-Slump Concrete Overlay

ANDREW D. HALVERSON and GLENN R. KORFHAGE

ABSTRACT

The design and construction of a state-of-the-art cathodic protection system for a reinforced-concrete bridge deck by the Minnesota Department of Transportation is described. The bridge selected was the 42nd Street Bridge (Bridge 9616) over I-35W in South Minneapolis. The system selected was a distributed-anode system with a low-slump concrete overlay as a wearing surface. The system was constructed in the summer of 1983. The cathodic protection system has primary and secondary anodes for current distribution. A primary anode system of platinized niobium wire placed transversely across the bridge feeds a secondary anode system of carbon strands placed longitudinally on the bridge. Both the wire and the strands are covered with conductive polymer concrete. Power from a rectifier is supplied to the anodes through a conduit running along the north crash rail of the bridge. Rehabilitation of the bridge was completed in 30 working days, and the system was activated in December 1983.

In 1982 the Minnesota Department of Transportation decided to pursue the design and construction of a state-of-the-art cathodic protection system for a bridge deck rehabilitation. This project was to be undertaken with the participation of the Demonstration Projects Division of FHWA as part of Demonstration Project 34, Cathodic Protection.

Minnesota had previously placed an early design of cathodic protection. This system was placed in 1975 on the Duluth Street Bridge on Trunk Highway (T.H.) 100 (Bridge 27002) in Golden Valley. This system utilized a conductive coke breeze layer stabilized with asphalt and containing the cathodic protection hardware covered by an asphalt overlay as a wearing surface (Figure 1). Because of the instability of the conductive coke layer, the asphalt wearing surface showed distress and was reconstructed in 1981 by cold milling off 1 in. of the original overlay and replacing that with 2 in. of new material. By 1983 the wearing surface once again exhibited surface distress. Although the cathodic protection system had functioned satisfactorily, it was believed that an updated design might provide a more stable wearing surface.

After an investigation of bridges slated for rehabilitation, it was decided to contract for the design and construction of a cathodic protection system on the 42nd Street Bridge over I-35W in South Minneapolis. The designer selected was Kenneth Clear of Kenneth C. Clear, Incorporated. The rehabilitation contract was awarded to the low bidder, Arcon Construction Company of Mora, Minnesota. Egan McKay Electric of Minneapolis was the subcontractor.

It was decided to use a distributed-anode cathodic protection system on the bridge with a low-slump concrete overlay for the wearing surface.

BACKGROUND

The 42nd Street Bridge (Bridge 9616) over I-35W in South Minneapolis was constructed in 1964. The bridge is a precast concrete beam span made up of four spans

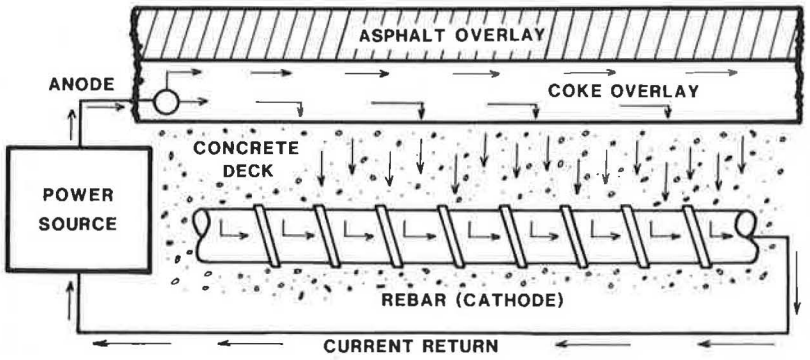

FIGURE 1 Trunk Highway 100 cathodic protection system.

(Figure 2). The two end spans are 25 ft on the west end and 31 ft on the east end. The two center spans are each 71 ft 6 in. long for a total length of 199 ft. The width of the roadway across the bridge is 52 ft, and there are 5-ft wide sidewalks on both sides. The roadway surface area is 10,348 ft^2 and the total sidewalk area is 1,990 ft^2, giving a total area of 12,338 ft^2 to be cathodically protected.

A September 1981 inspection of the 42nd Street Bridge revealed 5 percent delamination of the surface area of the roadway. The inspection also revealed that there were spalled areas on the caps at Piers 1 and 3 because of leaking of the expansion joints. The columns on the west pier (Pier 1) were in poor condition, and the ends on about 10 out of 24 of the precast girders (six each span) had also deteriorated because of the leaking expansion joints.

In July 1982 the Office of Research and Development did some additional testing of the 42nd Street Bridge. Delamination detection was done using a Delamtect. This supported the 1981 bridge inspection. Testing with a pachometer revealed that the concrete cover over the reinforcing steel was 1 in. to 2 3/4 in. The average depth of cover was 1 3/4 in. Drill dust samples were taken to determine the chloride in the bridge deck. Although there was a great deal of variation among the samples, average values were as follows: from 0 to 1/2 in., 4,300 parts per million (ppm); from 1/2 to 1 in., 1,900 ppm; from 1 to 1 1/2 in., 900 ppm; and from 1 1/2 to 2 in., 400 ppm.

A copper-copper sulfate half-cell was used to take potential readings on the bridge deck. This indicated that there was active corrosion at the bridge ends and at the expansion joints. There was also some active corrosion in the middle of the bridge deck.

With this information in hand, the design of the cathodic protection system of the 42nd Street Bridge began.

EXPERIMENTAL WORK

Design

The cathodic protection system for the 42nd Street Bridge is a distributed-anode cathodic protection system with a low-slump concrete overlay. Power is supplied to each of the four zones or spans of the bridge by a transverse primary anode system (Figure 3). The primary anode wire is 0.031 in. in diameter. It has a copper core with 35 percent of the cross-sectional area being niobium and a 25-μ-in. coating of platinum.

The anode is further distributed by placing longitudinal carbon strand conductors electrically continuous with the primary anodes. The carbon conductors are composed of 5 strands with 4,000 filaments per strand. These are then wrapped with Dacron to make the material fieldworthy. The carbon strands

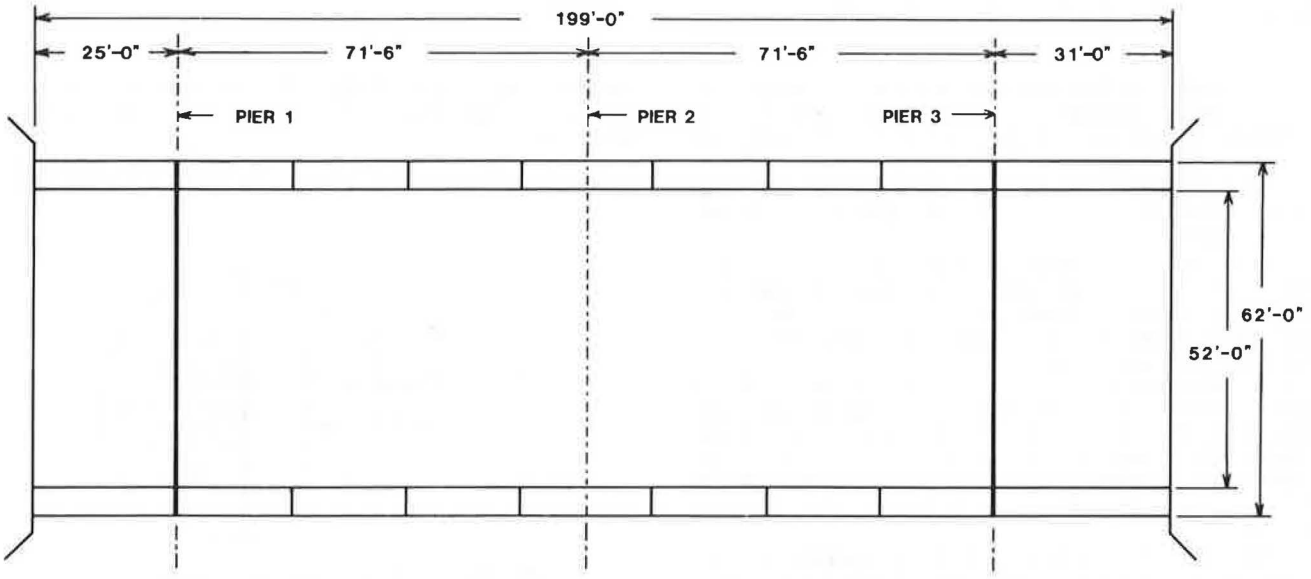

FIGURE 2 42nd Street Bridge over I-35W.

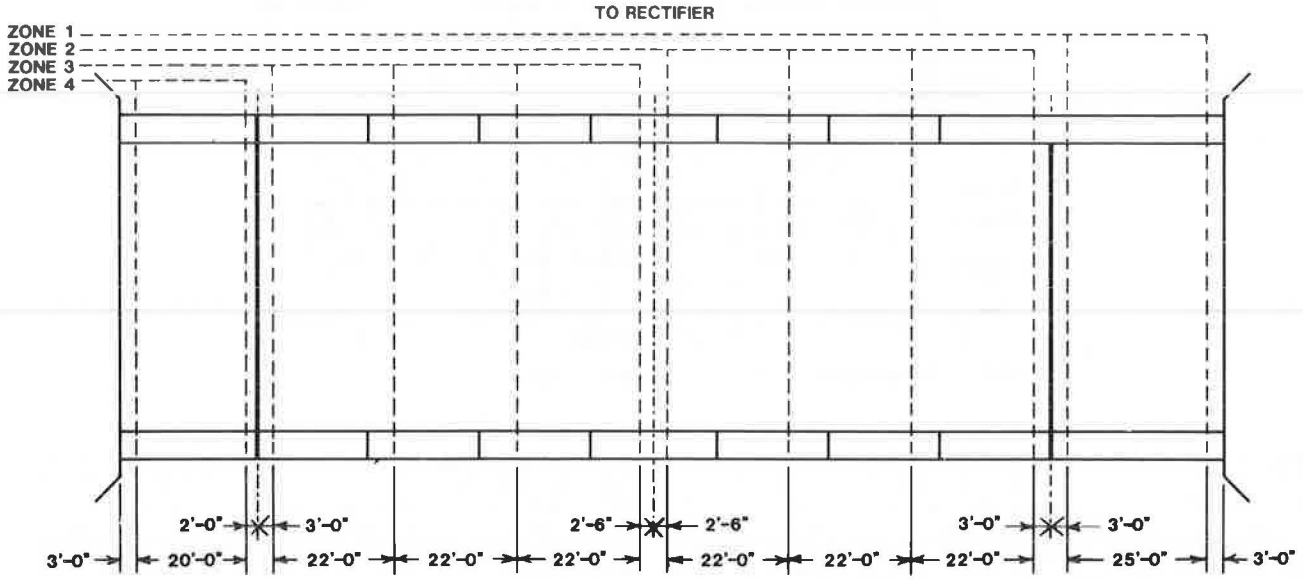

FIGURE 3 Platinized niobium primary anode system.

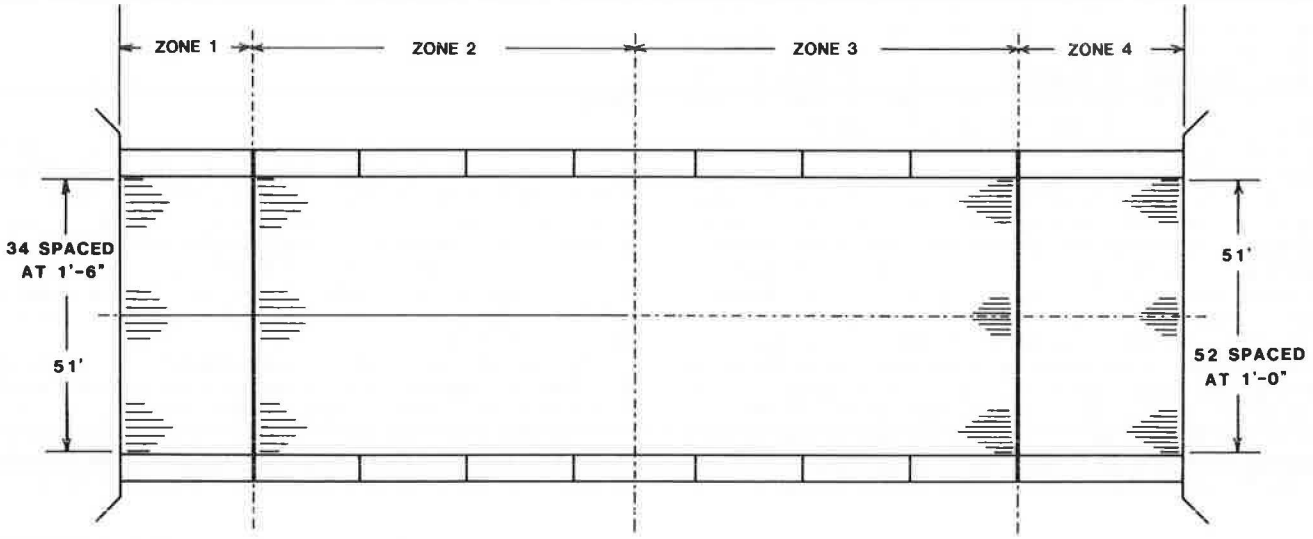

FIGURE 4 Carbon strand secondary anode system.

are 99 percent carbon and have a tensile strength of 250,000 psi. Secondary anodes are placed in two patterns (Figure 4). On half of the deck they are placed 1 1/2 ft apart and on the other half of the deck they are 1 ft apart. The two patterns were used to determine the most economical system for future applications.

The primary and secondary anodes are held on the deck with a ribbon of conductive polymer concrete (PC). This material provides additional anode material and protects the wire and carbon strands during placement of the overlay.

The sidewalks of the bridge are protected by a slotted cathodic protection system in which the same primary anodes are used but the wire and carbon strands are placed in slots cut in the sidewalk and backfilled with conductive PC (Figure 5). All carbon strands in the slotted sidewalk system are placed 1 ft apart.

Power for the distributed anode system is supplied by a rectifier with an alternating-current input of 115 V and 60 cycles capable of a direct-current output of 24 V and 14 A to each of the four zones. This would provide up to 3 mA per square foot of concrete.

Power from the rectifier to the distributed anodes is supplied through a buried rigid metallic conduit

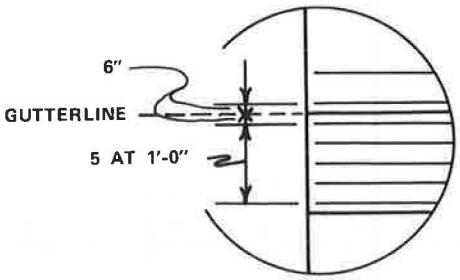

FIGURE 5 Cathodic protection of bridge sidewalks.

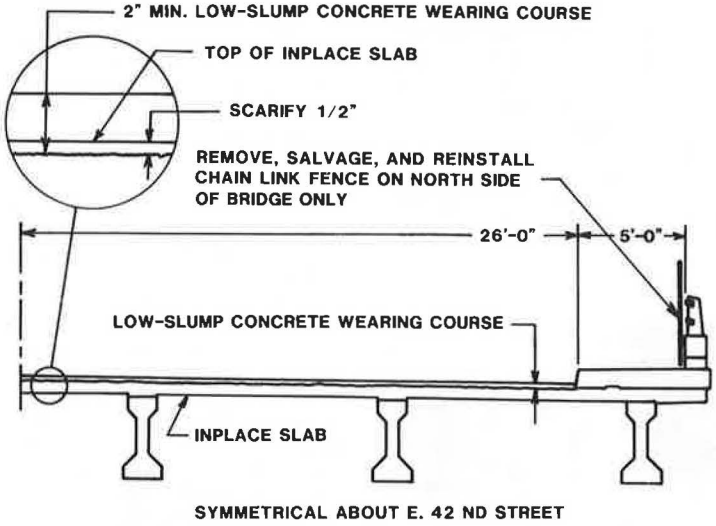

FIGURE 6 Typical section of 42nd Street Bridge.

from the rectifier to the bridge and polyvinyl chloride along the north crash rail of the bridge. Placement of the conduit on the bridge required removing and replacing a chain link fence (Figure 6).

The low bid for the rehabilitation of the 42nd Street Bridge was $163,200. This includes $3,500 for the rectifier, $37,900 for the cathodic protection system, and $2,000 for removal and reinstallation of the chain link fence. The total of $43,400 for the work related to cathodic protection is based on a price of $3.50/ft^2 of protected area.

Construction

Rehabilitation of the 42nd Street Bridge began July 11, 1983. After closing the bridge, the contractor milled off 1 in. of the bridge deck and began to repair the substructure. On July 19 and 20, the slots were cut in the sidewalk for the carbon strands and the platinized niobium wire anode. Concrete removals in delaminated areas and at the expansion joints also began at this time.

Holes were drilled through the sidewalk to drain the polyvinyl chloride conduit system carrying the wires that supply power to the deck. This proved to be a difficult task because of the amount of reinforcing steel in the deck. A hole was also drilled from the primary anode slot in the sidewalk through the curb to the bridge deck (Figure 7). This was done to lead the platinum wire from the sidewalk slot to the deck surface and back to the sidewalk slot on the other side of the bridge. By doing this, the contractor did not have to saw the face of the curb.

Miscellaneous steel in the deck was made electrically continuous with the reinforcing steel, and the reinforcing steel had a lead wire cadwelded to it to provide the system ground.

Corrosion probes were placed at the top and bottom reinforcing steel mats in each end span and at the top level in each center span (Figure 8). These probes consisted of a 6-in. piece of 5/8-in. reinforcing steel embedded in a 3 x 3 x 8-in. block of concrete containing about 15 lb of chloride per cubic yard of concrete.

The steel had a wire lead attached, and a ground wire was cadwelded to the reinforcing steel mat at a point near the probe. This, in effect, creates a strong corrosion cell. The effectiveness of the cathodic protection system can be revealed by the corrosion activity or lack of such activity in the corrosion probe.

FIGURE 7 Drilling hole through curb for primary anode wire.

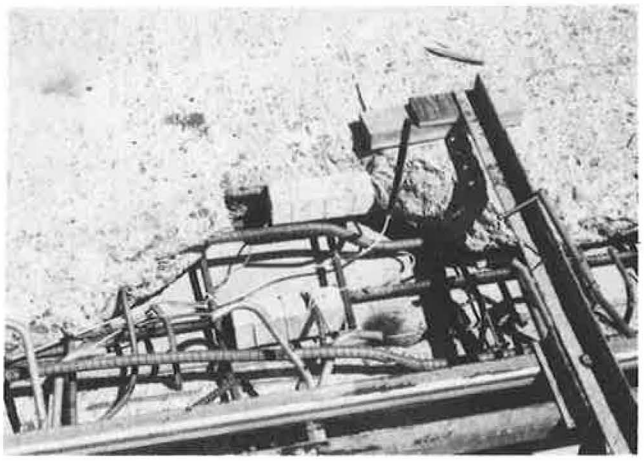

FIGURE 8 Corrosion probes at top and bottom mats.

A silver-silver chloride reference cell was placed in each span of the bridge on August 5 to provide control of the rectifier output. These were placed as close to the depth of the steel as spacing of the steel would permit. The reference cells were patched with a salt-bearing concrete proportioned and supplied by the designer. Before the reference cell was placed, the patch area was moistened. A bed of fresh concrete was prepared, the reference cell was placed in it, and the patch was completed (Figure 9).

FIGURE 9 Patching reference cell.

After the expansion joints were placed but before the cathodic protection system was installed, the contractor sandblasted the bridge deck.

Figure 10 shows the beginning of work on the distributed-anode system on August 11. The electrician is leading the platinized niobium wire from the sidewalk slot through the hole in the curb to the bridge deck and across the deck. Behind the electrician are wooden pegs placed in holes that were drilled in the bridge deck. The pegs are either 1 or 1 1/2 ft apart depending on the required spacing of the carbon strand secondary anodes. The carbon strand was strung out on the deck from one end of a zone to the other, wrapped around two pegs, and strung back to the other end. Wrapping the strand around these pegs allowed it to be pulled tight and the proper spacing of either 1 or 1 1/2 ft between the strands could be maintained until the PC ribbons were placed. After the PC was cured, the pegs were pulled and the excess carbon strand was removed.

Placing the conductive PC was a time-consuming process. It began with the combining and mixing of the resin and hardener. This was done outdoors where ventilation was no problem. Mixing was done in the container in which the resin had arrived. The resin was shipped in 1-gal units in Imperial gallon-sized metal cans.

The resin and hardener were then added to a heavy-duty plastic bag containing a preweighed amount of conductive coke. The liquids and coke were mixed in the plastic bag by using a rolling motion; this was carried out on a plastic-covered piece of plywood (Figure 11). The mixed PC was transferred to a pail and then to a hand-made hopper and extruder (Figure 12). After the conductive PC ribbon was placed, it was sprinkled with dry coke, which was beneficial to the cure of the PC.

The first plexiglass hopper and extruder was supplied by the designer of the cathodic protection system and was copied by the electrical subcontractor. Several of these plexiglass devices were used. With time, the PC would bond to the plexiglass

FIGURE 11 Mixing resin, hardener, and coke.

FIGURE 10 Passing platinum wire through curb.

FIGURE 12 Placing PC ribbon.

and start to clog the hopper and the extruder. This made for slower production and for a smaller ribbon. Specifications called for the ribbon to be 1 to 1 1/2 in. wide and 3/8 to 5/8 in. thick. It took a total of 14 hr to complete the first half of the bridge deck. The second half of the bridge was completed in about 8 hr. The first half of the low-slump overlay was placed August 12, the day following completion of half of the cathodic protection system and 1 month after work had begun.

Before the low-slump concrete was placed, a sand cement grout was placed on the bridge deck and brushed around. Concrete was supplied by a concrete mobile to a Bidwell paver.

The platinum wire for the second half of the protective system was coiled underneath a greased steel plate, which was paved over (Figure 13). Later a saw cut was made to provide a sharp vertical edge against which the remainder of the overlay was to be placed. When the excess concrete was removed, the steel plate was exposed, and the cathodic protection system was placed on the remaining behalf of the bridge deck.

FIGURE 13 Plate covering platinum wire.

Originally, the cathodic protection system was designed so that traffic could be maintained over the bridge during construction. However, rehabilitation of the bridge permitted complete closure of the structure. The only problem associated with this portion of the project was that a platinized niobium wire was cut with a jackhammer and had to be spliced. The grid system design should account for any future problem that may occur because of splicing or from any breaks that may develop.

On August 17 the distributed-anode system was placed on the south half of the bridge. On August 18 the bridge deck was cleaned, and the remainder of the riding surface was placed 2 days following the placement of the protective system, on August 19. This was started early in the morning in order to avoid the hottest part of the day. The paving went well. An Astroturf drag was used to provide surface texture, and transverse tining was placed by hand to within 1 ft of each gutterline. A sprayed membrane-curing compound was applied.

Following the paving of the bridge deck but before the bridge was opened, the sidewalk slot system of protection was placed. The slot system on the north side was placed on August 22 and 23 and the south side on August 24. The platinum wire was placed in the transverse slots and conductive carbon strands were placed in the longitudinal slots.

The conductive coke was weighed for each batch of PC mixed. A coloring agent was added to the coke filler to lighten the color of the material and make it more closely resemble the sidewalk concrete. The coke and coloring agents were thoroughly mixed.

The hardener and resin were combined and then mixed together. These were then added to the conductive coke material and mixed in the same manner as the ribbon material on the bridge deck. The corner was cut off the mixing bag, and the conductive PC was placed directly into the slot from the bag (Figure 14). Silica sand instead of coke was placed on the fresh polymer sidewalk because sand is lighter in color but still helps both curing and traction. It took three working days to prepare and complete the sidewalks of the bridge. It took a total of about 6 hr to place the conductive PC on each side. At the same time, the approaches were paved, and the bridge was opened late in the evening of August 24, 45 days after construction began. The remaining work on the conduit runs and junction boxes was done while there was traffic on the bridge deck.

FIGURE 14 Placing conductive PC in sidewalk slot.

Because of production delays, the rectifier was not received until December. It was promptly placed and activated on December 20. The rectifier is capable of 24 V direct current and 14 A for each of the four zones.

On the basis of E log I tests conducted before activation, the system is operating at the cathodic protection current. The corrosion probes in the bridge deck do not show corrosion activity. The system is operating at 0.3 A for Zone 1, the west end span, and 0.9 A for Zone 2. These zones have 1 1/2-ft secondary anode spacing. Zones 3 and 4, with 1-ft secondary anode spacing, are both operated off one circuit because of a defective circuit card. They draw a total of 1.2 A. Voltage varies but is about 1.5 V in all cases.

Extensive testing of the cathodic protection system could not be done in 1984. In April the control panel of the rectifier was stolen, and this was not replaced until the end of August 1984. The system was inoperable all summer. Testing will be done when time and weather permit. The system will then be changed to operate on four circuits as planned.

FINDINGS AND CONCLUSIONS

The rehabilitation of the 42nd Street Bridge went well. Although it took a great deal of time to place the conductive PC, the contractor managed to improve production after the first half of the deck had been completed.

There was a slight shortage of both the platinized niobium wire and carbon strand anode materials. One platinized niobium primary anode ended less than 1 ft short. This was probably the result of the accidental cutting and resultant splicing of the material. There was about a 3-ft shortage of carbon strand material. This can be accounted for in the method used to hold the wire in line on the deck. Over 200 ft was wasted at the ends of the zones where the turn was made with the carbon strand to parallel previous strands.

As mentioned earlier, it was difficult to drill through the bridge deck in order to provide a drain hole for the conduit run. Also, it would be desirable to have expansion joints between any two fixed points on the conduit run. This system has expansion joints, but at one location the polyvinyl chloride conduit pulled out of a junction box as temperature changed.

All things considered, the project was successful. The shortage of platinized niobium wire was handled by using carbon strand material. The shortage of carbon strand could not be corrected, but the break in the carbon strand was made between two primary anodes, and thus electrical continuity was maintained.

The new overlay was tested with the Delamtect shortly after construction. No delaminations could be found. The overlay has been through a harsh winter. There is some surface deterioration as a result, but there is no apparent cracking. The deterioration takes the form of scaling and is possibly the result of low entrained air in the concrete. Delamtect testing done in 1984 revealed some potential small delaminations. These were too small to confirm, but testing will continue.

The rectifier has been in operation only a short time, but early tests have indicated that this will be an efficient system to operate. The evaluation of the system will begin in the summer of 1985.

Publication of this paper sponsored by Committee on Corrosion.

Cathodic Protection of a Four-Lane Divided Continuously Reinforced Concrete Pavement

ANDREW D. HALVERSON and GLENN R. KORFHAGE

ABSTRACT

The design and construction in 1982 of a second cathodic protection system for continuously reinforced concrete pavement by the Minnesota Department of Transportation is described. Corrosion of the reinforcing steel in this type of pavement has been a severe maintenance problem. An initial cathodic protection research project was successful in retarding this corrosion, so the department contracted for the design of a second system. This resulted in three separate designs, each 1,800 ft long, with separate power sources. They are (a) a trench system with the anodes placed in a trench 4 ft deep by 1 ft wide (b) a shallow-post-hole system with the anodes placed in augered post holes 12 ft deep, and (c) a deep-post-hole system with the anodes placed in augered post holes 15 ft deep. The pavement is grounded every 200 ft of each roadway by attaching wire to the reinforcing steel. Construction began in October 1982 and was completed in 1983. The systems were activated in December 1983 at current levels determined by E log I tests. Initial testing of the systems based on readings taken on corrosion probes placed during construction has indicated that they will be effective. Extensive testing has been delayed because of equipment problems that have shut down one system.

The deterioration of continuously reinforced concrete pavement (CRCP) is a serious problem in the state of Minnesota. This deterioration is primarily the result of chloride-induced corrosion of the reinforcing steel and is similar to the problem afflicting concrete bridge decks.

It can generally be stated that the products that build up on the surface of the reinforcing steel as a result of corrosion occupy a great deal more volume than the steel from which they were formed. As these materials build up, they produce stress in the concrete matrix. Because of its low tensile strength and brittle nature, the concrete fails and cracks. The crack propagates to the surface, and spalling and potholing result.

The distress in CRCP is visible throughout the year in the form of old patches on the pavement surface, and the spalls and potholes are a particular problem in the spring (Figure 1).

FIGURE 1 Deterioration of CRCP.

BACKGROUND

The first CRCP in Minnesota was constructed in 1963 on Interstate 35 near Faribault in the southern part of the state. This was a test section of freeway nearly 11 mi long. The pavement was not jointed. It contained a high percentage of reinforcing steel, 0.5, 0.6, or 0.7 percent. It was intended that, with temperature change, the pavement would develop many small, closely spaced cracks held tight by the reinforcing steel; this would eliminate the need to saw, seal, and maintain pavement joints. The cracks developed as expected, but a maintenance-free pavement was not the result.

Construction of CRCP as a standard practice began in Minnesota in 1967 and, through the late 1960s, over 200 route miles were completed. Total lane mileage of CRCP is much higher, because the roads are multilane freeways and the additional mileage of ramps at interchanges should be included. By 1970 the construction of CRCP had been discontinued. Initial failures were already apparent. These were tension failures, evident in the form of open cracks where reinforcing had corroded, had been reduced in cross section, and had finally ruptured (1). By 1974 the oldest pavements began to exhibit isolated cases of spalling and shallow potholing. During 1975 maintenance operations to patch open holes became frequent, and by 1976 the maintenance reached a significant level.

In 1977 the Minnesota Department of Transportation (MnDOT) initiated a performance and condition review and a research investigation to examine the state of the art for rehabilitation of deteriorated CRCP. As part of the research, a critical section of pavement received a bituminous overlay, a marginally critical section was rehabilitated by removing the upper portion and any delaminated areas and overlaying with a low-slump concrete overlay, and another section was placed under cathodic protection.

The cathodically protected section of pavement is 1,000 ft on southbound I-35W in Blaine. The concept of cathodic protection of a highway pavement is new, but cathodic protection has been used for a number of years on pipelines, bridges, and more recently on other structures. In a technique from the pipeline industry, a current is impressed from a rectifier to a buried, remote anode to neutralize the corrosive current by polarizing the steel, making it entirely a current-receiving cathode (Figure 2).

The 1,000-ft section of I-35W is divided into two designs for cathodic protection. One-half of the section is protected with a a trench-type system, and the other is protected with a post-hole system. In the trench system a Duriron anode is placed 3 1/4 ft deep in a trench 4 ft deep. Anodes are placed every 50 ft and lie within a 1 1/2-ft-deep lift of conductive metallurgical coke breeze (Figure 3). In the post-hole system the anodes are also 50 ft apart. However, they are placed in a 10-ft-deep augered post hole (Figure 4). The anodes are contained in a galvanized sheet metal canister 8 in. in diameter and 4 1/2 ft long. The canister is filled with coke breeze, and the post hole is backfilled with coke breeze to a depth of 6 ft.

Visual observation of the cathodically protected pavement has revealed less surface distress and patching than is evident on adjacent unprotected pavement. In addition, in the summer of 1982, the department contracted with Donahue and Associates to conduct an investigation of selected segments of CRCP by using infrared thermography. This investigation, which included the original cathodically protected pavement, revealed numerous significant areas of delamination on unprotected pavement but only minor areas of delamination on the protected pavement.

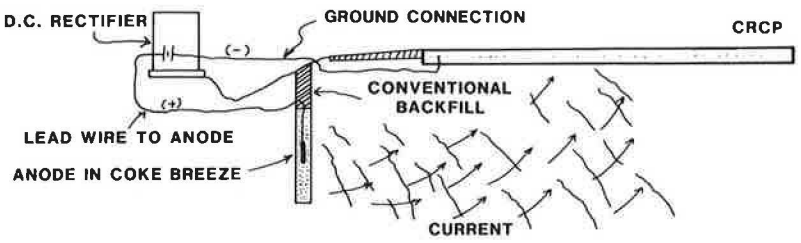

FIGURE 2 Cathodic protection of CRCP.

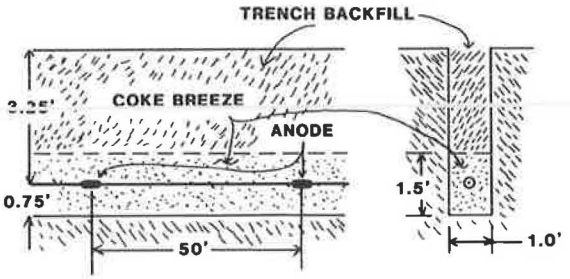

FIGURE 3 Trench-type cathodic protection system.

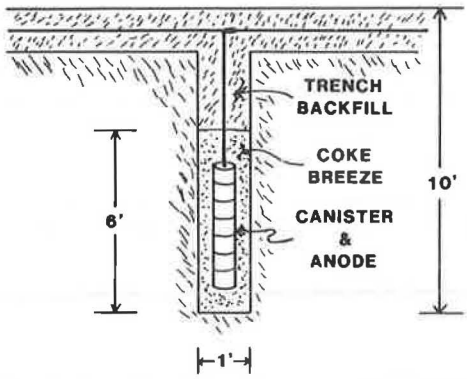

FIGURE 4 Post-hole cathodic protection system.

EXPERIMENTAL WORK

In 1982 at the request of the department's Oakdale District Office, efforts to design and construct 1 mi of cathodic protection for a segment of CRCP began. The segment chosen was a four-lane divided section of I-35E north of St. Paul. The department contracted with Kenneth C. Clear, Inc., to design the system. Rectifiers were ordered by the department, and bids were requested for construction of the project.

System Design

The section of I-35E to be protected is located in the city of Vadnais Heights, north of St. Paul. It begins at a bridge over LaBore Road Connection and the Burlington Northern Railroad (Bridge 9567) and ends at the White Bear Lake city limits. The pavement was constructed in 1970. It is 8 in. thick and contains 0.7 percent steel by cross-sectional area. The reinforcing steel consists of tied bars. The average daily traffic is 29,300.

Test results from a 1981 CRCP inventory survey (2) revealed about 2.3 in. of concrete cover over the reinforcing steel. Chloride contents, as determined by drill dust samples, were about 3,990 parts per million (ppm) from 0 to 1/2 in.; 2,550 ppm from 1/2 to 1 in.; 1,960 ppm from 1 to 1 1/2 in; 1,070 ppm from 1 1/2 to 2 in.; and 630 ppm from 2 to 2 1/2 in. Electrical potentials were taken with a copper-copper sulfate half cell. All readings taken revealed active corrosion. Delamination detection was done with a Delamtect. This revealed less than 1 percent delamination, which was corroborated by infrared thermography done in 1982 and 1983.

Efforts to build a cathodic protection system began April 9, 1982. It was decided that this second system should be built in the median of the freeway in order to protect both roadways. A consultant agreement for design and testing was signed in May. The design resulted in three separate systems, each with its own source of power. There are a trench system and two post-hole systems. Each of these is 1,800 ft long, and each has five zones with independent electrical control.

The first system is in a trench 4 ft deep by 1 ft wide. Nine inches of conductive metallurgical coke breeze is placed in the trench and compacted. The 2 x 60-in. Duriron anodes are 60 ft apart. There are six anodes per zone, which is 360 ft long. The anodes are covered with 9 in. of coke breeze, which is also compacted. The remainder of the trench is backfilled with excavated material (Figure 5).

The second system, immediately north of the trench system, is a shallow-post-hole system. The anodes are in 12-in. diameter post holes that are 12 ft deep and 36 ft apart. There are 10 anodes per zone. The 1 1/2 x 60-in. anode is contained in an 8-in. diameter galvanized metal canister 7 ft long. The anode is backfilled with coke breeze within the canister, and the canister is backfilled with coke breeze within the post hole (Figure 6).

The northernmost system uses deep post holes. The anodes are in 12-in. diameter post holes augered 15 ft deep that are 17 ft apart. There are 20 anodes per zone. The 1 1/2 x 60-in. anodes are in a 10-in. diameter galvanized metal canister that is 7 ft long. The anode is backfilled with coke breeze within the

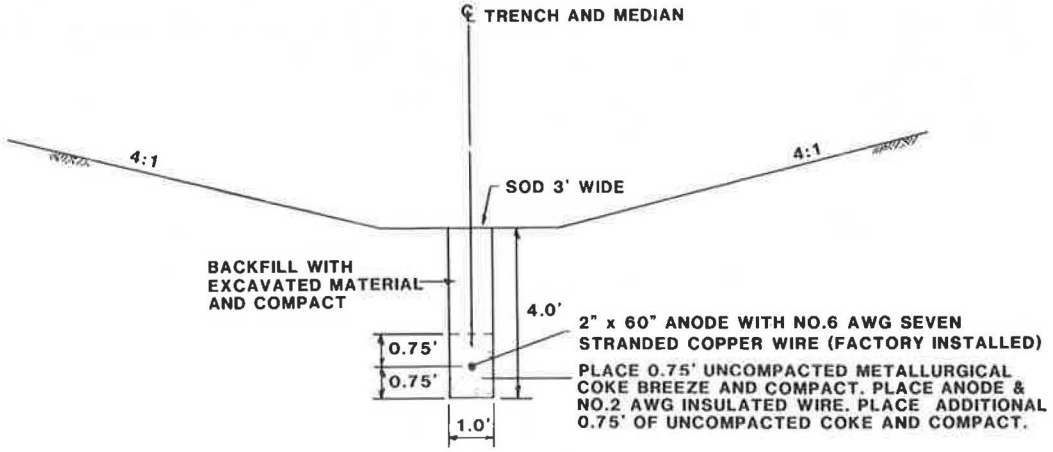

FIGURE 5 Trench-type cathodic protection system: construction details.

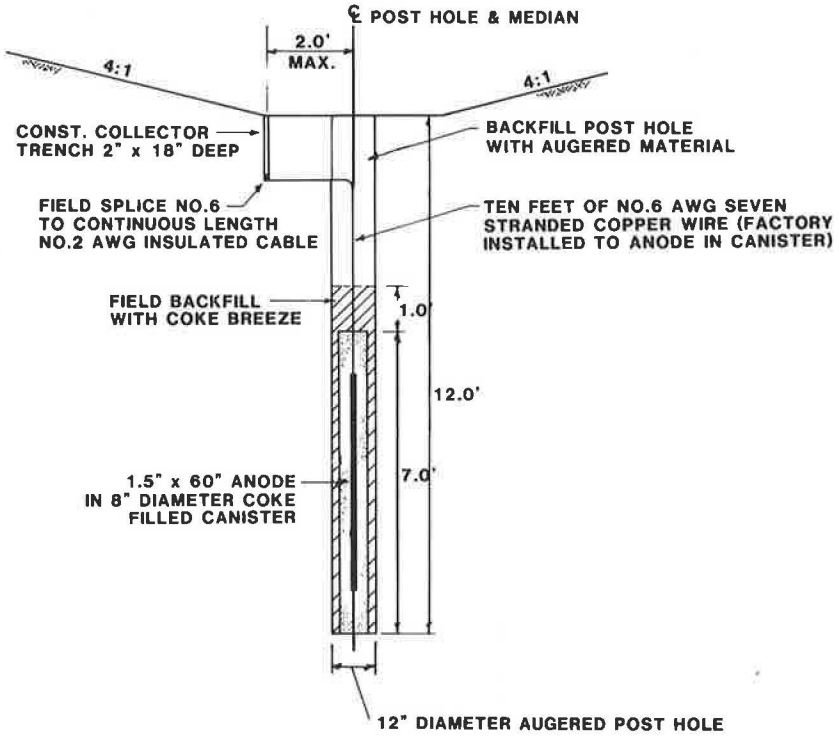

FIGURE 6 Shallow-post-hole system.

canister, and the canister is backfilled with coke breeze within the post hole (Figure 7).

The system is grounded every 200 ft. A ground wire is attached to the reinforcing steel. This wire leads to a header cable in a collector trench that is 4 ft off the edge of the pavement. The header cable is continuous along the northbound and southbound roadways for 5,400 ft (Figure 8). Power is supplied to each system by a rectifier with a 240-V alternating-current input. The rectifiers for the trench and shallow-post-hole systems are capable of an output of 50 V direct current at 32 A for each of the five zones. The rectifier for the deep-post-hole system is capable of an output of 80 V at 32 A per zone.

The deep-post-hole system was designed because part of the project is located on a fill section through a swampy area, which has higher soil resistivity. The trench and shallow-post-hole systems are lower in elevation than the deep-post-hole system and are in the fill in the swamp. The soil resistivities are similar there and much lower than that of the deep-post-hole system, which is on an ascending grade. The deep-post-hole system was designed to reach a wetter soil with lower resistivity.

Construction

The contract for the cathodic protection system, minus rectifiers, was put out for bids in August 1982. The contract was let at a low bid of about $131,000. Rectifiers were purchased by the state for about $38,000 and were to be installed by the contractor. Thus, the total cost of the system was $169,000, or about 70 cents ft^2. The contract was let September 10, 1982.

The contractor began work on October 11 by establishing traffic control. The contract allowed 10 working days during which the passing lanes of each roadway could be closed for construction. After those 10 days, only temporary lane closures were allowed.

The contractor first established the system grounds, which were made to the reinforcing steel at 200-ft intervals. A cable locator was used to find the transverse steel. A small milling machine was then brought in to grind the concrete to the depth of the steel (Figure 9). Jackhammers were used to further expose the steel, which was cleaned by using an electric drill with a wire brush. A number 8 stranded copper wire was cadwelded to the longitudinal and then the transverse reinforcing steel, and each cadweld was tested for soundness with a hammer. A hole was drilled through the soil and under the 4-ft-wide bituminous shoulder on the median side of each roadway to an 18-in.-deep collector trench (Figure 10). The trench was originally opened up with a backhoe at each ground connection and later completed with a trenching machine. The ground wire could then be passed under the shoulder without damage to the shoulder. A 9-in. section of 1/2-in. polyvinylchloride conduit was placed around the wire to counteract any shear effects at the edge of the concrete pavement. Figure 11 shows the conduit and the ground wire cadwelds.

A number 1 AWG insulated cable with high-molecular-weight polyethylene (HMWPE) insulation was placed in each collector trench and was continuous through the length of the trench. The number 8 AWG ground lead from the reinforcing steel was cadwelded to the number 1 header cable and enclosed in an epoxy encapsulation kit made for direct burial.

Each collector trench also contained three number 12 twisted wires, to be used as test leads for potential readings. The leads terminated in test stations buried along the shoulder (Figure 12), which made it possible to take electrical potentials on the surface of the pavement without running long lead wires and without running wires across the pavement.

The system grounds were patched with concrete.

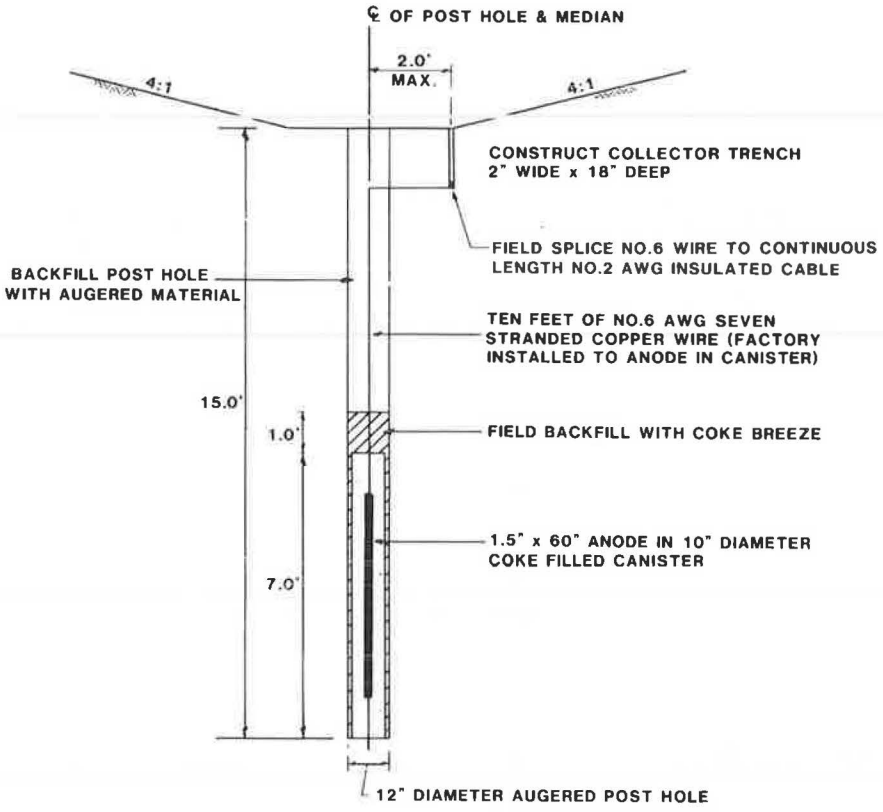

FIGURE 7 Deep-post-hole system.

Before patching, the reinforcing steel was sandblasted and then cleaned with compressed air. The holes were grouted and patches were then placed by using concrete supplied by a concrete mobile. Patches were sprayed with a membrane-curing compound.

A corrosion probe was placed in both roadways in each system in the passing lane near the centerline. The probe consisted of a 6-in. piece of 5/8-in. reinforcing steel with a number 8 stranded wire attached. The steel was cast in a 3 x 3 x 8-in. block of salt-laden concrete in order to create a strong corrosion cell. The concrete contained 15 lb of chloride per cubic yard of concrete.

The probe was placed at the level of the reinforcing steel in the pavement and the wire was passed through a saw cut to the edge of the pavement and then to the collector trench in the same manner as that used for the system grounds. Each corrosion probe also had its own ground wire. The probe was patched along with the grounds (Figure 13). The wire was sealed in the saw cut with epoxy. Test stations were provided for each corrosion probe.

The trench system was installed in a trench 4 ft deep by 1 ft wide excavated with a backhoe. The trench system was wired into five zones with six anodes in each zone cadwelded to a continuous length of number 2 AWG insulated cable between the anodes and the rectifier. Splice kits covered each weld.

The splice kits consisted of a plastic sheath placed around the cadweld. This sheath was then

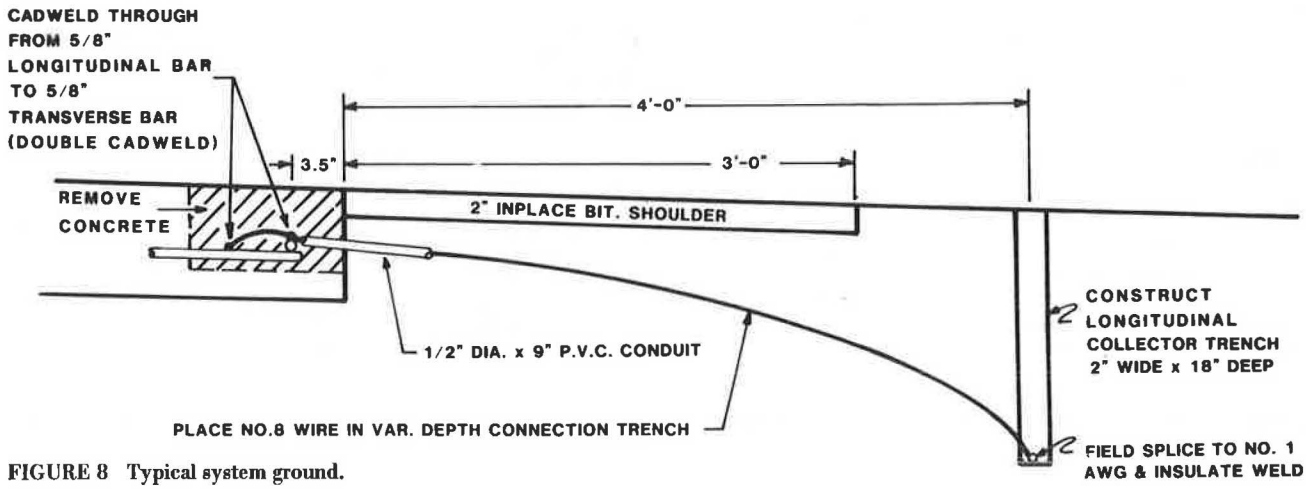

FIGURE 8 Typical system ground.

filled with a two-part epoxy that was shipped in a container with two compartments. The materials were combined by breaking the partition between the two components, and the epoxy was poured into the sheath. The epoxy was then allowed to harden (Figure 14) and the splice kits were tested with a holiday detector to ensure their effectiveness.

Construction of the trench system went well. The construction of the post-hole systems was another matter, however. The contractor worked on the deep system first. A high-speed drill was used to auger the 15 ft. The soil was a very fine sand. The sides of the post hole tended to collapse inward and this eventually became quite a problem. The anodes and canisters were lowered into the post holes by a choker using another truck with a boom (Figure 15). The canisters were then backfilled with coke breeze.

As mentioned, the soil posed a problem. The contractor started at the highest part of the project. As each hole was drilled, the work went to a lower level and came nearer the water table. The sides of the holes would not hold and the contractor had to

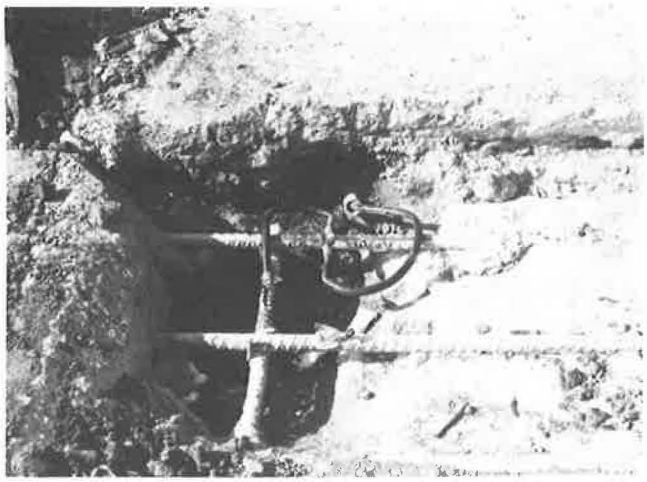

FIGURE 11 Completed cadwelds and conduit.

FIGURE 9 Concrete milling machine.

FIGURE 12 Test station.

FIGURE 10 Drilling under bituminous shoulder.

FIGURE 13 Corrosion probe.

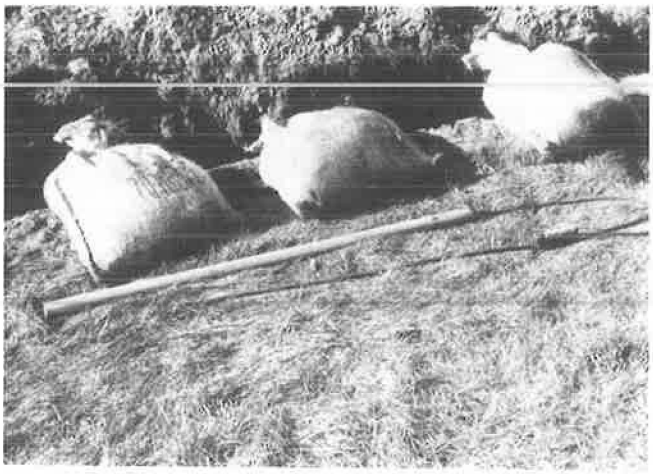

FIGURE 14 Completed splice kit.

FIGURE 16 Drilling in casing.

FIGURE 15 Lowering canister into post hole.

switch to a much slower auger. Eventually, the holes were predrilled with a higher-speed auger and completed at low speed in a casing (Figure 16).

When work stopped for the winter, the contractor had completed all but the lead wires for the anodes for the two post-hole systems and the placement of the rectifiers, which had not yet been delivered.

In the summer of 1983, the contractor made the cadweld connection of the number 8 AWG anode lead to the number 2 AWG header cable for each anode of the post-hole systems. A splice kit was used to cover each cadweld, and each splice kit was again checked with a holiday detector. A 3-in. rigid metallic conduit was passed under the roadway to carry the cables from the median to the rectifiers, which are located on the backslopes.

Also in the summer of 1983, the designer conducted E log I tests to determine the power levels at which the systems would be operated. All systems were finally activated in November and December 1983. The trench system and the post-hole systems were set to operate at between 8 and 9 A per zone. This results in about 8 to 9 V per zone for the trench system and 9 to 10 V for the shallow-post-hole system. The deep-post-hole system operates at from 7 to a maximum of 21 V per zone as the system gets into high-resistivity soil. The embedded corrosion probes showed no corrosion activity.

Extensive half-cell testing has not been completed. In the late summer of 1984, all five circuit cards in the rectifier for the trench system were lost because of electrical damage. The three systems have not been in operation at the same time since.

When all systems were operating at about 0.5 mA/ft^2 of concrete, the monthly operational costs were about $60, $70, and $100 for the trench system, shallow-post-hole system, and deep-post-hole system, respectively.

FINDINGS AND CONCLUSIONS

With the exception of the soil problem, the construction of the cathodic protection system was successful. The same contractor had built the original pavement protection system, but he was still not familiar with this type of work. If more projects are let, more efficient ways should certainly be found to build them.

The use of a cable locator and a milling machine in establishing the system ground worked quickly and well. Drilling under the shoulder for the ground lead was an excellent idea. However, when the system ground trench was not backfilled promptly, the sides collapsed at several locations and the shoulder was damaged.

The handling of the coke was difficult. It was delivered in 100-lb sacks on pallets. The material was stockpiled when delivered and had to be handled more than once before it was finally placed.

The cadwelding required some trial and error but went very well after that. The splice kits all checked out well with the holiday detector and only one failed to set properly. That one was removed and replaced.

The rectifiers were ordered in late September 1982 and they arrived late in April 1983. One unit was damaged during handling by MnDOT and was returned in July for inspection and a new cabinet. The repaired unit was received in November and was promptly placed.

Initial testing of the system has indicated that the corrosion probe can be polarized. This indicates that the reinforcing steel can be, too. Extensive copper-copper sulfate half-cell tests are sorely needed. This is work that was intended to be done in 1984, but the operation of one of the rectifiers was lost before the testing could be scheduled.

When the recent CRCP inventory is reviewed (2), it may be seen that, of all of the projects surveyed,

the reinforcing steel is at the minimum depth, all sections have chlorides in excess of the amount that induces corrosion, most sections have wide cracks, there is active corrosion on all CRCP, and most sections exhibit delaminations. Once again, more than 200 route-mi of CRCP are involved and at least four times that number of lane miles.

Cathodic protection is looked on as one possible solution to the CRCP problem. Any such decision will be influenced by the cost and effectiveness of the system.

REFERENCES

1. P.C. Hughes. Evaluation of Continuously Reinforced Concrete Pavement. Investigation 184. Office of Materials, Minnesota Department of Highways, St. Paul, 1970.
2. A.D. Halverson and M.G. Hagen. Continuously Reinforced Concrete Pavement Inventory. Investigation 200. Office of Research and Development, Minnesota Department of Transportation, St. Paul, 1982.

Publication of this paper sponsored by Committee on Corrosion.

Early Performance of Eight Experimental Cathodic Protection Systems at the Burlington Bay Skyway Test Site

DAVID G. MANNING and HANNAH C. SCHELL

ABSTRACT

The initial phases of a research program to develop an effective cathodic protection system for use on bridge substructures are described. Four experimental cathodic protection systems were installed on the columns of the Burlington Bay Skyway Bridge in Burlington, Ontario, in 1982 and four more were added in 1983. Seven were impressed-current systems and one was a galvanic system. Each system covered approximately 40 m^2 of concrete surface. Several types of instrumentation were developed to monitor the effectiveness of the cathodic protection. All eight systems are being monitored, and the data collected through July 1984 are presented. All the impressed-current systems were found to be effective in stopping corrosion, but the components of some systems were not sufficiently durable. Insufficient power was available from the galvanic system for it to be practical. The future work required to develop a full-scale operational cathodic protection system for bridge substructures is discussed.

Four experimental cathodic protection systems were installed on the columns of the Burlington Bay Skyway in Burlington, Ontario, in 1982 and four more were added in 1983. The project is part of a research program to develop a means of rehabilitating corrosion-damaged bridge substructures. The specific objectives of this project and the details of the test site were described in two earlier papers (1,2). This paper summarizes the important features of each system and their performance up to July 1984.

DESIGN AND CONSTRUCTION

With the exception of System 4, all the installations were impressed-current systems. Each impressed-current system was powered by an unfiltered full-wave rectifier operating under constant current control. A summary of the main features of each system is given in Table 1 and a more complete description follows.

Systems 1 to 4 were installed in the same con-

TABLE 1 Summary of Important Features of Systems 1-8

System No.	Primary Anode	Secondary Anode	Overcoat	Area (m^2)	Type
1	Conductive polymer[a]	None	Shotcrete	38	I
2	Conductive polymer[b]	Conductive paint[c]	None	38	I
3	Conductive polymer	PAN carbon fiber (south and west faces), pitch carbon fiber (north and east faces)	Shotcrete	38	I
4	Zinc ribbon	None	Shotcrete	38	G
5	Conductive polymer mesh[d]	None	Shotcrete	45	I
6	Conductive polymer (north and west faces), graphite (south and east faces)	Conductive paint[c]	Latex paint (east and west faces), none (north and south faces)	47	I
7	Conductive polymer precast (south and east faces), in situ (north and west faces)	PAN carbon fiber mesh (east, south, and west faces), PAN carbon fiber woven with fiberglass (north face)	Shotcrete	47	I
8	Platinized wire embedded in conductive paste	Conductive paint[c]	None (south face), latex paint (east and west faces), latex paint + tie coat (north face)	33	I

Note: I = impressed current; G = galvanic; PAN = polyacrylonitrile.

[a]Carbon fiber core.
[b]Platinized niobium copper wire core.
[c]The three conductive paints were of different compositions.
[d]Copper wire core.

figuration: three panels high on the south column face and two panels high on the remaining faces. This was done to determine whether protection of the third panel on the south face influenced corrosion activity over the adjacent unprotected faces. A "panel" refers to the area of one face between adjacent rustication strips. The rustication strips, which were at 1.22-m centers, are visible in Figure 1. Systems 5 to 8 were installed three panels high on all four faces.

FIGURE 1 Systems 1, 2, and 3 under construction, August 1982: System 1, right column; Systems 2 (upper) and 3 (lower), left column.

Before the cathodic protection systems were installed, the areas of delaminated concrete were removed and patched; all the surfaces were sandblasted and any exposed metal form ties were coated with epoxy.

An individual connection was made to each anode so that they could be powered independently to investigate different anode spacings.

System 1

Precast conductive polymer anodes were placed vertically on 450-mm centers as shown in Figure 1. The conductive polymer consisted of a vinyl ester binder with spherical carbon particles providing a specified resistivity of less than 10 ohm·cm. Two strands of 30,000-filament carbon fiber were embedded in the full length of each anode to increase conductivity. The fiber was made from a polyacrylonitrile (PAN) base. The anodes were cast by Ministry staff. The entire system was covered with a conventional portland cement shotcrete overcoat, nominally 40 mm thick.

System 2

The primary anodes were the same as those in System 1 except that a single strand of platinized niobium copper core wire was embedded in the full length of each anode. The anodes were placed horizontally on the column, connected at the corners to form three rings around the column at the level of the rustication strips. A secondary anode of water-based graphite-pigmented conductive paint was placed on the surface of the panels bordered by the anodes. The paint had low resistivity and promising durability characteristics, although it was not developed specifically for use on exterior concrete surfaces.

System 3

System 3 utilized the same type of primary anodes as those used in System 2. The anodes were placed vertically with two anodes at the third points of the long faces and one anode at the center of the short faces as shown in Figure 1. A secondary anode of carbon fiber was applied to form a network on the concrete surfaces. The fiber on each face was continuous, but there was no connection between adjacent faces. The south and west faces used a double strand of the 30,000-filament PAN fiber used for System 1. A 20,000-filament pitch-based fiber overbraided with Dacron was used on the north and east faces. The entire system was covered with 40 mm of conventional portland cement shotcrete.

System 4

This was the only sacrificial anode, or galvanic, system. Work elsewhere (3,p.135;4,p.63) had shown that various configurations of zinc anodes could provide adequate protection for steel reinforcement in concrete. The anodes used were in the form of a diamond-shaped (9 x 12-mm) zinc ribbon with steel

core by which connections to the anode could be made. The anodes were placed vertically on 150-mm centers. All the anodes on each face were connected to a single feeder cable that was connected, through a switch, to the reinforcement on the same face. The entire system was given a shotcrete overcoat 40 mm thick. Salt was added to the shotcrete to reduce its resistivity and also to ensure that the potential of the zinc remained active.

System 5

System 5 utilized a proprietary long-line conductive polymer anode recently introduced to the marketplace. It was used in combination with a shotcrete overcoat 40 mm thick. The anode was supplied in the form of an expandable mesh as shown in Figure 2. The length of anode on each face was 13.4, 10.7, 12.4, and 8.7 m/m^2 of concrete surface for the north, south, east, and west faces, respectively.

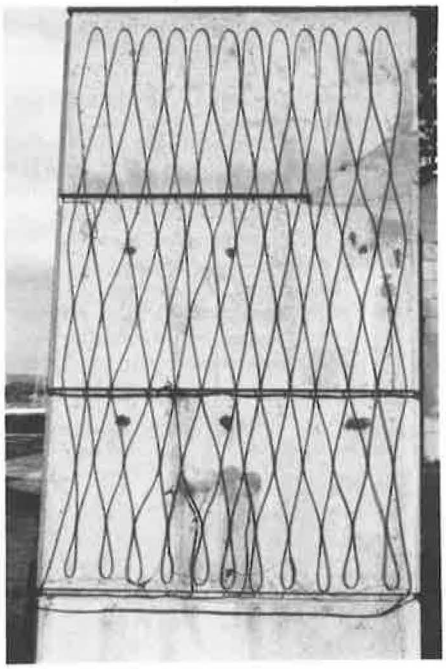

FIGURE 2 System 5, south face: expandable anode mesh before shotcreting.

System 6

As in System 2, System 6 employed a conductive coating as a secondary anode. The coating consisted of graphite in an acrylic solution. The primary anodes on the north and west faces were polymer concrete; graphite anodes were used on the other two faces. The anodes were attached by mechanical anchors and cemented to the column with poured-in-place conductive polymer to ensure a good electrical connection. The polymer concrete anodes were precast by the manufacturer and had a platinized wire core. The paint was chosen for use on the basis that it had demonstrated superior durability properties in an ongoing NCHRP study. Its resistivity was higher than that of the paint used in System 2.

The east and west faces were given two coats of latex paint to investigate the effect of an overcoat on the response of the system to changes in the moisture content of the environment. A view of the completed installation is shown in Figure 3.

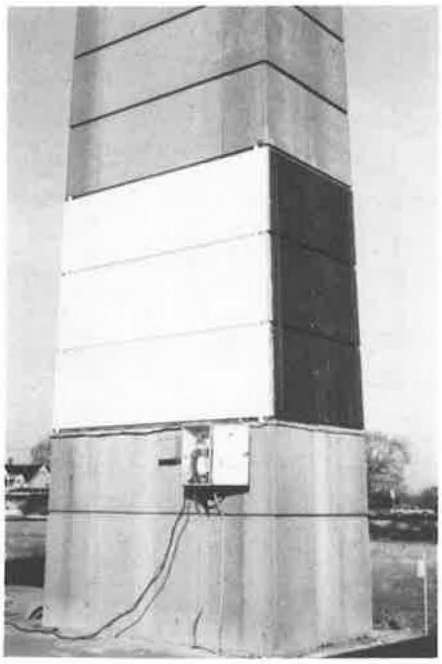

FIGURE 3 System 6: south face (with exposed conductive paint) and west face (with a latex overcoat on the conductive paint).

System 7

System 7 utilized the same type of 30,000-filament PAN carbon fiber used in System 3. Three faces of the column were covered with a mesh made up of fibers on a 75-mm grid spacing as shown in Figure 4. The north face employed a fiberglass mesh with carbon fiber interwoven vertically on 25-mm centers. Precast conductive polymer anodes were used on the south and east faces. Platinized wire covered by poured-in-place polymer concrete was used for the primary anodes on the other two faces. The entire system was covered with shotcrete.

System 8

System 8 was a proprietary system consisting of primary anodes of platinized wire embedded in a conductive paste and a secondary anode of a carbon-filled, water-based acrylic paint. Single vertical anodes were placed in the center of three of the column faces and two vertical anodes were placed at the third points of the west face as shown schematically in Figure 5. A latex paint overcoat was applied to the north, east, and west faces. A tie coat was also used between the conductive paint and the overcoat on the north face to improve the bond between the two.

INSTRUMENTATION

After a review of the experience of others (5,6), instrumentation consisting of macrocells, reference cells, current pick-up probes, current distribution probes, and electrical resistance probes was designed and installed in Systems 1 to 4.

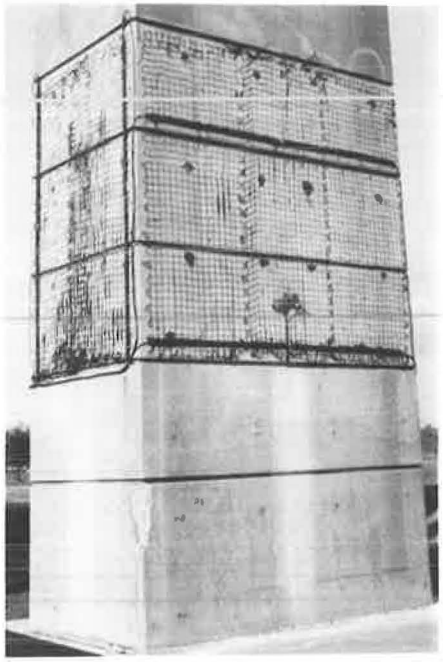

FIGURE 4 System 7: primary and secondary anodes on south and east faces before shotcreting.

The macrocell is a strong natural corrosion cell in which current flow can be measured. The ability of the cathodic protection to reverse the direction of current flow (i.e., to stop corrosion) is one indication of its effectiveness. A zinc-zinc sulfate reference cell and a thermocouple were embedded adjacent to each macrocell. The current pick-up probes consisted of short pieces of rebar embedded at the level of the reinforcing steel at various points in the structure. They were used to measure current density. The current distribution probes consisted of three current pick-up probes installed at the same locations but at different depths from the concrete surface. They were used to measure the variation of current density with depth. The electrical resistance probes were designed to give a quantitative measurement of corrosion in terms of metal loss per year.

The instrumentation and anode leads were terminated in a single junction box for each system. All the measurements were made at the junction box. Details of the fabrication and installation of the instrumentation and the method of making measurements have been given elsewhere (1,2).

The instrumentation used in Systems 5 to 8 was modified following 1 year's experience in monitoring Systems 1 to 4. The changes were as follows:

1. The electrical resistance probes did not function satisfactorily in Systems 1 to 4 and were not used.
2. The current distribution probes in Systems 1 to 4 gave very consistent data. It was decided that there was no reason to repeat the measurements in Systems 5 to 8.
3. Fewer macrocells were constructed in order to reduce installation costs.
4. In addition to the zinc-zinc sulfate reference cells, molybdenum-molybdenum oxide, silver-silver chloride, lead, and carbon cells were installed in System 5. Silver-silver chloride and molybdenum-molybdenum oxide cells were also installed in System 6 and Systems 7 and 8, respectively. In all cases, the additional reference cells were installed adjacent to the reinforcing steel but not adjacent to the macrocells. The number and location of the various types of instrumentation for a typical system are shown in Figure 5.

Throughout this study, the convention was to attach the positive lead of the voltmeter to ground.

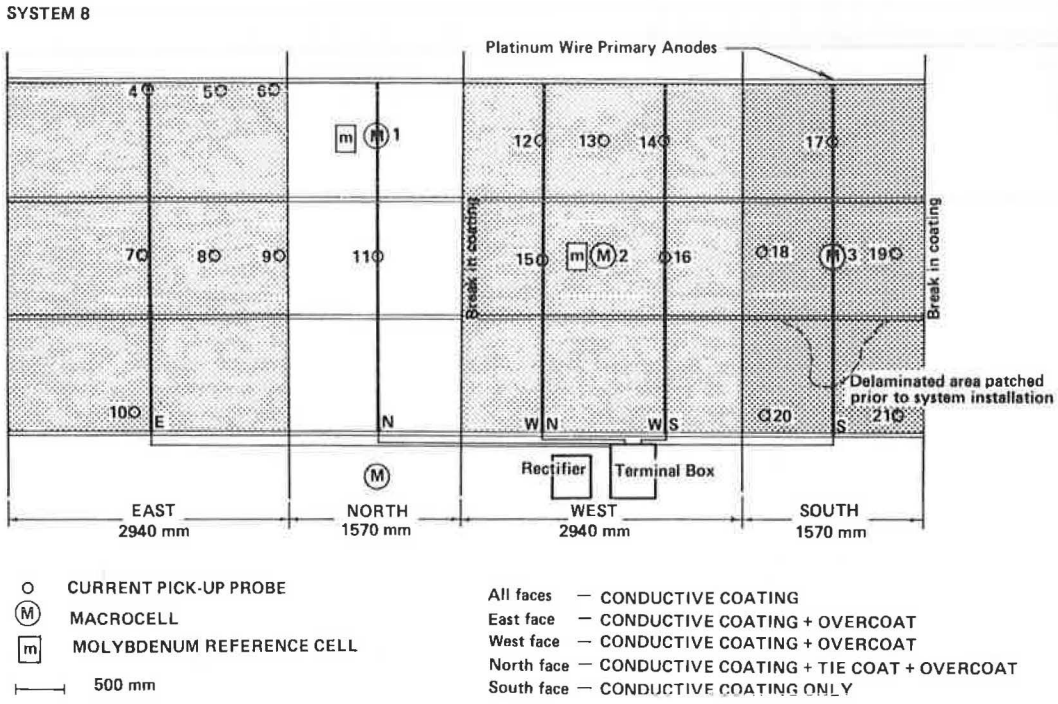

FIGURE 5 System 8: anode and instrumentation placement.

By using this procedure, a positive meter reading indicated that a probe (macrocell, pick-up, or distribution) is anodic (i.e., corroding). Conversely, negative readings indicate that a probe is cathodic (i.e., noncorroding). Resistance measurements were made with a Vibroground Model 263 meter. A Beckman Model 3010 meter was used for current and voltage readings and a Nicolet Model 3091 oscilloscope was used to measure the reference cell potentials.

OPERATION

Systems 1 to 4 were activated in October 1982. E-log I tests were conducted in order to determine the current required for protection according to the procedures given elsewhere (2;7,pp.287-332). The tests yielded an average protection current value of 418 mA, with values ranging from 250 to 780 mA. For purposes of comparison, the three impressed-current systems (1, 2, and 3) were all set at a constant current of 500 mA. This current level has been maintained (except when the systems have been intentionally switched off) throughout the monitoring period described in this paper. The sacrificial anode system was activated by connecting the anodes to the reinforcing steel of the column and had an initial driving voltage of approximately 300 mV.

Systems 5 to 8 were powered in November 1983 to maintain the same average current density (13 mA/m² of concrete surface) as that of Systems 1 to 3. Because the areas of these systems were not the same, as shown in Table 1, the current requirements also differed.

All the systems were switched off periodically for several days to several weeks and allowed to depolarize in order to observe depolarization characteristics. Different anode configurations were investigated in several of the systems.

RESULTS OF MONITORING PROGRAM

A summary of data collected from Systems 1 to 4 and Systems 5 to 8 during the October 1982 to July 1984 monitoring period reported here is given in Tables 2 and 3, respectively. Current densities in each system, in terms of concrete surface area, and the proportion of current flowing to each column face or anode region are shown. The average of the current shifts experienced during all the operating periods is given for the current pick-up probes and the macrocell probes in each system in terms of current density on the probe surface. High and low values of anode-to-rebar resistance are also shown. These results and other pertinent data are discussed in more detail in the following sections.

Impressed-Current Systems

Voltage

One requirement for satisfactory performance of a cathodic protection installation is that the protection current be maintained at an acceptable voltage level. For the three impressed-current systems installed in 1982, voltages were typically in the range of 3 to 6 V. Voltage levels were seen to vary in response to changes in temperature and humidity. Systems 1 and 3, with shotcrete overcoats, were generally stable and responded slowly to these changes. They exhibited slightly higher voltages during the winter months of 1983 and 1984, corresponding to increases in anode-to-ground resistance.

System 2 showed rapid and extreme responses to changes in temperature and humidity. Driving voltages of 13 to 14 V were experienced during the summer months in both 1983 and 1984, corresponding to periods of high anode-to-ground resistance in this system. Both poor mechanical contact between anode and paint and drying of the concrete surface below the paint contributed to this increased resistance. The system voltage dropped sharply in the fall of 1983, returning to the previous level of approximately 3 V, and remained there until the spring of 1984.

Voltage levels in Systems 5 to 8 during their initial 9 months of operation typically ranged be-

TABLE 2 Systems 1 to 4: Summary of Current, Current Density, and Resistance Data, October 1982 to July 1984

System	Anode or Column Face	Current Density on Concrete (mA/m²)	Portion of Current Flowing to Each Anode or Face (%)	Avg Current Shift During System Operation (μA/cm²)			Anode-to-Ground Resistance (Ω)	
				Macrocells		Current Pick-Up Probes		
				Winter	Summer		High	Low
1	Overall	13.2		-3.4	-2.9	-2.5		
	North face	10.4	12				29	7.7
	South face	14.3	26				34	15
	East face	18.3	35				38	7.1
	West face	13.9	27				46	20
2	Overall	13.2		-2.5	-0.6	-3.5		
	Top ring		35				30	4.2
	Middle ring		45				28	3.9
	Bottom ring		20				32	5.0
3	Overall	13.2		-3.7	-2.2	-5.3		
	East face							
	Anode 1	11.9	6				54	28
	Anode 2		18				26	23
	North face	14.1	17				30	20
	West face							
	Anode 1	16.6	21				18	15
	Anode 2		12				24	18
	South face	14.7	26				22	14
4	Overall	2.1		-0.4[a]		-0.2		
	North face		28				18	2.8
	South face		18				11	1.3
	East face		26				9	2.5
	West face		28				10	3.7

[a] Average of winter and summer readings.

TABLE 3 Systems 5 to 8: Summary of Current, Current Density, and Resistance Data, November 1983 to July 1984

System	Anode or Column Face	Current Density on Concrete (mA/m^2)	Portion of Current Flowing to Each Anode or Face (%)	Avg Current Shift During System Operation ($\mu A/cm^2$)			Anode-to-Ground Resistance (Ω)	
				Macrocells		Current Pick-Up Probes		
				Winter	Summer		High	Low
5	Overall	13.5		-5.9	-2.6	-3.2		
	North face	14.8	20				23	4.1
	South face	15.8	21				24	3.5
	East face	14.9	35				15	2.5
	West face	10.1	24				22	3.0
6	Overall	13.3		-7.0	-3.0	-6.1		
	North face	14.1	19				19	4.6
	South face	16.5	22				23	3.4
	East face	12.9	31				21	3.5
	West face	11.7	28				18	3.3
7	Overall	13.2		-3.3	-1.6	-3.4		
	North face	8.0	11				28	6.2
	South face	18.1	24				18	3.9
	East face	12.4	30				23	4.0
	West face	14.5	35				15	2.7
8	Overall	13.1		-4.8	-0.7	-5.2		
	North face	12.2	18				9.4	4.9
	East face		28				7.4	3.9
	South face	14.2	23				30	3.4
	West face							
	North		14				24	5.2
	South		17				14	3.7

tween 2 and 6 V. In all four systems, higher voltages were required during cold periods to maintain the constant system currents. In contrast to System 2, Systems 6 and 8, which also employed conductive paint anodes, showed no significant increase in voltage levels during hot dry periods.

Typical values of operating voltage for all eight systems are shown in Figure 6. For systems in which voltage levels during winter and summer differed significantly, average voltages are shown for each period, denoted in Figure 6 by W and S, respectively.

Macrocells

The initial application of cathodic protection current was sufficient in all the impressed-current systems to reverse current flow in the macrocells. That is, under cathodic protection, the corroding anode of the macrocell became a current-receiving cathode.

Average macrocell current shifts are shown for all eight systems in Tables 2 and 3. Where current shifts seen in winter and summer differed significantly, they are shown separately, denoted by W and S.

Typical macrocell data are shown in Figure 7, which is a plot of the current density on three of the macrocell probes in System 2 as a function of time during the 8 months following cell installation. Probe 2 was located outside the protected area and served as a control, remaining anodic through the monitoring period. In contrast, Probes 1 and 5 were cathodic during periods when current was applied but shifted in the anodic direction when the power was switched off.

Although the data shown in Figure 7 can be considered typical, some macrocells did not remain cathodic at all times. This usually occurred during periods of hot weather when the cells were more active or was associated with obvious areas of degradation of the anode in some of the systems.

There were also indications of long-term changes in macrocell behavior, which may or may not be at-

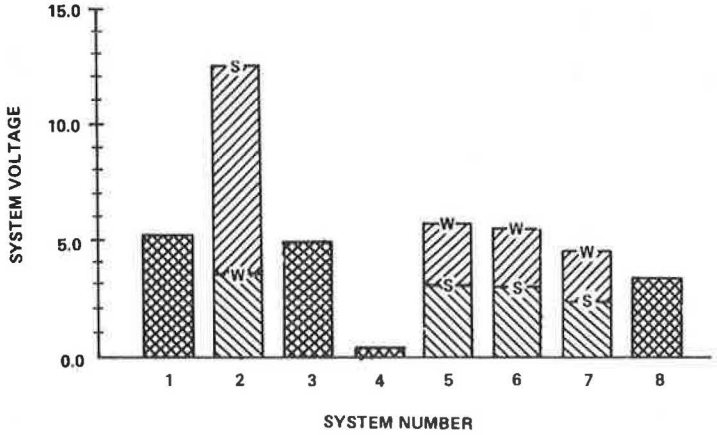

FIGURE 6 Typical operating voltages for Systems 1 to 8 (W and S denote winter and summer periods of operation, respectively).

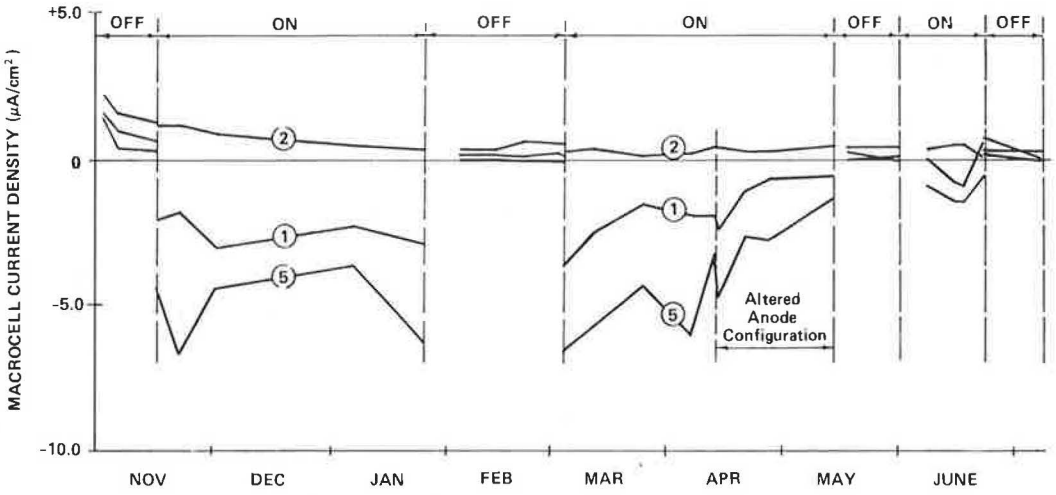

FIGURE 7 System 2: current density on macrocell probes 1, 2, and 5, November 1982 to June 1983.

tributable to the application of cathodic protection. The shift in current density between consecutive off and on periods gradually decreased. Eventually some macrocells remained cathodic even though other cells in the same system became anodic during periods of depolarization. This may indicate a decrease in the required protection current with time or migration of chloride ion away from the macrocell probe, which reduces the intensity of the galvanic cell. However, the control cells outside the limits of the cathodic protection in Systems 1 to 4 also showed decreasing current with time, although they continued to corrode whether the power was on or off. This makes the data more difficult to interpret and suggests that macrocells may be most useful as a monitoring tool shortly after installation but become less reliable at later stages.

Current Pick-Up Probes

The current density of 13 mA/m² applied to the concrete surface corresponds to an average of approximately 2.8 μA/cm² on the surface of the reinforcing steel. This figure was calculated on the basis of all the steel in the protected areas and includes two layers of main reinforcement. Current densities in all the impressed-current systems on probes embedded at the level of the first layer of reinforcement were typically in the range of -2 to -6 μA/cm² during periods when power was applied. During periods when the power was off, current flow to or from the pick-up probes was essentially zero. In contrast to the macrocell probes, there was no significant change from one off period to another.

The pick-up probes were also used to measure the uniformity of current flow within each system. System 1, with closely spaced primary anodes, and System 2, with a conductive paint secondary anode covering the surface, both showed an even distribution of current. Probe current densities were in the range of -1 to -4 μA/cm². In System 1, current densities decreased slightly as the distance from the supply end of the anode increased. This effect was not seen in System 2, indicating that the paint system provided superior current distribution. The magnitude of current densities measured in System 3 was higher than that seen in Systems 1 and 2, ranging from -4 to -8 μA/cm². Highest densities occurred directly beneath primary anodes, decreasing between anodes and reaching a minimum midway between anodes and column

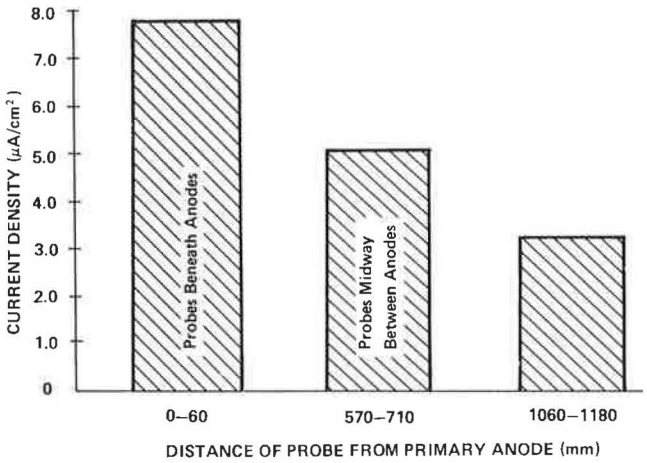

FIGURE 8 System 3: variation of probe current densities with distance from primary anode.

edges as shown in Figure 8. These minimum levels were comparable with values seen in Systems 1 and 2.

Current distribution in System 5 beneath the surface anode mesh was uniform throughout the system with an average current density on the pick-up probes of -3.2 μA/cm². Anodes on each face were initially powered from both ends, with an insulated wire interconnecting the anode mesh at approximately every fourth loop along the bottom of the mesh. This was done in order to introduce a degree of redundancy into the system and to ensure that later investigative coring of the concrete would not result in electrical isolation of portions of the mesh. This arrangement can be seen in Figure 2. It was found that it was sufficient to power each mesh from one end only because this caused no decrease in current densities or increase in driving voltage.

In System 6 current densities were relatively high, averaging -6.1 μA/cm². There was considerable variation over the system, with the highest densities experienced in the vicinity of the anodes and on the narrower north and south faces where the anodes were spaced 2.0 m apart. Very low densities were seen at the midpoints of the longer faces, which suggests that for this material a primary anode spacing of 3.8 m is too large.

System 7 had a relatively even current distribu-

tion over its surface. However, average surface current density on the north column face, with its fiberglass-carbon fiber anode, was approximately one-half the average current density on the other three faces (-8.0 mA/m² and -14.5 mA/m², respectively). This corresponds to a higher anode-to-ground resistance for this face.

Initially, the current distribution in System 8 was very uniform with an average current density on the pick-up probes of -5.2 μA/cm². There was a definite decrease in current densities experienced during the May-July period of 1984 compared with those of the preceding winter. This was particularly evident on the south and west faces corresponding to visible evidence of anode deterioration on those faces. As the conductive paint anode on the south face was broken down, probes in the affected areas no longer received current (this is discussed in more detail in the section on durability).

Alternative anode spacings were investigated in five of the systems. In System 1, alternate anodes were powered, which resulted in a doubling of anode spacing to 900 mm. In System 3, one primary anode was used to power a maximum length of 4.0 m of carbon fiber. These increased anode spacings resulted in unacceptable decreases in system current densities. In System 2 it was found that anode separation could be doubled to 2.5 m without a significant decrease in protection levels. System 7 was powered for a short time by one anode per face rather than two. This resulted in an extremely uneven distribution of current over the system, which was unacceptable. The positions of the anodes in System 8 were such that spacings of 2.8 and 3.7 m could be investigated by disconnecting appropriate anodes. The current density on the probes was maintained for the 2.8-m spacing but at 3.7 m, current densities on probes remote from the anode dropped substantially, indicating that the optimum anode spacing is in the range of 2.5 to 3.0 m.

Current Distribution Probes

The current distribution probes installed in Systems 1, 2, and 3 were designed to measure the variation of current density with depth compared with the current pick-up probes that were used to measure the uniformity of current over the concrete surface. The average results for the period October 1982 to April 1983 for all the probes embedded at 100, 180, and 250 mm in Systems 1, 2, and 3 are given in Figure 9. Thus the probes at the 250-mm depth received 15 percent of the current reaching the probes at the 100-mm depth even though the deeper probe was at a greater depth than the two layers of main reinforcement. The measurements showed that even deeply embedded steel received some beneficial effects from cathodic protection.

Reference Cells

Both static and instant-off potentials measured by the reference cells embedded in the seven impressed-current systems varied widely from cell to cell, although individual cells responded to current application in a consistent manner. Therefore, the voltage shift between static cell potential and instant-off potential during system operation, rather than the instant-off potential itself, was chosen for comparison with published protection criteria.

A polarization shift between static and instant-off potentials of -100 mV is one of a number of protection criteria described by Stratfull (7). For Systems 1 to 3, during the initial 8 months of operation, the applied current was more than sufficient to satisfy this criterion. Average polarization of the zinc-zinc sulfate cells in the three systems for this period was -230 mV, with values ranging from -187 mV to -301 mV. Polarization levels for the cells in Systems 1 and 3 remained in this range until deterioration of anode connections prevented current flow to all protected areas; this is described in more detail in the section on durability. System 2 experienced lower polarization shifts during hot summer periods when the specified current density could not be maintained because of increased circuit resistance. Control cells installed outside the protected areas in all three systems typically showed a gradual cathodic shift in potential during the 18 months after installation, though the reason for this is not clear.

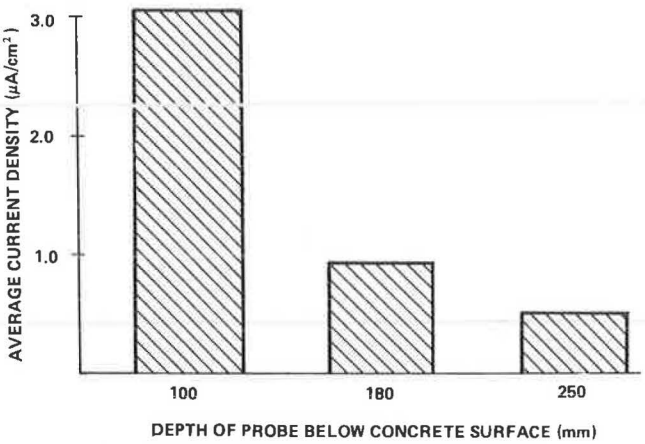

FIGURE 9 Current distribution probes, Systems 1, 2, and 3: average current received by probes at 100, 180, and 250 mm below concrete surface.

Polarization shifts seen in Systems 5 to 8 during the first winter months of operation were generally slightly greater than those seen in Systems 1 to 3, averaging -480 mV and ranging between -281 and -779 mV. A decrease in polarization was observed in most of the cells as temperatures increased in the spring, leading to an average polarization shift during the April-June period of -243 mV. In System 6 this decrease in polarization was particularly obvious in cells midway between anodes on the long column faces, where polarization shifts were less than -150 mV. Polarization shifts measured by the cells in System 8 during this period were reduced drastically, averaging -164 mV compared with -472 mV during the winter months. This was in part because the static potential of cells in this system moved significantly in the negative direction between winter and summer depolarization periods. This phenomenon was not observed to the same degree in cells in the other systems and the reasons for this difference have not been fully explained.

Considerable variation was seen among the five types of reference cells used. Zinc cells typically exhibited a wide range of values from cell to cell, with individual cells also varying significantly. Zinc cells were placed close to molybdenum cells at two locations. Although initially both pairs of cells showed similar polarization levels, in the summer months the molybdenum cells indicated a drastically reduced polarization shift, whereas the zinc cells changed little. The molybdenum cells used often produced an erratic signal and became particularly unstable at temperatures below approximately 5°C. The silver-silver chloride cells also

behaved in an erratic manner during periods of low temperatures. Graphite and lead cells appeared relatively stable and consistent over time, showing little variation with temperature or moisture conditions.

Galvanic System

Of the eight installations, the single sacrificial anode system was the one most affected by environmental temperature and humidity changes. Considerable fluctuation occurred on both a seasonal and day-to-day basis. The sum of the currents flowing to each face ranged from low values of 30 to 40 mA to highs of 100 to 160 mA experienced during the hot summer months of 1983 and 1984. These corresponded to surface current densities in the range of 1 to 4 mA/m^2, considerably less than those experienced in the impressed-current systems. The maximum currents were not sufficient to maintain reference cell polarization shifts meeting the protection criteria of -100 mV (7). During periods of low current flow, the reference cells experienced polarization shifts of only a few millivolts. None of the macrocells consistently experienced reversal of anodic current flow during system activation. Current densities on the pick-up probes were low. The average current densities on the macrocells and pick-up probes and the proportion of current flowing to each column face are shown in Table 2. The typical range of anode-to-rebar resistances is also shown. These resistances varied considerably but returned seasonally to the same levels. Because the driving voltage of a galvanic protection system is fixed, there is no means of maintaining current levels when circuit resistance increases. The driving voltages of 350 to 400 mV measured offered adequate protection to the steel only when circuit resistance was at a minimum. As noted by Schell et al. (2) the current output of the system was insufficient to meet present protection criteria.

DURABILITY

Although all the impressed-current systems functioned satisfactorily from the standpoint of cathodically protecting the steel, some of the components deteriorated in service. The winter of 1983-1984 was unusually severe. In addition to prolonged cold spells, there were frequent snowfalls. Deicing salts were routinely applied to the bridge deck with the result that chloride-laden runoff often flowed over the column surfaces below, as shown in Figure 10. As a result, the components, especially those on the south column faces, were exposed to numerous freeze-thaw cycles, often in the presence of salt solution.

After 8 months of operation, large areas of shotcrete on Systems 1 and 3 were delaminated. Unfortunately, the shotcrete was not checked for delamination after construction, so the time of delamination is uncertain. When a check was made again 1 year later, the areas of delamination had increased substantially and were cracked extensively. After approximately 5,000 amp-hr of operation, both systems exhibited a sudden increase in resistance between the anodes and the column reinforcing steel such that the maximum rectifier output of 15 V was no longer sufficient to maintain the current required. Systems 1 and 3 were switched off permanently in April 1984. Figures in Table 2 are based on data collected while the rectifier output remained at 500 mA.

The increased resistance was found to be the result of breakdown of the connections between the lead wires and the polymer concrete anodes. Coring revealed that corrosion had taken place where the copper lead wire was soldered to a short platinized wire protruding from the anode, even though the connections had been sealed. This emphasizes the need for carefully designed and well-insulated connections. It may be desirable to keep these connections outside the concrete where possible or to embed them within the anode (as was done for the primary anodes in Systems 6 and 7).

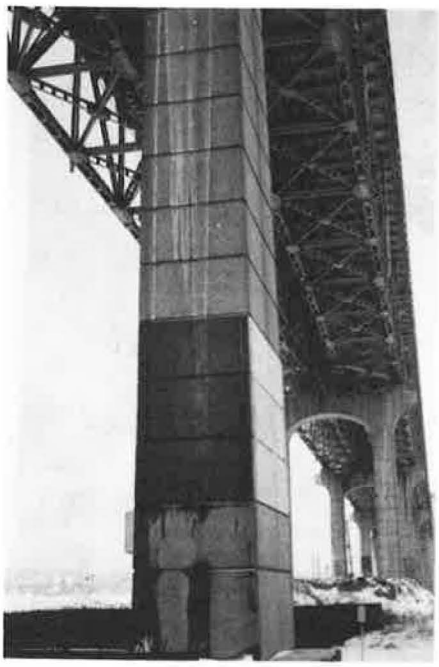

FIGURE 10 Typical exposure conditions of columns during the winter months (System 6 shown).

System 2 lost large patches of paint during the second winter. The paint peeled cleanly away from the concrete and most of the loss occurred on the south face, as shown in Figure 11. As in Systems 1 and 3, the primary anodes showed no damage. Deterioration of the connections was visible and appeared to account for the large increase in the resistance between the middle anode ring and ground. By March 1984, this resistance was so high that current was being distributed only by the top and bottom anode rings. The data in Table 2 summarize the performance of System 2 before March 1984.

There was no deterioration of the shotcrete in System 4. A core taken through an anode after 400 amp-hr of operation showed no visible corrosion.

Shotcrete applied to Systems 5 and 7 was sounded 28 days after placement and before current application to determine whether debonding of the shotcrete had occurred. The only significant area of debonding (approximately 0.8 m^2) was found on System 5, whereas System 7 had a few small scattered delaminations. The sounding was repeated in May 1984 after 7 months of activation. In both systems, a much greater area of shotcrete was found to be debonded. Minor cracking was seen in the vicinity of the rustication strips and the column corners. Anodes in both systems continued to perform well.

In System 6 there was no evidence of deterioration of either the conductive paint or the polymer and graphite primary anodes after 9 months of operation. There was some discoloration and minor cracking of

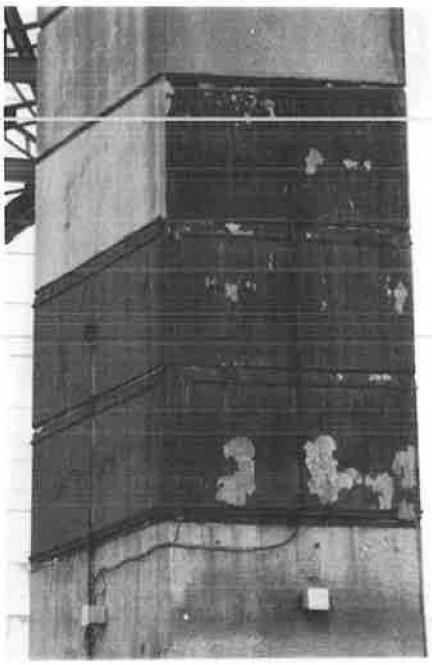

FIGURE 11 System 2: deterioration of conductive paint on south column face 15 months after application.

the latex overcoat in the vicinity of the primary anodes.

Gradual deterioration of the conductive paint anode in System 8 contributed to increased circuit resistance and poor current distribution within the protected area. After 9 months of operation, approximately 90 percent of the conductive paint applied to the south face had been lost. Moderate peeling of both paint layers occurred where the conductive paint was applied with an overcoat or an overcoat and a tie coat. Deterioration of the conductive paste applied over the platinum wire anodes resulted in exposure of portions of the wire to the environment at several locations. Data shown for this system in Table 3 cover only the period of operation from November 1983 to January 1984. During the spring and summer of 1984, the percentage of current flowing to the west and south faces of the column, where damage is greater, dropped to 24 percent (from 54 percent the previous winter). Current density on these faces, which are continuous, was reduced to 6.1 mA/m^2 from 14 mA/m^2.

CONCLUSIONS AND FUTURE WORK

Work in this program to date has indicated that it is possible to design cathodic protection systems that are practical for substructure applications. Current levels sufficient to provide protection to the column rebar can be maintained by suitably designed impressed-current systems. Data collected from probes embedded in the test systems indicate that an even distribution of current over the concrete surface can be achieved. Typically, the systems were able to maintain low driving voltages.

Construction and monitoring of these systems have identified several areas where development is required. There is a need for appropriate tests to identify suitable anode materials. Numerous materials are being introduced to the marketplace that appear promising, but no long-term performance data are available. It is necessary to devise accelerated tests that will simulate field conditions to allow prediction of anode service life and failure mode. Reference cells that are stable and reliable must be identified or developed if potential controlled rectifiers are to be practical and dependable for field use. There is also a need to study the durability of alternative connection details and to investigate the reasons for delamination of the shotcrete overcoat in the impressed-current systems. Studies in some of these areas have already been initiated.

The next major project in this program is a larger-scale demonstration project applying the most promising of the systems identified so far to a multicolumn bridge pier bent.

REFERENCES

1. D.G. Manning, K.C. Clear, and H.C. Schell. Cathodic Protection of Bridge Substructures: Burlington Bay Skyway Test Site, Design and Construction Phases. In Transportation Research Record 962, TRB, National Research Council, Washington, D.C., 1984, pp. 29-37.
2. H.C. Schell, D.G. Manning, and K.C. Clear. Cathodic Protection of Bridge Substructures: Burlington Bay Skyway Test Site, Initial Performance of Systems 1 to 4. In Transportation Research Record 962, TRB, National Research Council, Washington, D.C., 1984, pp. 38-50.
3. J.B. Vrable. Cathodic Protection for Reinforced Concrete Bridge Decks: Laboratory Phase. NCHRP Report 180. TRB, National Research Council, Washington, D.C., 1977.
4. D. Whiting and D. Stark. Galvanic Cathodic Protection for Reinforced Concrete Bridge Decks: Field Evaluation. NCHRP Report 234. TRB, National Research Council, Washington, D.C., 1981.
5. K.C. Clear. FCP Annual Progress Report--Year Ending Sept. 30, 1980, on Project 4K "Cost Effective Rigid Concrete Construction and Rehabilitation in Adverse Environments." FHWA, U.S. Department of Transportation, 1980.
6. C.E. Locke and C. Dehghanian. Embeddable Reference Electrodes and Chloride-Contaminated Concrete. Materials Performance, Vol. 18, No. 2, 1979, pp. 70-73.
7. R.F. Stratfull. Criteria for the Cathodic Protection of Bridge Decks. In Corrosion of Reinforcement in Concrete Construction (Alan P. Crane, ed.), Society of Chemical Industry, London, 1983.

Publication of this paper sponsored by Committee on Corrosion.

Fatigue and Freeze-Thaw Resistance of Epoxy Mortar

MRINMAY BISWAS, OMAR N. GHATTAS, and HERCULES VLADIMIROU

ABSTRACT

Results of tests to investigate resistance of epoxy mortar to fatigue and freeze-thaw exposure are reported. Fatigue resistance is evaluated by number of load reversals sustained against a repeated impactive loading at different temperature levels within the range of 0 to 150°F. The results indicate that fatigue resistance decays exponentially with increasing temperature. Freeze-thaw resistance is evaluated as it is affected by the presence of moisture in fine aggregates. The results indicate that basic material strength and stiffness as well as freeze-thaw resistance of epoxy mortar diminish markedly because of the presence of even a small amount of moisture.

High-strength, fast-setting epoxy mortar is used as an interface material between prefabricated components of modular structural construction. In transportation engineering, for example, epoxy mortar has been used in several full-depth bridge deck construction and rehabilitation projects. Figure 1 shows a typical application. In such a construction method, a series of precast concrete slabs are laid on the top of steel or precast concrete stringers, and the mortar is used in at least three different interface locations, namely, at the interface of stringer and deck slab as bedding material, at the joint between two adjacent slabs, and in the shear pockets containing the mechanical shear connectors. It should be pointed out that mortars using portland cement or acrylic polymers as binders have also been applied in similar modular construction systems. In any case, the mortar becomes an integral part of the structure and fully participates in all load transfer functions. The short-term and long-term performance of the structure depend on the integrity of the mortar connections, which in effect become the links of the structural system.

Short-term static strengths of epoxy mortar are known to be higher than those of usual portland cement concrete. Severe repeated loading and freeze-thaw exposure are two critical damaging factors for structural material. The knowledge of degradation resistance of epoxy mortar is important for the consideration of the durability of the material and of the structure.

MIX DESIGN

Preliminary experimentation indicated that mortars of trowelable to flowable consistency are produced with sand-to-epoxy weight ratios in the range of 3.5:1 to 2.5:1. The workability of wet mortar depends on the gradation and characteristics of sand and on the formulation of the epoxy compound used. A constant mix design was used for the fatigue and freeze-thaw tests reported here. Graded natural silica sand meeting ASTM C 778 (Standard Specification for Sand) was selected. In accordance with ASTM C 881-78 (Standard Specification for Epoxy-Resin-Base Bonding Systems for Concrete), a Type III, Grade 1, Class C epoxy compound was selected. This is a low-viscosity epoxy, specified for use as a binder in epoxy mortars or epoxy concrete at temperatures above 60°F. The components A and B were mixed at ratios of 3.33 to 1.0 by weight, as specified by the manufacturer. The sand and the epoxy binder were mixed at a ratio of 3:1 by weight. Bench and laboratory mixers with simultaneous rotary and planetary motion were used. A relatively slow speed of 75 rpm with three planetary rotations per revolution was used to avoid formation of excessive air bubbles. The mixing was done for a total period of 1.5 min per batch. The workability of the mix allowed convenient casting of the specimens. Some bleeding and plastic shrinkage were observed. Mild rodding was necessary to eliminate air bubbles from the specimen as much as possible.

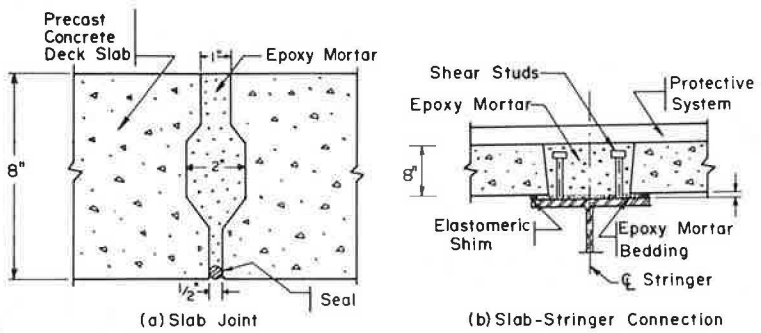

FIGURE 1 Typical application of epoxy mortar in modular bridge deck construction.

The mix design and the yield were controlled by using the physical data of the components as given in Table 1. The average compressive strength of the resulting material was 2,260 psi at room temperature, based on static tests on solid cylindrical specimens 2 in. in diameter x 4 in. long. It may be noted that this strength is somewhat lower than that of conventional portland cement concrete. This means that the use of ASTM C881 alone is not sufficient to guarantee the achievement of certain mortar strength.

TABLE 1 Physical Properties of Mortar Components

Component	Weight (g)	Volume (cm^3)	Computed Density (g/cm^3)
Graded sand	3700	2230	1.66
Component A	948	900	1.05
Component B	285	300	0.95
Epoxy mortar mix	4933	≈2460	≈2.005

FATIGUE RESISTANCE

Specimen Configuration

Figure 2 shows the specimen configuration for fatigue testing. A 1/2-in. layer of epoxy mortar was sandwiched between two plastic cylinders cut from 2-in. diameter cast acrylic rods. The overall size of the solid cylindrical specimens was 2 x 4 in. The specimen configuration was designed to simulate the use of epoxy mortar as an interface layer of moderate thickness between prefabricated or precast concrete modules. The faces of the acrylic cylinders were grooved to provide improved mechanical bond and to prevent excessive lateral deformation of epoxy mortar under axial load.

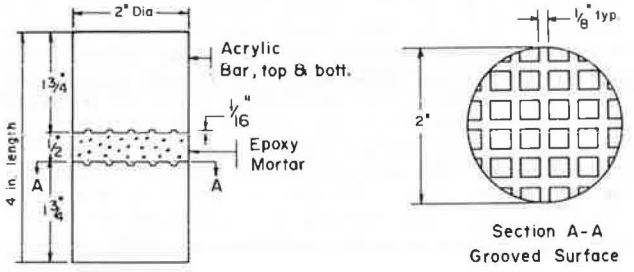

FIGURE 2 Sandwich cylinder specimen for fatigue testing.

Temperature Variable

Although epoxy resin is a thermosetting polymer and degradation of mechanical properties should be expected at a high temperature, say, about 350°F, the mechanical properties of epoxy mortar are reported to degrade at moderately elevated temperatures (1, pp.210-215). Results of static compressive strength tests on the sandwich specimens, as shown in Figure 3, confirm such reported variation of the properties of epoxy mortar with changes in temperature. In reference to Figure 3, the following points may be noted:

1. The average compressive strength of the epoxy mortar at room temperature (70°F) is 7,240 psi, on the basis of static tests on sandwich specimens. This is about three times higher than the value based on tests of bulk epoxy mortar cylinder specimens.

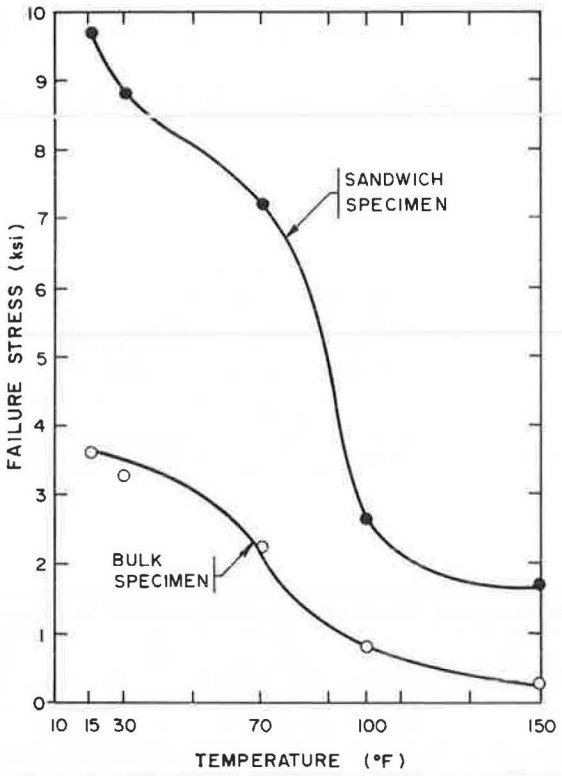

FIGURE 3 Static compressive strength of epoxy mortar at different temperature levels.

2. A precipitous drop of compressive strength at elevated temperatures was observed. Such a drop is characteristic of polymer resin and it is expected at a high temperature, but in the case of the subject mortar it occurred at about 80°F, which is not an unlikely temperature for bridge decks or other constructed facilities.

It is also evident that the mortar strength continued to rise with lowering of temperature. In fact, at 0 and 30°F, the epoxy mortar became so strong that frequently the acrylic cylinders failed before reaching the static failure load of the mortar. Because the strength of the usual epoxy mortar is expected to be higher than that reported here and because of the poor bond between the epoxy mortar and the acrylic cylinders, the use of acrylic cylinders is not recommended for such tests.

In any case, because of the observed and reported variation of the static strength of epoxy mortar with the variation of temperature, it was decided that fatigue resistance of the epoxy mortar material would be investigated at various temperature levels. Specific temperature levels of 0, 30, 65, 100, and 150°F were selected.

Time-Dependent Loading

The time-dependent loading used is shown in Figure 4. This is an invert haver-square waveform, a heavily punishing loading condition, representing an extreme situation of repeated impactive loading on a transportation structure. The valley load of (-) 7.0 kips represents a maximum compressive stress of 2,230 psi, which is about one-third of the static compres-

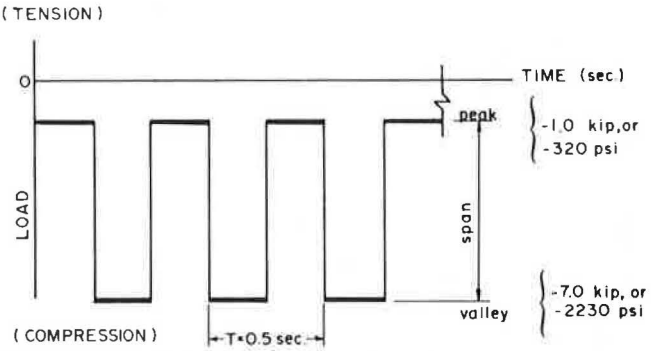

FIGURE 4 Typical haver-square waveform of repeated impactive fatigue loading.

sive strength of the sandwich specimen at room temperature. To avoid any separation of the specimen from the loading device, a peak load of (-) 1.0 kip was maintained. This was equivalent to a normal minimum compressive stress of about 5 percent of the compressive strength of the specimen at room temperature. In order to accommodate pronounced strength degradation at elevated temperatures, valley and peak loads of (-) 3.5 kips and (-) 0.5 kip, respectively, were also used. A frequency of 2 Hz (i.e., four load reversals per second) was used at all temperature levels.

Test Results

The summary of the test data is given in Figure 5, showing fatigue resistance as a number of load reversals sustained as a function of temperature level

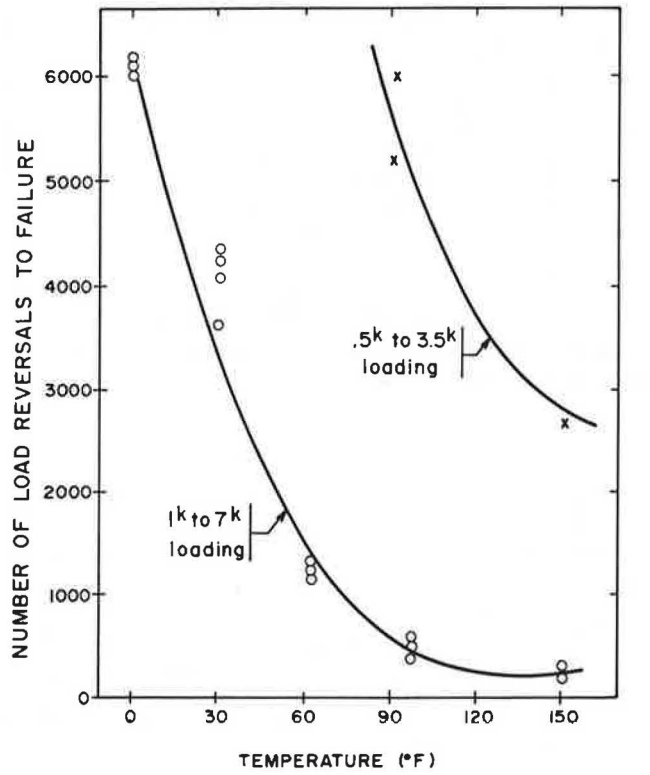

FIGURE 5 Fatigue resistance as number of load reversals sustained as function of temperature level.

plotted on linear scales. Because an exponential decay of strength was observed, the data were plotted on semilog scale, as shown in Figure 6. A nearly linear plot on this scale suggests a possible relation in the form of

$$N = A\exp(-kt) \quad (1)$$

where

N = number of load reversals sustained,
t = specimen temperature, and
(-k) = slope of ℓn(N) versus t curve, which in this case was about -0.2.

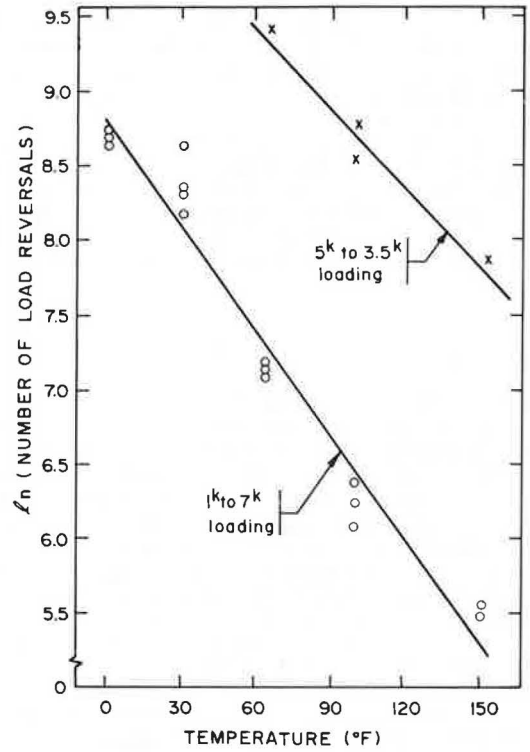

FIGURE 6 Logarithm of number of load reversals versus temperature level.

It appears that k represents a material fatigue property, and A, the intercept of the curve with the ordinate, would be a function of loading characteristics for a given material. It is evident, as expected, that for a given temperature, the number of load reversals sustained increases with the lowering of the magnitude of the maximum compressive load.

FREEZE-THAW RESISTANCE

It is generally claimed that epoxy mortar is unaffected by freeze-thaw exposure. Degradation of epoxy mortar due to freeze-thaw exposure, however, has been reported and discussed on occasion (2). Considering that water is the primary reason of freeze-thaw degradation in portland cement concrete, it may be suspected that incidental or inadvertent presence of water may also be the cause of possible freeze-thaw degradation of epoxy mortar. With this in mind, freeze-thaw experiments were designed to evaluate the effect of the presence of varying amounts of

water in the sand, the fine aggregate of the epoxy mortar.

Test Procedures

Freeze-thaw experiments were conducted generally in keeping with ASTM C 666-80 (Standard Test Method for Resistance of Concrete to Rapid Freezing and Thawing), Procedure A, and ASTM C 215-60 (Standard Test Method for Fundamental Transverse, Longitudinal, and Torsional Frequencies of Concrete Specimens).

The mortar mix design was the same as that described earlier, except that the measured amount of sand for a specific batch was premixed with a certain amount of added water. The amounts of water added were 0, 1, 2, 3, and 5 percent by weight of sand, respectively, for five different test batches. Typical specimen size was 3 x 4 x 16 in. The tests were conducted by using a freeze-thaw cabinet with a capacity of 18 specimens laid in a horizontal position. A temperature range of 0 to 40°F, cycling at approximately 4 hr (i.e., 2 hr of freezing and 2 hr of thawing) was used. Physical properties were measured initially and after the completion of 60 and 120 cycles. Three different physical properties were measured, namely, static modulus of elasticity, dynamic modulus of elasticity, and modulus of rupture.

Test Results

The static modulus of elasticity was evaluated by measuring midspan deflections due to transverse loads. The initial (i.e., before freeze-thaw cycling) average value of static E as a function of moisture content is shown in Figure 7. Substantial reduction in material stiffness with even small increments of water content was evident. Because freeze-thaw degradation is characterized by a relative reduction in material stiffness, relative values of static E as a function of number of freeze-thaw cycles are shown in Figure 8. It is evident from typical values corresponding to 1 and 2 percent moisture content that freeze-thaw degradation occurs at an increasing rate with increasing moisture content. Degradation is substantial after 60 freeze-thaw cycles, and measurement could not be practically taken for samples at 120 cycles because of extreme reduction of material stiffness.

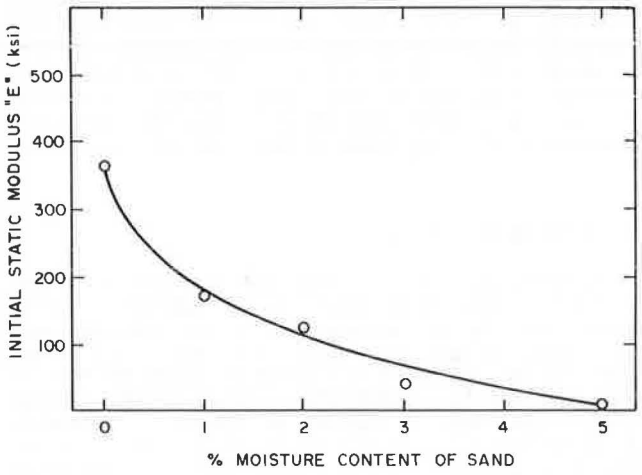

FIGURE 7 Reduction of initial static E with increasing moisture content.

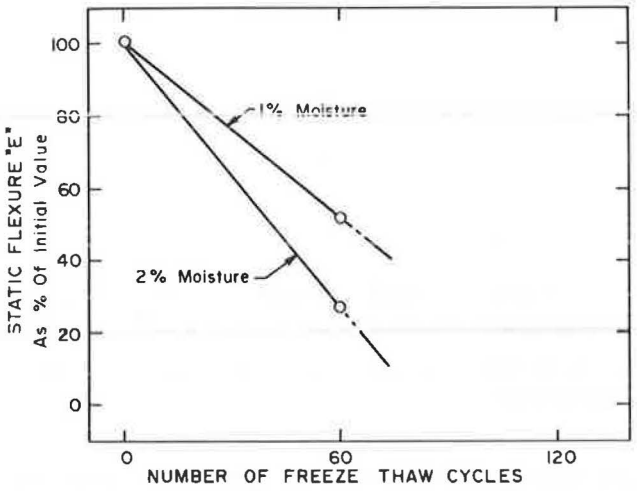

FIGURE 8 Reduction of relative value of static E with number of freeze-thaw cycles.

The dynamic modulus of elasticity was evaluated by measuring fundamental transverse frequency with instruments conventionally used for taking such measurements for portland cement concrete specimens. Relative values of dynamic E as a function of the number of freeze-thaw cycles are shown in Figure 9

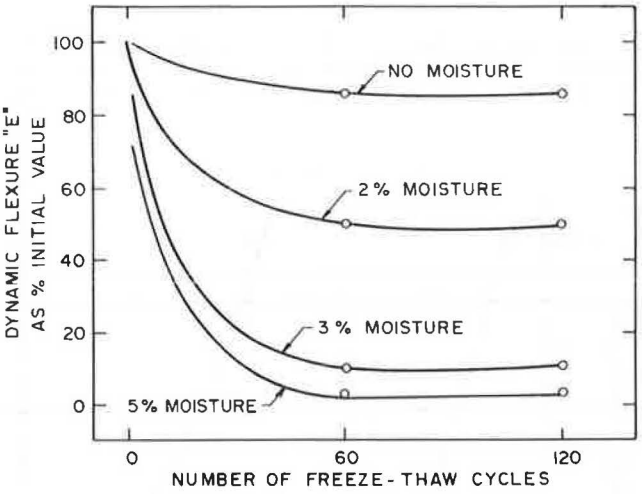

FIGURE 9 Reduction of relative values of dynamic E with number of freeze-thaw cycles.

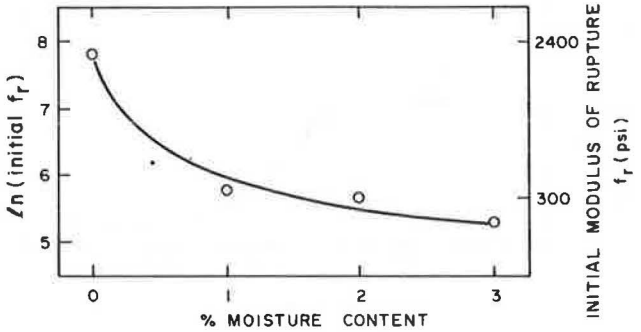

FIGURE 10 Initial modulus of rupture as function of moisture content.

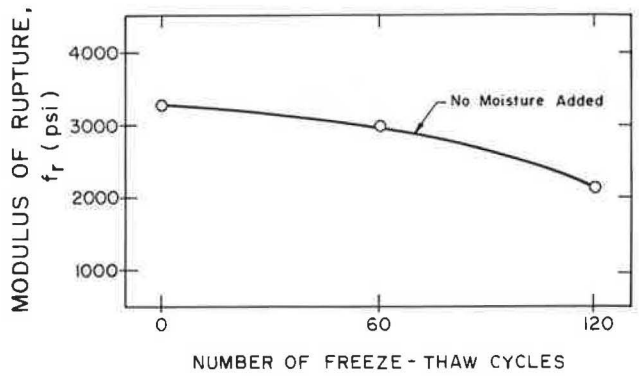

FIGURE 11 Degradation of modulus of rupture with increasing number of freeze-thaw cycles.

for varying moisture content. Increasing freeze-thaw degradation with increasing moisture content and substantial degradation after 60 cycles were evident. Small degradation due to freeze-thaw exposure was evident even for specimens with no added water.

Because the specimens remained intact after the conclusion of tests for static and dynamic E, the same specimens were utilized to obtain modulus of rupture (f_r), which was evaluated by failing the specimens in flexure. Even before any freeze-thaw cycling, the reduction in f_r is precipitous because of a small increment in added moisture. Initial f_r as a function of moisture content, plotted on a semilog scale, is shown in Figure 10. Even for specimens with no added water, degradation of f_r with increasing number of freeze-thaw cycles was evident, as shown in Figure 11.

CONCLUSIONS

Epoxy mortar is susceptible to fatigue damage due to repeated impactive loading. Within the range of 0 to 150°F, fatigue resistance degrades significantly with increasing temperature and improves with decreasing temperature.

All mechanical properties of epoxy mortar degrades significantly because of even a small amount of water added to the fine aggregate.

Epoxy mortar may be susceptible to freeze-thaw damage. Freeze-thaw resistance degrades significantly because of even a small amount of water added to the fine aggregate.

ACKNOWLEDGMENTS

Discussions with R.J. Schutz of Protex Industries and J. Heinen of Nash-Babcouck Engineering were invaluable in planning the work reported here. The Probond 831C Epoxy Bonding System was contributed by Protex Industries. Funding was provided by the Duke University Research Council, by the Richard Leach Endowment, and by the School of Engineering, Duke University. Tests for measurement of dynamic modulii were conducted at the facilities of the Virginia Highway and Transportation Research Council.

REFERENCES

1. K. Okada et al. Thermo-Dependent Properties of Polyester Resin Concrete. In Polymers in Concrete, American Concrete Institute, Detroit, Mich., 1978.
2. R.K. Ghosh. Concrete Repairs with Epoxy and Polymer Resins. In Highway Research Record 327, HRB, National Research Council, Washington, D.C., 1970, pp. 12-17.

Publication of this paper sponsored by Committee on Adhesives, Bonding Agents and Their Uses.

A Study of Bond Strength of Portland Cement Concrete Patching Materials

FRAZIER PARKER, JR., G. EDWARD RAMEY,
RAYMOND K. MOORE, and FORREST W. FOSHEE

ABSTRACT

Laboratory studies were conducted to evaluate bond strength between rapid-setting portland cement concrete (PCC) patching materials and PCC pavement. Slant shear and impact tests were used to evaluate bond strength development. Rapid-setting PCC, Roadpatch, and polymer concrete were evaluated. Manufacturer-recommended bonding agents were used with Roadpatch and polymer concrete. Portland cement grouts and epoxy were used with rapid-setting PCC. Nails installed along bond surfaces were evaluated as mechanical anchors. Testing was conducted after 6-hr curing for early-strength evaluation and after subjecting samples to cyclic temperature variations for durability evaluation. The slant shear test proved to be a valuable one for measuring bond strength development. Roadpatch and rapid-setting PCC provided desirable strength characteristics. Polymer concrete had superior early bond strength, but its long-term strength gain and durability were not as good as those of Roadpatch or rapid-setting PCC. Epoxy bonding agents were adversely affected by low temperatures and PCC grout was adversely affected by high temperatures. The inclusion of 1/8-in. diameter nail anchors along bond surfaces did not measurably improve bond strength.

The major focus of federal, state, and local highway agencies has shifted from construction of new facilities to maintenance, repair, and rehabilitation of existing facilities. The Interstate system is virtually completed, and older, more heavily traveled sections, which have experienced traffic that has often exceeded design weights and volumes, are requiring increased maintenance and often complete rehabilitation.

A large portion of heavily traveled urban Interstate pavements is composed of portland cement concrete (PCC). Before and during complete rehabilitation, patching of cracked and deteriorated areas, joint repair, and joint resealing are required. Heavy traffic conditions on urban freeways create difficult, hazardous, and costly maintenance operations. Speed of repair and strength and durability of the patch are at a premium. Patch strength and durability are directly related to the bond developed between the patch and the base concrete. The research reported here evaluated the relative bond strength developed between several rapid-setting patching materials and base concrete. The work also investigated sensitivity of strength development to the use of several bonding agents and anchors.

IMPORTANT PATCH PROPERTIES

High early strength is a major requirement of a rapid-setting patching material. Although minimum acceptable early-strength values have not been definitely established, O'Conner (1) has suggested compressive strengths of 300 psi at 2 hr and 2,500 psi at 24 hr. Ross (2) has suggested 6 hr as the maximum time that a patch could be allowed to cure before the road is opened to traffic within an 8-hr work shift. This value was used for early-strength evaluation.

A patch must be durable to withstand environmentally induced stresses without debonding. Bond strength durability was evaluated by comparing the strengths of specimens subjected to cyclic temperature variations with those of control specimens of the same age. One group was subjected to daily temperature variations of 80 to 120°F and a second group to variations of 15 to 50°F.

Patches are subjected to traffic-induced dynamic stresses, and therefore ductile behavior to provide energy absorption capacity and fracture resistance is desirable. Patch resistance to dynamic loading was evaluated by performing impact tests on overlays of patching materials bonded to base concrete. The energy absorbed during impact and failure of the test specimens was assumed to be indicative of the ductility of the composite specimens.

MATERIALS EVALUATED

Three rapid-setting materials--Roadpatch, polymer concrete, and a rapid-setting PCC--were evaluated. Roadpatch is a proprietary patching material. The particular polymer cementing agent used in the tests was a proprietary two-component methyl methacrylate system.

Each proprietary patching product was mixed and placed according to the manufacturer's recommendations. Gradations of the fine and coarse aggregates used as fillers in the patching materials are given in Table 1. Both were commercial materials produced by washing and grading natural sand-gravel. The predominant mineral constituent was quartz.

Roadpatch with Steel Fibers

Roadpatch is a fast-setting nonshrinking portland cement (PC)-base patching material. The manufacturer alleges 1-hr compressive strength of 1,500 psi with

TABLE 1 Aggregate Gradations

Sieve Size	Percent Fines by Weight: Coarse Aggregate	Percent Fines by Weight: Fine Aggregate
3/4 in.	100	–
1/2 in.	97	–
3/8 in.	59	100
No. 4	2	96
No. 8	–	85
No. 16	–	68
No. 30	–	39
No. 50	–	19
No. 100	–	7

0.005 percent expansion on setting. Ingredients, including steel fibers, are proportioned and packaged by the manufacturer. Coarse aggregate was added to this mixture (50 percent by weight) to serve as a filler material. A slurry consisting of the cementitious ingredients was used as a prime coat to enhance bonding.

Polymer Concrete

Polymer concrete consisted of a rapid-setting low shrinkage two-component methyl methacrylate system and coarse aggregate. In addition to a monomer and hardener, the manufacturer-supplied cementing system contained fine aggregate. To this, coarse aggregate (50 percent by weight) was added. The manufacturer alleges cured (45 min to 2 hr) compressive strengths, for the mortar, of 8,000 psi with 0.012 percent linear shrinkage. A two-component methyl methacrylate-based primer was used to enhance bonding.

Rapid-Setting PCC

Type III PC and 2 percent (by weight of PC) $CaCl_2$ were used to promote rapid strength development in the PCC. The mix had a water-cement ratio of 0.43, with the following ingredient proportions: water, 348 lb/yd^3; cement, 810 lb/yd^3; fine aggregate, 1,300 lb/yd^3; coarse aggregate, 1,400 lb/yd^3.

The problems associated with the use of $CaCl_2$ in concrete that contained steel were recognized. However, it was used in the study rather than one of the available nonchloride accelerators because of its established set-accelerating properties. Its use precluded the introduction of an additional variable for consideration.

Patches were constructed with no bonding agent applied to bond surfaces, with a neat-cement (Type III) grout, or with an epoxy grout as a bonding agent.

TESTING PROGRAM

Patch materials, bonding agents, and anchors were evaluated with a series of laboratory tests on patch material specimens, base concrete specimens, and composite specimens of patch material and base concrete. Static and impact loading were employed to measure material strength and bond strength between patch materials and base concrete. Specimens of various ages were tested to assess rate of strength gain. Specimens subjected to cyclic temperature variations were tested to assess environmentally related strength deterioration.

Test Procedure

Three types of laboratory tests were performed. Compressive tests were employed to evaluate the strength of patching materials and base concrete. Slant shear tests were used to evaluate bond strength between patch materials and base concrete. Impact tests were performed to evaluate dynamic bond strength and energy-absorbing capacity of patches. Compressive strength tests were performed according to ASTM Method C 39-72 on 4 x 8-in. cylindrical specimens. Slant shear and impact tests are described in the following paragraphs.

Slant Shear Test

Bond strength was assessed by a composite cylinder test called the Arizona Slant Shear Test (3), which has been adopted by ASTM as Method C 882-78 (Bond Strength of Epoxy-Resin Systems Used with Concrete). The specimens consisted of 4 x 8-in. composite cylinders of base concrete and patching materials as shown in Figure 1. Patching materials were cast on hardened half-volumes of base concrete having bond planes inclined at 30 degrees from the longitudinal axis of the cylinder. The bond surface was prepared by sandblasting to remove laitance and expose aggregate.

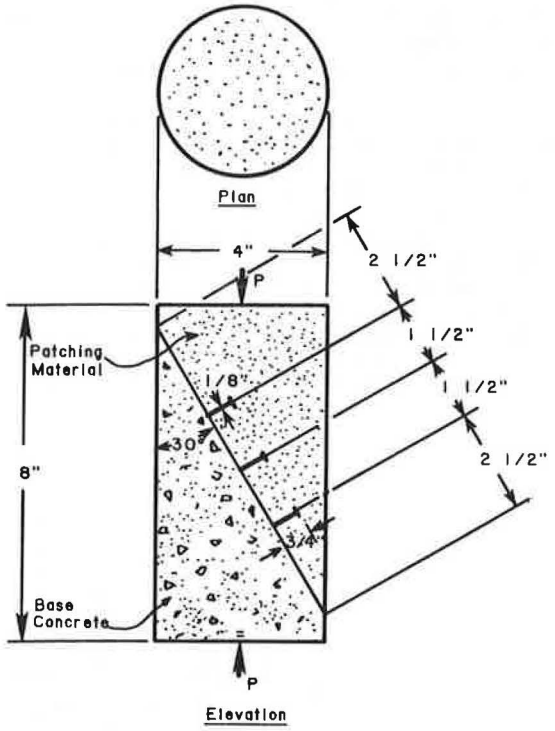

FIGURE 1 Slant shear specimen.

Three 1/8-in. diameter nails were grouted into the base concrete along the bond surface on part of the specimens to evaluate their effectiveness as anchors. The nails were centered in the bond area as shown in Figure 1.

The measure of strength from the slant shear specimens was computed by dividing the compressive axial load by the cross-sectional area measured perpendicular to the cylinder axis (12.57 in.^{2}). This indicates the compressive strength and is different

from the bond strength that would be obtained by dividing the component of axial load parallel to the bond surface (P cos 30 degrees) by the bond area 25.13 in.^{2}). Compressive strength was selected for comparative purposes and is reported here rather than pure bond strength because it permits direct comparison with compressive strength of patch materials and base concrete. It also permits utilization, for comparative purposes, of the results from approximately 20 percent of the specimens that did not experience pure bond failure. Bond strength can be obtained by multiplying the reported compressive strengths by 0.43.

Impact Test

The impact test was designed to measure the energy absorbed by a block-overlay specimen when struck by an impact load sufficient to cause fracture. The impact strength of the base concrete was determined by testing homogeneous specimens that were monolithically cast in a block-overlay configuration. The impact strength of patches was measured by using specimens composed of an overlay of patching material cast on a block of base concrete as shown in Figure 2. The bond surface was prepared by sandblasting.

Two 1/8-in. diameter nails were grouted into the base block along the bond surface on part of the specimens to measure their effectiveness in increasing energy absorption capacity. The nails were located as shown in Figure 2.

A frame-supported pendulum was used to perform the impact tests (4). The pendulum consisted of a steel rod (approximately 5 ft long) with an impact head (20.4 lb) bolted to one end and an axle welded to the other. The impact head was constructed of welded steel plates, which provided a smooth impact surface. The axle was mounted into roller bearings on either side of the frame, allowing the impact head to swing freely in an arc. A pointer attached to the axle registered the angle of inclination of the pendulum, and a following pointer attached to the frame measured the total angle that the pendulum swung through after being released.

After a test specimen was positioned and locked into the jig, the pendulum was raised to a horizontal position. The following pointer was adjusted to measure the angle that the pendulum would swing through from this horizontal position and the pendulum released. The pendulum rotated through an arc causing the leading plate of the impact head to strike off the overlay of the specimen. The impact occurred as the head swung through the lowest point of its arc. The specimen and impact head were aligned so that the leading plate of the impact head would strike the overlay flush across the face of contact.

It was found that the pendulum made a free-swing arc of 175.5 degrees. The 4.5 degree difference in angle was due to the inherent energy losses (caused by friction of the moving parts) of the machine. The energy dissipated by the fracture of the specimen could be determined from the difference in angle of the arc measured after impact and the free-swing arc of 175.5 degrees.

The relationship between the angle of pendulum rotation and the energy absorbed by the specimen during fracture is given by

$$E = 103.8 - 112.6[1.0 - \cos(A - 90°)] \quad (1)$$

where E is the energy absorbed by the test specimen during fracture in foot pounds and A is the angle measured from the horizontal to the maximum height of the pendulum after impact in degrees.

Test Series

Four groups of tests were designed to accomplish program objectives. Group 1 tests evaluated rapid bond strength development. Composite slant shear cylinders were loaded in compression to determine static strengths, and composite impact specimens were impact loaded to determine dynamic strengths. Group 1 specimens were tested after 6 hr of moist curing.

Group 2 tests evaluated long-term bond development. Composite slant shear cylinders were loaded in compression to determine static strengths and composite impact specimens were impact loaded to determine dynamic strengths. Group 2 specimens were tested after 3 days' moist curing and 30 days' air curing. The results were used as the basis for evaluating bond strength loss with weathering.

Groups 3 and 4 tests evaluated the durability of

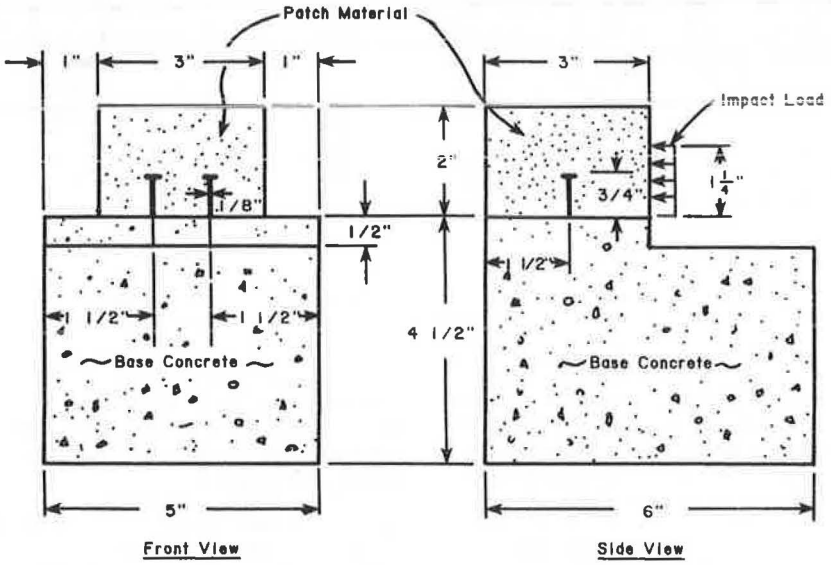

FIGURE 2 Composite impact specimen.

static and dynamic bond strength. Composite slant shear specimens were loaded in compression to determine static strength and composite impact specimens were impact loaded to determine dynamic strengths. Group 3 specimens were loaded after 3 days' moist curing followed by 30 days of exposure to cyclic high temperatures. Group 4 specimens were loaded after 3 days' moist curing followed by 30 days of cyclic freezing and thawing. Daily cyclic temperature variations for these groups are shown in Figure 3.

EXPERIMENTAL RESULTS AND DATA ANALYSIS

Data generated in the testing program are presented and analyzed in this section. Each reported compressive strength or energy absorption is the average from tests of two specimens. Comparisons between the strengths were made by using the F- and t-tests at a 5 percent level of significance. The F-test was used to compare standard deviations of the distributions. When the F-test permitted acceptance of the hypothesis of equal standard deviations, the t-test was used to compare mean strengths. When the F-test dictated rejection of the hypothesis of equal standard deviations, a modified t-test was used to compare mean strengths. The hypothesis of equal mean values was tested with the t- or modified t-test. Modes of failure, particularly for impact tests, had a significant effect on the test results and are considered along with quantitative static and impact strength data.

Strength of Base Concrete

Each test group contained control specimens that were cast from the same concrete batch used to form

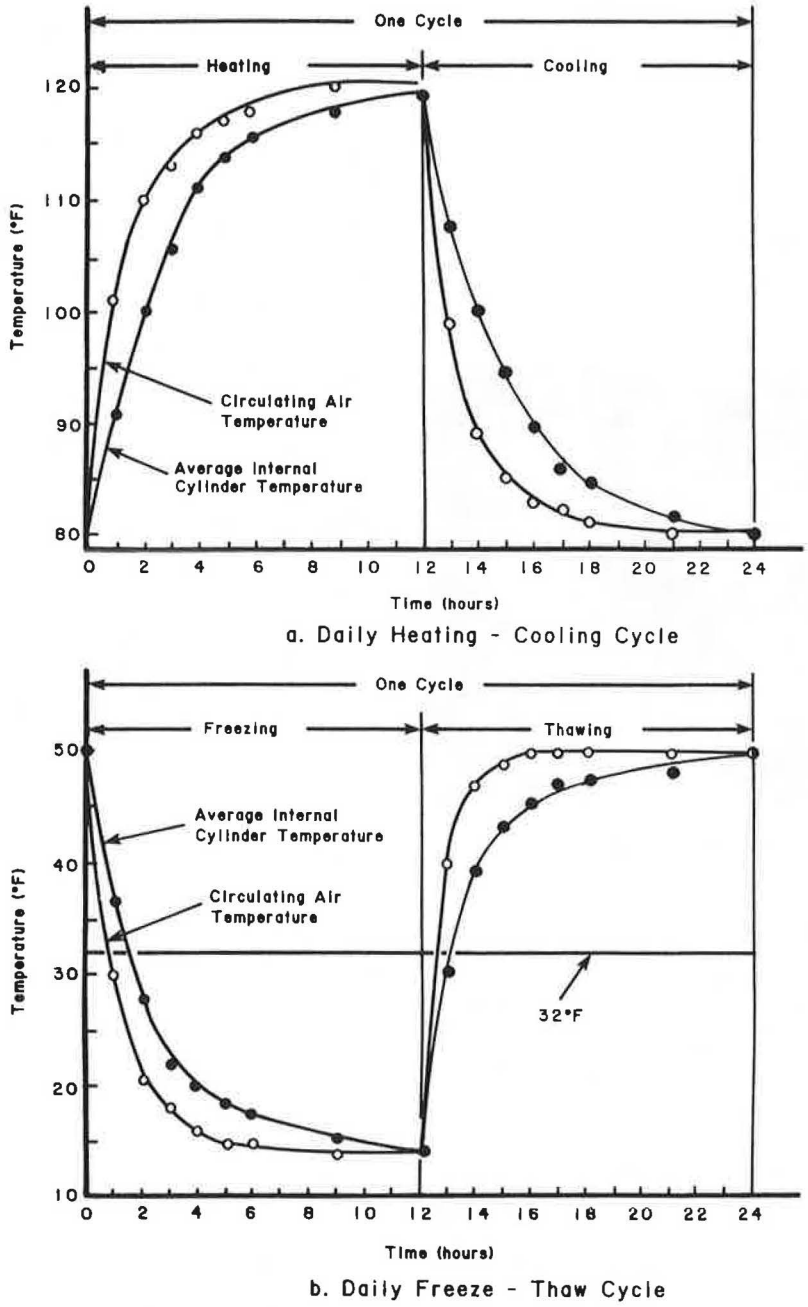

FIGURE 3 Simulated weathering process.

the half-cylinders and base blocks. These control specimens were moist cured for 28 days and then subjected to the same conditions as the composite specimens in the particular group. The intent was to provide bases for patching that would have strengths greater than those of the patch materials. Compressive strengths and energy absorption capacities of the homogeneous base concrete specimens are given in Table 2.

TABLE 2 Compressive Strength and Energy Absorption Capacity of Base Concrete

Test Series Designation	Average Compressive Strength (psi)	Average Energy Absorbed (ft-lb)
Group 1	6,088	51
Group 2	6,784	60
Group 3	6,545	65
Group 4	6,008	37

Failure Modes

Three modes of failure were observed in slant shear tests. These are shown in Figure 4 and were designated bond failures, bond or base failures, and bond or patch failures.

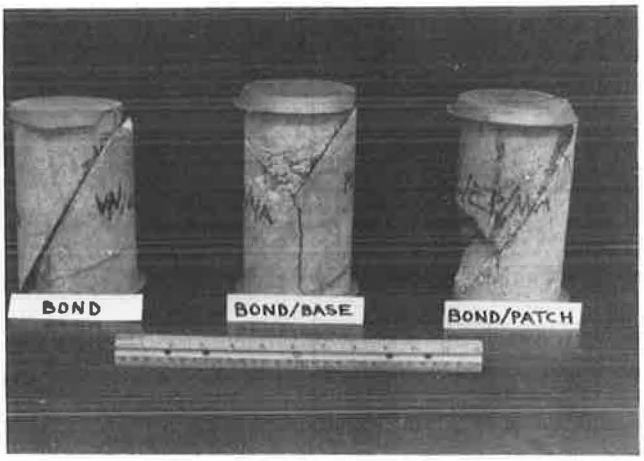

FIGURE 4 Failure modes for slant shear specimens.

Bond failures were the most common and were characterized by a sudden rupture along the bond surface at the maximum load. The bond or base and bond or patch failure modes occurred in one-third of the cured and weathered specimens. These were characterized by failure planes that deviated from the bonding plane into the base concrete or patching material.

The composite impact specimens exhibited four modes of failure. These are shown in Figure 5 and are designated bond failures, base failures, bond or base failures, and bond or patch failures. Bond failures occurred in only a portion of the 6-hr tests. Tests in Groups 2, 3, and 4 experienced one of the three latter failure modes. In these specimens the bond strength, or the residual strength provided by anchors, was sufficient to cause failure in the base or patch material.

FIGURE 5 Failure modes for composite impact specimens.

Variations in failure mode were undesirable because quantitative bond strength comparisons could only be made between specimens that had similar failures. Only 8 percent of the composite impact specimens exhibited pure bond failure; therefore, only qualitative comparisons of energy absorption capacities can be made. To provide quantitatively meaningful data the size of the base block would have to be increased to ensure failure along the bond surface.

Results from the slant shear test generally provided a sound basis for comparing relative bond strengths of patching materials and techniques. Approximately 80 percent of the composite cylindrical specimens exhibited bond failures.

Six-Hour Compressive Strengths of Patching Materials

Average 6-hr compressive strengths of the patching materials were rapid-setting PCC, 2,646 psi; Roadpatch, 1,930 psi; and polymer concrete, 4,357 psi. A graphic comparison of these strengths is shown in Figure 6. Comparisons with the t-test at the 5 percent level of significance indicated significant differences in mean strengths. The polymer concrete obviously developed the largest early strengths, but strengths of the PCC and the Roadpatch appear to be adequate for patching.

Six-Hour Strength

Results of Group 1 slant shear tests are presented in Figure 7. All specimens experienced bond failures. The anchored and unanchored polymer concrete specimens had strengths at least 56 percent greater than those of any of the other specimens. The unanchored PCC specimens with an epoxy prime had the lowest strength. This strength was significantly lower than that of the PCC specimens with no bonding agent. A general-purpose epoxy bonding system, with manufacturer-recommended Type II or III (ASTM C 881-78), was used for the prime coat. Specification pot life for the epoxy varied from 60 min at 50°F to 30 min at 90°F. A more rapid-setting epoxy formulation would likely have increased the rate of bond development.

A comparison of unanchored PCC specimens with no bonding agent and unanchored PCC specimens with a PC grout shows that the PC grout significantly increased the average strength. The strength increase was about 730 psi. A comparison of PCC with PC grout specimens

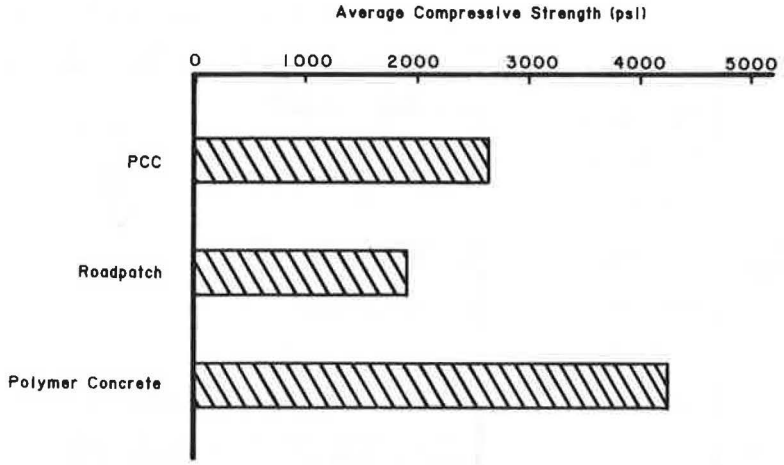

FIGURE 6 Average 6-hr compressive strengths of patching materials.

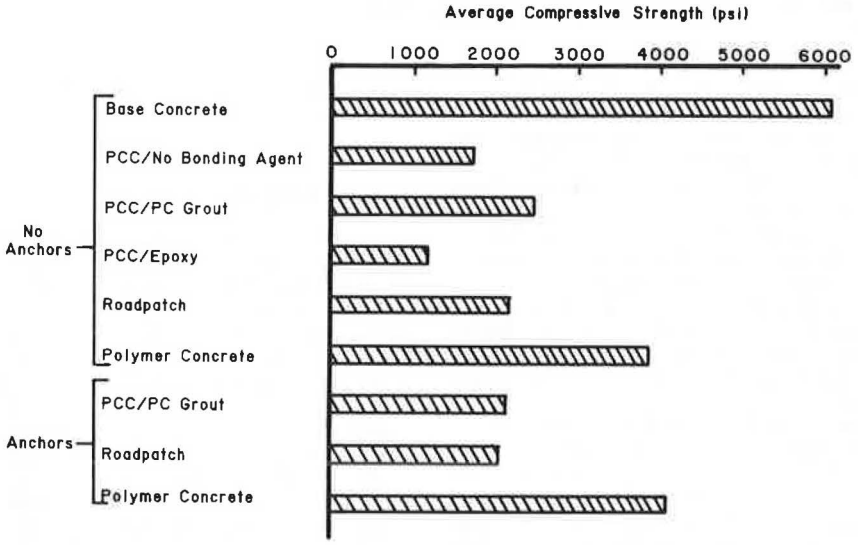

FIGURE 7 Average 6-hr compressive strengths: Group 1 tests.

and Roadpatch specimens reveals comparable strengths with no significant differences. Also, it appears that the presence of anchors did not appreciably increase slant shear strength. Comparison of anchored and unanchored strength for PCC with PC grout, Roadpatch, and polymer concrete revealed that there was no significant difference in the average strengths.

Results of Group 1 impact tests are presented in Figure 8. Only the unanchored PCC specimens with no prime or with PC grout experienced bond failures. Therefore, when energy absorption capacities are compared, the specimen's failure mode must be considered. Where failure modes were different, comparisons are by necessity qualitative.

From Figure 8 it can be noted that those specimens experiencing base or bond and base failures had energy absorption capacities between 42 and 61 ft-lb, which is similar to that measured for the base concrete (51 ft-lb). This is to be expected because these specimens failed through the base as did the homogeneous specimens of the base concrete. The bond strength in these specimens was sufficient to cause failure in the base and, thus, the similarities in energy absorption.

The unanchored PCC specimens with no bonding agent or with PC grout experienced bond failures and had the lowest energy absorption capacities. Comparison can be made between the static and dynamic strength of the unanchored epoxy-bonded PCC specimens. The average slant shear strength for these specimens was the lowest of all the patching materials and techniques. However, the impact specimens exhibited base failures and their average energy absorption capacity was the highest of all the unanchored specimens. Although the magnitude of energy absorption capacity is not significant, these results suggest that the strength of the epoxy-bonded specimens was sensitive to the loading rate, resulting in effective energy dissipation during dynamic (i.e., impact) loading but poor static strength.

The high energy absorption capacities of the anchored PCC and Roadpatch specimens and the bond-patch failure mode provide an interesting comparison with the anchored polymer concrete specimens. On the basis of measured energy absorption, the anchored PCC and Roadpatch were superior. However, on the basis of failure mode the polymer concrete was superior because failure occurred through the base. The high measured energy absorption capacities of the anchored PCC and Roadpatch were primarily due to the testing mechanism and failure mode. On impact, bond failure occurred and the load was transferred

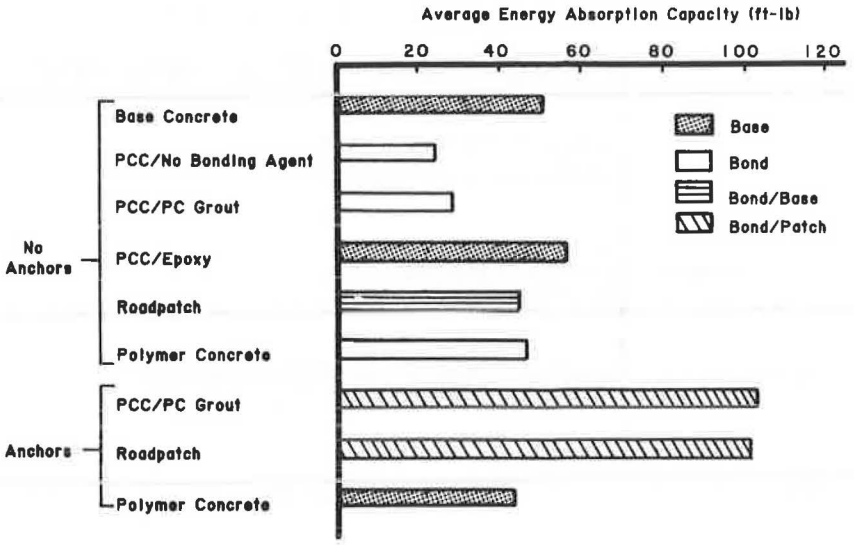

FIGURE 8 Average 6-hr energy absorption capacities.

to the ductile anchors. The anchors had sufficient strength to essentially stop the pendulum, thus giving an indication of high energy absorption. This behavior illustrates one of the benefits of anchors, which is that they hold the patch in place after bond failure occurs. This behavior also illustrates the improper application of the test for measuring bond strength of anchored specimens and suggests a remedial testing technique. A more appropriate procedure would be to increase the arc through which the pendulum rotated before striking the specimen until bond failure occurred. This loading procedure would provide comparable results for both anchored and unanchored specimens.

After the early-strength tests had been completed, several changes were made in the types of patching materials and techniques for Groups 2, 3, and 4. Testing of unanchored PCC specimens with no bonding agent was discontinued because of low strength and energy absorption capacity. Because the anchors had no measurable effect on strengths of polymer concrete and Roadpatch, anchored specimens of these materials were eliminated. The low strengths and large failure strains of unanchored epoxy-bonded PCC specimens indicated a need for anchors. The reasoning was that as strain occurred along this bond surface, a portion of the load would be transferred to the anchors, thus increasing bond strength of epoxy-bonded PCC patches.

Cured Strength

Control specimens (Group 2) were tested to establish a basis for assessing bond strength loss due to weathering and to assess long-term bond strength gain. Curing conditions were 3 days' moist cure followed by 30 days' air cure at 70°F. Groups 1 and 2 slant shear tests are presented in Figure 9 to facilitate comparison. Most specimens failed in pure bond although three exhibited a bond-base failure, indicating sufficient bond strength to cause base concrete failure. All cured specimens except those with epoxy bonding agents had compressive strengths in excess of 5,000 psi. The unanchored epoxy-bonded specimens did, however, exhibit the largest (415 percent) percentage strength increase. The anchored epoxy-bonded specimens had the smallest cured strength. Comparable 6-hr tests were not performed for this case, and thus no assessment of strength gain was possible. The polymer concrete specimens achieved the smallest strength gain (67 percent). The Roadpatch specimens achieved the largest cured strength (6,187 psi). However, when compared with

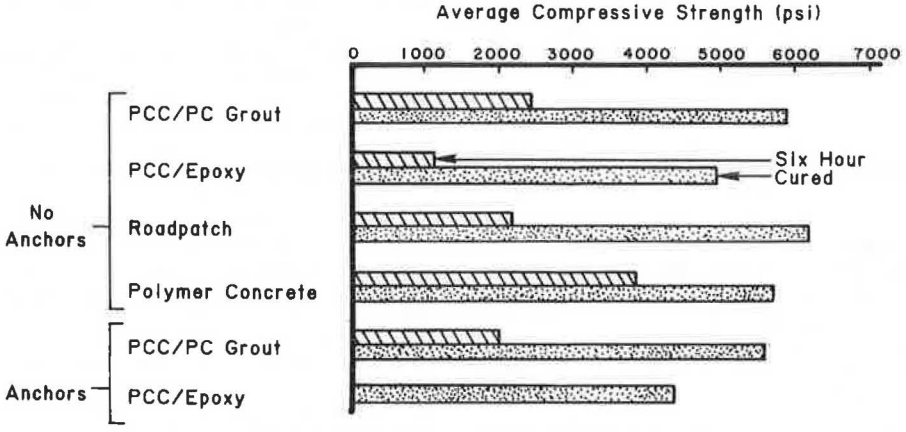

FIGURE 9 Comparison of 6-hr and cured strengths.

other cured strengths it was only significantly different (5 percent level) from that of the anchored epoxy-bonded PCC specimens.

All Group 2 impact specimens exhibited base failures, indicating sufficient bond strength to cause failure in the base block. Qualitatively, implications of impact results are that all materials and bonding techniques develop impact bond strengths capable of causing base failures; that is, they are the same as homogeneous specimens.

Weathered Strength

Results from slant shear specimens subjected to temperature variations are presented in Figure 10 along with control test data. Bond failure predominated and quantitative comparisons with control specimens provide valid indications of bond strength loss.

The PCC specimens (anchored and unanchored) with epoxy prime had the smallest strengths for Groups 2, 3, and 4. This is further evidence that the particular epoxy used was not beneficial for bond development and is particularly true for the cold weathered specimens, which have by far the least strength.

The unanchored and anchored PC-grout-bonded PCC specimens had lower (19 and 10 percent, respectively) strengths when subjected to the high temperatures. At a 5 percent level of significance, the strength of the unanchored specimens subjected to high temperatures was different from that of comparable cured specimens, but the strength of anchored high-temperature specimens was the same as that of comparable cured specimens. The fact that the 10 percent strength difference for anchored specimens is not significant is attributable to the large (1,632 psi) range for the weathered strength. At a 5 percent level of significance, the strengths of anchored and unanchored specimens subjected to low temperatures were the same as comparable cured strengths. It was reasoned that the reduced hot-weathered strengths were possibly due to drying and shrinkage of the grout bonding layer.

The strength of the hot-weathered epoxy-bonded PCC specimens was lower, whereas the strength of the hot-weathered anchored epoxy-bonded PCC specimens was higher than that of control specimens. These differences were not significant at a 5 percent level and no definitive conclusions can be drawn about the effects of high temperatures on epoxy bonding. However, the low temperatures had a significant (5 percent level) adverse effect on the strengths of unanchored and anchored epoxy-bonded PCC specimens. These strengths were only 47 and 63 percent, respectively, of the control specimens. This result is a consequence of the temperature dependency of the epoxy curing and a degradation of bond.

The patching materials least affected by the cyclic temperatures were Roadpatch and polymer concrete. Both the hot- and cold-weathered Roadpatch specimens exhibited strengths that were over 94 percent of the strength of the control specimens. At a 5 percent level of significance the strengths were the same. The polymer concrete specimens showed excellent resistance to high temperatures (only 1 percent decrease), but experienced a loss of strength (13 percent) when subjected to low temperatures. At a 5 percent level of significance the high-tempera-

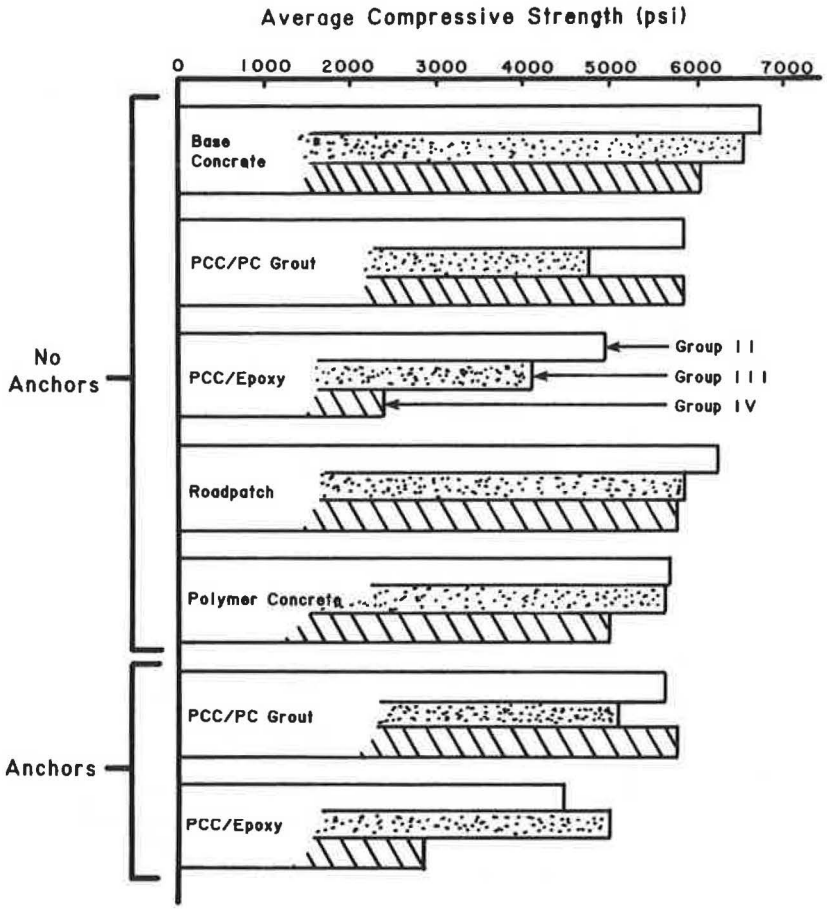

FIGURE 10 Comparison of cured and weathered strengths.

ture strength was the same but the low-temperature strength was different from the cured strength.

As in the 6-hr slant shear tests, the anchors had no discernible effect on the strengths. The anchors also failed to reduce strength loss due to variable temperature.

The modes of failure experienced by the slant shear specimens provided no indication that cyclic temperature variations caused a decrease in bond strength. In general, bond failures were observed for corresponding specimens in Groups 2, 3, and 4. The Group 4 anchored grout-bonded PCC specimens were an exception and exhibited bond-patch failure. No totally satisfactory explanation can be offered, but the retardation of strength gain of the PCC patch material appears plausible.

Control specimens and specimens subjected to high and low temperatures experienced base-block failures when impact loaded. As a consequence the measured energy absorption capacities are quantitatively inappropriate measures of bond strength.

Several qualitative comparisons may be made by examining the results from Groups 2, 3, and 4 impact tests. Epoxy-bonded specimens experienced base failures, indicating that the dynamic bond strength is sufficient to cause failure in the base blocks. This is considered further evidence that epoxy bonding is sensitive to rate of loading. With the slow rate of loading employed in the slant shear test the epoxy-bonded specimens experienced bond failures and gave lower strengths. Although there are inconsistencies and scatter (Figure 11), the energy absorption capacities of the epoxy-bonded specimens are comparable with strengths of other specimens in the same group.

The one instance where the measured energy absorption capacities were considered quantitatively significant was for the hot-weathered (Group 2) unanchored PC-grout-bonded PCC specimens. The weathered strength was only 53 percent of that of the control specimens (Figure 11), and these specimens experienced a bond-base failure rather than a base failure. The hot weathering process had an adverse effect on bond strength.

CONCLUSIONS

The objectives of this project were to evaluate rapid-setting PCC pavement patching materials, bonding agents, and anchor systems. The following conclusions summarize the major findings of the research:

1. Roadpatch and rapid-setting PCC provide desirable patch properties.
2. Polymer concrete had superior early bond strength but its long-term strength gain was not as good as that of the Roadpatch or rapid-setting PCC. Cold temperature weathering also caused a larger decrease in strength of polymer concrete.
3. Epoxy had a slow rate of strength gain and was adversely affected by low temperature; its bond strength was sensitive to rate of loading. Type III PC grouts improved bond strength but were susceptible to high-temperature weathering.
4. The inclusion of 1/8-in. diameter nails did not measurably improve bond strength, but it did increase the ductility and energy absorption capacity of the patches.

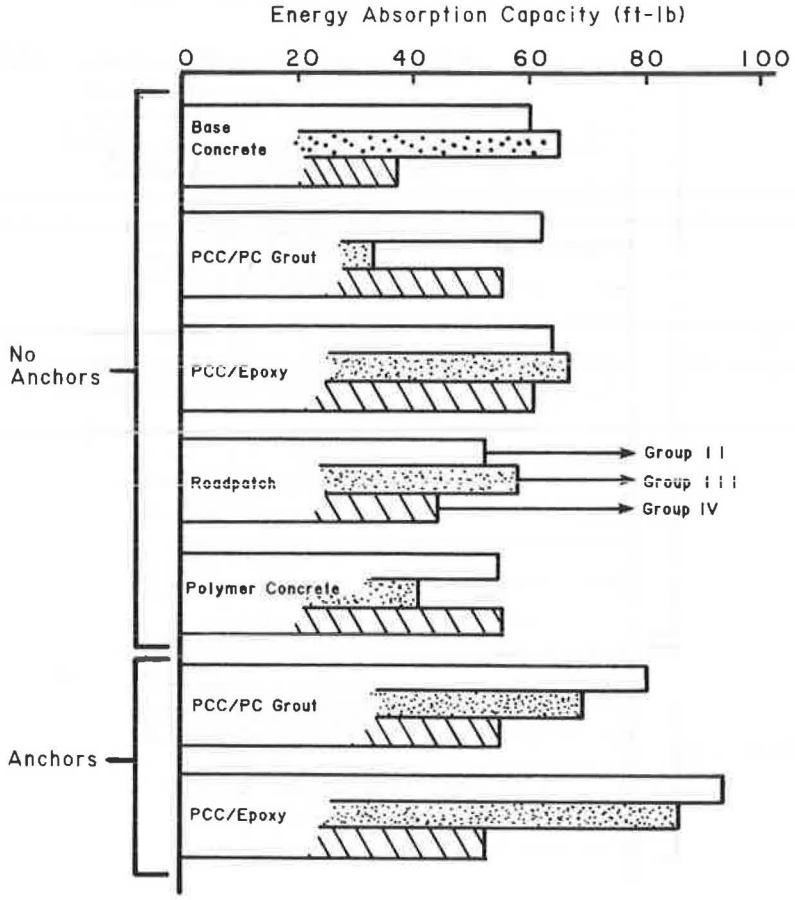

FIGURE 11 Comparison of cured and weathered energy absorption capacities.

5. The impact test, as used, was unsatisfactory for evaluating dynamic bond strength.

ACKNOWLEDGMENTS

The work reported in this paper was sponsored by FHWA, U.S. Department of Transportation, through the State of Alabama Highway Department (Alabama Highway Department Project 930-107). The authors are grateful for their sponsorship, assistance, and cooperation.

REFERENCES

1. D.L. O'Conner. Rapid Setting Cement Mortars for Concrete Repair. Report 3-09-71-020. Materials and Tests Division, Texas Highway Department, Austin, June 1971.
2. J.E. Ross. Rapid Setting Concrete Patching Study. Research Report 84. Louisiana Department of Highways, Baton Rouge, March 1975.
3. J.D. Kriegh. Arizona Slant Shear Test: A Method to Determine Epoxy Bond Strength. Journal of the American Concrete Institute, Vol. 73, No. 7, July 1976, pp. 372-373.
4. A.M. Strickland. An Experimental Evaluation of Rapid Setting Patching Materials Used in the Repair of Concrete Pavements. M.S. thesis. Auburn University, Auburn, Ala., 1982.

Publication of this paper sponsored by Committee on Pavement Maintenance.

Laboratory Evaluation of Four Rapid-Setting Concrete Patching Materials

G. EDWARD RAMEY, RAYMOND K. MOORE, FRAZIER PARKER, JR., and A. MARK STRICKLAND

ABSTRACT

Many proprietary patching products are available for the repair of portland cement concrete (PCC) pavement. These materials must cure rapidly to minimize delay and limit safety hazard exposure to both the traveling public and maintenance personnel. However, long-term strength and durability are equally important, although information concerning these properties and direct comparisons between patching alternatives is limited. Compressive strength, tensile strength, direct shear, and energy absorption tests were used to evaluate polymer concrete, magnesium phosphate cement, Roadpatch with steel fibers, and epoxy-bonded PCC. The split-cylinder tensile bond strengths of the patching materials were comparable to those of the base concrete. The shear bond strengths and energy absorption tests indicated that polymer concrete has good cured properties as a composite patch but may be susceptible to weathering or thermal deterioration. Roadpatch also had satisfactory cured strength properties but had better resistance to decreases in direct shear bond strength and tensile strength when exposed to simulated weathering. Roadpatch appeared to exhibit a good overall combination of characteristics that indicate satisfactory short-term and long-term durability. The epoxy-bonded PCC alternative demonstrated substantial strengths, but the slow rate of strength gain noted was a major disadvantage for potential field application. Magnesium phosphate concrete does not appear to be an attractive early cure material and it may be susceptible to damage from dynamic loading.

Portland cement concrete (PCC) pavement repair performed in urban areas requires rapid-setting patching materials to minimize the maintenance time. Heavy traffic conditions interacting with maintenance work create delay and safety hazards for both the maintenance crews and the traveling public. Rapid-setting patching materials also make possible the scheduling of patching activities in early morning hours. Thus, a pavement patch can be installed and the pavement section reopened to traffic without causing daytime delays.

Many properly applied rapid-setting patching ma-

terials have satisfactory short-term strength and bonding properties. However, long-term durability is also critical because premature debonding of patches creates further pavement deterioration and expensive repatching.

The major objective of the research reported here is to compare the strength and weathering resistance characteristics of selected rapid-setting PCC pavement patching compounds. A laboratory testing program evaluated material and bonding properties, which are fundamentally related to the durability and performance of spall-type patches. Patching materials currently used for shallow-depth surface repairs of PCC pavement slabs and bridge decks were selected. Previously published research indicated that these products possessed satisfactory material strength and short-term durability.

PATCHING MATERIALS

Polymer Concrete

The polymer concrete consisted of a liquid monomer, a premixed powdered hardener, and fine aggregate. One gallon of monomer was mixed with a 30-lb bag of hardener before the addition of 1 gal of pea gravel.

A coat of polymer primer was applied to base concrete to improve the bond before the polymer concrete was placed. The primer, mixed for application for normal weather conditions, was a two-component resin consisting of 1 qt liquid monomer mixed with 11 g of powdered hardener.

Magnesium Phosphate Cement (MPC)

Following manufacturer recommendations, one 50-lb sack of cement was added to 1 gal of water.

Roadpatch with Steel Fibers

Roadpatch was prepared by adding a liquid (one part Acryl 60 and three parts water) to a blend of powdered component and steel fibers to obtain mortar consistency with a 2- to 3-in. slump. A primer coat consisting of Acryl 60 and powdered component was applied to base concrete before the patching material was placed to improve bond.

Epoxy/PCC

An epoxy adhesive (a mixture of two liquid components in a 1:1 volumetric ratio) was applied to base concrete in a thin coat immediately before placement of rapid-setting PCC. The PCC mix design was one part water, two parts Type I cement, four parts natural sand, and six parts pea gravel by weight. In addition, the curing rate was accelerated by dissolving 1 percent (by cement weight) calcium chloride into the mixing water. The PCC was placed while the epoxy adhesive was still tacky.

Base Concrete

Mixture design and materials were identical to those of the rapid-setting concrete except that the calcium chloride was omitted.

TESTING PROCEDURES

Compressive Strength Testing

Cylinders of patching materials 3 in. in diameter by 6 in. were tested by using ASTM Test Method C 39 as a general guide.

Tensile Strength Testing

ASTM Test Method C496 was the general guide for tensile testing of 3-in. diameter by 6-in. cylindrical specimens. Homogeneous specimens were tested to evaluate tensile strengths of individual patching materials and composite cylinders (Figure 1a) were used to measure bond strength at the interface between base concrete and the patching material. Tensile testing was conducted by using flat steel platens; 8-in. long and 0.25-in. thick plywood strips were placed between the specimen and the platens.

Direct Shear Testing

A composite block specimen (Figure 1b) consisting of a 4-in. width of base concrete and a 2-in. cube of patching material cast on the top was subjected to a horizontal static load applied to the vertical face of the cube. Shear strength of the base concrete was obtained by using monolithically cast block-overlay configurations of the same dimensions.

Impact Testing

The composite block specimen (Figure 1b) was tested to evaluate energy absorption capabilities of the composites of patching material and base concrete. A

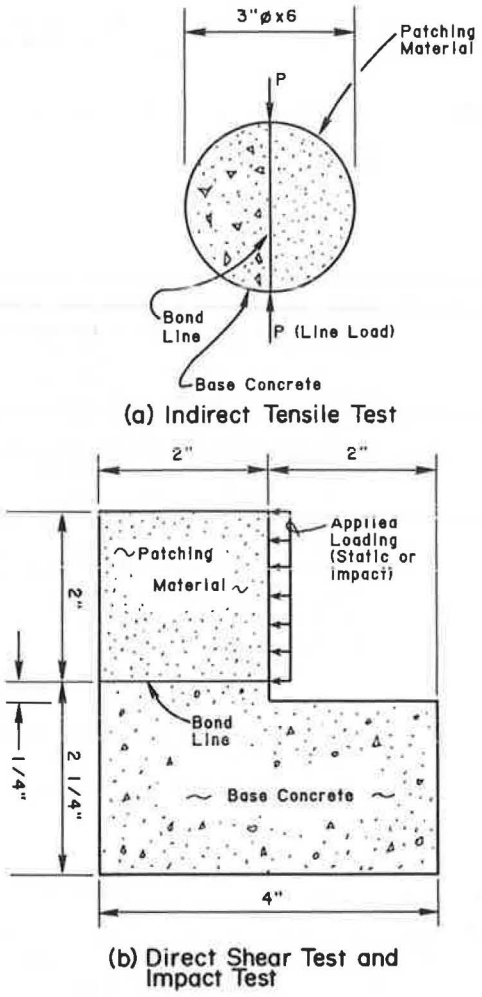

FIGURE 1 Laboratory test specimens.

pendulum impact testing machine was designed so that the pendulum arm was released from an initial horizontal position to swing through an arc and hit the vertical face of the cube at the lowest point of the arc. The energy loss caused by fracturing the bond between cube and base concrete, considered to be the maximum energy absorption capability of the composite of patch material and base concrete, was calculated on the basis of pendulum arc travel.

WEATHERING SIMULATION

One group of laboratory test specimens was placed in random order on metal racks inside a heating-refrigeration unit to simulate field weathering. A minimum 0.5-in. spacing was maintained between specimens and between the specimens and interior walls to provide adequate circulation. Specimens on the top rack were shifted to the bottom rack and other specimens were moved to the rack immediately above at 5-day intervals to prevent preferential temperature changes produced by the air circulation pattern in the unit.

The simulated weathering process is shown in Figure 2. The total time of exposure was 80 days and included two series of 20 daily cycles of freezing and thawing and two series of 20 daily cycles of heating and cooling.

EXPERIMENT DESIGN

Material and bond strengths of all patching materials vary with age and environmental conditions. Three test series described in Table 1 were employed to evaluate the effect of age and simulated weathering exposure.

Rapid-setting patching materials should provide a satisfactory patch in a short period of time. Thus, compressive, tensile, shear, and impact tests should evaluate early strengths and a Group 1 Test Series tested materials 6 hr after specimen preparation. A 6-hr curing period approximates the maximum time a maintenance crew could allow for the curing of typical field-installed patches during an 8-hr work day.

However, epoxy-bonded rapid-setting PCC specimens were tested after 24 hr of curing because a 6-hr curing period was not sufficient time for appreciable strength gains to take place.

Thermal durability of the patching alternatives is an important factor relating to long-term patch performance. Temperature changes may cause deterioration of patching material strength or bond to the patched concrete or both. Weathering resistance was determined by strength measurements following exposure to a series of cyclic temperature changes (Group 3 Test Series). These measurements were compared with corresponding strengths by using non-weathered test specimens in the Group 2 Test Series. Differences between Group 2 and Group 3 Test Series could be attributed to the simulated weathering because curing time was the same. Furthermore, Group 2 strengths can be related to the fully developed properties of the composites of patch material and base concrete.

The strengths shown on the bar graphs represent the means of three duplicate specimens. Coefficients

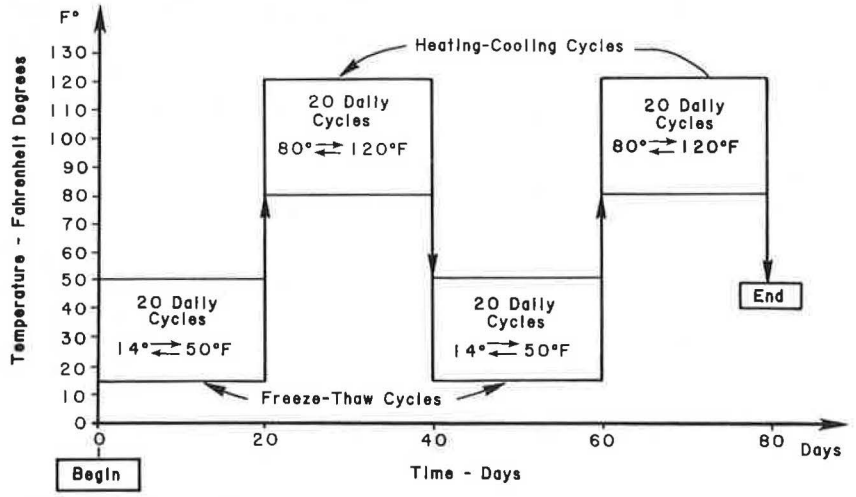

FIGURE 2 Simulated weathering program.

TABLE 1 Experiment Design

Test Series Designation	Age or Exposure of Specimens	Test Series Purpose	Testing Conducted
Group 1	6 hr moist curing in laboratory	Determine early strengths of patching materials and composite patches	Compressive strength, tensile strength, direct shear strength, impact resistance
Group 2	2 days moist curing and 81 additional days in laboratory environment	Determine matured strengths of patching materials and composite patches	Compressive strength, tensile strength, direct shear strength, impact resistance
Group 3	2 days moist curing, 1 day soaking in water, and 80 additional days of cyclic temperature changes	Determine durability potential and thermal degradation of patching materials and composite patches	Compressive strength, tensile strength, direct shear strength, impact resistance

of variation (CV) were also calculated, although the sample size was too small for statistical tests of significance to be utilized with meaning.

COMPRESSIVE STRENGTH RESULTS

As shown in Figure 3, the highest early age (Group 1) mean strength was associated with polymer concrete, followed by Roadpatch and MPC. The data for polymer concrete and Roadpatch had CVs less than 10 percent and the means appear to represent accurate values. The MPC CV exceeded 30 percent, and it appears that the mean compressive strength is overestimated by this limited data set. However, the early age compressive strengths of all three materials are adequate for making quick patch repairs. It should also be noted that the 24-hr average compressive strength of the rapid-setting PCC was 2,080 psi, which was lower than those measured at 6 hr for the proprietary patching products.

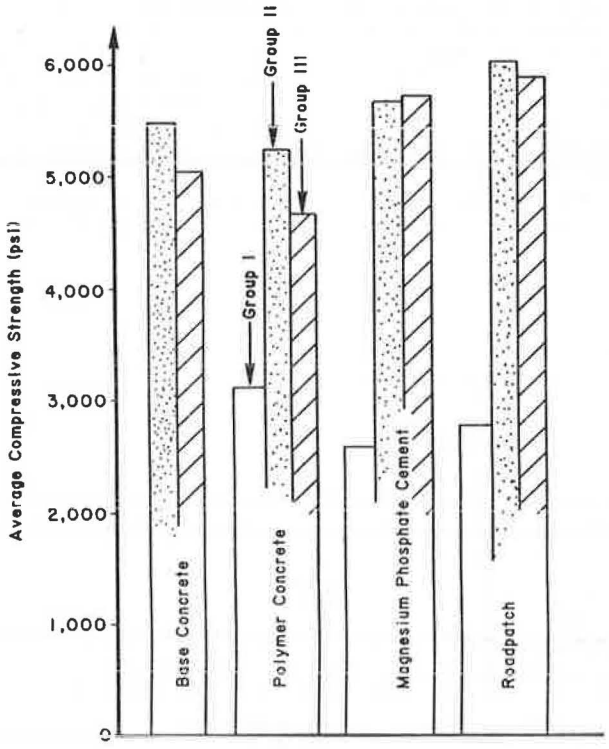

FIGURE 3 Compressive strength results.

Group 2 compressive strengths had minimal variation with CVs less than 20 percent for all materials. The final cured strengths of the patching products were approximately equal to the compressive strength of the base concrete.

A comparison of Group 1 and Group 2 strengths indicates that the patching materials continued to gain strength. This additional strength gain is an assurance that the compressive strengths of the patching materials are adequate for field application.

Group 3 (simulated weathering) results showed little variation (all CVs less than 10 percent). Simulated weathering did not affect the compressive strength of Roadpatch or MPC as much as it did for the base concrete or polymer concrete. Polymer concrete suffered the largest reduction in strength (11 percent). Comparison of Group 2 and Group 3 results suggests that Roadpatch and MPC may provide better weathering and thermal durability.

TENSILE STRENGTH RESULTS

The Group 1 means shown in Figure 4 indicate relatively small differences between patching materials. Homogeneous and composite polymer concrete data showed little variation (CVs less than 5 percent). However, considerable variation (CV greater than 25 percent) was associated with the MPC data. Therefore, the average tensile strength for MPC is not considered as valid as that for the other materials. It should also be noted that the 24-hr average tensile strength of the rapid-setting PCC was 340 psi, which was lower than those measured at 6 hr for the proprietary patching products.

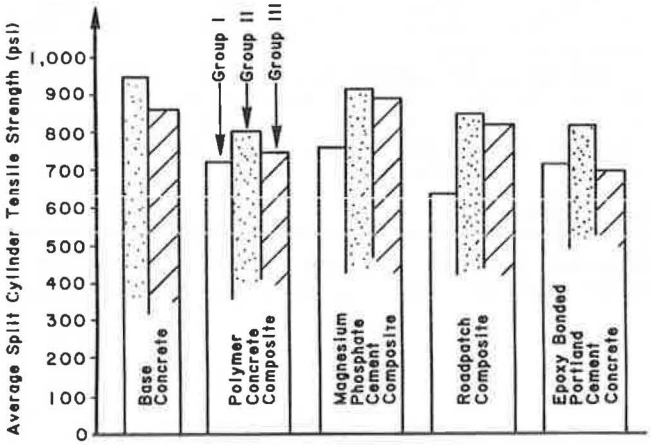

FIGURE 4 Split-cylinder tensile strength results.

The epoxy adhesive provided a strong bond for the concrete half-cylinders. However, the slow curing time of the epoxy renders the epoxy-bonded PCC unattractive for making rapid-patch repairs. The rate of strength gain of the epoxy used for bonding the PCC was very slow and approximately 12 hr was necessary before the epoxy stiffened so that it would not deform when touched. Considering the variance in the test data, it appears that polymer concrete is the better choice of material on the basis of Group 1 testing.

Relatively little variation was present in Group 2 results (all CVs equal to or less than 10 percent). Roadpatch exhibited the greatest tensile strength of the homogeneous test cylinders, which was approximately 30 percent higher than that of the other materials (data not shown in Figure 4). Composite cylinders of patching material and base concrete possessed tensile strengths approximately the same as those of the base concrete.

A comparison of Group 1 and Group 2 strengths indicated a notable increase in tensile strength with time for Roadpatch and a somewhat smaller increase for the other materials. As with the compressive strengths, the increasing tensile strengths are positive indicators that materials selected on the basis of early strength will be adequate in later months.

Comparison of Group 2 and Group 3 strengths indicated a 20 percent reduction in the average tensile strength of the homogeneous polymer concrete (not shown in Figure 4). A small reduction (approximately 7 percent) was also present in the average tensile

bond strength of the polymer concrete composite. As is shown in Figure 4, Roadpatch and MPC specimens exhibited a negligible reduction in bond strength. On the basis of the trends in Group 2 and Group 3 average tensile strengths, it appears that Roadpatch and MPC are better choices for rapid-setting materials.

DIRECT SHEAR RESULTS

Considerable data variation was noted during Group 1 testing, which could have been the result of small specimen size or the difficulty experienced in tracking the load on the block or overlay specimens with load cell or strain indicator instrumentation. Although the results shown in Figure 5 exhibit CVs in excess of 17 percent, a general evaluation of the relative shear bond strengths can be made. A comparison of Figures 4 and 5 indicates that direct shear strengths generally parallel the tensile strengths of the composite cylindrical specimens with the exception of the MPC composite. This material exhibited good tensile bond strength but poor direct shear bond strength.

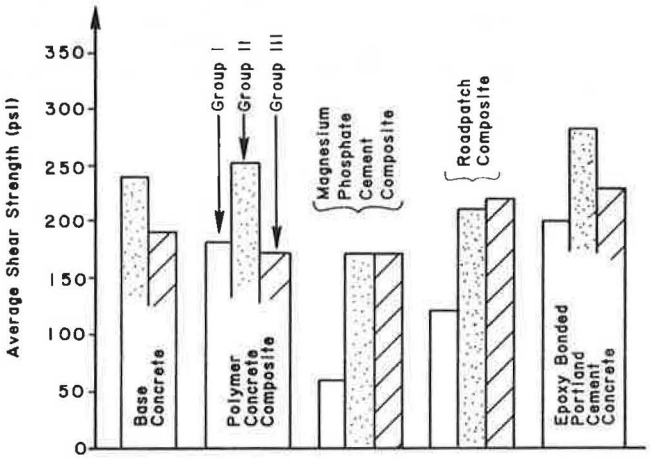

FIGURE 5 Direct shear strength results.

The shear bond strength of the composite epoxy-bonded concrete was very good, but undesirably long hardening time is a disadvantage with this material. On the basis of the differences in Group 1 direct shear results, polymer concrete appears to be the best choice.

A comparison of Group 1 and Group 2 results shows an increase in the average bond strengths with time. The Group 1 bonded composites exhibited average shear strengths in excess of those of the base concrete, although excessive curing time is required. Polymer concrete and Roadpatch test specimens exhibited average shear strengths comparable with that of base concrete.

The comparison of Groups 2 and 3 indicated that polymer concrete experienced a considerable loss (approximately 24 percent) of shear bond strength during the weathering process. The average shear bond strength of Group 2 and Group 3 MPC specimens was less than that of any of the other patching materials. The epoxy-bonded PCC displayed a weathered strength comparable with that of Roadpatch and a strength reduction (Group 2 versus Group 3) comparable with that of polymer concrete. Although significant variation was present in the results (CVs up to 30 percent), the relative performance of the Roadpatch material in the direct shear testing was good. It exhibited no loss in average bond shear strength and the data trend indicates that Roadpatch is the better choice on the basis of this criterion.

IMPACT TEST RESULTS

As is shown in Figure 6 for Group 1 tests, the polymer material had a higher average energy absorption capability than the other patching materials. The CV for these results was less than 8 percent. Roadpatch specimens (CV greater than 18 percent) also demonstrated a significant energy absorption capability. MPC composite specimens possessed low energy absorption capacity. The early age bond strength of MPC appears to be too low to dissipate energy in fracturing either the overlay (patching) material or base concrete. The specimens fractured through the bond line and the overlay broke away intact.

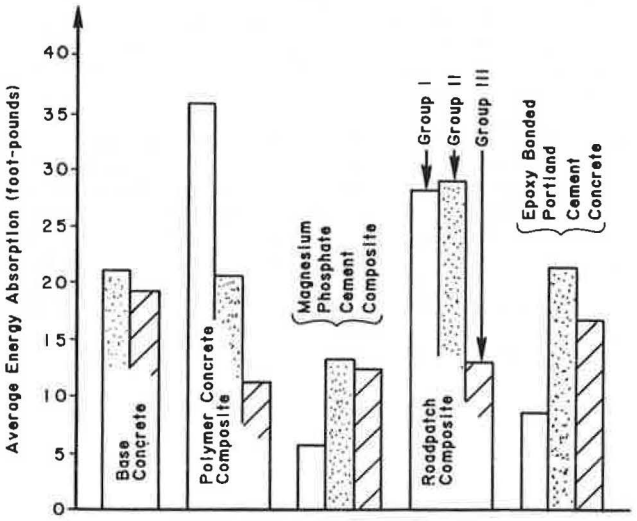

FIGURE 6 Average energy absorption results.

Group 1 epoxy-bonded PCC block and overlay specimens also had a very low energy absorption capability. Although this alternative demonstrated static strengths comparable with those of polymer concrete, low energy absorption capability would be undesirable for satisfactory field performance.

Roadpatch specimens exhibited the greatest average energy absorption capacity in the Group 2 results. MPC has a much smaller energy absorption capacity than any of the other patching materials. Group 3 data indicate that the energy absorption capabilities of polymer concrete and Roadpatch were severely reduced by exposure to the simulated weathering process. Both materials exhibited reductions of approximately 50 percent. Although MPC possessed the least unweathered energy absorption capacity, little deterioration was noted after exposure to simulated weathering.

CONCLUSIONS

The general conclusions concerning the relative performance of the patching materials are based on the trends in the laboratory results. Direct shear and impact test results exhibited significant scatter. Even with these discrepancies, an indication of shear bond strength and energy absorption capability

was evident. Consideration of the overall test results indicates that strength and bonding properties of the patching materials were directly related. Also, the durability of the homogeneous patching materials appears to be a good indication of the durability of their bond to base concrete.

Of the materials tested, polymer concrete exhibited the most ideal setting time. Polymer concrete appears to be the best of the materials tested in terms of early strength, which indicates that it would be suitable for making quick-patch repairs. However, polymer concrete displayed a relatively large loss of energy absorption capacity with age and a loss of strength after exposure to simulated weathering, which indicates a potential problem with long-term durability. Early age strengths and energy absorption capacities suggest that polymer concrete is probably the best choice of the materials tested for making rapid repairs to concrete pavements and bridge decks.

MPC does not appear to be an attractive early cure material. Comparison of early age strengths indicated that MPC had the least strength; it also had a very low energy absorption capacity. This material appears susceptible to damage from dynamic loading. However, an advantage of MPC is its thermal durability.

Early strengths of Roadpatch were relatively good. Test result trends indicated that the final cured strength and energy absorption capacity properties were the best of the rapid-setting materials tested. However, Roadpatch demonstrated a substantial loss of energy absorption capacity after simulated weathering, which may be indicative of a long-term durability problem.

Epoxy-bonded PCC patching materials used in this study are not recommended because the rate of strength gain of the epoxy adhesive and that of PCC were both too slow for completing a field patching repair within 1 working day. However, because the strengths of the test specimens were substantial and the energy absorption capacity and durability properties also were good as compared with those of other material alternatives, additional effort should be made to identify or develop a fast-curing epoxy and PCC mixture design. For situations in which rapid-setting time is not critical, this alternative, as tested in this study, is satisfactory.

ACKNOWLEDGMENTS

The research reported here was sponsored by FHWA, U.S. Department of Transportation, through the State of Alabama Highway Department (HPR Project 930-103) and administered by the Engineering Experiment Station, Auburn University, Auburn, Alabama. The authors gratefully acknowledge the contributions of Mac Roberts, Tom Cain, and Frank Holman of the Alabama Highway Department.

REFERENCE

1. G.E. Ramey and A.M. Strickland. An Experimental Evaluation of Rapid-Setting Patching Materials Used in the Repair of Concrete Bridges and Pavements. HPR Report, Research Project 930-103. State of Alabama Highway Department, Montgomery, 1984.

Publication of this paper sponsored by Committee on Pavement Maintenance.

A Field Evaluation of Factors Affecting Concrete Pavement Surface Patches

FRAZIER PARKER, JR., G. EDWARD RAMEY, RAYMOND K. MOORE, and JOHN W. JORDAN, JR.

ABSTRACT

Field studies were conducted to evaluate the effects of bonding agents, mechanical anchors, and consolidation and curing techniques on the performance of surface pavement patches constructed with Roadpatch and rapid-setting portland cement concrete. Specimens were constructed on the surface of an existing pavement and load tested. One series of load tests was conducted to evaluate portland cement (PC) grout and epoxy bonding agents; mechanical anchor systems made up of 1/8-in.-diameter nails, number 2 U-bars, and a number 6 U-bar; and combinations of bonding agents and anchor systems. A second series of tests was conducted to evaluate combinations of patch materials, bonding agents, and anchor systems when constructed with good to poor consolidation and curing techniques. Bonding agents improve the consistency and reliability of the bond with base concrete. The performance of PC grouts with rapid-setting PC patching material is recommended. The bond strength was insensitive to method of placement of grout, but uniformity and quality, as indicated by low water-cement ratios, are important in bond strength development. To be effective, anchors must have sufficient strength and stiffness. Anchors should have a cross-sectional area of at least 1/2 $in.^2$/100 $in.^2$ of bond area. Internal vibration and moist curing have a definite positive effect on early patch strength.

Although the Interstate system is virtually completed, the older and more heavily traveled sections are experiencing a rapid decline in serviceability. Pavements on the primary system are also experiencing similar performance problems that require spot maintenance. A large portion of these pavements are composed of portland cement concrete (PCC), especially in the urban areas. Spot repair maintenance is, at best, difficult to perform because traffic safety considerations require patching materials and construction procedures that minimize the time that the pavement is closed to traffic.

The research discussed here evaluated materials and techniques that can be used in constructing rapid-setting concrete pavement surface patches. The experimental program utilized an abandoned section of PCC pavement located near Auburn, Alabama, and has been reported on in more detail elsewhere (1,2).

TESTING PROGRAM

Several bonding agents, anchorage systems, and combinations of bonding agents and anchorage systems were evaluated in Series A tests. Series B tests evaluated the performance of various combinations of patch materials, surface preparation techniques, anchorage systems, and different consolidation and curing techniques.

The experimental patches were constructed on an abandoned section of US-280 located between Auburn and Opelika, Alabama. The pavement, consisting of 18-ft-wide, 8-in.-thick reinforced PCC slabs with 39-ft joint spacing, was in excellent condition with no visible cracking. The pavement concrete utilized natural sand and gravel with top-size gravel of approximately 1.5 in. Sawing and chipping of the pavement was difficult because of the primarily quartz composition of the aggregate. Although no concrete cores were tested, it appeared that concrete strength was quite high because no failures occurred in the pavement concrete during load testing of the patches.

Test Series A

These tests were designed to isolate and evaluate the effects of various bonding agents and anchorage systems. Test blocks 6 x 12 x 3 1/2 in. of rapid-setting PCC were cast directly on the surface of the existing pavement that had been abraded with an electric Roto Hammer and cleaned with a wire brush. The test specimen geometry had a 72-$in.^2$ bond surface area. Two test specimens of each of the following eight combinations of surface preparation and anchorage systems were cast:

1. A portland cement (PC) painted on,
2. A PC grout scrubbed in,
3. An epoxy tack coat,
4. Four number 2 U-bars,
5. One number 6 U-bar,
6. One number 6 U-bar and epoxy tack coat,
7. Eight nails, and
8. Control (no additional surface preparation).

After the load resistance performance of the foregoing specimens had been analyzed a second set was cast in replicas of two with the following surface preparation:

1. A PC grout painted on,
2. A "dry" PC grout broomed in, and
3. Control (no additional surface preparation).

Details of the anchored test specimens are shown in Figure 1.

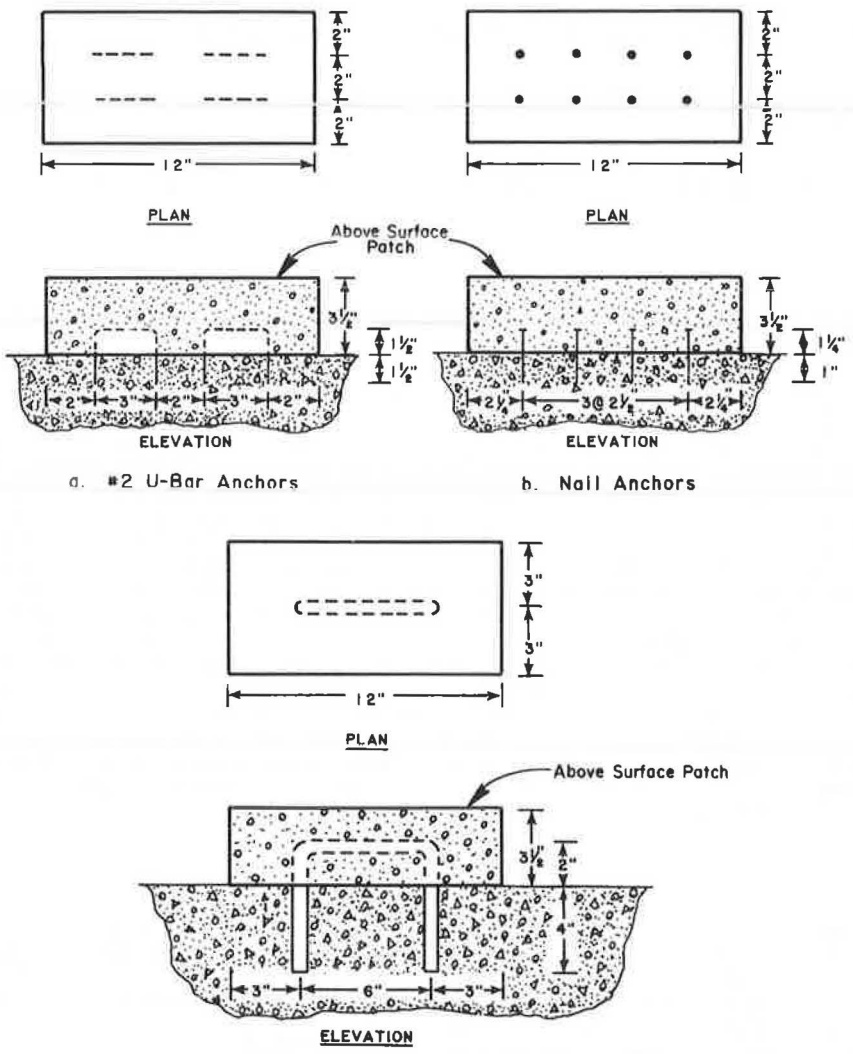

FIGURE 1 Details of anchorage systems, Test Series A.

The PCC pavement surface was scarified with an electric rotary hammer and cleaned with a wire brush to provide a clean, roughened bond surface with exposed aggregate. The second step was the installation of anchors (for the anchored specimens) consisting of nails and number 2 or 6 steel reinforcing bars bent into U-shapes. These anchors were grouted by placing a polyester mixture into holes drilled in the pavement surface.

Once the anchors were in place, forms were constructed, as shown in Figure 2, and the various bonding agents were applied to the roughened pavement surface. Rapid-setting PCC was placed and consolidated by thorough rodding. The specimens were covered with polyethylene sheeting and cured for 10 days before testing.

The jacking pedestal, shown in Figure 3, provided a reaction support for loading the specimens. Loads were applied with a 120-kip hydraulic jack and measured with a 100-kip electric load cell. Specimen movement was monitored with a 0.001 accuracy dial gauge. To eliminate tensile stresses along the bond surface, the load was applied at an angle of approximately 20 degrees with the pavement surface. This ensured that the line of action would pass through the kern of the bond area. Loads were applied until complete bond failure or specimen crushing occurred. When possible, specimen deformations were recorded.

Test Series B

Series B tests evaluated rapid-setting PCC and Roadpatch when utilized with various bonding agents, anchor systems, and consolidation and curing techniques.

The test setup for Series B was similar to that for Series A, shown in Figure 3. Although specimen dimensions and bond area remained the same, two details were different. A coloring admixture was added to the rapid-setting PC and Roadpatch to aid in determining whether failure planes passed through the base concrete, through the patch material, or along the interface. A loading face with an angle of 20 degrees from the vertical, shown in Figure 4, was cast on the specimens to eliminate the need for the angled bearing plate used in Series A.

Table 1 summarizes the comparisons between treatment combinations that can be made. The patch mate-

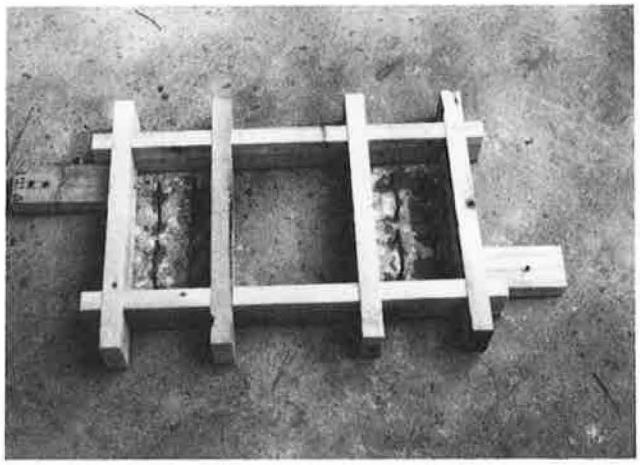

FIGURE 2 Forms for constructing test blocks.

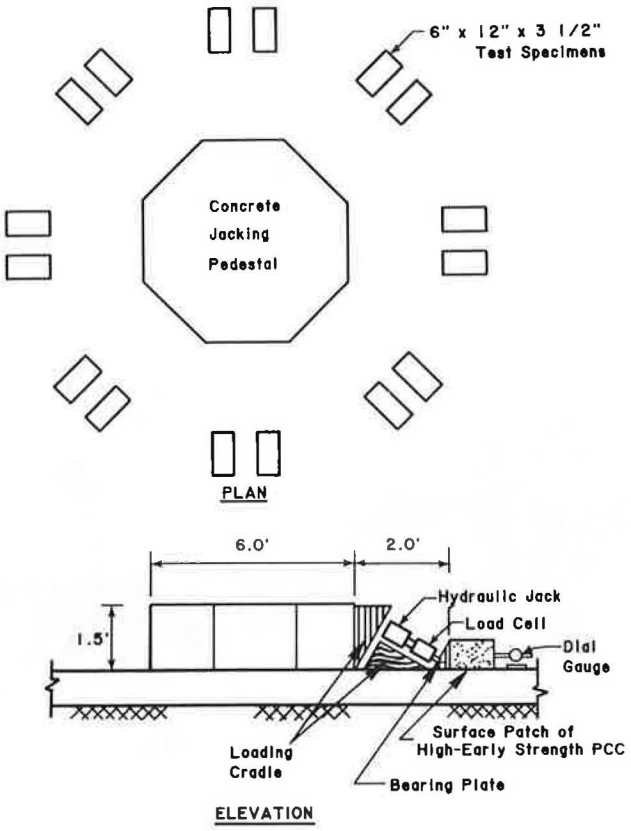

FIGURE 3 Field test set-up, Test Series A.

rials were rapid-setting PCC and Roadpatch. A cement grout was used as a bonding agent for the rapid-setting PCC and the manufacturer's recommendation of an acrylic slurry was used for the Roadpatch. Unanchored and anchored specimens were included and anchor details are shown in Figure 4. A number 4 U-bar anchor was selected as a compromise between the four number 2 and one number 6 U-bar systems used in Series A. Moist curing and simple exposure to existing conditions were employed. Two levels of compactive effort, internal mechanical vibration and minimal rodding, were employed.

Construction of the Series B test specimens was similar to that for Series A tests. That is, the pavement surface was abraded with a Roto Hammer, the number 4 U-bars were grouted into holes in the pavement with a polyester grout, forms were constructed, prime coats were applied to the bond surfaces, and patch material was placed. Twelve of the specimens were consolidated with internal vibrations, and four (two of PCC and two of Roadpatch) were consolidated with only minimal rodding to remove large visible voids.

The specimens were cured for 6 hr before testing. Twelve specimens were moist cured by being covered with wet burlap and polyethylene sheeting. Two samples of PCC and two of Roadpatch were not protected from moisture loss during curing.

EXPERIMENTAL RESULTS

Load test results for the two test series include failure load data, load-deformation responses, and qualitative information concerning modes of failure.

TABLE 1 Load Test Specimens: Test Series B

Patch Parameter	No. of Replicas PCC	Roadpatch
No anchors, moist cure, internal vibration	2	2
Anchors, moist cure, internal vibration	2	2
No anchors, exposure curing, internal vibration	2	2
Anchors, moist cure, minimal rodding	2	2

Material comparison

Anchorage effort comparison

Curing effort comparison

Consolidation effort comparison

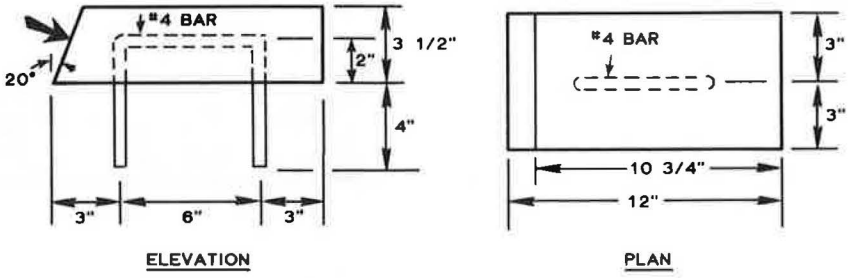

FIGURE 4 Details of specimens with number 4 U-bar anchors, Test Series B.

TABLE 2 Failure Modes and Loads: Test Series A

Surface Preparation	Failure Mode	Avg Peak Failure Load (kips)	Percent Difference
None	Bond failure, brittle-type failure	32	-
PC grout			
Painted on	Bond failure, brittle-type failure	29	-10.3
Scrubbed in	Bond failure, brittle-type failure	34	5.3
Broomed off	Bond failure, brittle-type failure	29	-10.3
Epoxy tack coat	Bond failure, brittle-type failure	45	39.9
One no. 6 U-bar anchor	Bond failure followed by cracking around U-bar and crushing, ductile-type failure	44	36.1
One no. 6 U-bar anchor and epoxy tack coat	Cracking around U-bar and crushing, no bond failure, ductile-type failure	48	48.0
Four no. 2 U-bar anchors	Bond failure followed by cracking around U-bars, ductile-type failure	44	36.1
Eight-nail anchors	Bond failure followed by immediate pullout of nails from the base concrete, brittle-type failure	27	-17.1

Because of differences in anchorage systems, loading conditions, and age at testing, absolute magnitudes of failure loads are only of general interest. Of specific interest are comparisons within a test series to assess the relative benefits of the various materials and techniques.

Test Series A

Results from the load tests in this series are summarized in Table 2. The percent difference relates to the control case, in which there was no surface preparation. In each case, the specimens without mechanical anchors experienced abrupt bond failures as shown in Figure 5 (top). This type of failure was probably caused by tensile stress concentrations resulting from application of the load.

With the exception of the specimens with nail anchors, the anchored specimens exhibited ductile-type failures; that is, the maximum load did not produce an abrupt catastrophic failure. Load-deformation measurements indicated that these specimens were able to sustain applied loads after bond failure. The U-bar anchors should extend the life of a patch by maintaining its structural integrity after bond failure. The nail anchors lacked the stiffness and pull-out strength necessary to provide significant load-carrying capacity after bond failure. The nails were pulled from the base concrete after bond failure occurred. The ratio of anchor cross-sectional area to bond area for the nails was only 0.00014, whereas for the number 2 U-bars and number 6 U-bars these ratios were 0.0055 and 0.0122, respectively.

Failure of specimens with U-bar anchors was characterized by splitting around the bars and crushing of the patch material as shown in Figure 5 (bottom). The U-bar anchors had sufficient strength and stiffness to produce a ductile-type load-deformation response. Typical load-deformation curves for anchored and unanchored specimens are shown in Figure 6. Note the considerable deflection necessary to significantly reduce the load resistance for the anchored specimen. The failure modes experienced by specimens with U-bar anchors suggest that their strength and ductility would be enhanced by a patching material with high tensile strength and ductility such as steel fibrous concrete.

With the exception of the nail anchors, the specimens with anchors performed well. When the specimens with the epoxy tack coat and number 6 U-bar, number 6 U-bar alone, number 2 U-bars, and

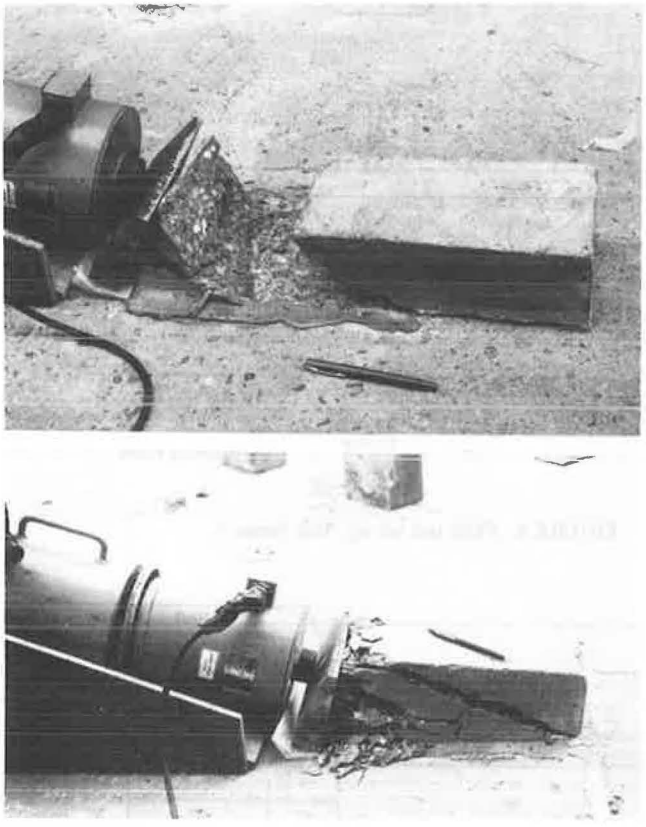

FIGURE 5 Typical failure modes, Test Series A: bond failure, unanchored specimens (top) and splitting and crushing, anchored specimens (bottom).

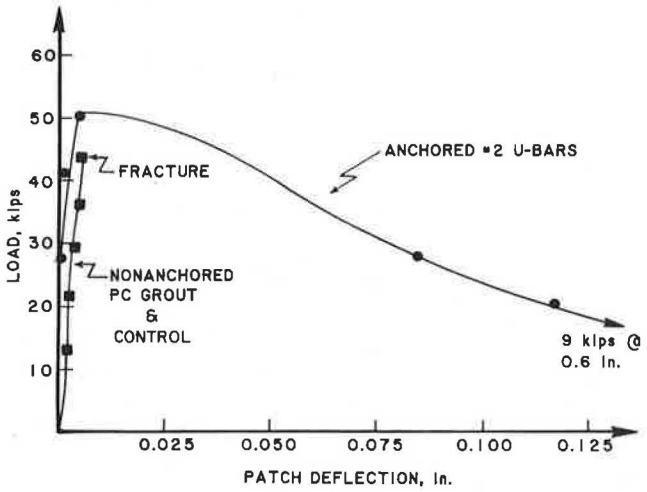

FIGURE 6 Typical load-displacement curves, Test Series A.

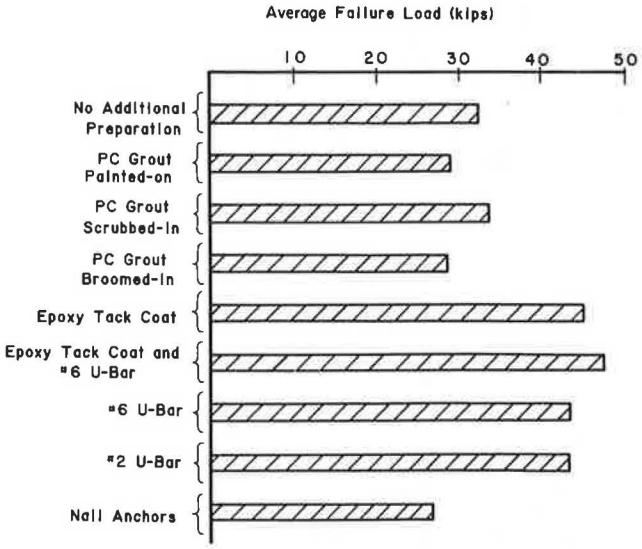

FIGURE 7 Comparison of failure loads, Test Series A.

nail anchors were compared with the control specimens, increases in average strength of 48, 36, 36, and -17 percent, respectively, were found. The increases, combined with improvements in ductility, make the use of anchors appear quite attractive. The role of the anchors in patch performance appears to be similar to that of reinforcing steel in concrete: the steel provides tensile strength, ductility, and toughness. On the basis of consistent and maximum load-carrying capacity, specimens with the epoxy tack coat and number 6 U-bar were superior. These specimens had the smallest variability in load-carrying capacity and exhibited no detectable bond failure. The failures resulted from splitting and crushing of the patching material. The average strength of these specimens was approximately 48 percent higher than that of the control specimens. this average strength is, however, only 6 percent higher than that for specimens with epoxy tack coat only and 9 percent higher than that for specimens with only number 6 U-bars. Further research is needed to fully determine the merits of combining an epoxy tack coat with a mechanical anchorage system. Of particular concern is the epoxy's slow strength gain and sensitivity to temperature.

Average failure loads are shown in Figure 7. Results from the control specimens cast with no bonding agent or anchors exhibited significant variations. Loads ranged from 65 to 7 kips with an average of 32 kips. The average load-carrying capacity for the unanchored specimens was not increased by the use of bonding agents. However, when failure load variability was compared, it was noted that the consistency of load-carrying capacity was significantly improved by using a PC grout bonding agent. Specimens with the PC grout painted or broomed on exhibited average strengths approximately 10 percent smaller than those of the control specimens with no additional preparation. However, these specimens demonstrated consistent failure load results.

Series A tests suggest no strong relationship between patch performance and the method utilized for application of the PC grout. As illustrated in Figure 7, the different methods produced similar results. Epoxy showed more promise as a bonding agent than PC grout. Average loads for the epoxy were higher than those for the PC grout specimens and approximately 40 percent higher than those for the control specimens. The strengths were comparable with those achieved with the number 6 U-bar and the number 2 U-bar anchors. However, earlier laboratory studies (3,4) have shown that the epoxy's rate of strength gain is relatively slow and sensitive to temperature.

Test Series B

Results from Series B load test specimens are given in Table 3. The specimens were loaded after 6 hr of moist curing. The failure modes were similar to those for comparable specimens in Test Series A. Unanchored specimens experienced bond failures, as shown in Figure 5 (top), which are characterized as brittle because of small failure displacements and abrupt losses of load resistance. Anchored specimens were characterized by bond failure, followed by slitting and crushing of the patch material. These were considered ductile because the specimens were able to sustain loads with increasing displacement after the peak load was achieved. The failure modes were similar to that illustrated in Figure 5 (bottom).

TABLE 3 Failure Modes and Loads: Test Series B

Patch Parameter	Failure Mode	Avg Peak Failure Load (kips)
PCC		
No anchors, moist cured, vibration	Bond failure, brittle-type failure	22
Anchored, moist cured, vibration	Bond failure followed by cracking around U-bar and crushing, ductile-type failure	20
No anchors, no curing, vibration	Bond failure, brittle-type failure	18
Anchored, moist cured, rodded	Bond failure followed by cracking around U-bar, ductile-type failure	20
Roadpatch		
No anchors, moist cured, vibration	Bond failure, brittle-type failure	24
Anchored, moist cured, vibration	Bond failure followed by cracking in plane of U-bar, ductile-type failure	18
No anchors, no curing, vibration	Bond failure, brittle-type failure	18
Anchored, moist cured, rodded	Crushing followed by bond failure and cracking around U-bar, ductile-type failure	12

Average values of peak failure loads (which is the maximum load on a load displacement curve) are presented in Figure 8. These loads and the modes of failure were used as the basis of comparison for evaluating the relative performance of the materials, the consolidation and curing procedures, and the anchor systems.

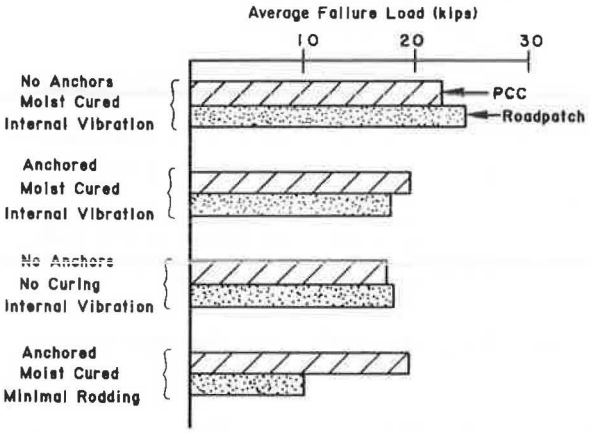

FIGURE 8 Comparison of failure loads, Test Series B.

As seen in Figure 8, the Roadpatch and the rapid-setting PCC performed about the same on the basis of load-carrying capacity. An exception was the minimal rodding case, but the difference was attributed to material sensitivity to consolidation effort. Comparing the average strengths of specimens with similar anchorage, consolidation, and curing conditions reveals no consistent pattern. The PCC specimens exhibited superior strength in two cases, but Roadpatch was stronger in the other two. On the basis of its superior ductility, exhibited through the retention of its structural integrity after displacements in excess of 1 in., Roadpatch appears to be the better of the two materials tested. As displacements approached 1 in., the PCC specimens tended to crack and be crushed.

Comparisons between the anchored and unanchored test specimens appear to contradict the results from Test Series A. In Series A, the anchored patches performed better than the unanchored patches, with the exception of the specimens with nail anchors. In that series, the increases in average strength compared with that of the control specimens for the specimens with epoxy tack coat and number 6 U-bar, number 6 U-bar alone, and number 2 U-bar were 48, 36, and 36 percent, respectively. However, as shown in Figure 8, the unanchored patches exhibited slightly greater load-carrying capacities than the anchored specimens. For PCC specimens, the difference between the unanchored and anchored mechanically vibrated and moist-cured specimens was about 10 percent. The difference between comparable Roadpatch specimens was 25 percent.

The poor performance of the number 4 U-bar anchorage system of Test Series B was due to in part to differences in size or arrangement of the anchors or both as compared with Test Series A. The one number 4 U-bar anchor provided a cross-sectional area of 0.40 $in.^2$, which gave a ratio of anchor to bond surface areas of 0.0055. In Series A, the four number 2 U-bars and the one number 6 U-bar provided, respectively, 0.4 $in.^2$ (0.0055) and 0.88 $in.^2$ (0.0122) of anchor area. The number 6 U-bars provide approximately twice the area and are stiffer than the number 4 U-bars, whereas the arrangement of four number 2 U-bars offers the advantage of reduced stress concentrations. The anchors, however, in both test series, served to provide ductility by retaining the integrity of the specimens and allowing for load transmittal after initial bond failure.

The importance of proper consolidation can be seen by comparing the specimens consolidated with internal vibration with those consolidated by minimal rodding. For the anchored, moist-cured PCC specimens, the average strengths were the same (19.9 kips). For comparable Roadpatch specimens, the strength of those that were mechanically vibrated was 32 percent larger than that of those that were minimally rodded. These results were influenced by the workability of the mixes used. The PCC mix was wetter and more workable, and thus the means of consolidation had no discernible effect. The Roadpatch mix was, on the other hand, quite dry and contained steel fibers; thus it was not as workable. Therefore, the mechanical vibration improved consolidation and significantly increased the strength of the Roadpatch specimens. Honeycombing was observed in the rodded Roadpatch specimens and further illustrates the need for mechanical vibration. On the basis of these results and the desirability of keeping the water:cement ratios of patching materials as low as possible, internal vibration is considered desirable.

A fourth comparison can be made between the moist-cured test specimens and those left unprotected against rapid moisture loss. Unanchored, vibrated, moist-cured PCC specimens had an average strength 20 percent higher than that of those left unprotected. Comparable Roadpatch average strengths were 26 percent higher. These results illustrate the importance of proper curing to ensure adequate early strength gain.

CONCLUSIONS

Major conclusions drawn from the results of this testing program are as follows:

1. The use of bonding agents improved the consistency and reliability of the patch bond with base concrete for the patches tested. Epoxy exhibited superior strength, but earlier laboratory studies (3,4) have shown that it has a slower rate of strength gain and is adversely affected by low temperature. Therefore, Type III PC grouts should be used as the bonding agent with rapid-setting PCC. The performance of PC grouts was insensitive to the method of placement. Uniformity of the grout and low water-cement ratios appear to be more important than method of placement.
2. The inclusion of mechanical anchors, in general, is beneficial in improving strength and ductility. These improvements are realized only if the anchors have adequate strength and stiffness. The nail anchors employed did not have adequate stiffness and embedment depth. The four number 2 U-bars and the one number 6 U-bar provided adequate stiffness to strengthen the surface patches. However, the one number 4 U-bar did not appear to provide adequate stiffness to strengthen the patch. Optimization of the size and number of anchors to best strengthen a patch was not achieved and should be addressed through additional research.
3. On the basis of the limited results from the anchored tests, it appears that anchors should have a cross-sectional area of at least 1/2 $in.^2$/100 $in.^2$ of bond area.
4. Internal vibration and moist curing have a definite positive effect on early patch strength.
5. Rapid-setting PCC manufactured with Type III

cement and an accelerator or the proprietary product Roadpatch can be successfully used for patching PCC pavements.

ACKNOWLEDGMENTS

The work reported in this paper was sponsored by FHWA, U.S. Department of Transportation, through the State of Alabama Highway Department (Alabama Highway Department Project 930-107). The authors are grateful for their sponsorship, assistance, and cooperation.

REFERENCES

1. F. Parker, G.E. Ramey, and R.K. Moore. Evaluation of Rapid Setting Materials and Construction Techniques for Concrete Pavement Patches. HPR No. 99, Research Project 930-107. State of Alabama Highway Department, Montgomery, 1984.
2. G.W. Jordan. Evaluation of the Performance of Various Rapid-Setting Concrete Pavement Patching Materials and Procedures by Field Testing. M.S. thesis. Auburn University, Auburn, Ala., March 1984.
3. A.M. Strickland. An Experimental Evaluation of Rapid-Setting Patching Materials Used in the Repair of Concrete Pavements. M.S. thesis. Auburn University, Auburn, Ala., March 1982.
4. F.W. Foshee. A Laboratory Comparison of Several Rapid-Setting PCC Pavement Patching Materials Used in the Repair of Concrete Pavements. M.S. thesis. Auburn University, Auburn, Ala., June 1983.

Publication of this paper sponsored by Committee on Pavement Maintenance.

Void Detection for Jointed Concrete Pavements

J. A. CROVETTI and M. I. DARTER

ABSTRACT

Procedures for the detection of voids or loss of support under jointed concrete pavements by using nondestructive deflection testing measurements are presented. A rapid field-applicable procedure is presented to quickly determine the presence of voids by analysis of the load and deflection response at slab-corners. A more detailed method is presented in which deflection measurements from center slab and corner locations are used to locate and determine the approximate size of any existing voids. The procedures were developed by using computer modeling of loadings with the ILLISLAB finite-element computer program. The procedures were field verified on several test projects. Basic guidelines for testing, locating joints or cracks requiring subsealing, and estimating grout quantities for jointed concrete pavements are presented.

The loss of support near transverse joints and working cracks because of the pumping of base or subgrade fines or both is one of several major causes of concrete pavement deterioration. Subsealing of locations with poor support by the injection of a grout mixture has become standard practice in many parts of the country. What has been lacking in this process is an established procedure to determine the locations along the pavement where loss of support exists. This deficiency has led many agencies to subseal on a blanket-coverage basis (e.g., all joints and working cracks), which has led to serious problems on several projects because it was not possible to determine (a) whether and where any voids existed in the first place, (b) an estimate of the grout quantity required to fill existing voids, and (c) the extent to which the voids were filled and support was restored.

Procedures were developed under NCHRP Project 1-21 at the University of Illinois for determining areas of loss of support (commonly called voids) by using nondestructive deflection testing (NDT) (1,2). Two different methods were developed:

1. A rapid and simple field method to give an indication of the existence of a void, and
2. A detailed approach to give an indication of the location and size of the void.

Both procedures were field tested at several different project sites.

BASIC APPROACH AND CONCEPTS

Computer modeling based on finite-element analysis was used to establish theoretical relations between

applied load and surface deflection for a wide variety of pavement conditions. These relations were then used as the basis for the formulation of the void detection procedures presented here.

Computer Modeling of Loadings

The computer program used to model the pavement's load-induced deflection response was the ILLISLAB finite-element program (3), which allows the user to input pavement material properties (layer thickness, elastic modulus, and Poisson ratio), loading conditions (magnitude, location, and area of load), and joint load transfer. The program then determines the theoretical surface deflections for specified nodal points on the slab.

A series of programs was run that varied slab thickness, slab modulus, subgrade support modulus, deflection load transfer, and void size to establish the effects of each of these parameters on pavement deflection. Deflection response was investigated at locations correlating to sensor locations commonly used on deflection testing equipment. To determine the effects of slab thickness on measured deflection, slab thicknesses of 8, 9, and 10 in. were examined. Subgrade stiffness values, modeled as spring constants acting at specified nodes (Winkler foundation k-value), were chosen to reflect the wide range of conditions that may be encountered in the field. Values ranging between 100 and 1,500 psi/in. were included.

Concrete slab modulus values were varied from 3,000,000 to 8,000,000 psi. Deflection load transfer across the transverse joint was varied to represent joint efficiencies of 0, 35, 65, and 100 percent. Voids were modeled as square areas located on one or both sides of the joint (equal area on both sides) by indicating a foundation support value of 0 psi/in. at all nodes inside the boundaries of these areas. Void sizes of 0, 4, 16, and 36 ft^2 were modeled on each side of the joint.

The effects of each of these variations were examined individually and in different combinations to determine whether any significance could be realized. Some of the findings of this computer modeling include the following:

1. Where full support exists, proportional variation of deflection due to available load transfer is independent (within testing accuracy limits) of slab thickness, slab modulus, and subgrade modulus;
2. Variations in deflection response due to void size are a function of both available load transfer and subgrade modulus when the void is located on only one side of the joint; and
3. Variations in deflection response due to void size are dependent only on subgrade moduli when equal-sized voids are located on either side of the joint.

Voids Under Slab

A void can be described as any unsupported area beneath the slab. The most common location for voids is along the outside edge of the driving lane at any transverse joint or working crack with poor load transfer. It is believed that these voids are created by a combination of excess moisture and independent large slab deflection in response to loading, which causes the erosion of subgrade or subbase fines or both.

Generally (but not always) this process begins under the leave side of the joint or working crack and expands in both the longitudinal and transverse directions. As the void increases in size, corner loadings along the outer edge force the leave slab to act as a cantilever, which generally leads to serious faulting and a corner break or diagonal crack across the slab.

Because of the heterogeneous qualities of the pavement, subdrainage, and loading conditions, void progression develops in a random pattern. For this reason, testing of individual joints is necessary to determine the location and extent of void development along any given project.

NDT Equipment

The NDT equipment utilized for void detection must be capable of (a) applying a reasonably heavy range of loads, (b) measuring the deflection directly beneath the center of the load, (c) measuring the deflection basin up to 36 in. (and preferably 72 in.) from the center of the loading plate at 12-in. intervals, and (d) simultaneously measuring slab deflections across joints and cracks for load transfer.

Vibratory steady-state devices such as the road rater and impact load devices such as the falling weight deflectometer (FWD) have been used successfully. The procedures outlined here were developed for use with these types of devices.

Deflection Load Transfer

Deflection load transfer, also commonly referred to as joint efficiency, is measured at the extreme outer corner of the slab and is computed as follows:

Load transfer (%) = (deflection of the unloaded slab/deflection of loaded slab) * 100

This load transfer can be the result of simple aggregate interlock, foundation stiffness, dowel bar shear transfer, or a combination of these mechanisms. Typical load transfer values measured along any given project may vary considerably and therefore each joint must be measured to determine the respective load transfer on each side of the joint.

Back-Calculation of Effective Slab Modulus

The magnitude of deflection variation with respect to void development varies as a function of slab modulus. It is therefore desirable to determine the effective slab modulus along each project before the implementation of the comprehensive void detection procedures. These modulus values may be back-calculated from NDT data by analyzing the deflection basin produced during center slab testing. This back-calculation process compares the measured deflection basin area and maximum deflection with theoretical values obtained through computer modeling to yield the appropriate slab modulus and foundation k-value for each slab tested.

Zero Voids Band

A key assumption of the comprehensive void analysis is that a certain percentage of the joints along the pavement will not have voids present. NDT measurements taken at these joints provide a reference from which subsequent void size predictions are based. Computer modeling was used to first establish a relationship between corner deflection and load transfer for fully supported slabs. Proportionally, this relationship was found to be constant over all

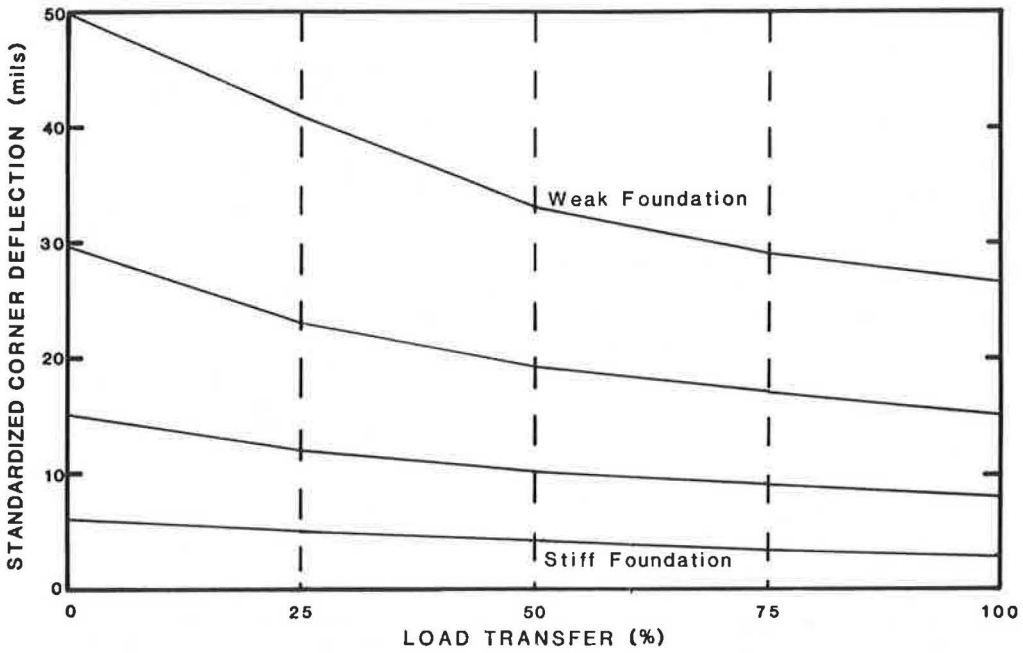

FIGURE 1 Corner deflection versus load transfer for fully supported slabs.

ranges of slab thicknesses and subgrade support values examined (8 to 10 in., 100 to 1,500 psi/in.), although the absolute magnitude of the corner deflections varies accordingly. Typical curves resulting from this analysis that represent deflection variation as a function of load transfer for fully supported slabs are shown in Figure 1.

The deflection responses shown in Figure 1 do not take into account any random variation that will be introduced into field deflection measurements because of the heterogeneous nature of both the portland cement concrete (PCC) slabs and foundation support along with load plate locating variations. The effects of field variables on corner deflections were examined by using data obtained with the road rater and FWD on new and lightly loaded slabs for which no voids existed. With these data, it was determined that the coefficient of variation of deflection testing response ranged from 10 to 15 percent. Therefore, assuming normality, the inclusion of all points plus or minus two standard deviations away from the sample mean on any given corner deflection or load transfer plot should include roughly 90 to 95 percent of all deflection measurements taken at those joints for which no voids exist. Including the effects of load transfer in this concept results in an error band located along a given theoretical mean curve. This resulting error band is called the "zero voids band." Figure 2 shows the location of this band as applied to deflection

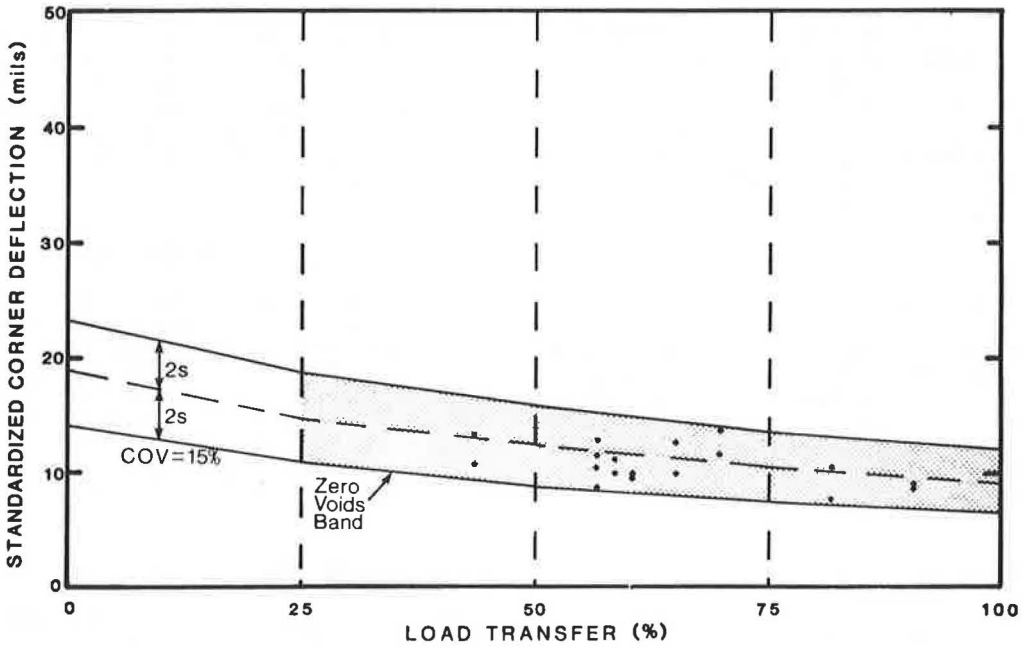

FIGURE 2 Zero voids band for newly constructed slabs on I-40, New Mexico.

measurements taken along a section of newly constructed slabs on I-40 in New Mexico.

Determining Corner Subgrade Support Value

In order to predict void size and locations at slab corners from deflection measurements, the effective subgrade support or k-value acting at the corner of a fully supported slab must be determined. With the ILLISLAB program it was found that for any given slab thickness, the effective corner subgrade support value is proportional to the deflection of a free corner (0 percent load transfer) in response to a corner load. Therefore, effective corner subgrade support can be determined rather easily.

Effects of Temperature

Temperature has two major effects on the slab, which affect measured deflections: slab curl and joint lockup. As the top of the slab warms from solar radiation, temperature differences between the top and bottom of the slab force it to curl downward. This may cause a reduction in deflection under load (and vice versa). The other effect occurs at the joints that lock up when the slab is warm and expands longitudinally. This produces a high load transfer at the joint and greatly reduces deflection. This joint lockup will also reduce the chance of finding voids that are located on only one side of the joint.

The combined effect of these two mechanisms can change slab corner deflections significantly. Temperature effects are considered in the procedures through restricting the measurement of deflections to a range of temperatures and testing primarily during early mornings or during ambient temperatures in the range of 50 to 80°F. Further testing and analysis are recommended to better quantify these effects so that they may be more fully incorporated into the void detection procedure.

Cracked Slabs

Cracks in slabs change the deflection patterns considerably, especially corner breaks or diagonal cracks near the joint. The void detection procedures presented here assume that the slabs are intact and that no cracks exist near the joints. If transverse cracks exist at 10 or more feet from the joint, they may be considered as joints and analyzed as such. However, slabs having a corner break or nearby diagonal cracks have had a loss of support, are difficult to stabilize, and should actually be considered for full-depth repairs.

VOID DETECTION PROCEDURES

The two methods of void detection developed will be presented by using actual data collected from various projects across the United States. The methods presented include (a) a rapid and simple method to indicate the existence of a void and (b) a comprehensive method to indicate the presence and approximate size of a void.

Rapid Void Detection Procedure

A rapid and fairly accurate procedure was developed to locate voids beneath slab corners. This method can be applied in the field and can give immediate indication of the existence of a void or of loss of support. Because available load transfer is not taken into account, exact void size determination is not possible. This method involves three basic steps as follows:

Step 1: Measure Corner Deflections. Measure pavement deflections at slab corners while the temperature range is between 50 and 80°F with a device that can apply at least three different load levels. Loadings should be chosen to encompass 9,000 lb, such as 6,000, 9,000, and 12,000 lb.

Step 2: Plot Results. Plot the measured results directly on a graph of load versus deflection as shown in Figure 3. Draw the best-fit straight line through all three points and compare this line with the line formed by the simple connection of the three points. Marked differences between these lines indicate possible void locations.

Step 3: Locate Voids. If the best-fit line is satisfactory, extend the line to the horizontal (deflection) axis and note the intercept value. Locations where no voids exist generally have intercept values along the horizontal axis of <0.002 in. Joints with no voids have also been found to have intercept values less than zero. Joints with voids generally have intercept values in excess of 0.002 in. with values increasing as void size increases.

This simple procedure can be applied both before and after subsealing to provide information as to the number of joints requiring subsealing and the effectiveness of the subsealing operation. An example of this procedure can be seen in the load deflection plot from a selected joint on Ohio I-77 as shown in Figure 4. Note that the leave-side response shifted after subsealing, which indicates a satisfactory stabilization of the slab.

Comprehensive Procedure for Void Detection

This procedure indicates the existence of a void and estimates its horizontal area (in terms of loss of support). It is somewhat complex but can easily be mastered after a few applications. Step-by-step procedures will be presented to outline the entire process. The structural characteristics of the test pavement used to illustrate the procedure are as follows: a 9-in. PCC slab over 4 in. of cement-treated base over a 12-in. sand subbase that has been subjected to heavy truck traffic for many years. Deflections were recorded under a 5,000-lb peak-to-peak vibratory load.

Step 1: Measurement of Deflections

The pavement scheduled for testing must first be divided into uniform subsections, which should include portions of the pavement with similar structural characteristics (thickness, age, base type, subgrade type). Further breakdown of these subsections may be necessary if pavement temperature fluctuations during testing exceed 20°F. Deflection measurements should only be taken if the ambient air temperature is between 50 and 80°F to avoid excessive slab curling and joint lockup.

Step 1a: Center Deflections

Center slab deflections should be taken for at least five sound slabs in each subsection. If this number of sound slabs does not exist, the minimum spacing

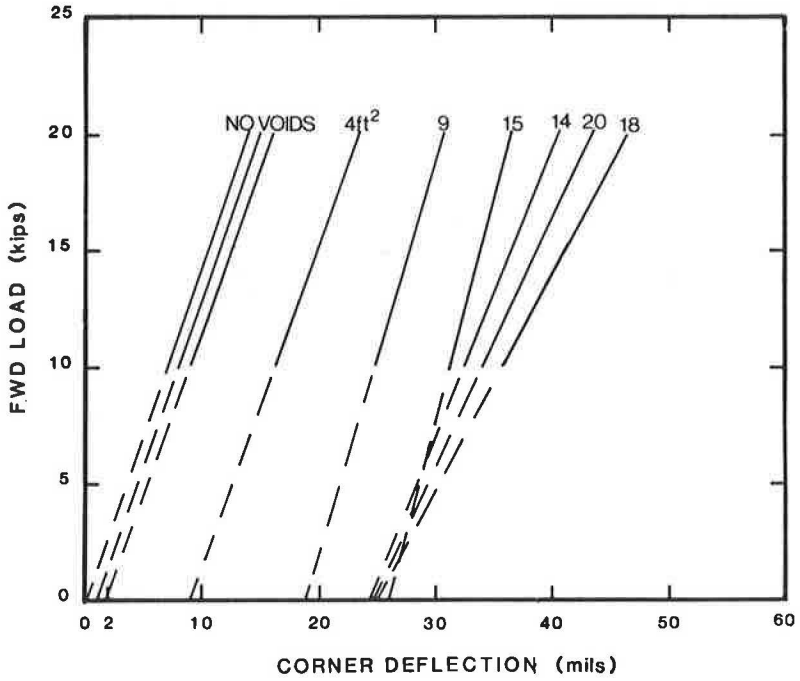

FIGURE 3 FWD load versus corner deflection (void sizes obtained from comprehensive method).

between the load cell and the nearest crack should be 6 ft as shown in Figure 5. The deflections for all four sensors along with the applied load should be recorded as shown in Table 1. Deflection measurements are recorded on Table 1 by using the notation Wij, where Wij corresponds to a measured deflection (W) at location i while the load is placed at location j. The six possible testing locations are shown in Figure 5. Additional values also listed in Table 1 will be explained later in this paper. When the FWD is used for deflection measurements, it is advisable to record only those deflections measured with an approximate 9,000-lb load.

Step 1b: Corner Deflections

Deflection measurements should be taken with the loading plate in the extreme corner of the slab (see Figure 5) on both the approach and the leave sides

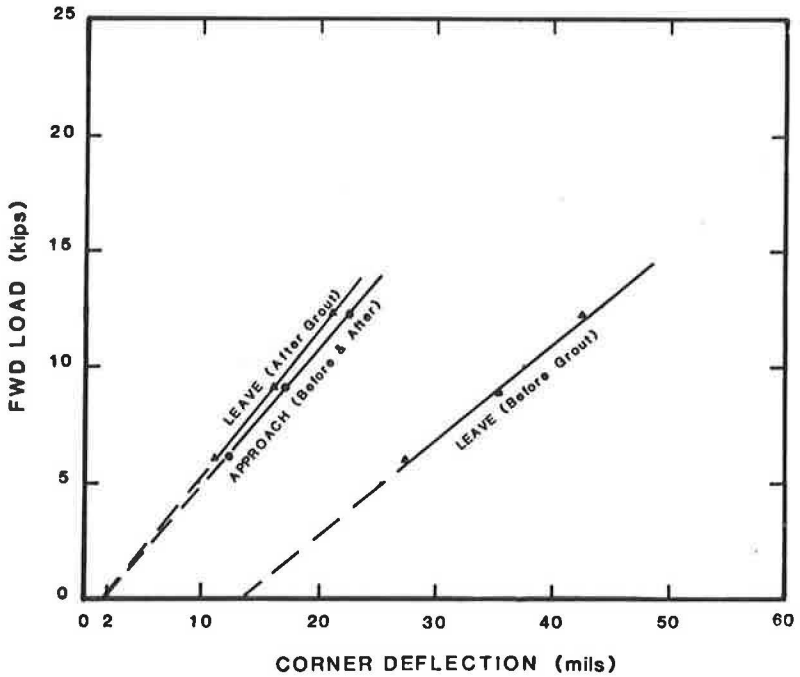

FIGURE 4 FWD load versus deflection before and after subsealing (I-77, Ohio).

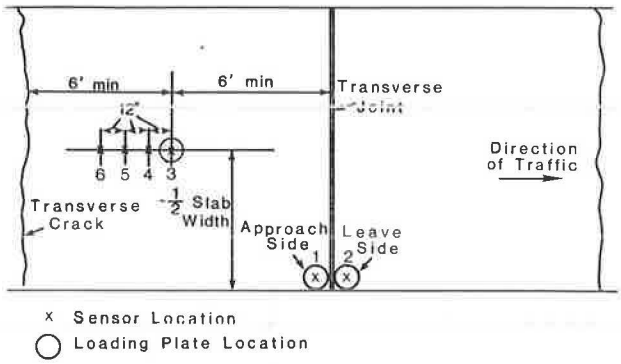

FIGURE 5 Load plate and sensor locations for center slab and corner deflection measurements.

of the joint. The second sensor should be located across the joint for at least one of these tests (and ideally for both) at each joint so that the existing load transfer at each joint can be determined. Deflections taken in the wheel path will not provide the accuracy required in void detection. Deflection measurements may be taken with any NDT equipment as long as the applied force to the slab is reasonably heavy (e.g., 5,000 lb or greater). Analysis of deflection data, however, suggests that the FWD provides the most accurate representation of a moving wheel load and is therefore recommended if a choice exists. Also, there is no significant preload weight for this equipment to bend the corner of the slab down before loading.

Measured deflections should be tabulated in a manner similar to that shown in Table 2. Again, if the FWD is used for deflection measurements, only

TABLE 1 Sample Void Analysis, Center Slab Deflections, 9-in. Slab

		Measured Values (mils)				Calculated Values			
Slab	Load (lb)	W33	W43	W53	W63	Area (in.)	d33 (mils at 9 kips)	Eslab (psi)	Badj
1	5,000	1.82	1.63	1.58	1.42	31.85	3.28	7.00E + 06	1.12
2	5,000	2.55	1.49	1.16	0.79	20.33	4.59		
3	5,000	2.67	1.65	1.51	1.31	23.15	4.81		
4	5,000	2.20	1.63	1.45	1.26	26.24	3.96	3.00E + 06	1.35
5	5,000	1.82	1.53	1.43	1.23	29.57	3.28	5.60E + 06	1.19
6	5,000	1.95	1.75	1.75	1.55	32.31	3.51	7.00E + 06	1.11
7	5,000	2.90	1.58	1.58	1.30	21.77	5.22		
8	5,000	2.48	1.80	1.64	1.30	25.79	4.46		
9	5,000	1.82	1.49	1.54	1.20	29.93	3.28	6.10E + 06	1.22
10	5,000	2.64	1.65	1.60	1.43	24.02	4.75		
11	5,000	1.85	1.65	1.48	1.40	30.84	3.33	7.00E + 06	1.12
12	5,000	2.86	1.67	1.52	1.28	22.07	5.15		
13	5,000	1.60	1.40	1.30	1.16	30.60	2.88	7.00E + 06	1.14
14	5,000	2.00	1.55	1.39	1.20	26.94	3.60	3.00E + 06	1.33
15	5,000	2.66	1.80	1.62	1.37	24.52	4.79		
Average								5.71E + 06	1.20
Ecorr									1.15

TABLE 2 Sample Void Analysis, Corner Deflections, 9-in. Slab

		Measured Values						Standardized Values			Void Size (ft^2) by Location	
Joint	Load (lb)	W11 (mils)	W22 (mils)	W12 (mils)	LT (%)	Ecorr	Badj	d11 (mils)	d22 (mils)	LT (%)	Approach Side	Leave Side
1	5,000	4.11	5.73	3.59	63	1.15	1.20	8.5	11.9	75	0	11
2	5,000	6.83	4.29	2.80	65	1.15	1.20	14.1	8.9	78	4	4
3	5,000	4.80	4.90	2.17	44	1.15	1.20	9.9	10.1	53	0	0
4	5,000	5.42	3.92	2.74	70	1.15	1.20	11.2	8.1	84	4	4
5	5,000	5.93	4.54	2.02	44	1.15	1.20	12.3	9.4	53	4	0
6	5,000	3.86	2.97	1.94	65	1.15	1.20	8.0	6.1	78	0	0
7	5,000	4.85	3.44	2.06	60	1.15	1.20	10.0	7.1	72	4	0
8	5,000	8.31	6.11	1.54	25	1.15	1.20	17.2	12.6	30	6	4
9	5,000	2.98	5.68	2.00	35	1.15	1.20	6.2	11.8	42	0	4
10	5,000	5.83	8.25	1.48	18	1.15	1.20	12.1	17.1	22	0	4
11	5,000	4.75	3.98	1.71	43	1.15	1.20	9.8	8.2	52	0	0
12	5,000	4.08	8.21	3.67	45	1.15	1.20	8.4	17.0	54	0	28
13	5,000	3.24	8.25	3.45	42	1.15	1.20	6.7	17.1	50	0	24
14	5,000	4.88	3.81	1.57	41	1.15	1.20	10.1	7.9	49	0	0
15	5,000	2.72	3.06	2.22	73	1.15	1.20	5.6	6.3	87	0	0
16	5,000	9.05	9.00	5.65	63	1.15	1.20	18.7	18.6	75	8	8
17	5,000	3.45	2.67	1.66	62	1.15	1.20	7.1	5.5	75	0	0
18	5,000	4.22	2.38	1.34	56	1.15	1.20	8.7	4.9	68	0	0
19	5,000	6.45	4.82	1.48	31	1.15	1.20	13.4	10.0	37	4	0
20	5,000	8.45	6.51	3.68	57	1.15	1.20	17.5	13.5	68	36	16
21	5,000	2.83	2.73	1.69	62	1.15	1.20	5.9	5.7	74	0	0
22	5,000	4.18	2.57	2.10	82	1.15	1.20	8.7	5.3	98	0	0
23	5,000	2.87	2.42	1.56	64	1.15	1.20	5.9	5.0	77	0	0
24	5,000	2.64	3.04	1.52	50	1.15	1.20	5.5	6.3	60	0	0
25	5,000	2.54	2.48	1.62	65	1.15	1.20	5.3	5.1	78	0	0
26	5,000	5.84	7.25	3.28	45	1.15	1.20	12.1	15.0	54	4	16
27	5,000	4.22	3.66	1.86	51	1.15	1.20	8.7	7.6	61	0	0

Note: LT = load transfer.

those deflections measured with an applied load near 9,000 lb should be recorded.

Step 2: Determination of Pavement Parameters from Center Deflections

The first task in this step is the calculation of the deflection basin area associated with each loading. This is accomplished by using the information obtained from center slab testing:

$$Area = (6/W33) * [W33 + (2 * W43) + (2 * W53) + W63].$$

The measured deflection W33 is then normalized to a 9,000-lb load by using the following formula:

$$D33 = W33 * (9{,}000\ lb)/(applied\ load),$$

where D33 is the normalized deflection in mils and W33 is the measured value in mils. The foregoing equation assumes a linear deflection response within the range of 5,000 to 15,000 lb. Deflections measured with loadings outside these limits may induce considerable error because of nonlinearity.

For each test location the calculated area and standardized deflection are used along with slab thickness to back-calculate the effective modulus of elasticity (E) of the slab. These E-values are then averaged to determine the average slab modulus for the subsection. Any values of E that are less than $3 * 10^6$ psi are suspect and should not be included in this average. Any values above $7 * 10^6$ psi should be considered to be $7 * 10^6$ psi for this analysis. See Table 1 for sample results.

The next task is a determination of the bending adjustment factor, Badj. This factor is computed for each test location as follows:

$$Badj = W33/W43,$$

where Badj is the bending adjustment factor and W33 and W43 are measured deflections at the center of the slab. Calculated values are averaged to obtain the representative bending adjustment factor for each subsection. The load transfer measured at each joint or crack is then multiplied by this average Badj to adjust for the slight bending of the slab between the first and second sensors, so that true load transfer across the joint is obtained (see Table 1 for sample results).

Step 3: Determination of Adjustment Factors to Standardize Corner Deflections

The measured deflections must be adjusted to a standard loading condition of 9,000 lb and a standard slab modulus of 4,000,000 psi. This is accomplished by graphically determining the elastic modulus correction factor, Ecorr. Once this value is known, the standardized deflections can be calculated by using the following equation:

$$dij = Wij * Ecorr * (9{,}000\ lb)/(applied\ load),$$

where

dij = standardized deflection,
Wij = measured deflection, and
Ecorr = elastic modulus correction factor.

(See Table 2 for sample results.)

Step 4: Determination of Adjusted Load Transfer

As mentioned previously, the measured load transfer (measured between sensors 1 and 2) must be adjusted by the Badj factor to reflect conditions that exist at the interface of the joint walls. This is accomplished by using the following equation:

$$Adjusted\ load\ transfer = measured\ load\ transfer * Badj,$$

where measured load transfer is (W21/W11) * 100 or (W12/W22) * 100 (W21 is deflection at location 2 with load at location 1, W11 is deflection at location 1 with load at location 1, W12 is deflection at location 1 with load at location 2, and W22 is deflection at location 2 with load at location 2). (See Table 2 for sample results.)

Step 5: Construction of the Void Detection Plot

The standardized deflections and adjusted load transfers are now plotted on the graph of deflection versus load transfer known as the void detection plot. Figure 6 is a plot of typical deflection data taken at consecutive joints along a project at both approach and leave corners.

Step 6: Determination of Zero Voids Band

To determine those joints for which no void exists, a family of zero voids curves is superimposed over the void detection plot. This family of zero voids curves is a series of curves drawn at various intercept values to represent the wide range of possible locations that may result because of field variables (e.g., slab thickness and subgrade stiffness). With these as guides, a curve is established that envelops the bottom of all the plotted data points. (There will be times when some extreme values or outliers will fall below this bottom line because of random statistical variation or errors in measurement. When the lower envelope is established, the number of outliers should be kept below 5 percent of the values falling in the completed zero voids band.) Deflection intercept values are then measured directly from this curve for each of the five main load transfer divisions (0, 25, 50, 75, and 100 percent). These intercepts are then multiplied by 1.43 to establish the intercepts for the mean zero voids curve and then by 1.86 to establish the intercepts for the upper limit on the zero voids band.

Step 7: Construction of Void Size Lines

The mean zero voids intercept at 0 percent load transfer is then used to graphically determine the effective corner subgrade support k-value. Once the effective corner support value is known, adjustment factors for each void size and load transfer can be determined. These adjustment factors are then applied to the mean zero voids intercepts at each major load transfer division to determine the intercepts for each of the various void sizes. Connecting these points results in the final graph as shown in Figure 7 (assuming a 9-in. slab thickness).

During this construction, all curves may be approximated as piecewise linear between the main load transfer divisions without introduction of significant error into the analysis. This concept will be illustrated on all void size lines. Void size lines that represent single-sided voids are shown as solid lines and those that represent equal-sized voids across the joint are shown as dashed lines. Single-sided void lines are not extended past the 75 percent line transfer lines because these high levels of load transfer (75 to 100 percent) are not normally conducive to developing a single-sided type of void pattern.

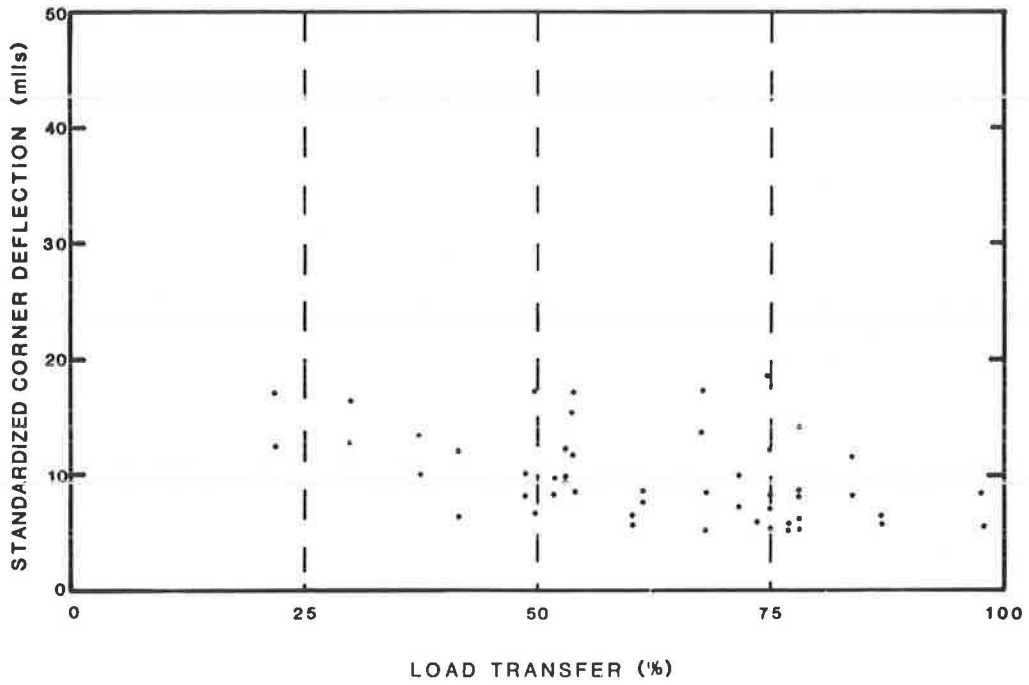

FIGURE 6 Typical plot of corner deflection versus load transfer.

Step 8: Determination of Void Sizes at Individual Joints

Approximate void sizes existing at each joint are found by using the following guidelines:

1. Points falling within or below the zero voids band are recorded as having no void.
2. Points falling above the zero voids band represent joints with voids developed. To size these voids, one must first determine whether a void exists on one or both sides of the joint. This is done by assuming that equal-sized voids exist across the joint if the deflections recorded at a joint (approach and leave sides) differ by no more than 15 percent.

One-Sided Voids

1. Any points falling between the upper limit of the zero voids band and the solid 4-ft² line are recorded as having a void of 4 ft².
2. Points falling between the 4- and 36-ft² void lines are interpolated as closely as possible.

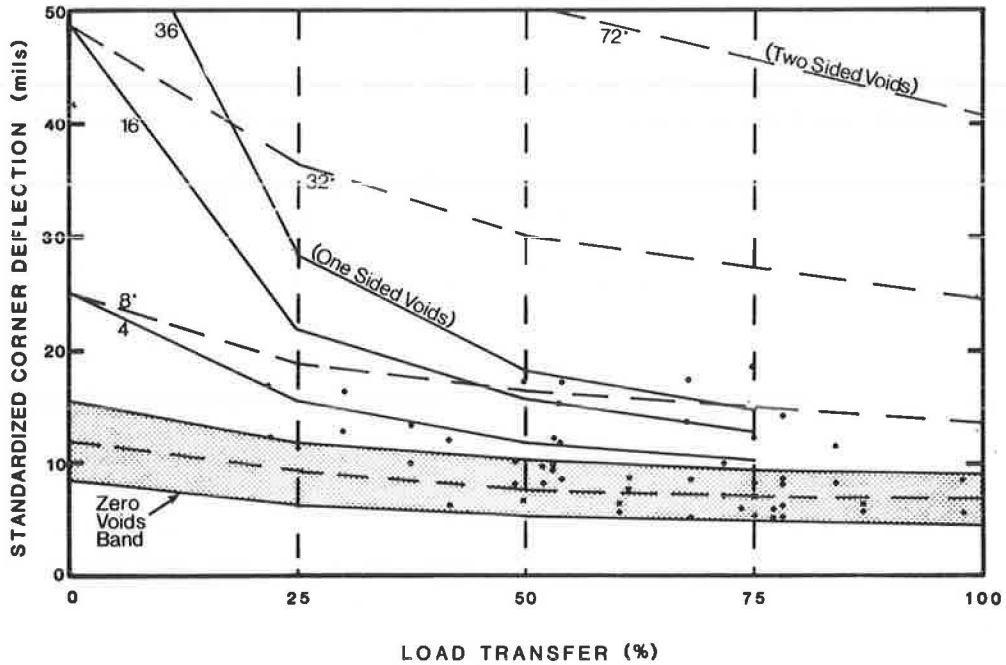

FIGURE 7 Completed void detection plot using typical deflection data.

3. Points above the 36-ft² line are recorded as 36 ft².

[Note: It is possible to have single-sided voids on both sides of a joint. This situation indicates voids of much different sizes (one large and one small).]

Double-Sided Voids

1. For points believed to have equal-sized voids, void predictions are based on only the larger measured deflection.
2. Points falling between the upper limit of the zero voids band and the 8-ft² line are recorded as 8 ft² (4 ft² on either side).
3. Points between 8 and 72 ft² are interpolated as closely as possible.
4. Points above the 72-ft² line are recorded as 72 ft² (a situation that rarely occurs).

Void sizes obtained by using Figure 7 have been entered in Table 2. This completes the void detection evaluation. The next step is to estimate the grout quantities required to fill these voids.

Step 9: Estimation of Grout Quantities

The amount of grout that is required to restore support for a given project logically should depend on the extent of voids that have developed beneath the slab or base. Experience has shown that this is true in general. However, the quantities of grout that are being pumped on projects today depend on several additional factors, including the amount of slab lift allowed during grouting (very important), the base type and condition, the subgrade soil type and extent of holes or discontinuities, shoulder type, and available channels for flow.

Thus, it is difficult to provide a reliable procedure for estimating the required grout quantities for a given project. During the demonstration projects for NCHRP Project 1-21, approximate grout quantities pumped during subsealing operations were obtained for joints with various predicted void sizes. Joints that indicated no voids (the deflection and load transfer point fell within the zero voids band) took an average of 1.8 ft³ of grout per joint. The deflections remained essentially the same after grouting as before grouting and thus no increase in support was achieved. In fact, sometimes an increase in deflection occurred at these joints. This grout may be going into the subgrade, under the shoulder, lifting the slab, and so on. For example, one joint that indicated no void took 6 ft³ of grout. If this amount of grout were actually filling a void of 36 ft², the depth would be 2 in. Thus, it is concluded that joints for which no loss of support or void development is indicated should not be subsealed because no structural benefits are obtained.

Joints for which the existence of voids are indicated from 4 to 36 ft² in horizontal size averaged between 2 and 3 ft³ of grout injected per joint. However, even here a substantial proportion of this grout must be going elsewhere than into the thin void beneath the slab or base. For example, a large void 36 ft² and 0.2 in. deep would require only 0.6 ft³ of grout to fill.

Even though it is believed that much of the grout being pumped is going somewhere other than into the actual void cavity, an average of 2 to 3 ft³ of grout per joint should be planned for joints where voids exist to ensure adequate dispersion and coverage of all existing cavities. Therefore, this quantity should be multiplied by the estimated number of joints and cracks with voids to estimate the overall grout quantity for the project. Joints for which no voids are indicated should not be subsealed.

For grout quantity estimation, a continuous sample of joints should be selected to represent the project under consideration (e.g., 25 consecutive joints per mile). These joints should be analyzed for voids by using the methods presented. The proportion of joints for which voids are indicated can then be determined. The sample project showed that voids existed at 14 out of 27 joints, or 52 percent. If this sample was chosen to represent a project 3 mi long with a joint spacing of 20 ft, the total grout quantity would be estimated as follows:

Total joints = (5,280/20) * 3 mi = 792,

Estimated number of joints requiring grout = 792 * 0.52 = 412,

Estimated grout quantity = 412 joints * 2.5 ft³/joint = 1,030 ft³.

SUMMARY AND CONCLUSIONS

The void detection procedures developed under NCHRP Project 1-21 are the result of a detailed 3-year study of both computer analysis and collected field data. During the study, emphasis was placed on simplicity and reliability of the resulting procedure. It is the authors' belief that if the procedures outlined here are followed, substantial savings, both in immediate rehabilitative costs and future maintenance costs, can be realized. The selective subsealing of only those joints and cracks that have loss of support is the most cost-effective way to restore support to jointed concrete pavements. Deflection testing provides assurance of restored support. If deflection measurements and void analysis are not performed before and after subsealing, there is no way to determine the benefit of the work. In addition, continued deflection monitoring of the pavement can show whether support is being maintained and grouting can be programmed if support is reduced.

ACKNOWLEDGMENT

This paper was prepared on the basis of a research project report entitled "Evaluation of Joint Repair Methods for Portland Cement Concrete Pavements." This project was sponsored by the American Association of State Highway and Transportation Officials, in cooperation with FHWA and was conducted in the National Cooperative Highway Research Program, which is administered by the Transportation Research Board of the National Research Council. The authors extend their appreciation to Paul Okamoto and Jeff Darling of the University of Illinois for their work on the initial phases of the void detection work.

REFERENCES

1. J.A. Crovetti and M.I. Darter. Appendix C: Void Detection Procedures. In Final Report, NCHRP Project 1-21, TRB, National Research Council, Washington, D.C., June 1984.
2. M.S. Hoffman. Mechanistic Interpretation of Nondestructive Pavement Testing Deflections. Ph.D. dissertation. Department of Civil Engineering, University of Illinois, Urbana-Champaign, 1980.

3. A.M. Tabatabaie and E.J. Barenberg. Longitudinal Joint Systems in Slip-Formed Rigid Pavements, Vol. 3: User's Manual. FAA and FHWA, U.S. Department of Transportation, 1979.

The contents of this paper reflect the views of the authors, who are responsible for the accuracy of the data. The contents do not necessarily reflect the official views or policies of the Transportation Research Board, the National Academy of Sciences, FHWA, the American Association of State Highway and Transportation Officials, or the individual states participating in NCHRP.

Publication of this paper sponsored by Committee on Pavement Maintenance.

Experimental Project on Grout Subsealing in Illinois: A 20-Month Evaluation

JAMES C. SLIFER, MARY M. PETER, and WILLIAM E. BURNS

ABSTRACT

Several experimental features were included in an undersealing project conducted by the Illinois Department of Transportation during the fall of 1983. This experimental project evaluated the performance of limestone-cement slurries versus that of pozzolan-cement slurries, the effects of admixtures (water reducer and superplasticizer) on these slurries, and the effects of various pumping pressures (10, 20, and 30 psi) on the undersealing operation. Initial studies indicated that the fly-ash grouts were generally superior to limestone grouts on the basis of the higher strengths exhibited by the fly-ash grouts regardless of admixtures, the greater improvements in deflections produced by the fly-ash mixes, the possible damaging effects produced by the limestone mixes when grouting is done in areas that display low initial deflections, and, finally, the greater flowability of the fly-ash mixes. Four slabs that were removed after undersealing verified this superior ability of the fly-ash grouts to flow into voids. Fly-ash grouts either with no admixture or with superplasticizer produced the greatest decrease in the pavement deflection at cracks and joints, whereas limestone grouts with admixtures produced the least decreases in deflections. It was also observed that, for a given pavement, a limiting deflection value exists below which deflections will not be reduced. In addition, if the initial deflection is low, it appears better not to grout the pavement, because deflections may increase. Pumping pressures investigated had a negligible effect on undersealing operations. Pavement deflections measured 7 and 20 months after undersealing supported the initial evaluations of undersealing materials.

Rehabilitation and restoration of portland cement concrete (PCC) pavements in Illinois have traditionally included the patching of failed areas followed by the placement of a bituminous overlay. Although overlaying the pavements will improve the ride quality, it does not correct the problems caused by the development of voids beneath the concrete slab. The purpose of undersealing or subsealing is to restore support to a pavement structure by filling these voids with grout under pressure without intentionally raising the pavement. The inclusion of pavement subsealing in conjunction with patching and resurfacing, therefore, appears to be a more effective rehabilitation technique.

Because of the projected increase in the use of this technique in the state, the Illinois Department of Transportation (IDOT) studied the design and proper application of grout slurries in undersealing. Specifically, this experimental project evaluated the performance of limestone-cement slurries versus that of pozzolan-cement slurries, the effects of admixtures on these slurries, and the effects of various pumping pressures on the undersealing operation.

EXPERIMENTAL PROCEDURES

Description of Test Area

A 71,000-ft section of a planned 3.15-mi restoration project was designated as the test section. This restoration project was performed on a four-lane divided concrete pavement segment of I-55 in Sangamon County, Illinois. The original pavement structure, constructed in 1963, consisted of 10-in. standard reinforced PCC pavement with load transfer contraction joints at 100-ft spacings over 6-in. Type A granular subbase material. Included in the restoration were full- and partial-depth patching, undersealing, underdrain installation, and profiling.

Experimental Features

In an attempt to learn more about the penetrating characteristics of grout, several variations in the mix design and injection pressures were planned. All test slurries were a combination of portland cement, the appropriate aggregate (limestone or fly ash), water, and, where indicated, the appropriate admixture (water reducer or superplasticizer). Six variations in the mix design were tested as follows:

1. Fly ash with superplasticizer,
2. Fly ash with no admixture,
3. Fly ash with water reducer,
4. Limestone with no admixture,
5. Limestone with water reducer, and
6. Limestone with superplasticizer.

In addition, three injection pressures--10, 20, and 30 psi--were chosen to investigate the feasibility of pumping grout at lower pressures to minimize the potential for pavement damage. The resulting design matrix is given in Table 1.

TABLE 1 Experimental Design Matrix

Section	Aggregate	Admixture	Pressure (psi)	Length (ft)
F-1	Fly ash	SP	30	300
F-2	Fly ash	SP	20	300
F-3	Fly ash	SP	10	300
F-4	Fly ash	None	30	300
F-5	Fly ash	None	20	300
F-6	Fly ash	None	10	300
F-7	Fly ash	WR	30	300
F-8	Fly ash	WR	20	300
F-9	Fly ash	WR	10	300
L-1	Limestone	None	30	300
L-2	Limestone	None	20	300
L-3	Limestone	None	10	300
L-4	Limestone	WR	30	300
L-5	Limestone	WR	20	300
L-6	Limestone	WR	10	300
L-7	Limestone	SP	30	300
L-8	Limestone	SP	20	300
L-9	Limestone	SP	10	300

Note: SP = superplasticizer; WR = water reducer.

Each test section consisted of three 100-ft panels. After each test section, a transition panel 100 ft long was designated before the next test section. The purpose of this transition panel was to allow the holding tank to be emptied and the appropriate mix design to be prepared. All test panels were located in the northbound driving lane of I-55.

Mix Designs

The limestone aggregate mix design selected was 1,499 lb of mineral filler (limestone dust), 589 lb of cement, and 938 lb of water. Water reducer (Hoycol, W.R. Grace Company) or superplasticizer (WRDA 19, W.R. Grace Company) was added at the rates of 8.5 or 17 oz per hundredweight of cement, respectively. Aggregate was required to meet the following gradation:

Passing Sieve No.	Percent Passing
30	100
100	92 ± 8
200	82 ± 8

The fly-ash aggregate mix design selected was 1,387 lb of fly ash, 605 lb of cement, and 915 lb of water. Again, a water reducer or superplasticizer was added at the rate of 8.5 or 17 oz per hundredweight of cement, respectively.

Field Operations

Deflection data were taken by IDOT on all experimental sections before grouting. The test method employed included the use of the Model 2008-X Road Rater with a peak-to-peak dynamic force of 8,000 lb operating at a frequency of 15 Hz. Measurements were taken in the outer wheel path 30 in. ± 5 in. from the outside pavement edge.

After deflection data were taken, a hole pattern was chosen. A three-hole and a five-hole pattern were used in this study and are shown in Figure 1. Either pattern was used on a given crack or joint. The holes, drilled with a pneumatic track drill, were 2 ± 1/4 in. in diameter and extended into the granular subbase approximately 4 in. Drilling was completed within 2 days before undersealing.

All the mixing and proportioning were done at the grout plant. The grout was mixed with an auger and sent to a holding tank until ready for pumping. Admixtures, when used, were added at the base of the auger by way of an automatic mechanical dispenser system.

The group packer was inserted into the drilled hole in the slab and pumping was initiated. A gauge mounted on the discharge pipe near the holding tank monitored the pumping pressure. Temporary surge pressures of short duration (1 to 3 sec), often exceeding 50 psi but maintained below 100 psi, were sometimes necessary to initiate grout flow. A Dynasonics Model UFT0601 (S/N 2965) Doppler flow meter indicated grout velocities and total volume. Also noted was the pumping time required to complete a given hole. A modified Benkelman beam was used to monitor the vertical movements of the slab. Lifting of the slab was kept below 0.05 in. total movement. Pumping was continued until (a) there was a significant movement of the gauge monitoring the slab lift; (b) slurry was forced up through a nearby crack, joint, or drilled hole; or (c) after a reasonable amount of time there was no indication of slab movement or grout take. Grout that was not routed to the packerhead for injection was recirculated back into the grout holding tank.

Samples of the grout mixtures were taken during the undersealing operations and were tested for compressive strength. Consistency of the mixtures was monitored with a standard flow cone. After pumping, the nozzle was removed and a temporary wooden plug was immediately inserted into the hole. These temporary plugs were removed after the back pressure

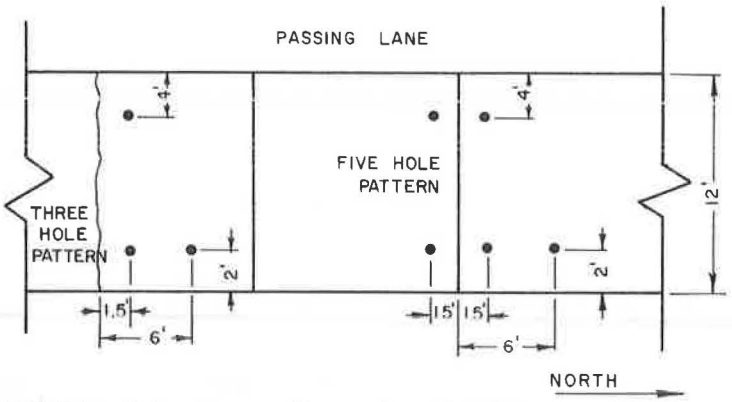

FIGURE 1 Hole patterns used in experimental section.

had subsided sufficiently to assure that the grout would not be forced out of the hole. On completion of the subsealing, all drill holes were grouted flush with the surface of the pavement with a sand-cement grout. Undersealing of the experimental section was begun September 22, 1983, and was completed by September 26, 1983.

Three days after the undersealing was completed, deflections were again measured. After a review of the deflection data, four locations were selected for removal of the slab and examination. Of the four locations, two were chosen from areas treated with limestone and two from areas treated with fly-ash mix. Of the two locations treated with a given aggregate mix, one location was chosen that displayed considerable improvement in deflection values and the other location was one that displayed a less than satisfactory change.

RESULTS

Pumping Pressures

Undersealing was performed at pressures of 10, 20, and 30 psi. At these low pumping pressures, total slab rise was easily maintained below the maximum of 0.05 in. The effects of pumping at pressures of 20 and 30 psi on the undersealing operation were negligible. However, time required for injection at 10 psi appeared to be longer. Because of the negligible differences at 20 and 30 psi, further results and discussion will be limited to an evaluation of materials.

Material Strength and Fluidity

Grout materials were evaluated on the basis of compressive strength, slurry fluidity or flowability, and ability to restore support to the pavement structure as indicated by the resulting deflection changes following treatment.

Samples of the grout mixtures were periodically taken during field operations and tested for compressive strength. Results are summarized in Table 2.

As shown in Table 2, fly-ash aggregate consistently produced mixes of greater strength; the highest strength is achieved with the mixture of fly ash and water reducer and the lowest with the limestone and no admixture. Only three of the six mix designs studied displayed compressive strengths greater than 1,000 psi. High compressive strengths may prove to be one solution to the problem of erosion.

Improved pumpability of the grout material will likely reduce wear to the pumping equipment, reduces clogging of the equipment, and, most important, improves the capability of the grout to fill voids. Average flow rates at 30 psi of the various mix designs as determined from Doppler flow meter data analysis are also given in Table 2.

TABLE 2 Compressive Strengths of Mix Designs and Average Flow Rates

Aggregate	Admixture	Avg Compressive Strength[a] (psi)	Flow Rate (ft^3/sec)
Fly ash	None	935	0.11
Fly ash	Superplasticizer	1,888	0.11
Fly ash	Water reducer	3,495	0.07
Limestone	None	628	0.04
Limestone	Superplasticizer	722	0.08
Limestone	Water reducer	1,089	0.04

[a]Compressive strengths were determined from 4-in. diameter cylinders (ASTM C 39) at 7 days.

As indicated, the fly-ash aggregate generally produced mixes capable of achieving greater flow rates; the greatest flow rate was achieved with the mixture of fly ash and superplasticizer and with fly ash and no admixture.

A Doppler flow meter was used in determining average flow rates. This nonintrusive measuring instrument is a suitable device for measuring the higher flow rates of grouting materials. Doppler flow meters are known, however, to be unreliable at lower flow rates typical of such a pressure-grouting operation.

An average of 2.00 ft^3 of grout was pumped per crack or joint in the test section treated with the fly-ash grout, whereas only 1.71 ft^3 of grout was injected per crack or joint in the test section treated with limestone grout. Only those cracks and joints with initial deflections, both leave and approach, that were in the range of $x \pm 1\sigma$ were included in these stated averages. Therefore, the possibility that a greater amount of fly-ash grout was pumped because of larger existing voids in the fly-ash test section was minimized. It is more likely that a greater amount of fly-ash grout was pumped because of its greater fluidity.

Deflection Analysis

Immediately Following Treatment

Deflection measurements were taken on all cracks and joints in the experimental section before undersealing operations began. Results, excluding those used for controls, are as follows (peak-to-peak dynamic force of 8,000 lb):

	Initial Deflection (mils)		
	Cracks and Joints	Cracks	Joints
Approach	7.45	7.10	7.83
Leave	7.94	7.42	8.51

Initial leave deflections were approximately 7 percent greater than initial approach deflections. Joint leave deflections were approximately 13 percent greater than crack leave deflections before grouting.

Three days after the undersealing in the experimental section had been completed, deflections were taken at all locations measured in the initial analysis. It is known that deflections fluctuate substantially with changes in such variables as temperature of the slab and moisture conditions of the subgrade (1). All experimental sections contained cracks or joints that were not treated and can therefore be considered experimental controls. These controls would indicate to what approximate degree the uncontrollable environmental conditions affected the deflection measurements stated here. The average approach deflections of those cracks and joints designated as controls increased 0.12 mil. Average leave deflections increased 0.10 mil.

Initial analyses indicated that grouting was effective in decreasing deflections that were higher than average but was ineffective for average or below-average deflection locations. That is, the greatest improvements will be experienced by those cracks or joints with unusually high initial deflections, and lesser degrees of improvement will be evident as the initial deflections approach that of the mean. Indeed, in several instances, those cracks or joints with below-average deflections experienced an increase in deflection after undersealing. An attempt to confirm these suspicions involved the analysis of cracks or joints with initial leave deflections that fell beyond the range of $x + 1\sigma$, where x is 7.94 mils and σ is 2.76 mils.

The average initial leave deflection of those cracks or joints that fell above $x + 1\sigma$ was 12.8 mils. After undersealing, this average deflection was decreased to 9.33 mils, a 27 percent decrease in mean deflection. When all cracks and joints with initial deflections greater than the average were included in the analysis, only a 21 percent decrease in measured deflection resulted. As indicated earlier, when a crack or joint with a low initial deflection is undersealed, deflections often increase. Evidence would appear to indicate that this is especially true when a limestone mix is used. Table 3 contains deflection measurements for those cracks and joints with initial approach and leave deflections less than or equal to the average. Initial approach deflection is 7.45 mils and initial leave deflection is 7.94 mils.

TABLE 3 Deflection Changes for Cracks and Joints Displaying Low Initial Deflections

	Aggregate	
	Fly Ash	Limestone
Approach		
Before (mils)	6.48	5.87
Immediately after (mils)	5.63	6.48
Percent improvement	13[a]	−10
Leave		
Before (mils)	6.43	5.81
Immediately after (mils)	5.48	6.85
Percent improvement	15	−18

[a]Decreases in deflections are considered positive and increases are considered negative throughout this paper.

As indicated in Table 3, leave deflections decreased by an average of 15 percent in sections treated with the fly-ash grout, whereas leave deflections increased by an average of 18 percent in sections treated with the limestone grout. Tables 4 and 5 contain these same deflection measurements for the designated mix designs. Table 4 contains the deflection information for the cracks and joints treated with the fly ash and the designated admixtures. Table 5 contains the deflection information for the cracks and joints treated with the limestone mix designs.

TABLE 4 Deflection Changes of Cracks and Joints Displaying Below-Average Initial Deflections and Treated with Fly Ash Mix

	Admixture		
	None	Superplasticizer	Water Reducer
Approach			
Before (mils)	6.00	6.88	6.54
Immediately after (mils)	4.75	6.44	5.71
Percent improvement	21	6	13
Leave			
Before (mils)	5.75	7.25	6.44
Immediately after (mils)	4.75	6.31	5.50
Percent improvement	17	13	15

TABLE 5 Deflection Changes of Cracks and Joints Displaying Below-Average Initial Deflections and Treated with Limestone Mix

	Admixture		
	None	Superplasticizer	Water Reducer
Approach			
Before (mils)	6.28	5.32	6.83
Immediately after (mils)	6.34	6.04	7.83
Percent improvement	−1	−14	−15
Leave			
Before (mils)	6.22	5.24	6.77
Immediately after (mils)	6.50	6.26	8.85
Percent improvement	−5	−19	−31

As Tables 4 and 5 show, the greatest decreases in deflections were obtained by the grout with fly ash and no admixture, whereas the greatest increases were obtained with the mixture of limestone and water reducer. These results would appear to indicate that blanket undersealing could have an adverse effect on below-average deflection areas, especially when a limestone grout mixture was used. On an intuitive basis, it appears that selective undersealing is a more efficient process in many situations regardless of mix design.

In an attempt to not be biased by the influence of treating below-average deflections, only those cracks or joints with above-average initial deflections were considered for further analyses and presented here. Deflection results for cracks and joints treated with the fly-ash and limestone grouts and showing above-average initial deflections are given in Table 6. As indicated, initial leave deflections were higher than initial approach deflections by approximately 15 percent and the greater amount of improvement (21 versus 15 percent) was experienced by the leave deflections. Initial joint deflections were similar to initial crack deflections and they both experienced approximately the same degree of improvement.

TABLE 6 Deflection Changes for Cracks and Joints Displaying Above-Average Initial Deflections

	Cracks and Joints	Cracks	Joints
Approach			
Before (mils)	9.39	9.27	9.47
Immediately following (mils)	7.98	7.89	8.05
At 7 months (mils)	7.43	7.57	7.33
At 20 months (mils)	6.54	6.50	6.57
Percent improvement			
Initially	15	15	15
At 7 months	21	18	23
At 20 months	30	29	31
Leave			
Before (mils)	10.81	10.76	10.85
Immediately following (mils)	8.52	8.55	8.50
At 7 months (mils)	8.10	8.64	7.72
At 20 months (mils)	6.02	6.14	5.92
Percent improvement			
Initially	21	21	22
At 7 months	25	20	28
At 20 months	44	41	45

Table 7 displays deflection changes for cracks and joints treated with either fly-ash or limestone aggregate. Inspection of Table 7 indicates that greater improvements in mean deflections were experienced by those cracks and joints undersealed with the fly-ash mix. These cracks and joints experienced a 33 percent decrease in leave deflections, whereas those undersealed with the limestone aggregate mix experienced only a 13 percent decrease. Likewise, a 26 percent decrease in approach deflections was noted for those cracks and joints undersealed with the fly-ash mix and only a 6 percent decrease for those undersealed with the limestone mix. On the average, improvements in deflections were 20 percent greater for areas treated with the fly-ash grout than for areas treated with limestone grout.

TABLE 7 Deflection Changes for Cracks and Joints Displaying Above-Average Initial Deflections

	Aggregate	
	Fly Ash	Limestone
Approach		
Before (mils)	9.94	8.99
Immediately following (mils)	7.38	8.41
At 7 months (mils)	6.72	7.94
At 20 months (mils)	5.91	6.97
Percent improvement		
Initially	26	6
At 7 months	32	12
At 20 months	41	22
Leave		
Before (mils)	10.88	10.76
Immediately following (mils)	7.31	9.39
At 7 months (mils)	6.97	8.91
At 20 months (mils)	5.69	6.24
Percent improvement		
Initially	33	13
At 7 months	36	17
At 20 months	48	42

Table 8 contains deflection information for cracks and joints treated with the fly-ash mix design and its designated admixtures. Table 9 contains the corresponding information for the limestone mix design. As Tables 8 and 9 indicate, the greatest improvements were produced by the fly ash with no admixture (an average decrease of 44 percent in the leave deflections) followed by the mixture of fly ash and superplasticizer (an average decrease of 36 percent in the leave deflection). The most disappointing results were produced by the limestone mixes with admixtures.

Of those areas treated with the limestone mix, only the limestone without admixture material reduced deflections (an average decrease of 27 percent in the leave deflections). The limestone aggregate with admixtures actually increased deflections; that is, the limestone mix with the superplasticizer admixture produced an increase of 3 percent in leave deflection measurements. Likewise, the limestone mix with the water reducer admixture also produced an average increase of 6 percent in leave deflection measurements.

TABLE 8 Deflection Changes for Cracks and Joints Displaying Above-Average Initial Deflections and Treated with Fly Ash Mix

	Admixture		
	None	Superplasticizer	Water Reducer
Approach			
Before (mils)	8.15	10.64	9.79
Immediately following (mils)	5.40	7.66	8.38
At 7 months (mils)	5.98	6.63	7.57
At 20 months (mils)	4.33	5.50	7.84
Percent improvement			
Initially	34	28	14
At 7 months	27	38	23
At 20 months	47	48	20
Leave			
Before (mils)	9.15	12.11	9.46
Immediately following (mils)	5.10	7.71	8.21
At 7 months (mils)	6.42	6.83	7.77
At 20 months (mils)	4.32	5.30	7.46
Percent improvement			
Initially	44	36	13
At 7 months	30	44	18
At 20 months	53	56	21

TABLE 9 Deflection Changes for Cracks and Joints Displaying Above-Average Initial Deflections and Treated with Limestone Mix

	Admixture		
	None	Superplasticizer[a]	Water Reducer
Approach			
Before (mils)	9.24	7.75	8.80
Immediately following (mils)	7.86	8.00	9.06
At 7 months (mils)	7.96	7.20	7.96
At 20 months (mils)	6.27	7.91	7.75
Percent improvement			
Initially	15	–3	3
At 7 months	14	7	10
At 20 months	32	–16	12
Leave			
Before (mils)	11.79	8.00	9.78
Immediately following (mils)	8.60	8.25	10.34
At 7 months (mils)	9.14	7.50	8.74
At 20 months (mils)	5.61	7.28	6.93
Percent improvement			
Initially	27	–3	–6
At 7 months	22	6	11
At 20 months	52	9	29

[a]Only one crack or joint treated with the limestone superplasticizer.

Twenty-Month Evaluation

Pavement deflections were remeasured 7 and 20 months after undersealing had been completed. Results supported many of the original evaluations of under-

sealing materials. Because temperature changes and other environmental conditions affect pavement deflections, all results are only relevant to a given period of time. That is, it is possible to compare the current performance of the undersealing materials; however, it is not possible to judge, with accuracy, the degree of change over time.

As Table 6 indicates, deflection improvements in joints were greater than those in cracks, although earlier deflections (both before treatment and immediately following treatment) had been similar. Leave deflections continued to show a greater amount of improvement than did approach deflections, probably because of large initial voids.

Deflection results for the cracks and joints treated with the fly-ash or limestone aggregate slurries are contained in Table 7. As expected, the cracks and joints treated with the fly-ash slurries generally continue to show a greater degree of improvement with time. A trend appears to be developing that shows the limestone-treated areas approaching the performance of the fly ash-treated areas. Immediately following treatment, leave slabs treated with the fly-ash slurries showed a decrease in deflections 20 percent greater than those treated with the limestone slurries. Seven months later this difference had decreased to 19 percent and most recently (20 months later) 6 percent, as shown in Table 7. The most likely explanation for this trend is the decreasing performance of the slabs treated with fly ash and water reducer and the increased performance of the slabs treated with the slurry that contained limestone and no admixture (see Tables 8 and 9) in comparison with other treated slabs.

At present, the mixes that have resulted in the greatest decreases in pavement deflections have been the fly-ash mixes with either the superplasticizer or without an admixture. The deflection measurements continue to indicate that poorest results occurred with slabs undersealed with the limestone slurries that contain admixtures.

One final comment should be made concerning the performance of the treated cracks or joints as compared with the untreated ones. Untreated cracks and joints were chosen mainly because, on the basis of visual evidence, undersealing was not necessary. Before undersealing, these pavement cracks and joints deflected an average of 7.9 mils. Cracks and joints that were to be treated deflected an average of 10.8 mils. Twenty months later, the leave deflections of untreated cracks and joints deflected an average of 4.8 mils. Treated cracks and joints deflected an average of 6.02 mils or only 26 percent more than the untreated ones. Cracks and joints treated with the mixture of fly ash and superplasticizer actually deflected less than the untreated controls, as shown in Figure 2. Therefore, it can be assumed that the treated areas are behaving similarly to the untreated areas and thus the undersealed pavement is performing adequately.

These results indicate, therefore, that greater improvements were achieved with a fly-ash aggregate mix. If an admixture is desired, it should not be of the water-reducing type. A superplasticizer with fly ash is acceptable and may be desirable because of strengthening characteristics produced by the superplasticizer. Reactions, however, can vary when pozzolans from different sources are combined with various admixtures. Mix designs must always be developed by using the specific pozzolan and additives. If a limestone aggregate mix is chosen, it should not be used in conjunction with either a superplasticizer or a water reducer.

In an attempt to develop a better method for estimating grout quantities, relationships between initial deflections and the volume of grout pumped were investigated. No strong correlations were found. It would appear, therefore, that initial deflections alone may not be a good basis for estimating grout quantities. The only effective method remains the use of historical averages. Approximately 0.86 ft^3 of grout was pumped into an average hole. This quantity falls within the average range previously noted by others.

Another research project was conducted by the University of Illinois simultaneously with the IDOT project (2). Procedures were developed under NCHRP Project 1-21 for void detection by using nondestructive deflection testing (NDT) for locating and dimensioning areas of voids beneath the pavement. Their comprehensive method requires three major inputs: (a) the thickness of the PCC slab, (b) deflection measurements taken at slab centers and corners along the pavement lane, and (c) measurement of deflection load transfer at the joint or crack.

Thirty-six joints were tested in the fly-ash grout

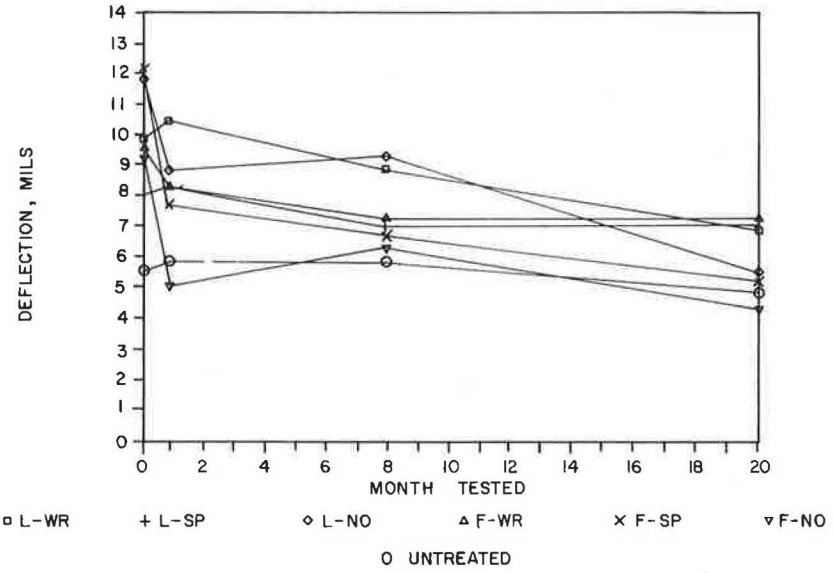

FIGURE 2 Deflection changes for treated and untreated cracks and joints (leave side only).

section and 36 in the limestone section. Fifty percent of the joints in the limestone section were found to have voids with an average size of 7 ft^2. Fifty-three percent of the joints in the fly-ash section were found to have voids with an average size of approximately 12 ft^2.

After grouting in the limestone section, voids were located at 61 percent of the joints and had an average size of approximately 10 ft^2. After grouting in the fly-ash grout section, voids were located at 28 percent of the joints tested and had an average size of approximately 8 ft^2.

Results of this study therefore supported the IDOT findings; that is, undersealing with a fly-ash grout can prove more efficient than undersealing with a limestone grout.

Slab Removal

Removal of the four slabs after undersealing operations also verified the superior ability of the fly-ash grouts to flow into the voids. The fly-ash grout successfully filled the voids and adhered to the bottom of the pavement and the aggregate base course. In one instance, only one of the three drilled holes injected with the limestone grout showed evidence of grout take. Fly-ash grout traveled from the adjacent lane to fill the void not filled by the limestone grout.

"Coning," fracturing of a conical portion on the underside of the concrete slab because of the drilling operation, was evident. Coning leaves the slab in a weakened condition and it will, in time, crack. Coning can be minimized by limiting the downfeed force of the drill.

Additional Project Observations

In addition to the experimental features of the test section, assessments of other factors in the undersealing operation were made. Specifically, the effect of undersealing on existing underdrain systems was observed and the capability of undersealing to stabilize poorly performing patches was investigated. Significant results are as follows:

1. Previously placed underdrains that had originally been backfilled with sand of FA-1 gradation were uncovered and inspected for grout intrusion. None was observed. It is believed that distressed pavements located where underdrains have been previously installed are candidates for pavement undersealing without significant risk to the underdrain system.
2. Several recently patched areas of I-55 displayed extremely high deflections and poor load transfer. These patches were successfully undersealed with a limestone grout. Deflections decreased by an average of 67 percent after grouting. One year later, however, pavement deflections were again as high as they had been before undersealing. Corings indicated that the grout was intact. Therefore it is believed that the void system simply redeveloped beneath the grouted pavement. It is believed that had these cracks at the patch and existing pavement interface been sealed, improvements would had proved more lasting.
3. A portion of I-55 previously patched and overlaid with bituminous concrete contained several rocking patches. Reflective cracking was soon to require maintenance. Patches were undersealed at the boundaries in an attempt to prolong the overlay life. Deflections decreased by an average of 13 percent.

CONCLUSIONS

1. The fly-ash grouts were stronger than limestone grouts treated with identical admixtures used in this study.
2. The fly-ash grouts were more flowable than limestone grouts.
3. Initial deflections at joints were slightly higher than those at cracks. Follow-up studies indicated that undersealing joints may prove more effective than undersealing cracks.
4. Initial leave deflections were slightly higher than initial approach deflections.
5. Fly-ash grouts either with no admixture or with superplasticizer produced the greatest decrease in the deflections of cracks and joints.
6. Limestone grouts with admixtures (superplasticizer or water reducer) produced the least decrease in deflection.
7. If initial deflections were low (below the calculated average for a given pavement), undersealing was ineffective. That is, cracks and joints treated with a limestone slurry experienced an increase in deflection readings and improvement was minimal when a fly-ash mix was used.
8. There appeared to be a limiting deflection value for a given pavement below which deflections would not be reduced. Similarly, greatest improvements were experienced by those cracks or joints with high initial deflections where voids and loss of support existed.
9. Initial deflection measurements in the wheel path alone were not a good basis for estimating grout quantities.
10. Undersealing, when done properly, can restore support to the pavement structure not only in the short term but also in the long term.

ACKNOWLEDGMENTS

The authors would like to thank the following individuals who contributed their time and efforts: David Wheat for programming assistance, David Berry for mix design development, and, finally, Ralph Baker, Jagat Dhamrait, Robert Riegel, and Michael Ripka for their technical assistance.

REFERENCES

1. Cement-Grout Undersealing and Slabjacking. Eres, Inc., Champaign, Ill., Dec. 1980.
2. Appendix C: Void Detection Procedures. In Joint Repair Methods for Portland Cement Concrete Pavements--Design and Construction Guidelines, NCHRP Report 281, TRB, National Research Council, Washington, D.C., (in preparation).

Publication of this paper sponsored by Committee on Pavement Maintenance.

Sealing Cracks in Bituminous Overlays of Rigid Bases

NORMAN E. KNIGHT

ABSTRACT

The objective of this project was to evaluate the effectiveness of seven polymer, rubber, or fiber-modified asphalt sealants and two asphalt emulsion sealants in sealing cracks in a bituminous concrete overlay on a rigid base. These nine sealants were compared with a filled asphalt cement, Pennsylvania Department of Transportation Class J-1. The sealants were observed to determine the effects of crack preparation, application methods, weather, and traffic on their performance. Inspections were conducted during different seasons to determine the condition of the sealants under weather extremes. The results of these inspections indicated that three sealants--Prismoseal A-2, AC-20 with Fibre-Pave, and AC-20 with rubber--performed significantly better than the remaining seven sealants and will be adopted for use in Pennsylvania. In addition, Superseal IIIA and Sof-Seal LM were recommended for further evaluation in sawn joints. H-1 with rubber, E-3, and CRF were not recommended for use because their performance, although satisfactory, was not outstanding.

The objective of this project was to evaluate the effectiveness of seven polymer, rubber, or fiber-modified asphalt sealants and two asphalt emulsion sealants in sealing cracks in a bituminous concrete overlay on a rigid base. These nine products were evaluated in comparison with a mineral-filled asphalt cement sealer, Pennsylvania Department of Transportation (PennDOT) Class J-1, which is a high-flow material, is tracked away from the crack by traffic, and is brittle in cold weather.

The experimental products were to be observed for a period of 36 months in an effort to do the following:

1. Compare the performance of the nine sealants with that of Class J-1 sealer;
2. Compare the performance of field blends of granulated rubber with AC-20 and H-1 and the prepackaged rubber or asphalt sealants;
3. Compare the effects of temperature extremes on the performance of the various products;
4. Determine whether the hot compressed air (HCA) lance improves the sealant bond;
5. Determine whether it is necessary to rout the cracks before the sealants are placed;
6. Determine whether the use of the squeegee improves the sealant performance;
7. Determine whether these materials are extruded by pavement movement;
8. Determine whether the materials are displaced by traffic;
9. Evaluate the overband method of crack sealing, as demonstrated by Prismo Universal Corporation;
10. Compare the performance of Class E-3 (CRS-2) asphalt emulsion with that of a proprietary emulsion formulated specifically as a crack sealant; and
11. Compare material and application costs.

PROJECT LOCATION

The project was located on Trunk Route 415 between Dallas and Harvey's Lake, Luzerne County, Pennsylvania (Figure 1). Sealing operations were performed between Station 1245 in Harvey's Lake and Station 1349 approximately 1 mi north of Dallas. Sealants were applied in the transverse cracks of the two outer lanes of the three-lane pavement (Figure 2). The longitudinal joints between the outside lanes and the center passing lane were also sealed. Seven of the sealants were applied in April 1981 and the remaining three sealants were placed in October 1981.

PREPARATION OF CRACKS

In the past, when cracks were filled with Class J-1 material, no crack preparation was performed by PennDOT. All materials used on this project except the Class E-3 and CRF emulsions, which can be applied to damp surfaces, require the cracks to be clean and dry.

Except for a short portion of Section 5, all cracks were routed by using a Crafco router to create a reservoir for the sealant at the top of the crack. This allowed more sealant material to be placed in the crack and to spread over a thicker cross section (1). The cracks were then brushed with a Crafco power brush and blown clean with a low-pressure backpack air blower. The surface of the routed area remained granular and dusty after the low-pressure air was used.

Prismo Universal Corporation introduced a material from England, Prismoseal A-2, that did not require routing. The crack was heated and blown clean with hot compressed air (HCA) at 3000°F and 3,000 fps. This procedure heated the bituminous concrete and flushed a small quantity of free asphalt to the surface along the crack. A clean, tacked surface was provided for the crack sealant material, which was placed by overseal banding, or using a metal box with a cutout to spread the approximate width and depth of 2 x 1/8 in.

Moisture was a problem on this project because of frequent rain showers. Application of the sealants was delayed until the pavement had lost some of its moisture, but the pavement was deemed not sufficiently dry when portions of Sections 2 and 3 were placed. A torch was then used on Section 3 to further dry the cracks. A leaking sewer line permitted water to flow up through the pavement in portions of

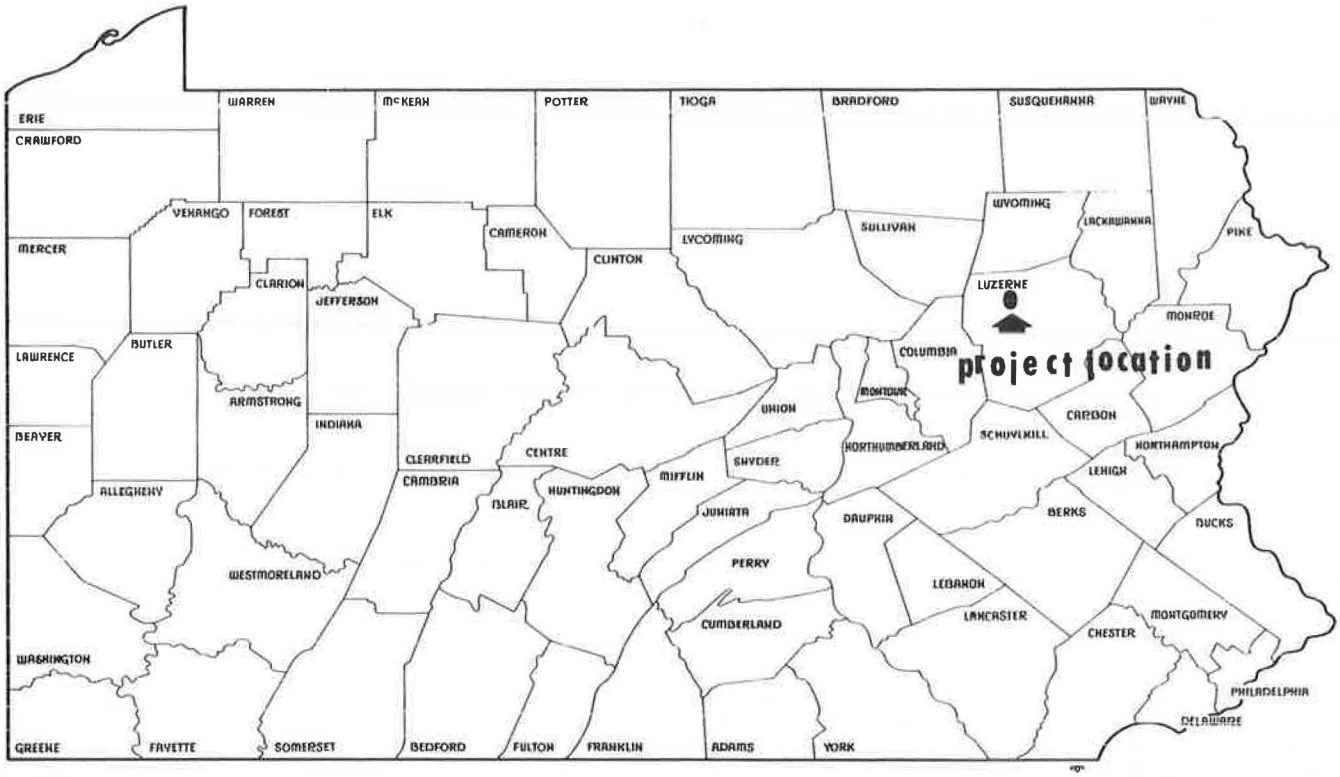

FIGURE 1 Location map.

Sections 3 and 5. These portions were sealed but were excluded from the area to be evaluated.

APPLICATION AND MATERIAL DESCRIPTION

Hot-poured sealants were applied from double boiler heating kettles and were pumped through an application wand directly into the crack and then smoothed with a squeegee. A small portion of Section 4 was placed without the squeegee operation to determine whether this procedure was necessary when Sof-Seal LM crack sealer was applied. The squeegee promoted the bond between the sealer and pavement and lowered the surface of the sealant below the pavement level, thus preventing the sealer from being affected by tires and snowplow blades. Prismoseal A-2 and AC-20 with Fibre-Pave were placed with special applicators and did not require squeegeeing.

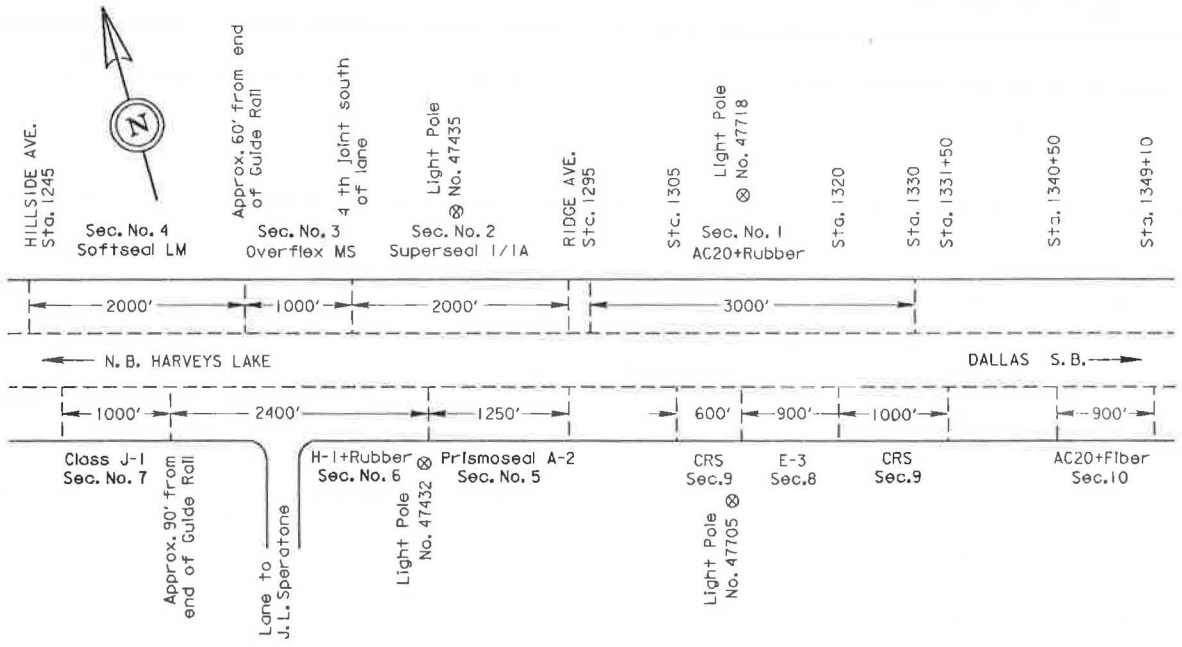

FIGURE 2 Crack Sealing Project LR 177, Luzerne County, Pennsylvania.

TABLE 1 Application Data

Section	Material	Producer	Application Temperature (F°)	Quantity Used (gal)	Cracks Filled (linear ft)	Coverage (ft/gal)
1	AC-20 with rubber		350	160	8,634	58
2	Superseal IIIA	Superior Products Company, Inc.	390-400	50	3,000	60
3	Overflex MS	Crafco, Inc.	375-385	25	1,500	60
4	Sof-Seal LM	W.R. Meadows, Inc.	375	42	2,500	70
5	Prismoseal A-2	Prismo Universal Corporation	350	60	1,250	20
6	H-1 with rubber	–	350	25	2,900	96
7	Class J-1	–	285	25	1,800	80
8	Class E-3	–	180	25	1,300	52
9	CRF emulsion	Witco Chemical Corporation	Ambient[a]	30[b]	1,600	53
10	AC-20 with fiber[c]	Hercules	285	70	1,350	19

[a]40° F. [b]Estimated gallons. [c]Fibre-Pave 5010.

Ten materials were placed on this project (Table 1), including Class J-1, which was placed in Section 7 as the control. Details of the application of these products follow.

Section 1: AC-20 (75 Percent) with Powdered Devulcanized Rubber (25 Percent)

The material in Section 1 was blended in the field by adding prepackaged granulated rubber to the circulating hot asphalt cement in the double boiler. Final mix temperature was 350°F. The addition of the rubber improved the resistance to flow over the plain asphalt cement and decreased the susceptibility to low-temperature cracking. When hot, this material flowed slightly from the cracks, but it adhered well as it cooled with no pick-up by vehicle tires.

Problems associated with the field mixing of this material were as follows:

1. The requirement that either a source of hot asphalt be reasonably close to the sealing project or a distributor be on the project to refill the heating kettle was cumbersome. Neither alternative was desirable because of the time lost in sending the heating kettle to the asphalt source and the cost associated with maintaining a distributor and operator for the small daily quantities of asphalt required on sealing projects. According to PennDOT policy, maintenance forces did not use a distributor for supplying asphalt. The heating kettle was filled at the nearest bituminous concrete plant.
2. The proper proportions of asphalt and rubber were not always maintained. Proportioning was difficult, especially when a partially filled kettle was recharged.

Section 2: Superseal IIIA

Superseal IIIA was manufactured by Superior Products Company, Inc., and consisted of a mixture of materials compatible with asphalt-concrete pavements. The material, prepackaged in a ready-to-use form, was heated in a double boiler-type melter-applicator.

This material had poor adhesion, especially on moist or dusty surfaces. It was readily worked loose by using a finger.

Section 3: Overflex MS

Overflex MS was a premixed, prepackaged blend of 25 percent vulcanized rubber and 75 percent asphalt cement manufactured by Crafco, Inc. This product adhered very well and exhibited excellent resistance to flow and extrusion from the reservoir routed into the crack.

Section 4: Sof-Seal LM

Sof-Seal LM was a premixed, prepackaged combination of polymeric compounds manufactured by W.R. Meadows, Inc. It was susceptible to moist or dusty surfaces as shown by the ease with which the material was pulled loose from the pavement by using a finger. There was also slight flow when the material was placed in the crack.

Section 5: Prismoseal A-2

Prismoseal A-2 was a single-component, highly modified rubberized asphalt dispersion manufactured by Prismo Universal Corporation. Although this product was designed to be placed without routing, it was applied on only a small portion of this section in that manner; the remaining portion was prepared by routing. The crack was cleaned by being blown with hot compressed air. A band of material was then placed on top of the pavement surface. The material used on this project was supplied in paper bags, but in future it will be packaged in meltable plastic bags. The paper adhered to the sealant blocks and required considerable time to remove before the sealant could be placed in the heating kettle. This material adhered well and did not flow from the cracks. It was not extruded by traffic.

Section 6: H-1 (75 Percent) with Powdered Devulcanized Rubber (25 Percent)

The material in Section 6 was a field blend of granulated rubber as used for Section 1. The only difference between this blend and the AC-20 with rubber was the penetration of the base asphalt. The H-1 had 250 to 300 penetration versus 60 to 120 for the AC-20 asphalt.

The problems associated with this material were the same as those for AC-20 and rubber--the requirements for a source of hot asphalt and blend control. The higher-penetration base asphalt flowed more readily from the crack, especially on superelevated curves. This material also was extruded by traffic.

Section 7: Class J-1

Class J-1 was an asphalt cement blended with approximately 20 percent mineral filler. This material had been used extensively by PennDOT maintenance forces. It has high flow, is subject to low-temperature

cracking, and is extruded by traffic. Past practice had been to pour the sealant on the road surface over the crack, thus subjecting the soft sealant to extrusion by traffic. On this project, the cracks were routed to form a reservoir below the surface of the pavement.

Section 8: Class E-3 Asphalt Emulsion

Class E-3 was an unmodified standard asphalt emulsion (AASHTO, CRS-2) that was used in comparison with the CRF emulsion. Application techniques were the same as those for the CRF sealant. Because E-3 will not withstand freeze-thaw cycling, it had to be stored in a heated storage tank or in drums that were protected from freezing.

Section 9: CRF Emulsion

CRF emulsion was a proprietary emulsified asphalt crack filler that was handled at ambient temperatures and formulated to withstand freeze-thaw cycling. This material was placed by using a pouring bucket. With this material, the crack did not have to be blown clean because the sealant was very fluid and wetted any particles in the reservoir. Sand was then spread over the sealed cracks and the sealant was permitted to cure approximately 1 hr before exposure to traffic. The advantages of this product were as follows:

1. It did not require a heating kettle, which saved the cost of heating the sealant and the wages of an operator;
2. It was available in 55-gal drums. These were easy to handle and store and were reclosed at the end of one work day and reused the next; and
3. It reportedly withstands freeze-thaw cycling. This permitted the unused portions to remain on the truck at the end of the work day and to be stored at a yard near the job site.

A disadvantage is its storage life of 6 months, as reported by the manufacturer, which is too short for normal PennDOT maintenance operations. Material not used in one sealing season is retained for use in the next season. The 6-month storage life would require all purchased CRF sealant to be used in one season.

Placing the sand cover on the CRF sealant was the slowest part of the operation and two men were required to keep up with the pouring of the sealant. The excess sand was unsightly and was blown around by traffic immediately after the work area was opened.

Section 10: AC-20 with Hercules Fibre-Pave 5010

Section 10 sealant was a blend of AC-20 and 7 percent of fine-denier, short polypropylene fibers. It was mixed in the field by addition of the fiber to the hot asphalt cement. This required a source of hot asphalt cement, which presented the same problem as that with blends of rubber with AC-20 and H-1 discussed previously. The blended sealant was applied with a wand supplied by Hercules and was placed without using a squeegee. Application was very fast. The sealant had good adhesion and did not flow from the crack.

MATERIAL AND APPLICATION COSTS

A complete valid cost analysis of the methods used to prepare the cracks and to apply the sealants on this project was not possible because of the limited quantities placed and because of the experimental nature of these methods of preparation and application. A major portion of the placement of all 10 sealants used the same preparation and application techniques, permitting comparison by the same PennDOT maintenance standards for production rates and labor costs for all materials. These costs are as follows:

With routing:	
One foreman at $8.51/hr + 55 percent overhead	= $13.19,
One equipment operator at $7.61/hr + 55 percent overhead	= 11.80,
Five maintenance workers at $6.51/hr + 55 percent overhead	= 50.45,
Equipment costs	= 40.56,
Total	= $116.00/hr.
Without routing:	
One foreman at $8.51/hr + 55 percent overhead	= $13.19,
One equipment operator at $7.61/hr + 55 percent overhead	= 11.80,
Two maintenance workers at $6.51/hr + 55 percent overhead	= 20.18,
Equipment costs	= 20.00,
Total	= $65.17/hr.

The unit cost, cost per linear foot, and daily costs for application of the sealants based on the PennDOT maintenance standards are given in Table 2. Material costs for the premixed sealants were approximately twice as much as those for the field-mixed sealants. This extra material cost may be offset by the savings in labor from not having to obtain hot asphalt cement and by the assurance of having a higher-quality sealant blend. The lowest-cost product was the Class E-3 asphalt emulsion. The cost per gallon for E-3 shown in Table 2 was on the basis of a bulk bid and was lower than that for sealants for which smaller shipping units, such as drums, pails, or boxes, are used. If protected from freezing or used only during warmer weather, this emulsion could be an economical sealant material. Sof-Seal LM was the most expensive sealant and cost approximately twice as much as the other premixed sealants.

In reality, differences in productivity would exist because of varying material consistencies and application techniques. These actual rates could only be determined on a production job where the crew was familiar with the use of the particular sealant material. New standard rates could then be determined for each and the in-place unit costs adjusted accordingly.

INSPECTIONS

Three on-site inspections were performed: March 1982, July 1982, and March 1984. These months were chosen to evaluate the sealants after exposure to weather extremes. Temperatures before the March inspections were approximately 0 to 10 degrees above zero and before the July inspection it was over 90 degrees. Inspections were made by two representatives from the Bureau of Bridge and Roadway Technology and one from the Bureau of Maintenance and Operations. Each observer rated the performance of each sealant by using the following criteria:

1. Resistance to extrusion by traffic,
2. Resistance to oxidation or embrittlement,
3. Resistance to particle intrusion,
4. Resistance to flushing,
5. Effect of cold weather,

TABLE 2 Comparison of Application and Material Costs

Section	Material	Cost per Gallon ($)	Coverage (ft/gal)	Material Cost per Linear Foot ($)	Total Cost of Labor and Material per Linear Foot ($)	Cost per Day of Material at 160 gal/day ($)	Daily Labor Costs ($)		Total Cost per Day of Standard Application Amount[a] ($)	Total Cost per Day of Standard Application Amount[b] ($)
							With Routing	Without Routing		
1	AC-20 with rubber	1.58	58	0.03	0.10	253	870	–	1,123	1,120
2	Superseal IIIA	3.25	60	0.05	0.12	520	870	–	1,390	1,344
3	Overflex MS	2.94	75	0.04	0.11	470	870	–	1,340	1,232
4	Sof-Seal LM	6.40	70	0.09	0.16	1,024	870	–	1,894	1,792
5	Prismoseal A-2	2.25-3.00	20	0.11	0.15	360-480		490	850-970	1,680[c]
6	H-1 with rubber	1.58	98	0.02	0.09	253	870	–	1,123	1,008
7	Class J-1	1.58	80	0.02	0.09	253	870	–	1,123	1,008
8	Class E-3	1.10	52	0.02	0.09	176	870[d]	–	1,046	1,008
9	CRF emulsion	2.85	53	0.05	0.12	456	870[d]	–	1,326	1,344
10	AC-20 with fiber									
	Field mixed	1.34	19	0.07	0.11	214		490	704[c]	1,232[c]
	Premixed	2.52	19	0.13	0.17	403		490	893[c]	1,904[c]

[a]Maintenance standard: 160 gal/day.
[b]Maintenance standard: 11,200 ft of cracks per day.
[c]Figures may be misleading for materials that do not require routing, because actual production would be greater than the standards. Because this was such a small application and start and stop times varied, valid application rates for the various materials could not be determined.
[d]Does not require heating kettle but does require dump truck for sand.

6. Ability to bond to pavement,
7. Abrasion resistance, and
8. Ability to rebond.

During the March 1982 inspection each of the sealants was rated poor, fair, or good on each of the foregoing rating criteria (Table 3). In July 1982 only an overall rating of poor, fair, or good was assigned to each sealant, as follows:

1. Good: AC-20 with Fibre-Pave, AC-20 with rubber, H-1 with rubber, and Prismoseal A-2.
2. Fair: E-3, CRF, Overflex MS, and Superseal IIIA.
3. Poor: Sof-Seal LM and J-1.

For the final inspection in March 1984, a numerical value was assigned to each rating: 0.5 for very poor to 4.0 for excellent. A value was assigned to each performance category by each evaluator, which permitted a score to be derived for each product and a numerical value to be determined for minimum performance. Twenty was chosen as the minimum acceptable performance score. No evaluation of the Class J-1 joint sealant was made during the March 1984 inspection because it was deemed to have failed in all categories. Results of this inspection are shown in Table 4.

INSPECTION RESULTS

AC-20 with Rubber

AC-20 with rubber showed no extrusion from the crack, was elastic and soft, did not track, and did not have an excessive amount of intrusions. During the March 1982 inspection, the sealant could be pulled loose from the road surface and moisture was present underneath; when the July inspection was conducted, the sealant had a tight bond to the pavement. The kneading action of the traffic was beneficial. The overall score for this sealant during the final inspection was 21.0. This product ranked third.

Superseal IIIA

The performance of Superseal IIIA was fair. No bleeding or tracking by traffic was evident, but

TABLE 3 Summary of Evaluations: March 1982

Characteristic	AC-20 with Rubber	Superseal IIIA	Overflex MS	Sof-Seal LM	Class J-1	H-1 with Rubber	Prismoseal A-2	CRF Emulsion	Class E-3	AC-20 with Fibre-Pave
Resistance to extrusion by traffic	Good	Good	Good	Good	Poor	Fair	Good	Poor	Poor	Very good
Resistance to oxidation or embrittlement	Fair	Good	Good	Good	Poor	Fair	Good	Fair	Fair	Good
Resistance to particle intrusion	Good	Very good	Good	Very good	Poor	Good	Good	Good	Good	Good
Resistance to flushing	Good	Very good	Good	Good	Poor	Fair	Good	Fair	Fair	Good
Effect of cold weather	None	None	None	None	Brittle	None	Can be gouged by snowplow blades	None	None	None
Ability to bond to pavement	Good	Poor	Fair	Poor	Good	Good	Good	Good	Good	Good
Abrasion resistance	Fair	Good	Poor	Good	Fair	Fair	Good	Fair	Fair	Good
Ability to rebond	Good	Poor	Poor	Poor	Good	Good	Good	Good	Good	Good

TABLE 4 Summary of Ratings: March 1984 Inspection.

	AC20+ RUBBER			SUPERSEAL 111A			OVERFLEX MS			SOF-SEAL LM			H-1 + RUBBER			PRISMO-SEAL A-2			CRF			E-3			AC20+ Fiber		
RATER	H	C	K	H	C	K	H	C	K	H	C	K	H	C	K	H	C	K	H	C	K	H	C	K	H	C	K
RESISTANCE TO EXTRUSION BY TRAFFIC	3	3	3	3	3	3	2	2	3	1	2	3	2.5	3	1	3	3.3	3.5	2	2	1	1.5	1	1	3	2	3.5
RESISTANCE TO OXIDATION OR EMBRITTLEMENT	2.5	3	3	1.5	1	2	2	3	2	2	3	3	2.5	3	1	3	3.3	3.5	2	2	3	1	1	1	3	2	3.5
RESISTANCE TO PARTICLE INTRUSION	2.5	2	3	3	3	3	2	2.5	3	1	1	1	2	2	1	3	3.3	3.5	1.5	2	3	1	1	3	3	2	3
RESISTANCE TO FLUSHING	2.5	2	3	3	3	3	3	2	3	1	3	3	2	2	1	3	3.3	3.5	2	3	1	1.5	2	1	2	2	3
EFFECT OF COLD WEATHER	2.5	2	2	1	1	1	1.5	2	2	2	3	3	1.5	3	2	3	3.2	3	2	2	2	1.5	1	1	3	3	3
ABILITY TO BOND TO PAVEMENT	2.5	3	3	1	1	1.5	1.5	1	1	1	1	1.5	1.5	1	1	3.5	3.1	2.5	2.5	1	3	1.5	1	3	3	4	3
ABRASION RESISTANCE	2.5	3	3	3	2	3	1	2	1.5	1	3	3	1.5	2	1	3	3.3	3	2	3	1	1.5	3	1	3	2	3
ABILITY TO REBOND	3	2	2	1	1	0.5	1.5	1	1	1	1	0.5	1.5	2	3	4	3.2	2	2	3	2	1.5	2	3	4	2	3
RATING, POINTS	21.0	20.0	22.0	16.5	15.0	17.0	14.5	15.5	15.5	10.0	17.0	17.0	15.0	18.0	11.0	25.5	24.0	20.0	24.5	17.0	17.0	17.0	11.0	12.0	14.0	24.0	19.0	25.0
RATING, RANK	3			9			5			6			7			1			4			8			2		
ACCEPTABLE	YES			NO			NO			NO			NO			YES			NO			NO			YES		

0.5 Very Poor
1.0 Poor
1.5 Poor/Medium
2.0 Medium
2.5 Medium/Good
3.0 Good
3.5 Very Good
4.0 Excellent

Note: Class J-1 was not evaluated.

almost all cracks had extensive areas of bond failure. Some areas of bond failure observed during the March 1982 inspection had rebonded when exposed to the higher summer temperatures. Loosening of the aggregate in the bituminous concrete pavement during preparation of the crack by routing may be partially responsible for the poor bond. This sealant had an average score of 16.0 during the March 1984 inspection; the moderately high score reflects the good properties of the sealant and indicates that it may perform satisfactorily when placed in a clean sawn joint of a bituminous overlay. This sealant ranked ninth.

Overflex MS

Overflex MS exhibited some loss of bond and was severely abraded by traffic. After exposure to higher summer temperatures, little healing of the edge cracks was evident. The average score was 15.5. This sealant ranked fifth.

Sof-Seal LM

Large areas of Sof-Seal LM were lost from the crack by traffic action; the remaining areas had poor bond and could be pulled from the crack by hand and when released would pull back like a rubber band. The sealant remained soft and had good weather resistance. This product may be suitable for sawn cracks and will be further evaluated under those conditions. The score for this sealant averaged 14.7 and it was ranked sixth.

Class J-1

The performance of Class J-1 sealant was unsatisfactory. It flowed out of the crack on superelevated curves and into the crack in other areas. Intrusions were common. This product was rated poor during the 1982 inspections and was not rated in 1984 because of its poor condition. This product was rated tenth.

H-1 with Rubber

H-1 with rubber was a field blend of H-1 (250-300 penetration) asphalt cement and granulated devulcanized rubber. It is the same as AC-20 with rubber except for the softer base asphalt cement. The performance was similar to that of the AC-20 with rubber, but the sealant flowed from the crack on superelevations and migrated into the crack. The score for this product averaged 14.7 and it was ranked seventh.

Prismoseal A-2

The performance of Prismoseal A-2 was good. Some loss was evident on high portions of the lane where snowplow blades scalped the surface, but the sealant was resistant to extrusion and particle intrusion. The portion placed over the cracks prepared by the hot lance adhered better and retained more sealant. The average score for this sealant was 24.5 and it was ranked first. The portion that was prepared by routing and without the hot lance was scored 20.0 by one observer.

CRF Emulsion

CRF emulsion was one of the two cold-applied sealants. It was poured into the routed crack and then covered with sand aggregate. There was no control over the ratio of aggregate to emulsion; therefore, some areas of the crack appear to be low in sealant content and some rich in sealant. Where exposed to traffic, the asphalt worked to the surface and was

extruded onto the adjacent pavement surface, forming a seal around the crack. Where the sealant was not exposed to traffic, some erosion of the sealant was evident. CRF performance varied from good to poor and appeared dependent on the ratio of sand to emulsion and to exposure to traffic. The average score was 17.0 with a ranking of fourth.

E-3 Emulsion

E-3 emulsion was cold applied with a cover of sand. In areas where it was not kneaded by traffic, the sealant was brittle and eroded by water. There was considerable variance in the performance of this sealant from one crack to another and in different portions of the same crack, which may be due to the varying ratios of emulsion to sand. The average score was 13.3 with a rank of eighth.

AC-20 with Fibre-Pave

The performance of AC-20 with Fibre-Pave was ranked medium to excellent on all evaluation criteria. When inspected in March 1982 after one winter of exposure, the sealant had a fuzzy, matted appearance, with fibers extending up from the surface of the asphalt. The overband could be pulled loose by hand and considerable moisture had accumulated under the sealant, but when inspected in July 1982 the sealant had a smooth surface and was tightly bonded to the roadway. The performance of this product over the areas of multiple cracks indicates that it may be useful as a wider seal-coat type of application on multiple cracks or alligatored areas. This sealant has good resistance to extrusion by traffic. The average score was 22.7 with a ranking of second.

CONCLUSIONS AND RECOMMENDATIONS

1. The performance of the sealants used on this project indicates that a crack sealant, under normal field conditions, must be able to coat and bond to surfaces that may be damp or dusty or both. The sealants that have high cohesive strengths and thus high resistance to intrusion of incompressibles generally require cleaner and drier pavement surfaces for satisfactory bond. Sealants that are a blend of straight asphalt cement and a modifier, such as rubber or fiber, bond well to dusty or damp surfaces. Emulsion-based sealants are unaffected by damp surfaces.
2. All products, with the exception of the Class J-1 sealant, would perform well as sealants for cracks. The roadway conditions on this project were severe; free water was flowing under and through the overlay during much of the test period. However, three of the products tested, AC-20 with rubber, AC-20 with Fibre-Pave, and Prismoseal A-2, scored significantly higher than the other products and therefore it was decided that only these three be considered for recommendation as approved department sealants.
3. The AC-20 with Fibre-Pave 5010 is a blend of polypropylene and AC-20. The blend must not exceed a temperature of 300°F; therefore, a precautionary note should accompany any instructions for its use.
4. The application of Prismoseal A-2 would require different pumps on the heating kettles because of the silica filler used in the sealant. It is anticipated that a change in the type of filler will be made, which would permit the application through existing equipment.
5. It is recommended that the department continue to use AC-20 with devulcanized rubber.
6. The use of H-1 with devulcanized rubber as a replacement for AC-20 with rubber is not recommended because the base asphalt cement is inherently too soft.
7. Superseal IIIA and Sof-Seal LM are recommended for additional evaluation for use in sealing joints sawn in bituminous concrete overlays.
8. The use of Class J-1 crack sealant should be discontinued; its service life is very short, less than 1 year.
9. The use of cold asphalt emulsions for crack sealing, although suitable, is not recommended because the other acceptable products have a longer estimated service life with little, if any, additional cost.
10. It is further recommended that the AC-20 with rubber, AC-20 with Fibre-Pave 5010, and Prismoseal A-2 be placed by overbanding with an approved applicator.
11. It is recommended that the hot-lance method of surface preparation be further evaluated for efficiency and cost-effectiveness.

REFERENCE

1. M.C. Belangie and D. Anderson. Evaluation of Flexible Pavement Crack Sealing Methods in Utah. Report FHWA/UT-81/1. Utah Department of Transportation, Salt Lake City, Jan. 1981.

Publication of this paper sponsored by Committee on Pavement Maintenance.

The Importance of Sealant Modulus to the Long-Term Performance of Concrete Highway Joint Sealants

SHERWOOD SPELLS and JERRY M. KLOSOWSKI

ABSTRACT

Preliminary laboratory and field results are summarized that demonstrate the value of modulus testing in evaluating the initial and long-term elastomeric properties of several generic sealants. The effects of accelerated weathering on the elastomeric properties of these sealants are examined and an illustration is given of how changes in modulus can affect the sealant's ability to withstand vertical shear caused by pavement deflections under traffic. Laboratory results indicate that all samples tested have the ability to withstand some vertical shear. The number of shear cycles that a sample is able to withstand after accelerated aging has been related to changes in the sealant's modulus property. Of the samples studied, low-modulus silicones maintained their modulus property and withstood the largest number of shear cycles. Test procedures and methods used in this study are described.

Considerable effort currently is focused on the restoration of U.S. highways. Diamond grinding and slab stabilization are among the techniques used to rehabilitate concrete pavements; joint resealing plays a key role in the total restoration process.

The role of the joint sealant is to prevent problems associated with water, incompressibles (e.g., dirt, small stones), and deicing chemicals that enter the joint from the surface. This type of infiltration results in erosion of pavement foundation, concrete spalling, and corrosion of embedded metals. If there is no surface seal or if the seal has failed, these problems associated with infiltration will be accelerated.

The joint sealant generally represents the smallest part of a new construction or rehabilitation project, but the performance demands placed on it are enormous. Selecting the correct sealant for the application thus is critical. Several tests can help the highway engineer in his evaluations. These tests are well known in the rubber industry, but many highway engineers may not be aware of them or may not fully appreciate the value of the information they provide.

As a result, tests that can be used to demonstrate the sealant's ability to maintain its elastomeric properties are often not used. With long-term sealant performance being the goal for new construction and rehabilitation, tests that can provide information regarding the elastomeric properties of generic sealants should be more closely examined.

Modulus testing in accordance with ASTM D-412 is one rubber test method that can be used as a tool to study a sealant's rubber or elastomeric characteristics. By definition, modulus is the force required to extend a rubber tensile bar to a specified percent elongation. This modulus value, at a specific elongation, will generally be different for each generic class of sealant:

Sealant Studied	Typical Modulus Value at 150 Percent Elongation (psi)
Low-modulus silicone	26
Two-component organic polymer	33
Polyurethane	68
Polysulfide	118

Regardless of the generic class, significant changes in the modulus values during testing can provide information about that particular sealant under similar field conditions. For example, an effective joint sealant must maintain its elastomeric properties at low temperatures. By measuring modulus values at room and low temperature, the effects of low temperature on the sealant's properties can be determined. If a significant increase in modulus is observed (i.e., the sealant becomes significantly stiffer) at low temperature, its success as a sealant may be diminished. The ability of a sealant to maintain its elastomeric properties can be determined by conducting accelerated tests such as weathering and heat aging.

Significant positive or negative changes in modulus values would indicate that elastomeric properties are changing, and actual field performance will depend on the extent of these changes. Thus modulus values obtained from various tests can provide information regarding the sealant's basic generic elastomeric properties; these properties ultimately control the sealant's long-term field performance.

In the field, the sealant must maintain its elastomeric properties as long as possible to accommodate the movement associated with concrete pavements. Horizontal movement (thermal expansion and contraction) capability is a well-recognized criterion for a joint sealant. But in the last few years studies have shown that the sealant is subjected to vertical shear movements also (resulting from pavement deflections) (1-3). These pavement deflections occur when traffic crosses a jointed pavement beneath which there are voids or when the pavement has curled as a result of the temperature differential between the top and the bottom. The frequency, number, and size of these vertical deflections that occur will depend on traffic volume (especially truck traffic), temperature, and pavement conditions. The ability to withstand vertical shear may partly explain why some sealants that pass laboratory extension and compression tests have limited field success. If the sealant does not possess sufficient elastomeric properties initially or it looses its elastomeric properties (i.e., there is a significant modulus change), these shear movements can contribute to sealant failure

(adhesive or cohesive or both). Thus, the ability to possess and maintain rubber properties becomes extremely important.

How temperature, modulus, and the retention of modulus after accelerated weathering affect the ability of several sealants to withstand vertical shear is examined. The test methods and equipment are also discussed.

TEST METHODS, PROCEDURES, AND EQUIPMENT

Two types of sealant test specimens were prepared for this study. The first type consisted of rubber slabs approximately 1/8 in. thick. These rubber slabs were used to determine modulus values. The second type was a test joint where the sealant bead between two concrete blocks was 1/2 in. wide x 1/2 in. thick x 2 in. long. The blocks were prepared according to ASTM procedures. These test joints were used for shear testing. Both types of test specimens were allowed to stay at room temperature (75°F, 50 ± 5 percent relative humidity) for 30 days before the start of testing.

ASTM D-412 was the method used to determine modulus. This method measures the force required to extend rubber tensile bars to a specified percent elongation. With the appropriate die, rubber tensile bars were cut from the cured rubber slabs. The modulus values were determined on an Instron tensiometer equipped with an environmental chamber. Figure 1 shows the inside of the test chamber with a test specimen between the gaps. This chamber can be operated above and below ambient conditions (-90 to 450°F). The study conditions were limited to -35 to 150°F. Measuring rubber properties (i.e., modulus)

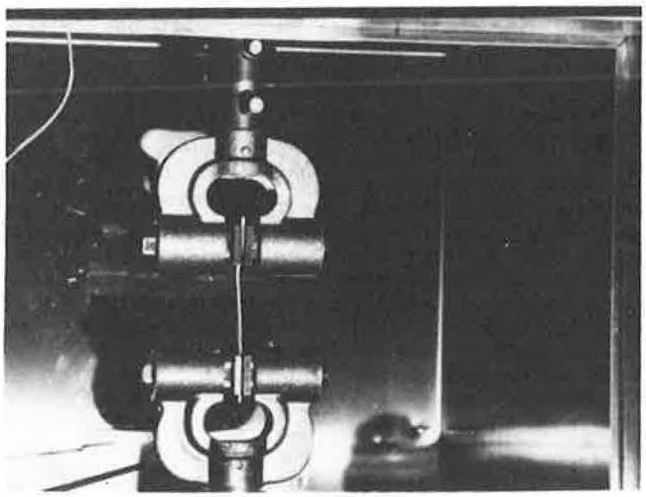

FIGURE 1 Environmental chamber with test specimen.

at various temperatures allows one to determine how temperature affects elastomeric properties and ultimate field performance. For example, at low temperature the sealant may become too stiff to accommodate movement. Or at high temperatures, the sealant may be too soft to reject stones. All samples were allowed to equilibrate at the specified temperature before the start of modulus testing. The only modification in the ASTM D-412 procedure was to reduce the rate of pull from 20 in./min to 2 in./min. The slower pull rate allowed for a more accurate modulus measurement because a few aged samples failed quite rapidly at the higher pull rate.

The shear tester used in this study (Figure 2) is a slight modification of one originally designed and built by the Research Branch of the Georgia Department of Transportation. This equipment simulates the vertical pavement deflection caused by one truck crossing a joint. The sample holder is divided into movable and unmovable halves. The movable half provides positive and negative 1/8-in. deflections at 144 rpm through an off-center cam attached to an electric motor. The 1/8 in. causes more deflection than that reported in field studies (2,3) but does provide a safety factor (2,4). In other words, a sealant that can maintain its elastomeric properties and withstand a large deflection in the laboratory will have a higher probability of field success. The 144-rpm deflection simulates the rate of deflection caused by a truck approaching and crossing a joint at 55 mph, with joint spacing of 30 ft.

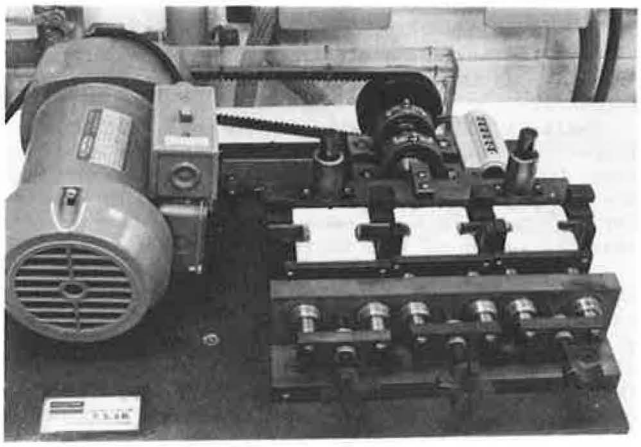

FIGURE 2 Shear tester.

Accelerated weathering tests allow one to simulate quickly the effects of natural weathering [ultraviolet (UV) exposure, rain] on various materials in the laboratory rather than relying solely on long-term outdoor testing. This type of testing can simulate in only a few months the effects of 1, 2, or 5 years or more of natural weathering on elastomeric materials.

Accelerated weathering was conducted according to ASTM G53-77 (Figure 3). This procedure uses UV radiation from fluorescent lamps and condensation to simulate rain and dew. In contrast to the traditional carbon-arc-accelerated weathering test, this method allows longer operating time at significantly reduced cost. The standard conditions are 4 hr of UV exposure at 60°C and 4 hr of condensation at 40°C. Samples (tensile bars and joint specimen) were placed in the weatherometer for the specified time and then allowed to stand at room conditions for 24 hr before modulus or shear testing was started.

RESULTS AND DISCUSSION

Sealing highway and airport joints requires that the sealant remain elastomeric under a variety of climatic conditions. Over the years, many different materials labeled as elastomeric or rubber joint sealants have been used, but the field performance has been less than desirable for truly elastomeric materials. The effect that environmental conditions

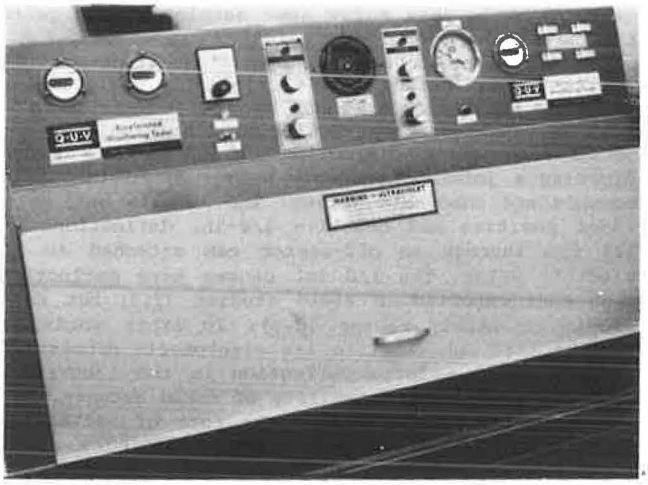

FIGURE 3 Accelerated weathering machine.

have on the sealant's elastomer or rubber properties is part of the reason for this undesirable performance.

Sealants will generally become more flexible as temperature increases and less flexible as temperature decreases. However, the temperature range and the extent to which significant changes in elastomeric properties will occur depend on the generic characteristics of that particular sealant.

The modulus values at 150 percent elongation for each sealant studied were tabulated earlier. Only one sample from each class was studied, and that sample is believed to be representative of that class. For other specific sealants in a given class, the actual modulus values may be different from the values shown. The effect that a specific temperature has on the elastomeric properties can be determined by measuring the sealant's modulus at that temperature by using the representative sealants shown earlier.

Modulus as a Function of Temperature

The data in Figure 4 show that the modulus of each sealant changes with temperature. The size and nature of these changes are dependent on the particular sealant and the temperature. The changes in modulus as a function of temperature represent changes in the sealant's flexibility. As temperature decreases, the modulus increases and flexibility decreases for all sealants. The rate of change was most pronounced in the range -35 to 0°F. For nonsilicone, the range 0 to 50°F showed quite pronounced changes as well. The only significant change noted for the silicone was in the range -35 to -20°F. Although the rate of modulus change varies with each sealant, and some were quite dramatic, some degree of flexibility still exists at the low temperatures, because the best specimens could still be stretched and tested.

From the viewpoint of application, the change in flexibility with decreasing temperatures translates into an increase in the sealant's cohesive character. With increased cohesion, more stress is placed on the sealant internally and on the bond line. These stresses ultimately can lead or significantly contribute to failure. Ideally, these forces should be as small as possible to prevent stress buildup. Thus, some aspects of the long-term field performance will depend on the sealant's capability to maintain elastomeric properties over the temperature range expected at a particular location. Serious consideration should be given to low-temperature effects if the sealant is to be used under low temperatures.

Modulus as a Function of Accelerated Weathering

Retention of elastomeric properties after weathering is as important to field performance as initial wide-temperature flexibility. The temperature range in which any sealant can remain elastomeric and perform effectively may be narrow but sufficient for a particular geographic location. However, if on weathering that particular sealant does not retain those elastomeric properties, then performance, even over a narrow temperature range, will be limited. Figure 5 shows how the modulus value of each sealant is affected by accelerated weathering. As shown, only the low-modulus silicones showed virtually no change in modulus value, which illustrates the retention of elastomeric properties. The other elastomerics showed two types of behavior. The polyurethane became harder and increased in modulus of elasticity. The polysulfide and other two-part

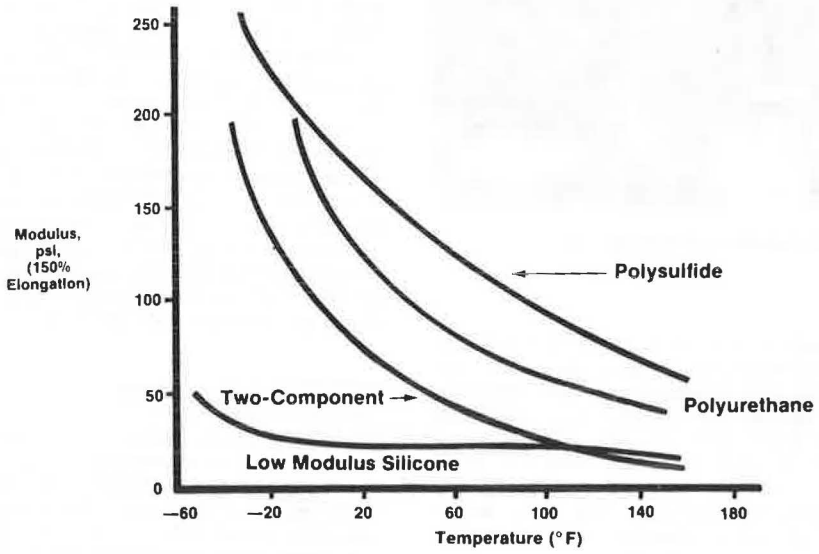

FIGURE 4 Effect of temperature on initial elastomeric properties.

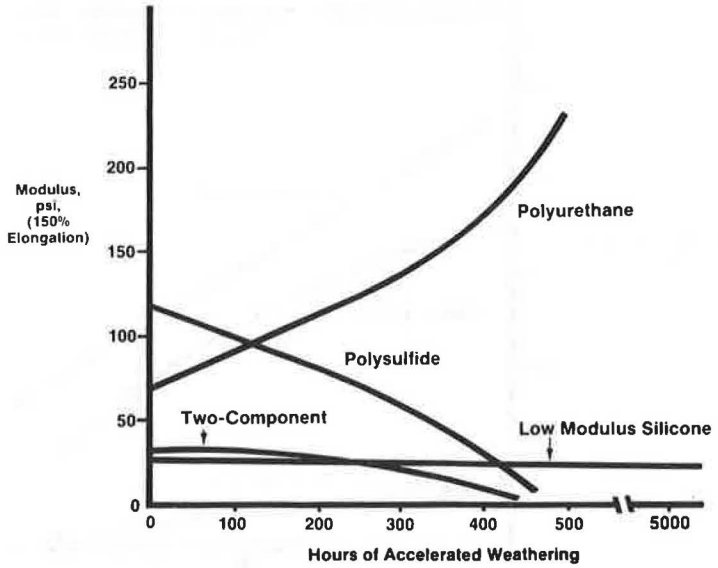

FIGURE 5 Effect of accelerated weathering on elastomeric properties.

product became harder when tested to shore A but actually showed a decrease in modulus of elasticity as a function of weathering. (The authors make no effort to explain the results with the sealants studied, only to report them.) The 500-hr accelerated weathering is not considered unduly severe when sealants for most U.S. locations are considered. Field performance will depend on the sealant's ability to remain elastomeric under the weathering conditions expected. Because weathering conditions vary the rates of change as well as the absolute value of the elastomeric properties, curves like those generated here should be important when a sealant is considered for a given location.

Vertical Shear Testing

Flexible elastomeric properties will control a sealant's ability to withstand joint movements in the field caused by thermal changes (expansion and contraction) and traffic (vertical pavement deflections). Depending on field conditions, both movements can occur at the same time. In the case of vertical deflections, these can occur because of small voids that exist beneath the pavement or because of the curling due to a temperature differential or both. Under traffic, these deflections will be positive and negative and in turn will subject the sealant to a rapid shearing action. This shear force on the sealant is expected to be the most severe during the winter months when the joints are widest (sealant extended) and pavement slabs can move independently (i.e., no load transfer device or no aggregate interlock of slabs). Because this shearing movement is in addition to the thermal movement, the sealant must maintain flexibility to accommodate both types of movement. The number of shear cycles that a sealant is exposed to for a given period will depend on traffic volume and pavement conditions. Because of weight, only truck traffic is believed to be significant in causing pavement deflection at the joints. The number of trucks per day on the Interstate system varies greatly, but many officials believe that 3,000 trucks per day is representative of typical truck volume on the average roadway. With each truck having three axles, this would expose the sealant to 9,000 deflections per day or 810,000 deflections for a 3-month winter period. In order to withstand such a large number of deflections, the sealant must maintain its flexible elastomeric properties (i.e., show minimal modulus change). In addition, the number and rate at which these deflections occur would indicate that the sealant's ability to withstand these shear forces can be as important as--possibly more important than--the ability to withstand thermal movement.

The number of shear cycles that a sealant can withstand initially and after accelerated weathering is another measure of its elastomeric properties. If a sealant maintains its elastomeric property after accelerated weathering, no change in the number of shear cycles would be expected. As shown in Figure 6, each sealant has the ability to withstand cyclic shear.

Under accelerated conditions of 25 percent sealant extension, ± 1/8-in. deflection at -18°F, each sample was continuously cycled until 1/4 in. of adhesive or cohesive failure or both was observed. All samples had the ability to withstand some shear stress. Except for the low-modulus silicone, all samples showed a reduction in their shear movement capability as a function of accelerated weathering. Low-modulus silicones showed no signs of failure after 1,000,000 cycles. In addition, a 9-in. concrete core, which was removed from I-75 in Georgia containing a 5-year-old, low-modulus silicone sealed joint, was put into the test machine for 1,000,000 more shear cycles and showed no failure.

Temperature will also affect the number of shear cycles that a sealant is able to withstand. Although not studied in detail, initial results show that as temperature increases, the observed number of shear cycles also increases. For example, an unaged polysulfide sealant exceeded 200,000 cycles without failure when tested at room temperature but less than 100,000 cycles at -18°F. A similar observation was made for the other nonsilicone sealants. This shows the effect temperature has on flexibility and is consistent with the curves of modulus versus temperature in Figure 4. This information provides some insight into why a particular sealant may give the desired field performance in another location. With this understanding, the engineer can better select sealants suited for a particular geographic location and traffic density and thus obtain maximum field performance for that sealant.

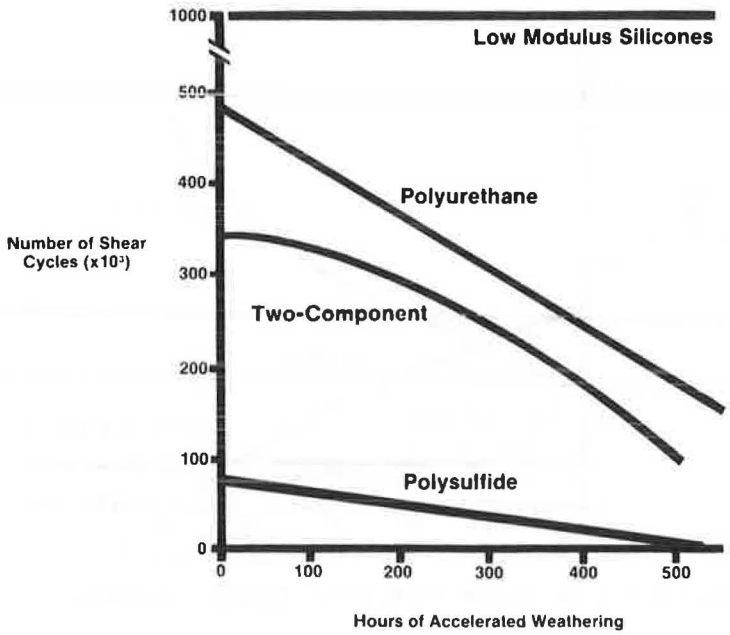

FIGURE 6 Effect of accelerated weathering on shear cycles.

CONCLUSION

The information presented in this paper represents some of the initial investigations into studying the relationship between a sealant's elastomeric rubber property and its ability to withstand vertical shear caused by pavement deflections under traffic. Geographic location, time of year, traffic volume, and pavement condition will determine the number, size, and frequency at which these deflections will occur. The sealant's success will depend on a better understanding of the application requirements and selection of a sealant that can meet those requirements.

Field performance of sealants used in concrete joints depends on the sealant's elastomeric rubber properties and the ability to maintain those rubber properties. As the ability to maintain those properties increases, longer useful life will be the expected field performance. Modulus testing according to ASTM D-412 is one method that can be used to measure a sealant's rubber properties. When used in conjunction with accelerated tests (i.e., weathering), modulus can indicate changes in rubber properties that are caused by environmental conditions. Thus, the engineer can use these laboratory tests to develop a better relationship between actual field performance and laboratory results. This testing could be used to explain why certain classes of sealants, or sealants within a class, show differing field performance in various geographic locations and establish minimum requirements for various sealants to meet application requirements.

The initial results from this study indicate that vertical shear can contribute to failure of the sealant. The ability of the sealant to withstand this type of movement initially and over the long term is related to the sealant's modulus at various temperatures and how the modulus changes with aging. The results indicate that all truly elastomeric sealants are capable of withstanding this type of movement for various periods of time. Except for low-modulus silicon, all samples tested showed a decrease in the number of shear cycles. This decrease has been attributed to a change in the sealant's rubber or modulus property with changes in temperature or aging.

As previously mentioned, the preliminary results represent the initial findings. Additional work is needed to study other variables (e.g., rate and duration of deflections). But modulus testing provides a tool by which to monitor changes in rubber properties and then match the sealant with the performance requirements.

REFERENCES

1. J.B. Thornton. Highway Joint Sealing. Adhesive Age, Aug. 1983.
2. W. Gulden and J.B. Thornton. Pavement Restoration Measures to Precede Joint Resealing. In Transportation Research Record 752, TRB, National Research Council, Washington, D.C., 1980, pp. 6-15.
3. 1. Minkarah, J.P. Cook, and S. Jaghoory. Vertical Movements of Jointed Concrete Pavements. In Transportation Research Record 990, TRB, National Research Council, Washington, D.C., 1984, pp. 9-16.
4. H. Allen. Report of Committee on Warping of Concrete Pavement. Proc., HRB, Vol. 25, 1945, pp. 199-250.

Publication of this paper sponsored by Committee on Sealants and Fillers for Joints and Cracks.

Maintenance Repainting of Structural Steel: Chemistry and Criteria

BERNARD R. APPLEMAN

ABSTRACT

The conditions and requirements for maintenance painting of structural steel are considerably different from those for the initial painting. One of the most important differences is the nature of the surface encountered. The ability of an applied paint to adhere depends on the characteristics of the surface as well as on the wetting and spreading properties of the paint. The degradation of the paint film is both cause and effect of the corrosion of the steel. Empirical plots of rust versus time are typically exponential; however, the low reliability and precision of such data indicate the need for better techniques for characterizing and evaluating coatings. Maintenance engineers need practical criteria for evaluating the condition of a structure and for deciding when and how much to repaint. Existing standards from ASTM and the Steel Structures Painting Council are suitable for obtaining quantitative ratings for small uniform areas of steel. Commonly used methods for assessing total surface condition are qualitative. A modification of these two approaches can provide quantitative, detailed, and more meaningful evaluations of the condition of a complex structure. This approach also can provide estimates of the need for future painting.

The phrase "maintenance repainting" may appear redundant to some readers. It was chosen deliberately to emphasize that one maintains a structure by applying paint to a surface that already has had a coat of paint; this makes it quite different from steel that has never been painted.

Repainting of previously painted steel represents by far the majority of structural steel painting each year, yet the understanding of basic processes and the technology available to the practitioner are far less advanced than those for painting of new steel. Some of the special considerations needed in maintenance painting are highlighted with a focus on two of these items: chemical interactions at the surface and practical criteria for decisions on repainting.

The major features of maintenance and initial painting are compared first. One of the most important differences between previously painted structural steel and new steel is the nature of the surface encountered. The discussion covers the major types of surfaces and their characteristics and the requirements for adhesion and compatibility.

Then the techniques for characterizing and evaluating the performance of coated structural steel are discussed. This leads to an assessment of the types of criteria needed for maintenance painting. Two of these types are discussed in some detail: criteria for the existing condition of the coating and steel and criteria for when and how much to repaint. The discussion includes a review of existing industry and government criteria and a proposed modification of these standards. Finally, examples are given of predicting future degradation patterns.

INITIAL PAINTING VERSUS REPAINTING

The major differences between initial painting and repainting are listed in Table 1. For a new structure, the painting is usually included in the design plans and specifications. Funds are earmarked for the painting. All structural steel parts, except for faying surfaces and other noted areas, are painted; surface preparation (e.g., blast cleaning) and priming are done in the shop under relatively controlled and defined conditions. Moreover, there are numerous painting and inspection guides and extensive performance data available from professional organizations and manufacturers.

TABLE 1 Initial Painting Versus Repainting

Category	Initial Painting	Repainting
What to paint	Predetermined	Survey and analysis required
Funding	Capital funds	Maintenance funds
Schedule	Construction and erection deadlines	Not set, often deferred
Application conditions	Shop, controlled environment, easy access	Field site, weather factor, scaffolding, etc.
Metal surface	Uniform, clean metal	Variable, contaminated
Paint selection	Data, guides available	Few guides, no performance data

In contrast, for maintenance painting, in general, there is no clear definition of what structures or parts of structures are to be or need to be painted. The funds for repainting must come from already tight maintenance budgets. These funds are often sporadic, which makes advance planning difficult. Unfavorable field conditions (e.g., weather, scaffolding) for surface preparation and application are familiar to all.

One of the most significant features of maintenance painting is the variability of the surface, a subject to be examined subsequently. Finally, in spite of and perhaps because of these unfavorable factors, there is a great lack of standards, cri-

teria, and guidelines for the maintenance painting of structural steel.

SURFACES, ADHESION, AND COMPATIBILITY

Common types of surfaces encountered on previously painted structural steel are as follows: blast-cleaned steel, tight rust and millscale, aged paint, and organic and inorganic contaminants. Materials such as loose rust, popped millscale, and nonadhering paint, which would normally be removed by the minimal surface preparation techniques, have been excluded.

Table 2 gives some characteristics of four surfaces. The surface energy (or wettability) is a measure of the ability of a droplet of liquid to spread out and make intimate contact with a surface (1,2). A high surface energy signifies good wettability, and vice versa. Of course, wetting depends on the liquid as well. The surface area is a measure of the number of bonding sites on the surface. A high surface area is desirable for good adhesion. One of the major beneficial effects of abrasive blasting is to increase the surface area of the steel.

TABLE 2 Surface Characteristics

Characteristic	Substrate			
	Blast-Cleaned Steel (Oxide)	Tight Rust	Aged Alkyd	Oil Film
Surface energy (dynes/cm)	>40	35-38	30-35	~25
Wettability	High	Medium	Medium	Low
Surface area	High	High	Low	Variable
Bond strength to metal	Very high	High	Medium	Low
Specific properties	Thin, dense, stable	Thick, porous	Brittle, fully reacted	Very thin layer

The ultimate objective of painting is to produce a coating that will adhere to and protect the metal. Thus, it is important that the surface to which the paint is applied have a strong bond to the underlying metal. The thin oxide of a freshly blasted metal will be strongly bonded to the metal, as will tight rust. Less well adherent are aged alkyd paints, which tend to be brittle, and thin oil films, which may interact with the solvent or polymer of the applied paint. Table 2 also lists some other properties that may affect interactions between paint and surface.

In consideration of what is required for an applied paint to form a strong, durable bond to the metal surface, the first requirement is for the paint to form a continuous film on the surface. This entails good wetting and spreading. Wetting depends on the nature of the interactions (both chemical and physical) between paint and surface. It is a thermodynamic property.

Spreading depends on the kinetics of film formation. Of importance is the liquid paint's viscosity, both as applied and during the spreading. Processes such as solvent evaporation and chemical reaction will increase the viscosity and reduce the spreading rate.

Once the paint has spread out and formed a film, it must be capable of establishing permanent bonds to the surface. The strength of adhesion depends on several factors: the chemical interaction between paint film and surface moiety, the total number of bonds, and the bond distance. The bond strength falls off rapidly with distance. Any contaminant on the surface can preclude any direct bond between paint and surface molecules.

Several commonly used maintenance paints will be examined in light of the requirements for film adhesion. Paints are composites whose properties depend on the various components. The surface energies given in Table 3 are based primarily on the solvents; reliable data on the paints themselves (3,pp.F33-F36;4) were not available.

TABLE 3 Properties of Paints Affecting Film Adhesion

Property	Paint			
	Oil-Alkyd	Vinyl	Epoxy	Inorganic Zinc
Surface energy (dynes/cm)	25-30	30-35[a]	30-35[a]	25-30[a]
Wettability	Good-excellent	Fair	Fair-good	Fair-good
Viscosity stability	Good-excellent	Poor	Poor-fair	Poor
Bond to metal	Polar	Primary (slight)	Primary (strong)	Primary
Bond to organic	Polar and primary	Polar	Polar (strong)	Polar (weak)

[a]These data are based on solvent properties.

Non-oil-containing, so-called "high-performance" paints (vinyl, epoxy, and zinc-rich) all have volatile solvents, so that very rapid increases in viscosity follow application. They all can form direct valence (primary) bonds to blast-cleaned steel, the substrate for which they were primary developed. The oil-containing paints form only polar bonds with metal. The epoxy and oil-alkyd paints have a higher proportion of polar groups capable of bonding to organic surfaces.

The overall strength of adhesion for the different surfaces considered is shown in Table 4. The numbers in parentheses are the solid and liquid surface energies. The general rule is that a liquid will wet a surface whose critical surface energy of wetting is greater than the liquid's surface energy (1). Note that vinyls and epoxies tend to form good bonds to existing vinyls and epoxies, but these are not nearly so common on older structures as oils and alkyd paints.

TABLE 4 Overall Strength of Adhesion

Paint	Substrate			
	Blast-Cleaned Steel (>40)[a]	Tight Rust (35-38)	Aged Alkyd (30-35)	Oil Film (~25)
Oil-alkyd (25-30)[a]	G	G	G	F-P
Vinyl (30-35)	E	F	F	P
Epoxy (30-35)	E	G	F	P
Inorganic zinc (25-30)	E	G-F	F-P	P

Note: E = excellent, G = good, F = fair, P = poor.

[a]Solid and liquid surface energies in dynes per centimeter.

PERFORMANCE OF COATINGS AND STEEL

The application and adhesion of a paint are necessary but not sufficient conditions for substrate protection. Also required of a paint is long-term ability to maintain its integrity and prevent corrosion of the metal. These constitute the performance of a coating system. A few aspects of paint performance

will be examined briefly. Major factors responsible for coating degradation and steel corrosion will be identified. Also to be discussed and illustrated are observed patterns of coating degradation with time and the deficiencies of empirical plots of rust versus time.

It is important to emphasize that performance depends on the condition of both the coating and the steel and that the two influence each other. Coatings degrade from the outside (moisture, abrasion, ultraviolet radiation), the interior (internal stress, film embrittlement, leaching of additives), and from the inside (undercutting, rust, blisters). The process of corrosion causes the coating to degrade more rapidly than it otherwise would.

Metallic corrosion requires a source of water and oxygen along with areas of differences in steel potential. While intact, a good barrier coating can limit the access of water and oxygen. As the coating degrades (i.e., film breaks and disbonding), it provides less and less of a barrier. Thus, the degradation of the coating leads to increased rate of corrosion in the metal.

The combined effects of the coating and steel performance are an example of negative synergism. The corrosion of the metal accelerates the degradation of the coating, and the breakdown of the coating accelerates corrosion. This phenomenon is important because it helps explain the observed rates and patterns of deterioration in coated steel.

Figure 1 shows some examples of generalized performance behavior with time. The top curve (A) represents a property in which the rate of degradation decreases with time and the bottom curve (B) a property in which the rate of degradation increases with time. The corrosion of bare steel in the atmosphere

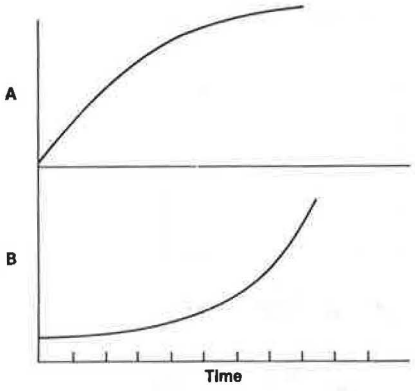

FIGURE 1 Typical performance attributes versus time.

is a property that follows example B (5,6). The decrease in corrosion rate after 1 or 2 years (Figure 2) is attributed to the protective nature of the loose oxide formed.

Plots of percent rust versus time, on the other hand, tend to follow pattern B, as shown in Figure 3 (7). In fact, because of this accelerating degradation pattern, a linear scale is not well suited for characterizing rust versus time for coated steel. ASTM, the Steel Structures Painting Council (SSPC), and others have adopted a logarithmic scale. This will be discussed later.

The particular example given is a smoothed curve based on large amounts of empirical data. Most of the time it is not practical to produce plots such as these. Even when it is, there are problems re-

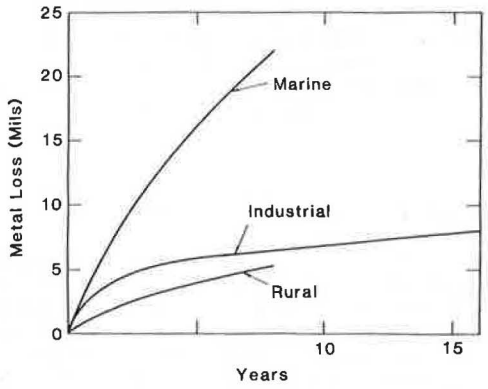

FIGURE 2 Corrosion of bare carbon steel.

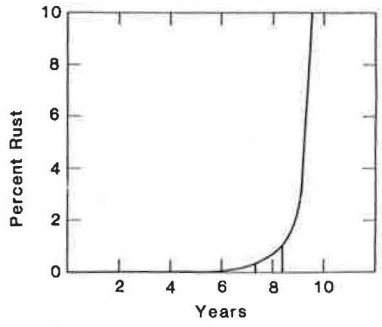

FIGURE 3 Deterioration of coated steel.

garding their interpretation. Frequently the conditions under which data were obtained (e.g., salt fog test) are not representative of actual environments for which information is needed. Even where data are from outdoor panel tests or structures themselves, there are large variations in the coating system used, the type of surface, or the exposure environment. These items, particularly the first, have been widely discussed in the literature.

A related factor is the lack of statistical reliability of most reported performance data. Because of the large amount of scatter, it is frequently necessary to prepare and evaluate several replicate test specimens. In evaluating performance of field data, even larger numbers of surfaces must be examined. Most tests do not provide enough replicate data to establish error limits (degree of reliability).

Finally, in monitoring the performance of coated steel, the inspector or researcher evaluates and records visual properties such as percent of surface rusted, number and type of blisters, and degree of chalking. It is unfortunately not practical to detect more fundamental quantities such as underfilm rust, electrical potential of steel, changes in polymer tensile strength, or internal stress.

It is hoped that eventually techniques will be available to monitor these properties in situ. This would provide earlier indications of deterioration of performance and facilitate coating system testing and timely maintenance painting. There is a considerable amount of effort directed toward understanding and monitoring basic processes. For example, Lehigh University and National Bureau of Standards researchers and others are investigating how corrosion initiates and spreads under a film and are developing more quantitative methods for evaluating

coating performance. These studies should provide the coatings scientists with better knowledge of the fundamental processes of coatings and steel degradation and eventually lead to more efficient and accurate methods for monitoring and evaluating field performance.

CRITERIA NEEDED FOR MAINTENANCE REPAINTING

However, the current crisis in structural maintenance cannot wait for these techniques. What can be done about the immediate needs for corrosion protection? How can better advantage be taken of existing technology? In particular, how can the maintenance engineer or inspector be assisted in carrying out more effective corrosion protection?

The start is to identify the major decision points or criteria for maintenance painting. A criterion is defined as a standard of judgment. The criteria are as follows:

- Condition of existing paint and steel,
- When to repaint,
- How much to prepare and paint, and
- What paint system to use.

Fist, a standard is needed for the condition of the existing paint and steel. The second and third of the foregoing criteria depend on the condition of the structure as well as on the philosophy or objective of the maintenance painting program. The final criterion listed depends partially on these factors and also on individual preferences and experience. It will not be addressed in this paper.

CRITERIA FOR COATING AND STEEL CONDITION

As discussed earlier, the performance of coatings on steel is normally evaluated by visual properties. Coatings specialists are all familiar with ASTM standards for quantitative evaluation of defects. The most widely used standard is ASTM D-610 (Degree of Rusting). A numerical value from 1 to 10 is assigned on the basis of the percentage of surface rusted (Figure 4). The correspondence between D-610 rust rating and percent rust is as follows:

Percent Rust	Rust Rating (R)
≤0.01	10
0.03	9
0.1	8
0.3	7
1.0	6
3.0	5
10.0	4

As noted, there is a mathematical logarithmic relationship between the two:

$$R = -2X \langle \log (\% \text{ Rust}) \rangle + 6 \quad (1)$$

where R is the rusting rating.

The ASTM standards evaluate a single specific defect each (e.g., rusting for D-610 or blistering for D-714). SSPC specification SSPC PA-4 (8) provides a rating scheme that recognizes the need to account for both coating defects and steel corrosion when decisions are made on repainting (see Table 5). SSPC PA-4 rates the total surface area affected by paint

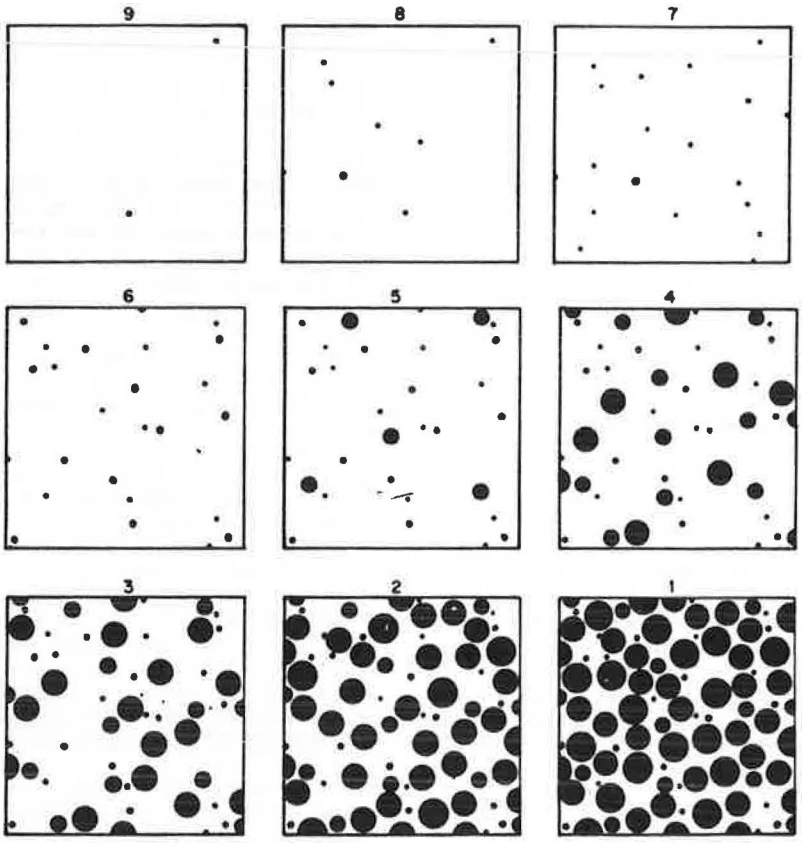

FIGURE 4 Rating of painted steel surfaces as a function of percent of area rusted (ASTM D-610/SSPC-Vis 2).

TABLE 5 SSPC PA-4: Maintenance Painting of Oil-Alkyd Paint

Condition	Paint System Defect	Surface Area Affected (%)	Equivalent Rust Rating	Surface Preparation Required
1	Rust, loss of topcoat	<0.1	9	Solvent clean (SP-1)
2	Rust, blisters; loose mill scale; loose paint	0.1-1.0	8-6	Hand clean (SP-2)
3	Rust, blisters; hard scale; loose paint	1-10	6-4	Hand clean, feather edges
4	Rust, pits; nodules; loose paint	10-50	4-1	Blast clean (SP-6), feather edges
5	Totally deteriorated	50-100	0	Blast clean entire area

system defects (e.g., loose paint, blistering, rust) by using the ASTM equivalency scale. This rating scheme also reduces the total number of conditions from 10 to 5.

ASTM-type standards were developed and intended for evaluating small test specimens. They are difficult to use on real structures because of the nonuniformity of rusting and coating degradation. Because of this, several users have developed rating schemes that take into account the entire surface area. An example is that of the British Standards Institute (9), which has established five conditions for a painted structure:

Condition 1: sound paint;
Condition 2: chalking, loss of topcoat;
Condition 3: thin film, blistering, pinhead rusting;
Condition 4: sound film, rusted areas < 25 percent; and
Condition 5: rusted areas > 25 percent.

However, there appears to be a need for some intermediate rating between Conditions 3 and 4.

An example of an industrial-user rating scheme is the following (10):

Condition	Failure Requiring Preparation	Insufficient Topcoat Thickness
1	0-5	0-5
2	6-20	6-25
3	21-35	26-100
4	36-60	100
5	61 or more	100

The conditions are based on a visual estimation of the percent of surface requiring preparation. A secondary consideration is the percent of the surface area showing loss of topcoat. Both of these schemes are based on qualitative, broad-brush evaluations of general surface condition. There is no definition for what type of surface requires preparation or how to determine this. Unless one has an experienced inspector, these schemes could result in highly erratic recommendations.

PROPOSED SCHEME FOR RATING TOTAL SURFACE AREA

It is possible to apply more quantitative assessment techniques for rating large surface areas. One such proposed scheme consists of four steps:

1. Identify the major structural elements (e.g., plates, girders, braces);
2. Subdivide each of these parts into ratable areas, defined as ones with a relatively uniform coating or steel condition; then visually or otherwise estimate the percentage of the total surface covered by the rating area;
3. Assign a numerical or semiquantitative rating to each rating area; these can be limited to ASTM rust ratings or can include multiple defects such as those described earlier; and
4. Compile the data.

Clearly, the final rating will not consist of a single percentage rating or general condition statement, but rather will reflect the complex patterns of coating and steel degradation. Of course, the user could always establish an overall condition rating of the structure that is a distillation of the ratings of the individual parts.

This technique is most suitable for relatively large surface areas. For small equipment and structures with intricate configurations, it is often more feasible to assign a single rating to an entire unit or subunit. An experienced inspector can assign a single rating for a larger structure if the total amount of deterioration and the degree of nonuniformity are not too great.

An example illustrated is a bridge with about 40 fascia plates (Figure 5). Approximately 12 plates showed some evidence of deterioration. For some there were only a few spots (5 percent of the surface with a rating of 9). On Plate 3, 10 percent of the surface had a rating of 4 (Figure 6), and on Plate 4, 40 percent had a rating of 6 (Figure 7). A rust rating of 8 is shown in Figure 8. The second example is a storage tank. Most of the structure (90 percent of the painted surface) showed no visible signs of rust or paint breakdown (Figure 9). By using the method outlined previously, it was determined that about 3 percent of the entire surface had a degradation rating of 9 according to ASTM D-610 (Figure 10). Another 3 percent received a rating of 8 (Figure 11), and 4 percent of the surface received a rating of 7 (Figure 12). These ratings were based on total defects, including rust breakthrough and topcoat cracking.

In some instances it might be appropriate to determine the percentage of the surface area showing a rating of 8 (Figure 8) or worse. For the tank example a total of 7 percent of the surface was rated as 8 or worse. For this tank, a walk-around inspection would yield an overall rating of 9. Alternatively the inspector could identify the number

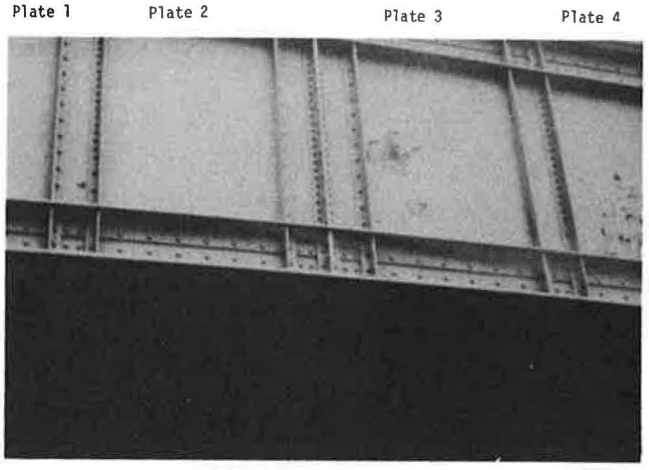

FIGURE 5 Rating of plates on highway bridge.

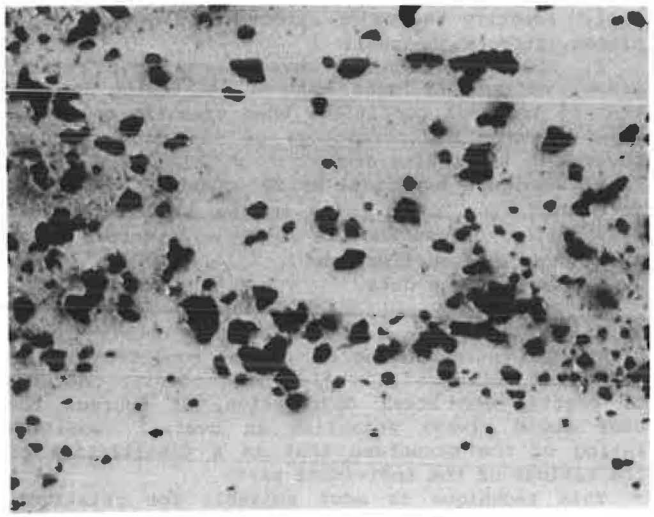

FIGURE 6 ASTM D-610 rust rating of 4.

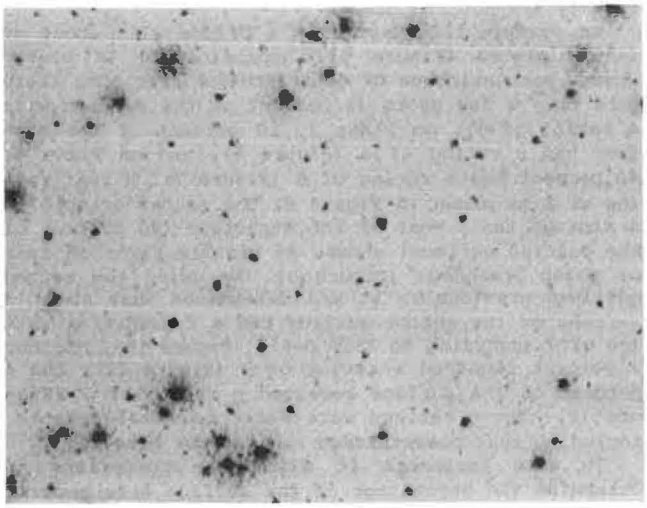

FIGURE 7 ASTM D-610 rust rating of 6.

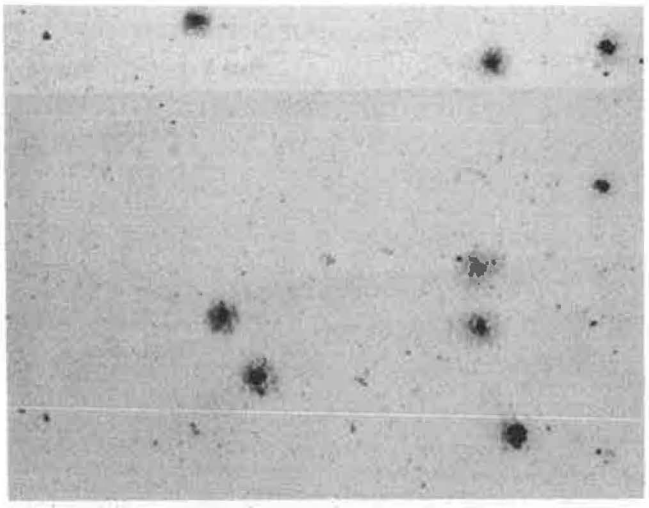

FIGURE 8 ASTM D-610 rust rating of 8.

of plates requiring 0 to 10 percent, 10 to 50 percent, or 100 percent repainting. For the bridge example Plates 1 and 2 required 0 to 10 percent repainting, whereas Plates 3 and 4 required 10 to 50 percent repainting. It is important to establish a systematic, consistent procedure that takes into account the number of components and structures to

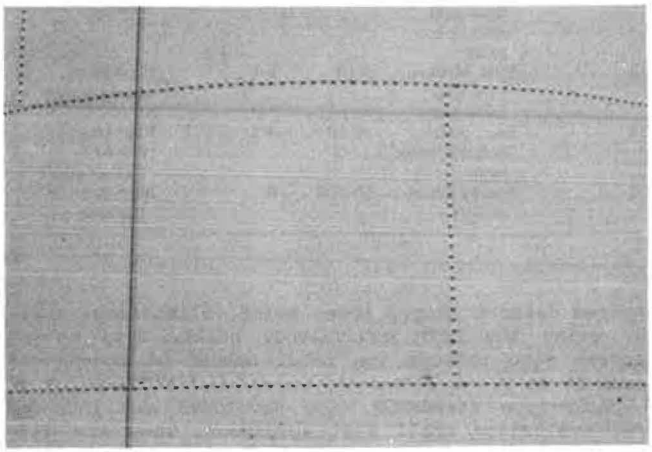

FIGURE 9 Portion of tank with ASTM rust rating of 10.

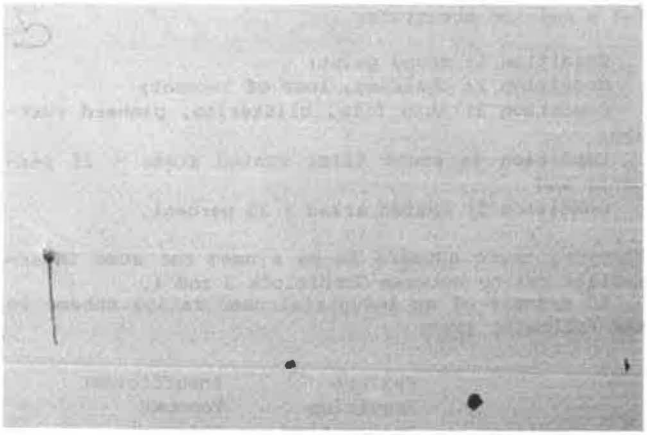

FIGURE 10 Portion of tank with ASTM rust rating of 9.

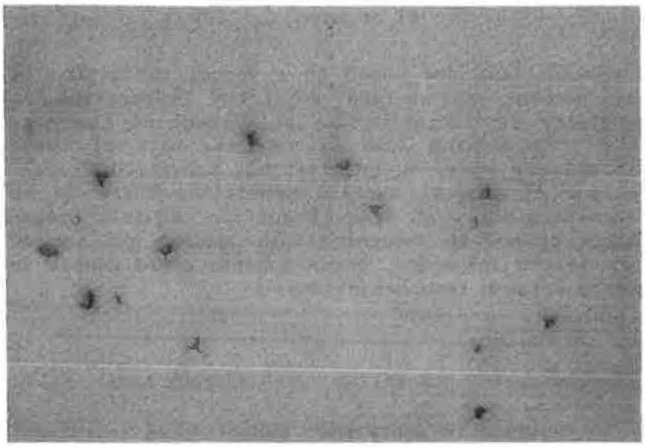

FIGURE 11 Portion of tank with ASTM rust rating of 8.

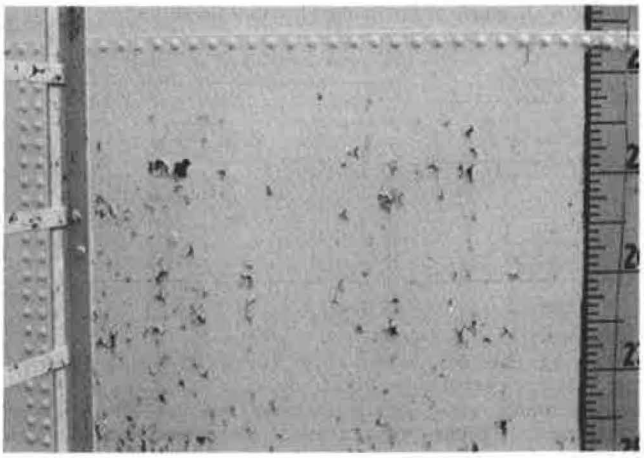

FIGURE 12 Portion of tank with ASTM rust rating of 7.

be rated, the uniformity of the surface condition, and the eventual use of the results. Use of numerical ratings for the individual areas can prove advantageous in estimating future degradation, as will be discussed later.

CRITERIA FOR WHEN AND HOW MUCH TO REPAINT

The preceding has been concerned with criteria for evaluating the structure's condition. Also of interest are criteria for when and how much to repaint. These depend to a great extent on the painting philosophy or objective. Painting to maintain appearance at the least cost will likely require repainting at an earlier stage than if preventing metal loss were the primary objective. A structure will be painted still less frequently, and even then only in critical areas, if maintaining structural capacity is the only requirement.

It is also important to distinguish between situations in which repainting is already mandated and the only questions are "how much" (and "how") and situations in which one also must decide whether to paint now or to wait ("when"). Several examples will be given of published criteria for when and how much to paint.

SSPC PA-4 is an example of a "how much" criterion (8). It prescribes what to do on the basis of existing conditions (Table 5). It does not specify, for example, whether it is preferable to paint at Condition 1 or 2. Other authorities, however, do include such recommendations. Repainting is frequently specified when a structure reaches an ASTM D-610 rating of between 7 and 8 (11). The industrial-user rating scheme cited earlier recommends painting when coating passes from Condition 2 to 3. However, if appearance is of little import, the author suggests waiting until the surface reaches Condition 5, at which point 100 percent abrasive blast cleaning is recommended. This example highlights the need for a maintenance painting philosophy in formulating repainting criteria.

DETERMINING FUTURE CONDITION OF PAINTED STEEL

Another important factor in estimating the condition and time for repainting is the interval between the survey and the actual inspection. Frequently budgets and schedules must be prepared 1 or 2 years in advance. Thus, the inspector may have to estimate what the condition of the paint and steel will be in the future.

The California Department of Transportation rating system for bridges includes tips for estimating how long it takes to go from Code 4 (rust starting along edges) to Code 5 (requires repainting within 5 years) (12). For a red lead alkyd paint system, the telltale signs are enlarging rust "freckles," and peeling of the topcoat and exposure of the primer. Rapid deterioration has been observed within 1 year for some systems in marine atmospheres.

Windler (13) suggests assigning coating priorities based on the condition of the metal and the coating. He recommends immediate recoating of areas showing an ASTM D-610 rust rating of 4 or less and of areas where coating exhibits marginal adhesion. Recoating is recommended within 12 to 24 months in areas showing ASTM ratings of 6 to 8 and topcoat delamination. Repainting of other areas, including those with minor localized spot rusting, can be delayed more than 2 years.

RUST RATINGS LINEAR WITH TIME

In order to estimate or predict what the condition of a structure will be in 2 or 3 years, information is needed on the rate of degradation as well as on the current coating and steel condition. A rearrangement of some data shown earlier (Figure 3) is given in Figure 13. Figures 13 and 14 (7) show ASTM D-610 rust ratings (instead of percent of rust) versus time. The data suggest that the rate of deterioration in the ASTM rust rating is approximately linear with time. This is equivalent to the statement that the percentage of surface rusting is approximately exponential with time, because the ASTM rating system is essentially an exponential scale.

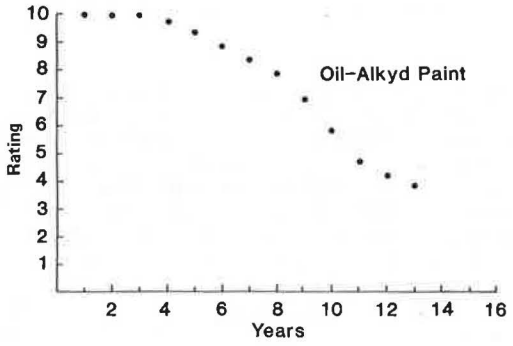

FIGURE 13 ASTM rust rating in industrial environment.

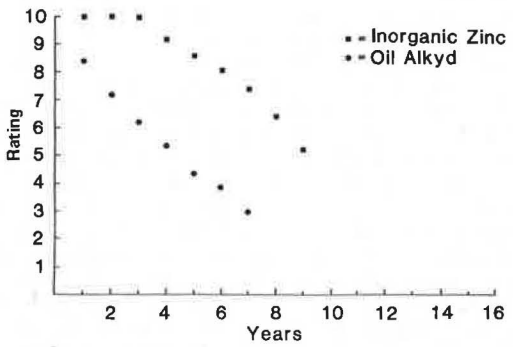

FIGURE 14 ASTM rust rating in marine environment.

There are also in some instances apparent threshold or induction periods lasting up to several years, during which no rust is observed. This time period depends on the type and thickness of coating and the exposure environment and is one of the most frequently used criteria for comparing coatings. This threshold period varies enormously, ranging from as little as 1 to 2 years for an alkyd in a marine environment to 15 to 20 years for an inorganic zinc in a mild or rural environment (Figures 13 and 14).

However, the slopes of these curves have considerably less variability than the thresholds. For most systems studied, the slope ranges between 0.5 and 1.0 ASTM units per year. These observed rates can be used to construct high and low ranges for predicted corrosion rates for an oil-alkyd paint in an industrial environment (Figure 15). The high-rate curve has a threshold of 2 years and a deterioration rate of 1.0 ASTM unit per year. The low-rate curve has a threshold of 4 years and deteriorates at 0.5 ASTM unit per year.

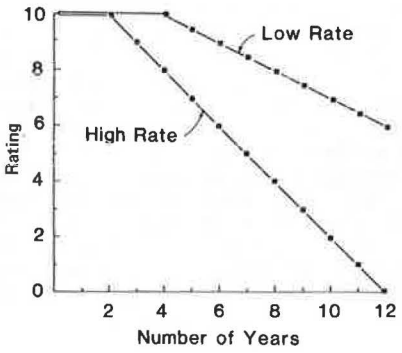

FIGURE 15 Estimating ASTM rust rating from high and low corrosion rates.

These curves can be used to estimate future corrosion effects and from those to determine future maintenance painting needs. This evaluation requires the ratings of the current condition of the structure. The example used is the tank shown in Figures 8-12. Future condition can be estimated on the basis of the graphs of high and low degradation rates (Figure 15). For example, under the high-degradation-rate assumption (1.0 ASTM unit per year), in 2 years the 10-rated areas would drop to 8, the 9-rated areas would drop to 7, the 8-rated areas to 6, and so on. Under the low-degradation-rate assumption (0.5 ASTM unit per year), the 9-rated areas would drop to 8, the 8-rated areas to 7, and so on, after 2 years. (Because of the threshold effect, it is assumed that for the first year the 10-rated areas do not degrade in the low-rate analysis.)

The ultimate objective of such an analysis would be to determine when the structure will require repainting. In this case (oil-alkyd paint over hand-cleaned steel in an industrial atmosphere), repainting is often stipulated when a large portion of the surface reaches a condition rating of 8. The ratings showed that currently 7 percent of the surface has a rating of 8 or worse (3 percent at 8, 4 percent at 7). This is the proportion of the surface that would require surface preparation by wire brushing if the structure were to be repainted. After 1 year, that would increase to between 6 and 10 percent (Table 6). After 2 years, this proportion is 10 to 100 percent and after 3 years 33 to 100 percent. These figures indicate that repainting cannot be deferred for 3 years. Even 2 years may be too long to wait, because if the corrosion rate is in the high range, the entire structure will have a rating of 8 or worse. Thus, some action is required for the following year, either repainting or reinspection. The latter would determine whether painting could be deferred for one more year.

TABLE 6 Example of Predicting Structure Condition

Current Condition		Projected Condition (% of surface)					
		1 Year		2 Years		3 Years	
ASTM Rating	Percent of Surface	High	Low	High	Low	High	Low
10	90	0	90	0	45	0	0
9	3	90	2	0	45	0	67
8	3	3	3	90	3	0	24
7	4	3	5	3	3	90	3
8 or worse	7	10	8	100	10	100	33

This example illustrates the value of conducting regular systematic surveys and documenting and applying the observed trends. The model predictions are approximations. They are dependent on the reliability and accuracy of the data used to derive the degradation curves. In applying the results, the user must be aware of the limitations of predicting coating behavior. In many cases, the input data can be modified to approach more closely existing conditions of a specific structure. Although far from being precise or proven tools, the methods proposed are expected to be an improvement over crude "guesstimating" or "eyeballing" techniques commonly used for making maintenance painting decisions.

SUMMARY AND CONCLUSIONS

The differences between maintenance painting and initial painting have been highlighted. One of the most important differences is the nature of the surface encountered. The wetting and spreading properties of paints and the characteristics of various surfaces determine the adhesion of the paint to the steel. Once paint is bonded to steel, its ability to protect steel from corrosion and retain its integrity is the problem to be addressed. The performance characteristics of coated steel versus time have been described and the negative synergism, deficiencies in current evaluation techniques, and possible improvements were noted.

A more immediate problem is to assist maintenance engineers in evaluating structural condition and deciding when and how much to repaint. Existing ASTM, SSPC, and other published criteria were reviewed and a technique was described for obtaining quantitative ratings for an entire structure. This approach may require some modification for different structures and conditions. It also may be used to estimate the need for future painting. These as well as more conventional standards and techniques, though far from perfect, can be effective tools in the effort to maintain, preserve, and protect the nation's public structures in the least costly and most efficient manner.

REFERENCES

1. W.A. Zisman. Surface Energetics of Wetting, Spreading, and Adhesion. Journal of Paint Technology, Vol. 44, Jan. 1972, pp. 42-57.
2. T.C. Patton. Surface Tension. In Paint Flow and Pigment Dispersion (Ch. 9), 2nd ed., John Wiley and Sons, New York, 1979.

3. C.R.C. Handbook of Chemistry and Physics, 64th ed. C.R.C. Press, Inc., Boca Raton, Fla., March 1983.
4. M. Tellor. Corrosion Resistant Zinc Paints. In Proceedings of Zinc Protective Coatings Conference, Zinc Institute, Inc., New York, 1981.
5. C.P. Larrabee. Mechanisms of Atmospheric Corrosion of Ferrous Metals. Corrosion, Vol. 15, 1959, p. 526.
6. F.W. Fink and W.K. Boyd. The Corrosion of Metals in Marine Environments. Battelle DMIC Report 245, Bayer and Company, Inc., Columbus, Ohio, 1970.
7. S. Frondistou-Yannas. Coating and Corrosion Costs of Highway Structural Steel. Report FHWA-RD-79-121. FHWA, U.S. Department of Transportation, March 1980.
8. Guide to Maintenance Painting with Oil-Alkyd Paint. SSPC PA-4. Steel Structures Painting Council, Pittsburgh, Pa., Nov. 1982.
9. Code of Practice for Protective Coating of Iron and Steel Structures Against Corrosion, Section 5: Maintenance. BS 5493. British Standards Institute, London, 1977.
10. S.P. Thompson. Managing a Maintenance Painting Program to Reduce Costs. Materials Performance, Vol. 21, No. 10, 1982, pp. 48-51.
11. A.H. Roebuck and G.H. Brevoort. Coating Work Costs and Estimating. Paper 145. Presented at CORROSION/82, National Association of Corrosion Engineers, Houston, Tex., 1982.
12. B.F. Deason. Methods of Evaluating Paint Conditions on Existing Steel Structures. California Department of Transportation, Sacramento, Dec. 1980.
13. F.J. Windler. The Corrosion Survey: An Engineer's Guide to Maintenance Painting Specifications. Paper 35. Presented at CORROSION/83, National Association of Corrosion Engineers, Houston, Tex., 1983.

Publication of this paper sponsored by Committee on Structures Maintenance.